Imaging of Brain Connectivity in Dementia: Clinical Implications for Diagnosis of its Underlying Diseases

Beeldvorming van de hersenconnectiviteit bij dementie: klinische implicaties voor de diagnose van onderliggende aandoeningen

Rozanna Meijboom

alzheimer
nederland

Publication of this thesis was financially supported by Alzheimer Nederland

Cover design: Rozanna Meijboom
Thesis layout: Ton Everaers
Printing: Ipskamp Printing

ISBN: 978-94-028-0469-0

Imaging of Brain Connectivity in Dementia: Clinical Implications for Diagnosis of its Underlying Diseases

Beeldvorming van de hersenconnectiviteit bij dementie: klinische implicaties voor de diagnose van onderliggende aandoeningen

Proefschrift

ter verkrijging van de graad van doctor aan de
Erasmus Universiteit Rotterdam
op gezag van de
rector magnificus

prof.dr. H.A.P. Pols

en volgens het besluit van het College voor Promoties.

De openbare verdediging zal plaatsvinden op
dinsdag 31 januari 2017 om 13.30 uur

door

Rozanna Meijboom
geboren te Rotterdam

Erasmus University Rotterdam

Erasmus

PROMOTIECOMMISSIE

Promotoren:

Prof.dr. A. van der Lugt
Prof.dr. J.C. van Swieten

Overige leden:

Prof.dr. C.M. van Duijn
Prof.dr. F. Barkhof
Dr. M.W. Vernooij

Co-promotor:

Dr. M. Smits

Voor mijn opa Dik (1922-2010) en oma Nel (1925) van Bebberen-Valken
Ik wens dat iedereen, net als zij, oud wordt met gezonde hersenen

TABLE OF CONTENTS

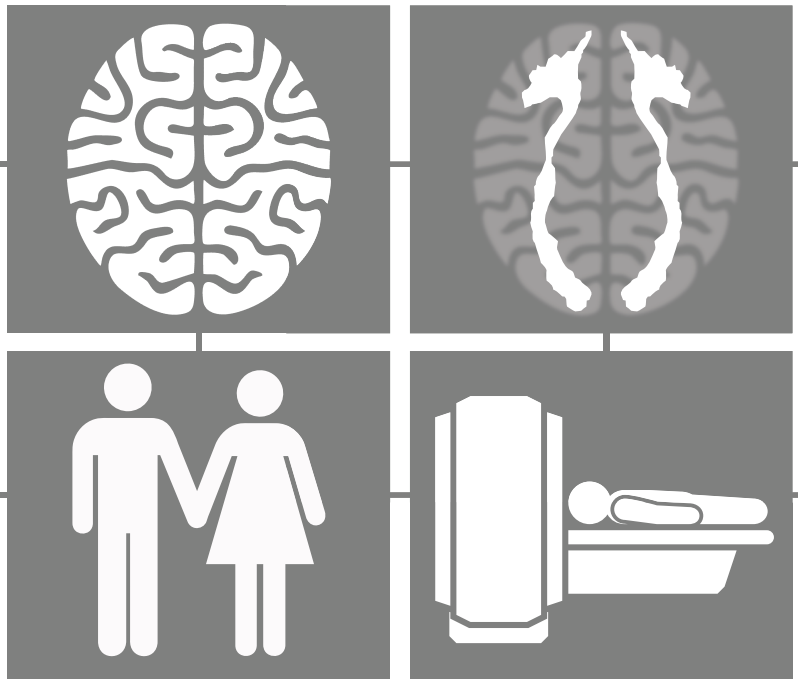

Chapter 1

General Introduction

Dementia is a neurodegenerative disorder affecting white matter (WM) and grey matter (GM) in different regions of the brain. Dementia generally occurs over the age of 65 years, but may also occur before the age of 65 years, i.e. presenile dementia [1]. In 2010 it was estimated that 35.6 million people worldwide suffered from dementia, and it was predicted that this number will nearly double every 20 years [1,2]. Few studies have investigated the prevalence of presenile dementia specifically [3], but the World Health Organization estimated in 2012 that presenile dementia may account for 6-9% of all dementia cases [1]. The two most common underlying diseases of presenile dementia are Alzheimer's disease (AD) and frontotemporal dementia (FTD) [4].

FTD is the umbrella term for several dementia subtypes affecting the frontal and/or temporal lobes. The two main variants of FTD are behavioural variant FTD (bvFTD) and semantic dementia (SD) [5].

BvFTD is mainly characterised by behavioural symptoms: disinhibition, apathy, loss of sympathy or empathy, stereotypical behaviour and hyperorality [6], but may also present with cognitive deficits in executive functioning [6] and memory [7,8]. Of note is that this clinical profile may not be as apparent in early stages of bvFTD when symptoms may still be unspecific. Brain abnormalities on conventional (structural) magnetic resonance imaging (MRI) are predominantly observed as GM atrophy of the right or bilateral frontal lobe(s) and the anterior temporal lobes [9–11]. Again, these abnormalities may only be evident in later disease stages. GM atrophy patterns such as these are likely underlying bvFTD behavioural symptomatology, as the bilateral frontal lobes are important for behaviour [12,13].

A syndrome controversially related to bvFTD is phenocopy FTD (phFTD). PhFTD is a rare and poorly understood syndrome with symptomatology very similar to that of bvFTD, but some aspects of phFTD are essentially different. In phFTD, core bvFTD symptoms, such as apathy, behavioural disinhibition, and loss of insight [14], are usually not accompanied by cognitive and brain abnormalities as is the case in bvFTD. PhFTD patients show a cognitive profile that ranges from normal to suggesting bvFTD [15–18] and have a relatively intact performance of daily living activities (ADL) [14,18]. These clinical features in phFTD appear stable over time, whereas in bvFTD patients progression of cognitive deficits is evident [18–21]. On conventional (structural) MRI, phFTD patients show no or only borderline abnormalities [19,21] in the frontal - and temporal - regions, which are typically affected in bvFTD [22]. As bvFTD patients may initially also present without structural MRI abnormalities, early-stage distinction between phFTD and

bvFTD may be difficult. Patients often remain undiagnosed or receive an alternative psychiatric diagnosis. A pathophysiological explanation for phFTD symptomatology is currently not available.

In contrast with this bvFTD spectrum, the SD variant of FTD is characterised by a language disorder affecting mainly the left hemisphere of the brain. SD presents with impaired confrontation naming and impaired single-word comprehension as core features, and may additionally present with impaired object knowledge and surface dyslexia [23]. On conventional (structural) MRI, SD predominantly shows anterior temporal lobe atrophy in the left hemisphere [10,11,23]. This likely underlies the specific language symptomatology as the left hemisphere is important for language functioning [24]. Language deficits seen in SD and other language variants of FTD may complicate differential diagnosis with atypical cases of AD presenting with early-stage language symptomatology [25,26].

AD is the most common disease underlying (presenile) dementia. It is mainly characterised by memory deficits, specifically by difficulties in learning and remembering new information. AD may also present with other cognitive deficits such as impaired reasoning and handling of complex tasks, visuospatial deficits and impaired language functioning [25]. In early stages however, symptoms may still be mild and unspecific, and AD may present with early-stage changes in social behaviour or executive functioning [27–29]. This may complicate differential diagnosis of AD and bvFTD, especially as early-stage symptoms in bvFTD may also be unspecific and memory deficits can occur [29,30]. Additionally, although in later stages of AD GM atrophy of the temporo-parietal lobes is usually observed on conventional (structural) MRI [25], in early stages this atrophy pattern may still be unclear.

Overall, early (differential) diagnosis of diseases underlying dementia may be difficult. Correct early diagnosis is important for several reasons. First, existing medication that may slow down progression in dementia (e.g. acetylcholinesterase inhibitors) will be most beneficial in a specific dementia subtype. Second, being aware of the nature of a patient's dementia will help both the patient and the family develop coping strategies and prepare for the future. Third, it will allow medication trials to target defined patient groups. Fourth, it is likely that future medication will be most beneficial when administered in the early stages - or even presymptomatically. In conclusion, it is of great importance to improve early (differential) diagnosis in dementia. In this thesis I investigate the potential use of advanced MRI for the differential diagnosis of diseases underlying dementia in the presenile dementia population.

As mentioned above, MRI is used to support diagnosis of dementia subtypes by means of brain imaging. However, in early disease stages, such as in AD and bvFTD, conventional (structural) MRI may still appear normal or show diffuse brain abnormalities unspecific for a dementia subtype [21,31,32]. More advanced MRI techniques, such as diffusion tensor imaging (DTI), resting state functional MRI (rs-fMRI) and arterial spin labelling (ASL) may aid (differential) diagnosis by detecting more subtle abnormalities that remain unrevealed using structural MRI [33].

The first and second techniques, DTI and rs-fMRI, can be used to assess brain connectivity, in terms of WM microstructure (Figure 1a) and functional connectivity (Figure 1b) respectively. Changes in WM microstructure are approximated by looking at diffusion of water molecules in the brain. For this purpose, several diffusion measures are used: fractional anisotropy (FA, i.e. directionality of diffusion), mean diffusivity (MD), radial diffusivity (RD, i.e. diffusion perpendicular to the axis) and axial diffusivity (AxD, i.e. diffusion along the axis). A decrease in FA suggests loss of directionality of diffusion, which has been suggested to indicate abnormal microstructure of the WM. Likewise, an increase in mean diffusivity indicates increased diffusion in all directions of a WM tract, i.e. less restricted movement of water molecules, is also thought to represent changes of WM microstructure. An increase in RD and AxD has been suggested to reflect respectively myelin [34] and axonal changes [35]. As both FA and MD are combination measures of RD and AxD, abnormalities of FA and MD may be induced by changes in either. Resting state functional connectivity changes are investigated in terms of patterns of brain activity that co-vary between different regions of the brain, so called resting state networks. A widely studied and well-defined resting state network is the default mode network (DMN), consisting of the precuneus, posterior cingulate cortex, inferior parietal lobule, lateral temporal cortex and medial prefrontal cortex [36] (Figure 1b). In this network, increased functional connectivity reflects neuronal activity changes that have become more congruent between regions. This may point to a brain mechanism compensating for early diminished neuronal functioning [37,38]. The degree of increased connectivity may reflect the brain's remaining ability of compensation, ultimately reversing to decreased connectivity as neuronal dysfunctioning progresses.

The third technique, ASL, can be used to assess GM perfusion in the whole-brain or in regions of interest (Figure 1c). Additionally, advanced post-processing tools may improve the use of conventional MRI enabling detection of smaller GM volume changes and combination of GM volumes with other MRI measures.

Taken together, these advanced MRI techniques detect subtle brain abnormalities in structure and function, which may aid clinical diagnosis in dementia.

Clinical differential diagnosis may especially benefit from objective quantitative advanced MRI measures, such as diffusion values. This allows us to identify dementia patients by comparing them to reference values of the healthy population. Additionally, advanced MRI techniques also allow us to combine WM and GM measures and to investigate relationships between subtle changes of WM and GM in dementia.

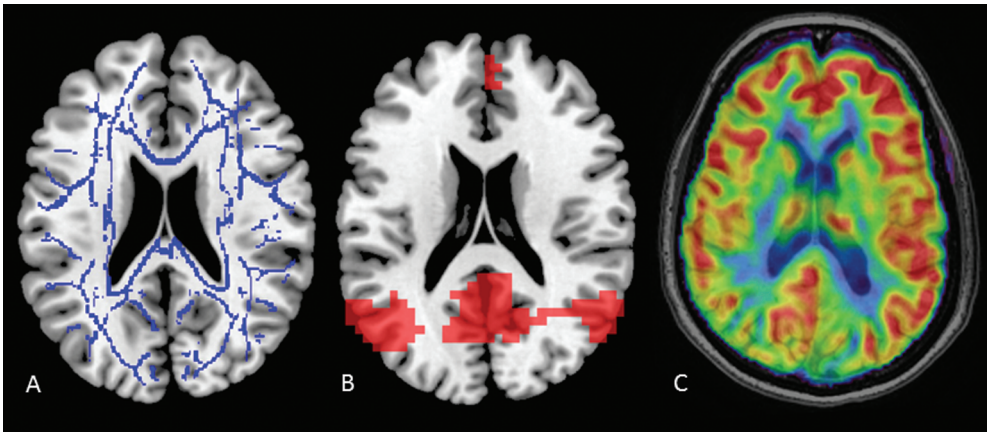

Figure 1. Axial images of (A) a white matter skeleton created by post-processing of diffusion tensor imaging, (B) resting state functional magnetic resonance imaging, and (C) arterial spin labelling in healthy participants. The white matter skeleton is depicted in blue (A). Default mode network functional connectivity of the inferior parietal lobules, posterior cingulate cortex/precuneus, and medial prefrontal cortex is shown in red (B). Grey matter regions with the highest perfusion are shown in red (C).

In **section 2** of this thesis I investigate subtle brain abnormalities in early-stage presenile AD and bvFTD. In **chapter 2.1** I explore the diagnostic utility of quantitative measures of tract-specific WM microstructure and functional connectivity of the DMN for early-stage and long-term differentiation of AD and bvFTD. **Chapter 2.2** investigates whether there is coherence between regional abnormalities of WM microstructure and GM volume and perfusion in AD and in bvFTD.

In **section 3** I investigate associations between subtle brain abnormalities and clinical symptomatology in AD, bvFTD and SD. In **chapter 3.1** I address functional associations between early-stage symptomatology and abnormalities of WM microstructure in both bvFTD and AD. In **chapter 3.2** I explore lateralization of WM microstructure and functional connectivity abnormalities in SD and bvFTD, which may be underlying their differential symptomatology.

Section 4 investigates whether phFTD and bvFTD may belong to the same

disease spectrum by exploring whether there are subtle brain abnormalities in phFTD that are similar to those seen in bvFTD. Functional DMN connectivity and microstructural WM abnormalities will be discussed in **chapter 4.1**, and quantified perfusion and GM volumes in **chapter 4.2**. In **chapter 4.3** I will address longitudinal changes in individual phFTD patients by looking at cognition, WM microstructure, GM volumes and perfusion.

In **chapter 5** I will provide an overview of the main findings and discuss the methodological considerations, clinical implications and future perspective of this research.

REFERENCES

1 World Health Organization. Dementia: A public health priority. 2012.

2 Prince M, Bryce R, Albanese E, *et al.* The global prevalence of dementia: A systematic review and metaanalysis. *Alzheimer's Dement* 2013;9:63–75.e2. doi:10.1016/j.jalz.2012.11.007

3 Rossor MN, Fox NC, Mummery CJ, *et al.* The diagnosis of young-onset dementia. *Lancet Neurol* 2010;9:793–806. doi:10.1016/S1474-4422(10)70159-9

4 Greicius MD, Geschwind MD, Miller BL. Presenile dementia syndromes: an update on taxonomy and diagnosis. *J Neurol Neurosurg Psychiatry* 2002;72:691–700.http://www.ncbi.nlm.nih.gov/pubmed/12023408

5 Neary D, Snowden JS, Gustafson L, *et al.* Frontotemporal lobar degeneration: A consensus on clinical diagnostic criteria. *Neurology* 1998;51:1546–54. doi:10.1212/WNL.51.6.1546

6 Rascovsky K, Hodges JR, Knopman D, *et al.* Sensitivity of revised diagnostic criteria for the behavioural variant of frontotemporal dementia. *Brain* 2011;134:2456–77. doi:10.1093/brain/awr179

7 Irish M, Devenney E, Wong S, *et al.* Neural substrates of episodic memory dysfunction in behavioural variant frontotemporal dementia with and without C9ORF72 expansions. *NeuroImage Clin* 2013;2:836–43. doi:10.1016/j.nicl.2013.06.005

8 Smits LL, van Harten AC, Pijnenburg YAL, *et al.* Trajectories of cognitive decline in different types of dementia. *Psychol Med* 2015;45:1051–9. doi:10.1017/S0033291714002153

9 Rascovsky K, Hodges JR, Knopman D, *et al.* Sensitivity of revised diagnostic criteria for the behavioural variant of frontotemporal dementia. *Brain* 2011;134:2456–77. doi:10.1093/brain/awr179

10 Karageorgiou E, Miller BL. Frontotemporal lobar degeneration: a clinical approach. *Semin Neurol* 2014;34:189–201. doi:10.1055/s-0034-1381735

11 Bocti C, Rockel C, Roy P, *et al.* Topographical patterns of lobar atrophy in frontotemporal dementia and Alzheimer's disease. *Dement Geriatr Cogn Disord* 2006;21:364–72. doi:10.1159/000091838

12 Cummings JL. Frontal-subcortical circuits and human behavior. *Arch Neurol* 1993;50:873–80. http://www.ncbi.nlm.nih.gov/pubmed/8352676.

13 Bonelli RM, Cummings JL. Frontal-subcortical circuitry and behavior. *Dialogues Clin Neurosci* 2007;9:141–51.http://www.pubmedcentral.nih.gov/articlerender.fcgi?artid=3181854&tool=pmcentrez&rendertype=abstract.

14 Hornberger M, Shelley BP, Kipps CM, *et al.* Can progressive and non-progressive behavioural variant frontotemporal dementia be distinguished at presentation? *J Neurol Neurosurg Psychiatry* 2009;80:591–3. doi:10.1136/jnnp.2008.163873

15 Bertoux M, de Souza LC, Corlier F, *et al.* Two Distinct Amnesic Profiles in Behavioral Variant Frontotemporal Dementia. *Biol Psychiatry* Published Online First: 2013. doi:10.1016/j.biopsych.2013.08.017

16 Hornberger M, Piguet O, Kipps C, *et al.* Executive function in progressive and nonprogressive behavioral variant frontotemporal dementia. *Neurology* 2008;71:1481–8. doi:10.1212/01.wnl.0000334299.72023.c8

17 Irish M, Graham A, Graham KS, *et al.* Differential impairment of source memory in progressive versus non-progressive behavioral variant frontotemporal dementia. *Arch Clin Neuropsychol* 2012;27:338–47. doi:10.1093/arclin/acs033

18 Mioshi E, Hodges JR. Rate of change of functional abilities in frontotemporal dementia. *Dement Geriatr Cogn Disord* 2009;28:419–26. doi:10.1159/000255652

19 Davies RR, Kipps CM, Mitchell J, *et al.* Progression in frontotemporal dementia: identifying a benign behavioral variant by magnetic resonance imaging. *Arch Neurol* 2006;63:1627–31. doi:10.1001/archneur.63.11.1627

20 Garcin B, Lillo P, Hornberger M, *et al.* Determinants of survival in behavioral variant frontotemporal dementia. *Neurology* 2009;73:1656–61. doi:10.1212/WNL.0b013e3181c1dee7

21 Kipps CM, Davies RR, Mitchell J, *et al.* Clinical significance of lobar atrophy in frontotemporal dementia: application of an MRI visual rating scale. *Dement Geriatr Cogn Disord* 2007;23:334–42. doi:10.1159/000100973

22 Rosen HJ, Gorno-Tempini ML, Goldman WP, *et al.* Patterns of brain atrophy in frontotemporal dementia and semantic dementia. *Neurology* 2002;58:198–208.http://www.ncbi.nlm.nih.gov/pubmed/11805245

23 Gorno-Tempini ML, Hillis a E, Weintraub S, *et al.* Classification of primary progressive aphasia and its variants. *Neurology* 2011;76:1006–14. doi:10.1212/WNL.0b013e31821103e6

24 Ocklenburg S, Beste C, Arning L, *et al.* The ontogenesis of language lateralization and its relation to handedness. *Neurosci Biobehav Rev* 2014;43:191–8. doi:10.1016/j.neubiorev.2014.04.008

25 McKhann GM, Knopman DS, Chertkow H, *et al.* The diagnosis of dementia due to Alzheimer's disease: recommendations from the National Institute on Aging-Alzheimer's Association workgroups on diagnostic guidelines for Alzheimer's disease. *Alzheimers Dement* 2011;7:263–9. doi:10.1016/j.jalz.2011.03.005

26 Galton CJ. Atypical and typical presentations of Alzheimer's disease: a clinical, neuropsychological, neuroimaging and pathological study of 13 cases. *Brain* 2000;123:484–98. doi:10.1093/brain/123.3.484

27 Bathgate D, Snowden JS, Varma A, *et al.* Behaviour in frontotemporal dementia, Alzheimer's disease and vascular dementia. *Acta Neurol Scand* 2001;103:367–78.http://www.ncbi.nlm.nih.gov/pubmed/11421849

28 Jenner C, Reali G, Puopolo M, *et al.* Can cognitive and behavioural disorders differentiate frontal variant-frontotemporal dementia from Alzheimer's disease at early stages? *Behav Neurol* 2006;17:89–95.http://www.ncbi.nlm.nih.gov/pubmed/16873919

29 Varma AR, Snowden JS, Lloyd JJ, *et al.* Evaluation of the NINCDS-ADRDA criteria in the differentiation of Alzheimer's disease and frontotemporal dementia. *J Neurol Neurosurg Psychiatry* 1999;66:184–8.http://www.ncbi.nlm.nih.gov/pubmed/10071097

30 Hallam BJ, Silverberg ND, Lamarre AK, *et al.* Clinical presentation of prodromal frontotemporal dementia. *Am J Alzheimers Dis Other Demen* 2007;22:456–67. doi:10.1177/1533317507308781

31 Gregory CA, Serra-Mestres J, Hodges JR. Early diagnosis of the frontal variant of frontotemporal dementia: how sensitive are standard neuroimaging and neuropsychologic tests? *Neuropsychiatry Neuropsychol Behav Neurol* 1999;12:128–35.http://www.ncbi.nlm.nih.gov/pubmed/10223261

32 Rosso SM, Heutink P, Tibben A, *et al.* [New insights in frontotemporal dementia]. *Ned Tijdschr Geneeskd* 2000;144:1575–80.http://www.ncbi.nlm.nih.gov/pubmed/10965365

33 Sperling RA, Aisen PS, Beckett LA, *et al.* Toward defining the preclinical stages of Alzheimer's disease: Recommendations from the National Institute on Aging-Alzheimer's Association workgroups on diagnostic guidelines for Alzheimer's disease. *Alzheimer's Dement* 2011;7:280–92. doi:10.1016/j.jalz.2011.03.003

34 Song S-K, Sun S-W, Ramsbottom MJ, *et al.* Dysmyelination Revealed through MRI as Increased Radial (but Unchanged Axial) Diffusion of Water. *Neuroimage* 2002;17:1429–36. doi:10.1006/nimg.2002.1267

35 Song S-K, Sun S-W, Ju W-K, *et al.* Diffusion tensor imaging detects and differentiates axon and myelin degeneration in mouse optic nerve after retinal ischemia. *Neuroimage* 2003;20:1714–22. doi:10.1016/j.neuroimage.2003.07.005

36 Buckner RL, Andrews-Hanna JR, Schacter DL. The brain's default network: anatomy, function, and relevance to disease. *Ann N Y Acad Sci* 2008;1124:1–38. doi:10.1196/annals.1440.011

37 Borroni B, Alberici A, Cercignani M, *et al.* Granulin mutation drives brain damage and reorganization from preclinical to symptomatic FTLD. *Neurobiol Aging* 2012;33:2506–20. doi:10.1016/j.neurobiolaging.2011.10.031

38 Bookheimer SY, Strojwas MH, Cohen MS, *et al.* Patterns of brain activation in people at risk for Alzheimer's disease. *N Engl J Med* 2000;343:450–6. doi:10.1056/NEJM200008173430701

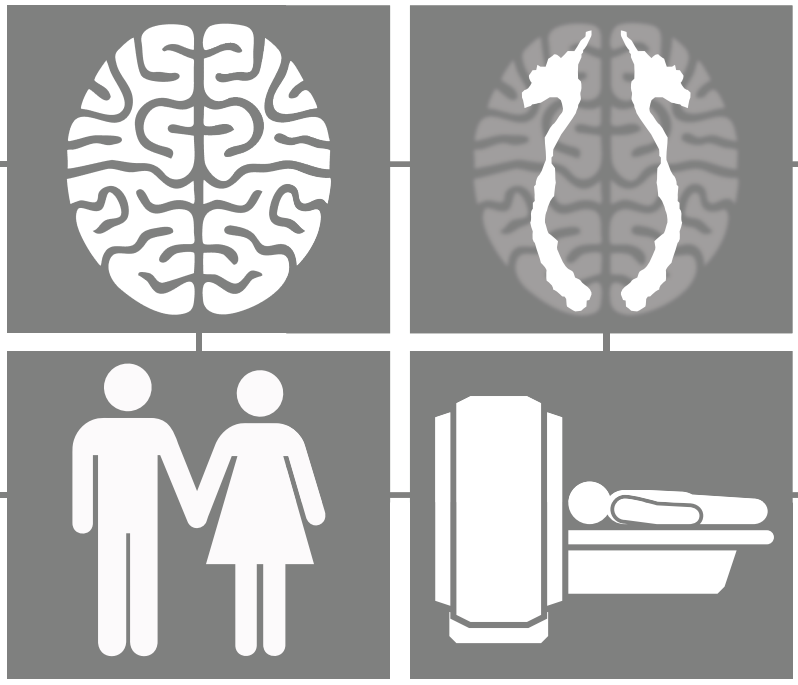

Section 2

Advanced MRI in Alzheimer's disease and behavioural variant frontotemporal dementia

Chapter 2.1

Quantitative early-stage and long-term differentiation of Alzheimer's disease and behavioural variant frontotemporal dementia using tract-specific microstructural WM and functional connectivity measures

Rozanna Meijboom
Rebecca M.E. Steketee
Leontine S. Ham
Dante Mantini
Esther E. Bron
Aad van der Lugt
John C. van Swieten
Marion Smits

Submitted

ABSTRACT

This study investigated quantitative measures of tract-specific white matter (WM) microstructure and functional default mode network (DMN) connectivity to explore clinical applicability for early-stage and long-term differential diagnosis of Alzheimer's disease (AD) and behavioural variant frontotemporal dementia (bvFTD).

Eleven AD and 12 bvFTD early-stage patients, and 18 controls underwent diffusion tensor imaging and resting state functional magnetic resonance imaging at 3T. All AD and 6 bvFTD patients underwent the same protocol at 1-year follow-up. Functional connectivity measures of the DMN and WM tract-specific diffusivity measures (fractional anisotropy, mean, radial and axial diffusivity) were determined for all groups. All measures were compared between the three groups at baseline, and between patients at follow-up. Additionally, the difference between baseline and follow-up diffusivity measures in AD and bvFTD patients were compared.

Functional connectivity of the DMN was not different between groups neither at baseline nor at follow-up. Diffusion abnormalities were observed widely in bvFTD and regionally in the hippocampal cingulum in AD. The extent of the differences between bvFTD and AD were diminished at follow-up yet abnormalities were still more pronounced in bvFTD, specifically in the cingulate cingulum and inferior fronto-occipital fasciculus. The rate of change was very similar in bvFTD and AD.

Quantitative tract-specific microstructural WM abnormalities, but not quantitative functional connectivity of the DMN, may aid early-stage and long-term differential diagnosis of bvFTD and AD. Specifically, pronounced microstructural WM changes in anterior WM tracts characterise bvFTD, whereas microstructural WM abnormalities of the hippocampal cingulum characterise AD.

1. INTRODUCTION

Presenile dementia is dementia with an onset before the age of 65 years. The two most common underlying disorders are Alzheimer's disease (AD) and behavioural variant frontotemporal dementia (bvFTD) [1]. AD is characterised by an episodic memory disturbance for recently learned as well as for learning new material, together with at least one other cognitive disturbance [2]. In contrast, bvFTD is mainly characterised by behavioural problems such as disinhibition, apathy and loss of empathy [3]. In later stages of AD and bvFTD, predominance of cognitive impairment in AD and social/executive impairment in bvFTD [4,5] aid differential diagnosis. However, differential diagnosis can be difficult in early stages of AD and bvFTD, as symptoms may still be mild and unspecific. BvFTD patients may present with memory deficits [6,7] and AD patients with changes in social behaviour or executive functioning [5,7,8]. Magnetic resonance imaging (MRI) supports diagnosis, but in early disease stages conventional (structural) MRI may still appear normal or show diffuse brain abnormalities unspecific for a dementia subtype [9–11]. More advanced MRI techniques, such as diffusion tensor imaging (DTI) and resting state functional MRI (rs-fMRI) may aid differential diagnosis by detecting more subtle abnormalities that remain unrevealed using structural MRI [12].

DTI is used to assess white matter (WM) microstructure of the brain. Previous studies have observed more pronounced microstructural WM abnormalities in bvFTD than in AD [13,14] and have suggested an anterior-posterior division of WM abnormalities in bvFTD and AD. Microstructural WM abnormalities are observed in anterior brain regions in bvFTD, such as the cingulate cingulum, genu of the corpus callosum (or forceps minor) and uncinate fasciculus, whereas microstructural WM changes in AD are localised in more posterior brain regions, such as the splenium (or forceps major) and the hippocampal cingulum [15–17]. Rs-fMRI is used to assess functional connectivity between grey matter (GM) regions that together form functional brain networks. A widely studied network is the default mode network (DMN), known to be affected in both AD and bvFTD [18]. Previous research has shown DMN differences between AD and bvFTD - mostly in the posterior DMN -, specifically decreased DMN connectivity in AD and increased DMN connectivity in bvFTD.

Clinical diagnosis may especially benefit from objective quantitative measures derived from DTI and rs-fMRI in differentiating subtypes of dementia patients, and patients from healthy persons, using group-specific reference values. In this study we explore the diagnostic utility of quantitative measures of tract-

specific WM microstructure and functional connectivity of the DMN for early-stage and long-term differentiation of AD and bvFTD.

2. METHODS

2.1 Participants

Patients were recruited in the Alzheimer Centre Southwest Netherlands. Inclusion criteria were an age between 40 and 70 years; suspected diagnosis of early AD [2] or bvFTD [3]; a Mini-Mental State Examination [19] (MMSE) score of ≥ 20. Exclusion criteria were contraindications for MRI; an expected loss to follow-up within one year; other neurological disorders; a different cause of dementia; alternative psychiatric diagnosis; past or current substance abuse. Diagnosis of either AD or bvFTD was confirmed after at least one year follow-up. Patients underwent the MMSE as part of their routine clinical diagnostic work-up.

Healthy controls, matched for age and gender, and without neurological or psychiatric history, were recruited through advertisement. Controls underwent neuropsychological testing and the MMSE as part of this study to rule out cognitive impairment.

The study was approved by the local medical ethics committee. All participants gave written informed consent.

2.2 Image acquisition

MRI was performed on a 3T GE Discovery MR750 system (GE Healthcare, Milwaukee, WI, US). See Table 1 for acquisition parameters. Patients underwent identical MRI protocols at baseline (T0) and at one year follow-up (T1). Controls underwent MRI at T0 only.

For anatomical reference, a high-resolution three-dimensional (3D) inversion recovery (IR) fast spoiled gradient echo (FSPGR) T1-weighted (T1w) image was acquired. DTI scans were acquired with spin-echo echo planar imaging (EPI) sequence and functional scans with a gradient echo EPI sequence with full coverage of the supratentorial brain. For functional scans participants were instructed to think of nothing in particular, to focus on a fixation cross and to remain awake.

Table I. Acquisition parameters.

	T1w	DTI	fMRI
FOV (mm)	240	240	240
TE (ms)	3.06	84.5*	30
TR (ms)	7.90	7930	3000
ASSET factor	2	2	2
Flip angle	12°	90°	90°
Acquisition matrix	240x240	128x128	96x96
Slice thickness (mm)	1	2.5	3
Volumes (slices per volume)	1 (176)	28 (59)	200 (44)
Duration (min)	4.41	3.50	10.00
Diffusion-weighted directions	n/a	25	n/a
Non-diffusion weighted images	n/a	3	n/a
Maximum b-value (s/ mm2)	n/a	1000	n/a
TI (ms)	450	n/a	n/a

T1w = T1-weighted, DTI = diffusion tensor imaging, fMRI = functional magnetic resonance imaging, FOV= field of view, TE = echo time, TR = repetition time, ASSET = array spatial sensitivity encoding technique, TI = inversion time.
*TE for DTI was set to minimum. This number represents the average TE. The range of TE was 81.9-90.8 ms.

2.3 Demographical analysis

Between-group differences in age were tested using a one-way ANOVA. Between-group differences in MMSE score were tested using a Welch-ANOVA and post-hoc Games-Howell t-tests, due to unequal variance across groups. Gender was compared across groups using chi-square tests. Analyses were done using IBM SPSS Statistics (version 21.0, New York, USA) with a significance threshold of $p<0.05$.

2.4 Grey matter (GM) volume analysis

GM volumes were calculated according to the methods described in Bron et al. (2014) [20]. GM volumes were obtained from the T1w image using the unified tissue segmentation method of SPM8 (Statistical Parametric Mapping, London, UK), after which intracranial volume (ICV) was calculated. Then, GM volume was divided by ICV to correct for brain size. GM volume (%ICV) was compared between all groups at T0 and between bvFTD and AD at T1 using a one-way ANOVA and post-hoc Bonferroni tests (IBM SPSS Statistics, version 21.0, New York, USA).

2.5 Microstructural white matter (WM) analysis

Data were analysed using FMRIB Software Library (FSL5, Oxford, UK) [21–23]. Data were corrected for motion and eddy currents using Eddy Correct and then skull-stripped using BET [24].

Tracts known to be associated with cognitive functions such as language, executive functioning and memory were selected for tractography: anterior thalamic radiation [25,26], cingulum [27], forceps major [25,28], forceps minor [25,29,30], inferior fronto-occipital fasciculus [31–33] , inferior longitudinal fasciculus [31,34], superior longitudinal fasciculus [34,35] and uncinate fasciculus [27,29,33]. The genu and splenium of the corpus callosum were represented by respectively the forceps minor and major.

Automated probabilistic tractography (AutoPtx) [36] was used to apply a tensor fit with DTIFIT [37], followed by a FNIRT registration and a BEDPOSTX probabilistic model fit for each participant. PROBTRACKX [37,38] was then run for all selected WM tracts using default space seed, target, stop and exclusion masks available in AutoPtx [36], resulting in a participant-specific tract density image. Tract density images were normalised by dividing them by the number of fibres included in the tract-image and then binarised for WM tract segmentation, based on the best-fit segmentation thresholds established by De Groot et al. (2015) [84] (see supplemental (suppl) Table 1 for thresholds).

Diffusivity images were masked with thresholded tract images using FSLstats, to acquire median fractional anisotropy (FA), mean diffusivity (MD), radial diffusivity (RD) and axial diffusivity (AxD) for each tract.

Further WM analyses were done using IBM SPSS Statistics (version 21.0, New York, USA). First, WM microstructure values at T0 were compared between AD, bvFTD and controls using an ANOVA and post-hoc Bonferroni t-tests, unless an age effect was present. Age effects were investigated using linear regression and, if necessary, taken into account using an ANCOVA. TE variation - induced by the minimum setting during scanning - could not be accounted for by means of regression analysis as ANOVA revealed higher TE for AD than for bvFTD and controls. The effect of varying TE is expected to be small, however a possible bias may have been introduced. In case of unequal variances across groups, between-group differences were investigated using a Welch-ANOVA and post-hoc Games-Howell t-tests. Second, WM microstructure values at T1 were compared between AD and bvFTD, following the same approach as for the baseline analyses. Two diffusion measures for separate WM tracts with both unequal variance across groups and age effect were excluded from the analysis. Third, AD and bvFTD WM microstructure values at T0 were subtracted from WM microstructure values at T1 to establish the difference score per diffusion metric per tract. These difference scores (rate of change) were then compared between AD and bvFTD using the same approach as for baseline WM metrics.

2.6 Functional connectivity analysis

Using regions of interest (ROIs) of the Hammers atlas (30 atlases with 83 ROIs; http://brain-development.org/brain-atlases) [39], GM regions making up the default mode network (DMN) were selected for functional analysis: bilateral medial prefrontal cortex (mPFC), bilateral lateral temporal cortex (LTC), bilateral inferior parietal lobule (IPL), bilateral precuneus, bilateral posterior cingulate cortex (PCC). All ROIs were normalised to Montreal Neurological Institute (MNI) space.

Functional and structural data were first preprocessed using Statistical Parametrical Mapping (SPM8, Wellcome department, London, UK). Spatial preprocessing consisted of manual realignment of functional and structural data to the anterior commissure, realignment of functional data, coregistration of functional and structural data, segmentation of structural data into grey matter and white matter with a light clean, and normalisation to MNI space with a resampling size of $3mm^3$ for functional and $1mm^3$ for structural data. Further preprocessing and analysis were performed using the connectivity toolbox by Mantini [40,41]. Functional data were scrubbed, smoothed with a Gaussian kernel of $5mm^3$ and cor-

rected for motion, WM and cerebrospinal fluid signals. Additionally, band-pass filtering (0.009-0.08 Hz) was applied.

For each DMN ROI, the blood-oxygenation-level dependent (BOLD) signal was calculated by averaging the BOLD signal of all voxels within the ROI. Subsequently, the average BOLD signal of each DMN ROI was correlated with all DMN ROI separately to assess functional connectivity. A Fisher's r-to-z transformation was then applied to allow for analysis of between-group functional connectivity differences. For both T0 (AD, bvFTD, controls) and T1 (AD, bvFTD) data, functional connectivity between ROIs was established for each group using a random-effect analysis corrected for multiple comparisons (false discovery rate (FDR)<0.001).

Functional connectivity differences at T0 between AD, bvFTD and control and differences between AD and bvFTD at T1 were assessed using an ANCOVA ($p<0.05$) with GM volume (%ICV) as covariate and post-hoc two-sample t-tests corrected for multiple comparisons (FDR<0.05).

3. RESULTS

3.1 Participant and disease characteristics

Eleven AD patients, 12 bvFTD patients and 21 controls were included in the study (see Table 2). Patients underwent MRI at T0 and at T1 one year later (mean 378 days); controls underwent MRI at T0 only. Three controls were excluded due to incidental structural imaging findings. Three bvFTD patients were excluded from the functional connectivity analysis due to missing rs-fMRI data. Six bvFTD patients did not undergo MRI at T1 and hence were excluded from T1 data analysis.

Table 2. Demographic characteristics.

Group	N	Mean age	Mean MMSE
BvFTD	12 (6 male)	60.3 (7.7)	26.6 (2.8)
BvFTD T1	6 (3 male)	64.0 (3.6)	-
AD	11 (8 male)	62.8 (5.0)	25.3 (2.0)
AD T1	11 (8 male)	63.3 (5.0)	-
Controls	18 (8 male)	59.8 (6.7)	29.1 (1.0)

BvFTD = behavioural variant frontotemporal dementia, AD = Alzheimer's disease, N = sample size. Values given as Mean (standard deviation). MMSE = Mini-Mental State Examination.

Data from 11 AD patients at T0 and T1, 12 bvFTD patients at T0 (9 for the rs-fMRI analysis) and 6 bvFTD patients at T1, and 18 controls at T0 were used for the analysis.

Participants did not differ in age at T0 ($F(2,38) = .498$, $p>0.05$), age at T1($t(15) = 0.311$, $p>0.05$), gender at T0 ($\chi^2(2,38) = 2.288$, $p>0.05$), or gender at T1 ($\chi^2(1,15) = 0.88$, $p>0.05$). MMSE score was different between groups ($F(2, 17.1) = 20.213$, $p<0.001$), and was lower in both patient groups compared with controls. MMSE score did not differ between AD and bvFTD.

3.2 Grey matter (GM) volume (%ICV)

Total GM volume (%ICV) was significantly lower in bvFTD (0.30%ICV, standard deviation (SD) 0.04) compared with both AD (0.33%ICV, SD 0.03) and controls (0.36%ICV, SD 0.03) at T0 ($F(2,38) = 13.837$, $p<0.001$), but not different between AD and controls. At T1, total GM volume (%ICV) was different between AD and bvFTD ($t(15) = -2.266$, $p<0.039$), and was significantly lower in bvFTD (0.27%ICV, SD 0.05) than in AD (0.32%ICV, SD 0.04).

3.3 White matter (WM) microstructure

3.3.1 Baseline (T0)

AD in comparison with controls (Table 3) showed higher MD only in the *right* hippocampal cingulum.

BvFTD in comparison with controls (Table 3) showed lower FA and higher MD, RD and AxD in the *bilateral* hippocampal cingulum, inferior fronto-occipital fasciculus, uncinate fasciculus, and forceps minor. Higher MD, RD and AxD in bvFTD compared with controls were additionally observed in the *bilateral* anterior thalamic radiation and superior longitudinal fasciculus. Further, lower FA and higher MD and RD in bvFTD compared with controls were observed in the *bilateral* cingulate cingulum.

BvFTD in comparison with AD (Table 3) showed lower FA and higher MD, RD and AxD in the *bilateral* inferior fronto-occipital fasciculus and uncinate fasciculus, and forceps minor. Higher MD, RD and AxD in bvFTD compared with AD was additionally observed in the *bilateral* anterior thalamic radiation, superior longi-

Table 3. Mean FA (x10^{-3}), MD (x10^{-3}), RD (x10^{-3}), AxD (x10^{-3}) for each WM tract, for bvFTD, AD and controls at T0.

WM tract	L/R	FA			MD			RD			AxD		
		BvFTD	AD	Controls	BvFTD	AD	Con-trols	BvFTD	AD	Controls	BvFTD	AD	Controls
ATR	L	320.44	328.95	327.82	**0.90**	0.83	0.81*	**0.73**	0.68	0.67	**1.27**	1.18	1.15*
ATR	R	315.64	320.27	322.81	**0. 93**	0.83	0.82	**0.76**	0.69	0.68	**1.31**	1.17	1.16*
CGC	L	**392.62**	417.66	438.54	**0. 86**	0.80	0.81	**0.67**	0.61	0.60	1.26	1.20	1.23
CGC	R	**355.58**	384.25	403.92	**0. 87**	0.81	0.81*	**0.70**	0.63	0.62	1.23	1.17	1.19
CGH	L	**221.51**	256.26	266.75	**0. 97**	0.88	0.84*	**0.85**	0.76	0.72*	**1.27**	1.19	1.13*
CGH	R	**213.55**	244.43	264.69	**1.04**	**0.88**	0.84*	**0.91**	0.76	0.72*	**1.34**	1.19	01.16*
IFOF	L	**380.55**	403.52	415.33	**0.89**	0.83	0.82	**0.68**	0.64	0.62	**1.30**	1.23	1.23
IFOF	R	**380.37**	402.05	425.34	**0.89**	0.84	0.82*	**0.70**	0.64	0.61	**1.31**	1.24	1.24*
ILF	L	373.10	383.60	388.35	**0.86**	0.83	0.82	**0.67**	0.64	0.63	**1.25**	1.21	1.19
ILF	R	382.13	389.16	403.75	**0.86**	0.83	0.82	**0.67**	0.64	0.62	**1.27**	1.22	1.20*
SLF	L	310.14	327.78	330.49	**0.84**	0.80	0.79	**0.69**	0.65	0.65	**1.16**	1.12	1.11
SLF	R	309.32	325.56	330.63	**0.84**	0.80	0.79	**0.70**	0.65	0.65	**1.17**	1.12	1.12
UF	L	**294.48**	329.90	355.41	**0.95**	0.83	0.82*	**0.79**	0.68	0.65*	**1.29**	1.17	1.17*
UF	R	**282.49**	323.75	338.02	**0.98**	0.85	0.84*	**0.83**	0.69	0.68*	**1.33**	1.19	1.19*

FMi	n/a	**319.98**	387.77	421.05	**0.96**	0.85	0.82*	**0.78**	0.66	0.62*	**1.30**	1.23	1.23
FMa	n/a	383.12	372.15	399.79	0.83	0.83	0.80	0.64	0.64	0.61	1.30	1.30	1.29

FA = fractional anisotropy, MD = mean diffusivity, RD=radial diffusivity, AxD=axial diffusivity, WM=white matter, bvFTD = behavioural variant frontotemporal dementia , AD=Alzheimer's disease, ATR = anterior thalamic radiation, CGC = cingulum (cingulate), CGH = cingulum (hippocampal), IFOF = inferior fronto-occipital fasciculus, ILF = inferior longitudinal fasciculus, SLF = superior longitudinal fasciculus, UF = uncinate fasciculus, FMi = forceps minor, FMa = forceps major, L= left, R=right.
*=Unequal variance, significance tested with Welch-ANOVA.
Vs other patient group$_{p<0.05}$
Vs controls$_{p<0.05}$

Table 4. Mean FA (x10^{-3}), MD (x10^{-3}), RD (x10^{-3}), AxD (x10^{-3}) for each WM tract, for bvFTD and AD at T1.

WM tract	L/R	FA		MD		RD		AxD	
		BvFTD	AD	BvFTD	AD	BvFTD	AD	BvFTD	AD
ATR	L	341.44	341.57	0.92	0.86	0.74	0.69	1.33	1.24
ATR	R	309.17	328.47	0.96	0.87	0. 79	0.71	1.37	1.23
CGC	L	392.49	443.31	0.88	0.82	excluded	excluded	1.28	1.22*
CGC	R	346.15	396.49	0.88	0.82	0.71	0.63	1.24	1.19
CGH	L	246.78	240.96	0.96	0.90	0. 82	0.78	1.27	1.20
CGH	R	220.07	248.85	1.03	0.97	0. 91	0.81*	1.31	1.33
IFOF	L	370.40	407.22	0.91	0.85	0.71	0.64	1.32	1.26*
IFOF	R	311.60	403.42*	0.88	0.85	0.67	0.65	1.30	1.26
ILF	L	357.26	383.46	0.90	0.85	0.71	0.65	1.28	1.23*
ILF	R	371.54	384.99	0.87	0.84	0.68	0.66	1.27	1.23
SLF	L	310.15	325.04	0.87	0.83	0.72	0.68	1.19	1.17
SLF	R	306.60	325.68	0.90	0.84	0.75	0.68	1.26	1.18
UF	L	271.33	323.24	1.03	0.90	0.87	0.73	1.35	1.25
UF	R	262.51	317.80*	1.16	0.87*	1.00	0.71*	1.53	1.21*
FMI	n/a	331.97	376.31	0.92	0.87	0.74	0.66	1.36	1.35
FMA	n/a	285.17	378.20	1.20	0.92	1.02	0.71	1.54	1.33

FA = fractional anisotropy, MD = mean diffusivity, RD=radial diffusivity, AxD=axial diffusivity, WM=white matter, bvFTD = behavioural variant frontotemporal dementia , AD=Alzheimer's disease, ATR = anterior thalamic radiation, CGC = cingulum (cingulate), CGH = cingulum (hippocampal), IFOF = inferior fronto-occipital fasciculus, ILF = inferior longitudinal fasciculus, SLF = superior longitudinal fasciculus, UF = uncinate fasciculus, FMi = forceps minor, FMa = forceps major, L= left, R=right.
*=Unequal variance, significance tested with Welch-ANOVA.
Vs other patient group$_{p<0.05}$

Table 5. Mean difference score (T1 minus T0) of FA ($x10^{-3}$), MD ($x10^{-3}$), RD ($x10^{-3}$), AxD ($x10^{-3}$)for each WM tract, for bvFTD and AD.

WM tract	L/R	FA		MD		RD		AxD	
		BvFTD	AD	BvFTD	AD	BvFTD	AD	BvFTD	AD
ATR	L	9.80	8.75	0.03	0.03	0.02	0.02	0.05	0.05
ATR	R	-9.84	5.81	0.02	0.04	0.03	0.02	0.03	0.06
CGC	L	-5.59	20.23	0.01	0.01	0.01	0.0003	0.002	0.01
CGC	R	-29.77	10.44	0.02	0.01	0.03	0.001	-0.002	0.01*
CGH	L	13.84	-19.95	0.03	0.01	0.02	0.01	0.04	-0.003
CGH	R	-5.78	-1.84	0.03	0.08	0.04	0.05	0.02	0.14
IFOF	L	-5.42	-3.17	0.01	0.01	0.02	0.01	0.02	0.02
IFOF	R	-73.01	-4.87*	-0.003	0.01	-0.01	0.01	-0.008	0.02
ILF	L	-12.86	-1.62	0.03	0.01*	0.03	0.01	0.04	0.02*
ILF	R	-13.69	-8.00	0.01	0.01	0.02	0.01	0.01	0.01
SLF	L	1.28	-3.97	0.03	0.03	0.03	0.03	0.04	0.05
SLF	R	6.20	-2.72	0.04	0.05	0.02	0.04	0.07	0.06
UF	L	-25.28	-12.54	0.09	0.07	0.10	0.06	0.08	0.07
UF	R	-13.80	-10.44	0.15	0.02*	0.15	0.02*	0.17	0.02*
FMa	n/a	-37.71	-3.78*	0.08	0.04	0.09	0.03*	0.04	0.06
FMi	n/a	-30.22	-13.49	0.23	0.07	0.23	0.06	0.24	0.10

FA = fractional anisotropy, MD = mean diffusivity, RD=radial diffusivity, AxD=axial diffusivity, WM=white matter, bvFTD = behavioural variant frontotemporal dementia , AD=Alzheimer's disease, ATR = anterior thalamic radiation, CGC = cingulum (cingulate), CGH = cingulum (hippocampal), IFOF = inferior fronto-occipital fasciculus, ILF = inferior longitudinal fasciculus, SLF = superior longitudinal fasciculus, UF = uncinate fasciculus, FMi = forceps minor, FMa = forceps major, L= left, R=right.
*=Unequal variance, significance tested with Welch-ANOVA.
Vs other patient group$_{p<0.05}$

tudinal fasciculus, and *right* hippocampal cingulum. Lower FA in bvFTD compared with AD was additionally observed in the *left* hippocampal cingulum. Further, bvFTD in comparison with AD showed higher MD and RD in the *bilateral* cingulate cingulum, and higher AxD in the *right* cingulate cingulum.

3.3.2 Follow-up (T1)

BvFTD in comparison with AD (Table 4) showed lower FA and higher MD and RD in the *right* cingulate cingulum and *left* inferior fronto-occipital fasciculus. Additionally, higher MD in bvFTD compared with AD was observed in the *left* cingulate cingulum and lower FA in the *left* uncinate fasciculus, and forceps minor. No differences were observed in AxD.

3.3.3 Rate of change

The rate of change (Table 5) of FA in the cingulum was different between bvFTD and AD. Specifically, the rate of change of FA in the *right* cingulate cingulum was higher in bvFTD compared with a lower change in AD, whereas the rate of change of FA in the *left* hippocampal cingulate was lower in bvFTD compared with a higher change in AD. Additionally, the rate of change of AxD in the *right* inferior fronto-occipital fasciculus was also different between bvFTD and AD, namely it was lower in bvFTD compared with higher in AD.

3.4 Functional connectivity

DMN functional connectivity was not significant for each group at T0 (Figure 1) and at T1 (Figure 2). Between-group differences in functional connectivity of the DMN at T0 (Figure 1) or at T1 (Figure 2) were also not significant.

As groups did not differ in DMN functional connectivity at both T0 and T1, added value and/or sensitivity of the rate of change analysis was not expected and consequently it was not performed.

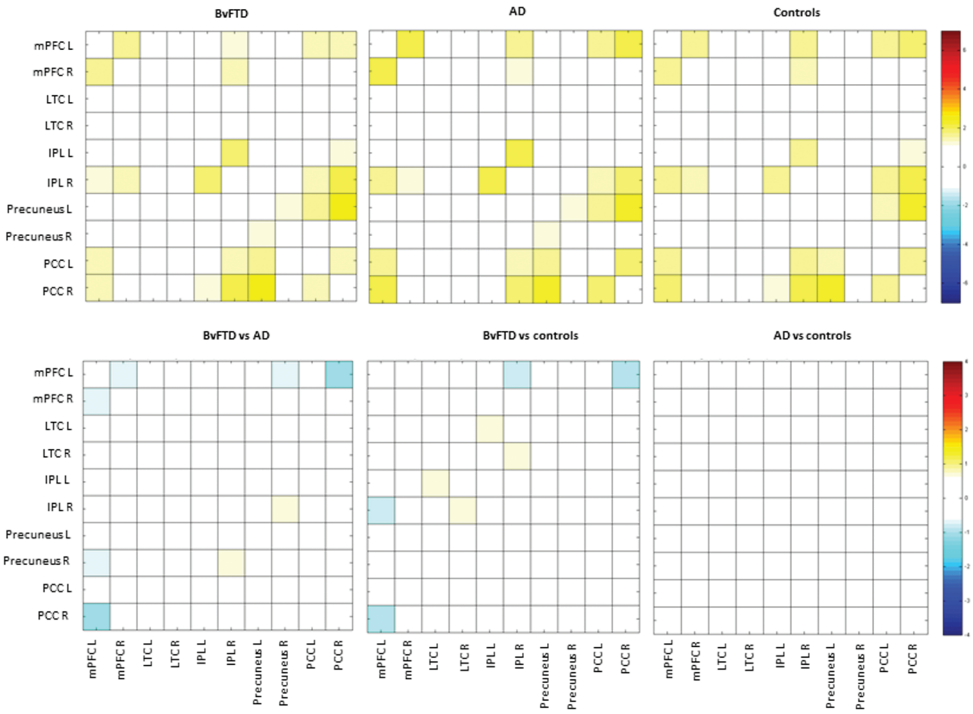

Figure 1. Non-significant default mode network (DMN) connectivity (p>0.05; $FWE_{corrected}$) at baseline (T0). DMN functional connectivity for behavioural variant frontotemporal dementia (bvFTD), Alzheimer's disease (AD) and healthy controls is shown in row one. Between-group differences for DMN functional connectivity are shown in row two. Colours represent the t-values of between-region functional connectivity.

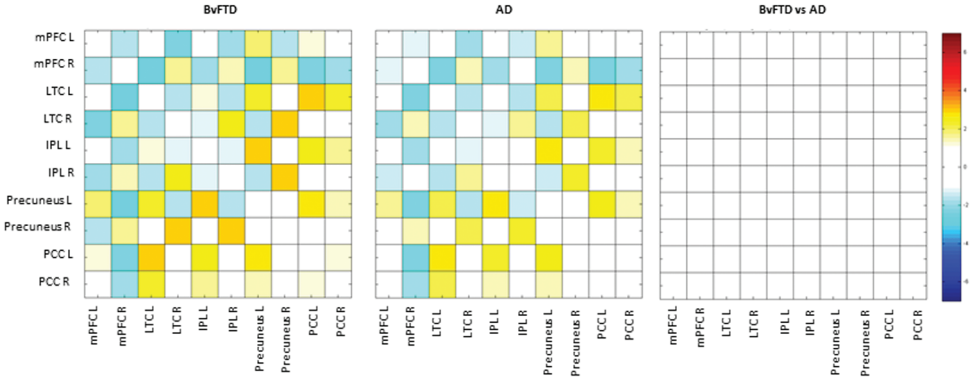

Figure 2. Non-significant default mode network (DMN) connectivity (p>0.05; $FWE_{corrected}$) at follow-up (T1). DMN functional connectivity for behavioural variant frontotemporal dementia (bvFTD) and Alzheimer's disease (AD) is shown in column one and two respectively. Between-group comparison for DMN functional connectivity is shown in column three. Colours represent the t-values of between-region functional connectivity.

4. DISCUSSION

In this study we observed that quantitative tract-specific microstructural WM abnormalities, but not quantitative functional DMN connectivity, may aid differential diagnosis of bvFTD and AD. Tract-specific microstructural WM abnormalities were observed in several WM tracts in bvFTD, whereas they were only seen regionally in AD. At follow-up, differences in tract-specific microstructural WM abnormalities between bvFTD and AD became less pronounced , although they were still stronger in bvFTD. Despite the diminished differences, the rate of changes was very similar between bvFTD and AD.

Quantitative microstructural WM abnormalities were seen in bvFTD and AD in different WM tracts, suggesting a differential diagnostic role for assessing diffusion values in a clinical context. Tract-specific WM microstructural abnormalities were evident in bvFTD in all WM tracts investigated, but most pronounced in the forceps minor, hippocampal cingulum, cingulate cingulum, inferior fronto-occipital and uncinate fasciculus. These WM tracts have been associated with cognitive domains characteristically affected in bvFTD [42], namely the forceps minor with disinhibition and executive functioning [29,43], the hippocampal cingulum with memory and executive functioning [44–46], the cingulate cingulum with cognitive control [47], the inferior fronto-occipital fasciculus with social cognition and emotional functioning [48–51], and the uncinate fasciculus with apathy, disinhibition and behavioural dyscontrol [29,52–54]. Unsurprisingly, WM abnormalities were not observed in the forceps major, a posterior WM tract associated with visuospatial functioning, such as perceptual speed and topographical orientation [55,56], a domain generally preserved in bvFTD [57,58].

Microstructural WM abnormalities in bvFTD were evident in comparison with both AD and healthy participants, but even more pronounced in comparison with the latter. This smaller difference between bvFTD and AD suggests that microstructural WM abnormalities, although to a much lesser extent, are also present in AD. The subtle microstructural WM abnormalities observed in the hippocampal cingulum only in AD compared to controls suggests an important implication of this WM structure in AD. The hippocampal cingulum has been associated with memory functioning [45,59], which is characteristically impaired in AD [60].

Thus, for the differentiation between early-stage AD and bvFTD, microstructural WM abnormalities of the hippocampal cingulum in absence of other WM tract changes is indicative of AD, whereas widespread, mostly anterior, WM mi-

crostructure abnormalities (e.g. uncinate fasciculus, hippocampal and cingulate cingulum, forceps minor) is indicative of bvFTD.

At follow-up, microstructural WM abnormalities were also more pronounced in bvFTD than in AD, mainly in the *left* inferior fronto-occipital fasciculus and *right* cingulate cingulum, and also in the *left* uncinate fasciculus and the forceps minor. These specific WM tracts may be important for differentiating between bvFTD and AD in later stages, as microstructural WM abnormalities of other WM tracts were no longer different between bvFTD and AD upon follow-up.

Cingulum involvement is in line with previous literature showing classification of bvFTD and controls to be best achieved using FA in the cingulum bundle [61]. Why it is the *right* cingulum that seems to be differentially affected is not entirely clear. Functional differentiation between the left and right cingulate cingulum has not been extensively investigated. One study has associated the *right* cingulate cingulum with visual working memory in bvFTD [27], but this finding should be interpreted with caution as previous research [62] has pointed out methodological issues concerning the task used to measure visual working memory, and consequently this task has been discarded by the manufacturer (*http://www.pearsonclinical.com/psychology/products/100000281/wechsler-memory-scale--fourth-edition-wms-iv.html#tab-details*). Another study has associated the right cingulate cingulum with cognitive control (e.g. problem solving, reasoning, behavioural flexibility) in MCI [47]. A possible explanation may be that cognitive control in bvFTD is more affected than in AD.

The inferior fronto-occipital fasciculus has been associated with a variety of cognitive domains, such as visual spatial information processing [63], emotion recognition [51], executive functioning [46,64], and psychiatric symptoms [65]. The *left* inferior fronto-occipital fasciculus has been specifically associated with language [66], processing speed and verbal/visual learning [67], and psychosis [68]. Many of these cognitive domains have been associated with bvFTD [69–71]. Although to our knowledge a direct association between the inferior fronto-occipital fasciculus and cognitive/behavioural performance in bvFTD has not been previously reported, our finding suggests there may be a link between bvFTD symptomatology and the observed abnormalities in this WM tract.

The uncinate fasciculus and forceps minor are both known to play an important role in bvFTD and are associated with characteristic bvFTD symptoms [29,43,52,54], such as disinhibition and executive dysfunctioning [3]. However, both the uncinate fasciculus and forceps minor have also been implicated in AD [45,72], which may explain why the differences in WM microstructure between

AD and bvFTD were not as pronounced (decreased FA only) as in the inferior fronto-occipital fasciculus.

Taken together, differences in WM microstructure between bvFTD and AD seem to be diminished at one year follow-up. This may be explained by the fact that with advancing of the AD disease process, WM microstructure changes more rapidly. Some studies have shown longitudinal microstructural WM changes in AD [73–75], and in bvFTD [61], but to our knowledge none has compared the rate of change of longitudinal abnormalities between AD and bvFTD. The rate of change in this study, in terms of the difference in diffusivity abnormalities between baseline and follow-up, showed a faster decline in WM microstructure of the *right* cingulate cingulum in bvFTD, and the *left* hippocampal cingulum and *right* inferior fronto-occipital fasciculus in AD. First, in line with changes at follow-up observed in this study and previous literature [61], these rates of changes may suggest a differential involvement of the cingulum, in which the anterior part is more affected in bvFTD and the posterior part in AD. This is supported by the macrostructural frontotemporal (anterior) and temporoparietal (posterior) involvement in respectively bvFTD and AD [76,77]. Second, the *left* inferior fronto-occipital fasciculus showed more pronounced changes in bvFTD at follow-up, and the *right* inferior fronto-occipital fasciculus showed a faster rate of change in AD, suggesting a differential hemispheric involvement for these two neurodegenerative disorders. However, whether the left and right inferior fronto-occipital fasciculus are associated with different, potentially disease-specific, symptomatology remains speculative. As described above, the inferior fronto-occipital fasciculus has been associated with many different cognitive functions but has as yet not been specifically linked to AD or bvFTD. However, our results suggest that such a link between the left inferior fronto-occipital fasciculus and bvFTD, and the right inferior fronto-occipital fasciculus and AD, may be present.

MD and RD differences between bvFTD and AD were most pronounced and thus seem more sensitive for early-stage differentiation of AD and bvFTD than FA and AxD. This suggest that myelin abnormalities are more pronounced in the early stages of bvFTD, as RD is thought to represent myelin damage [78], AxD axonal loss [79], and MD and FA a combination of these measures. At follow-up, AD and bvFTD could be best differentiated by FA, although differences in MD and RD were also evident. This again suggests that myelin changes are more pronounced in bvFTD than in AD, which is also supported by the absence of AxD differences at follow-up. Axonal abnormalities may develop to a similar extent in later stages of AD and bvFTD. Overall, however, differences in FA, MD and RD were diminished at follow-up, suggesting that myelin changes may also develop in AD, similar to bvFTD. In conclusion - in line with previous literature [16,61] - it is recommended

to use FA, MD and RD to differentiate between AD and bvFTD, but not AxD as this is less different between groups.

Functional DMN connectivity between AD and bvFTD was not different in our quantitative approach. Previous literature comparing AD and bvFTD observed differences in regions of the DMN using whole-brain independent component analysis [18,80–82], such as increased parietal DMN connectivity in bvFTD and decreased parietal DMN connectivity in AD. However, in this study we aimed to assess a different approach that may be used clinically, i.e. a quantitative measure of functional connectivity between DMN regions. The small sample size of this study, and thus low power, may have left possible group effects undetected. However, clinical use warrants sensitivity of measures at an individual patient level, hence a low sensitivity of quantitative functional DMN connectivity does not seem suitable for individual diagnostics.

This study knows some limitations. First, the small sample size limits interpretation of results and may particularly lead to underestimation of between-group differences. However, the findings of this study are in line with the literature and may indicate clinical utility of DTI, but not rs-fMRI, on an individual patient level. Second, sample size was smaller at follow-up than at baseline due to patients who were too ill to return for follow-up. This may have induced an underappreciation of long-term abnormality severity and rate of change differences.

In conclusion, quantitative tract-specific microstructural WM abnormalities, but not quantitative functional connectivity of the DMN, may aid differential diagnosis of bvFTD and AD at early-stage and in the longer-term. Specifically, pronounced microstructural WM changes in anterior WM tracts, in particular the *right* cingulate cingulum and *left* inferior fronto-occipital fasciculus, may differentiate bvFTD from AD, and microstructural WM abnormalities of the hippocampal cingulum, in absence of other microstructural WM changes, may differentiate AD from bvFTD.

REFERENCES

1 Greicius MD, Geschwind MD, Miller BL. Presenile dementia syndromes: an update on taxonomy and diagnosis. *J Neurol Neurosurg Psychiatry* 2002;72:691–700.http://www.ncbi.nlm.nih.gov/pubmed/12023408

2 McKhann GM, Knopman DS, Chertkow H, *et al.* The diagnosis of dementia due to Alzheimer's disease: recommendations from the National Institute on Aging-Alzheimer's Association workgroups on diagnostic guidelines for Alzheimer's disease. *Alzheimers Dement* 2011;7:263–9. doi:10.1016/j.jalz.2011.03.005

3 Rascovsky K, Hodges JR, Knopman D, *et al.* Sensitivity of revised diagnostic criteria for the behavioural variant of frontotemporal dementia. *Brain* 2011;134:2456–77. doi:10.1093/brain/awr179

4 Neary D, Snowden JS, Northen B, *et al.* Dementia of frontal lobe type. *J Neurol Neurosurg Psychiatry* 1988;51:353–61.http://www.ncbi.nlm.nih.gov/pubmed/3258902

5 Bathgate D, Snowden JS, Varma A, *et al.* Behaviour in frontotemporal dementia, Alzheimer's disease and vascular dementia. *Acta Neurol Scand* 2001;103:367–78.http://www.ncbi.nlm.nih.gov/pubmed/11421849

6 Hallam BJ, Silverberg ND, Lamarre AK, *et al.* Clinical presentation of prodromal frontotemporal dementia. *Am J Alzheimers Dis Other Demen* 2007;22:456–67. doi:10.1177/1533317507308781

7 Varma AR, Snowden JS, Lloyd JJ, *et al.* Evaluation of the NINCDS-ADRDA criteria in the differentiation of Alzheimer's disease and frontotemporal dementia. *J Neurol Neurosurg Psychiatry* 1999;66:184–8.http://www.ncbi.nlm.nih.gov/pubmed/10071097

8 Jenner C, Reali G, Puopolo M, *et al.* Can cognitive and behavioural disorders differentiate frontal variant-frontotemporal dementia from Alzheimer's disease at early stages? *Behav Neurol* 2006;17:89–95.http://www.ncbi.nlm.nih.gov/pubmed/16873919

9 Gregory CA, Serra-Mestres J, Hodges JR. Early diagnosis of the frontal variant of frontotemporal dementia: how sensitive are standard neuroimaging and neuropsychologic tests? *Neuropsychiatry Neuropsychol Behav Neurol* 1999;12:128–35.http://www.ncbi.nlm.nih.gov/pubmed/10223261

10 Kipps CM, Davies RR, Mitchell J, *et al.* Clinical significance of lobar atrophy in frontotemporal dementia: application of an MRI visual rating scale. *Dement Geriatr Cogn Disord* 2007;23:334–42. doi:10.1159/000100973

11 Rosso SM, Heutink P, Tibben A, *et al.* [New insights in frontotemporal dementia]. *Ned Tijdschr Geneeskd* 2000;144:1575–80.http://www.ncbi.nlm.nih.gov/pubmed/10965365

12 Sperling RA, Aisen PS, Beckett LA, *et al.* Toward defining the preclinical stages of Alzheimer's disease: Recommendations from the National Institute on Aging-Alzheimer's Association workgroups on diagnostic guidelines for Alzheimer's disease. *Alzheimer's Dement* 2011;7:280–92. doi:10.1016/j.jalz.2011.03.003

13 Zhang Y, Schuff N, Ching C, *et al.* Joint assessment of structural, perfusion, and diffusion MRI in Alzheimer's disease and frontotemporal dementia. *Int J Alzheimers Dis* 2011;2011:546871. doi:10.4061/2011/546871

14 Zhang Y, Schuff N, Du A-T, *et al.* White matter damage in frontotemporal dementia and Alzheimer's disease measured by diffusion MRI. *Brain* 2009;132:2579–92. doi:10.1093/brain/awp071

15 Daianu M, Mendez MF, Baboyan VG, *et al.* An advanced white matter tract analysis in frontotemporal dementia and early-onset Alzheimer's disease. *Brain Imaging Behav* Published Online First: 29 October 2015. doi:10.1007/s11682-015-9458-5

16 Mahoney CJ, Ridgway GR, Malone IB, *et al.* Profiles of white matter tract pathology in frontotemporal dementia. *Hum Brain Mapp* 2014;35:4163–79. doi:10.1002/hbm.22468

17 Lu PH, Lee GJ, Shapira J, *et al.* Regional differences in white matter breakdown between frontotemporal dementia and early-onset Alzheimer's disease. *J Alzheimers Dis* 2014;39:261–9. doi:10.3233/JAD-131481

18 Zhou J, Greicius MD, Gennatas ED, *et al.* Divergent network connectivity changes in behavioural variant frontotemporal dementia and Alzheimer's disease. *Brain* 2010;133:1352–67. doi:10.1093/brain/awq075

19 Folstein MF, Folstein SE, McHugh PR. 'Mini-mental state'. A practical method for grading the cognitive state of patients for the clinician. *J Psychiatr Res* 1975;12:189–98.http://www.ncbi.nlm.nih.gov/pubmed/1202204.

20 Bron EE, Steketee RME, Houston GC, *et al.* Diagnostic classification of arterial spin labeling and structural MRI in presenile early stage dementia. *Hum Brain Mapp* 2014;35:4916–31. doi:10.1002/hbm.22522

21 Jenkinson M, Beckmann CF, Behrens TEJ, *et al.* FSL. *Neuroimage* 2012;62:782–90. doi:10.1016/j.neuroimage.2011.09.015

22 Woolrich MW, Jbabdi S, Patenaude B, *et al.* Bayesian analysis of neuroimaging data in FSL. *Neuroimage* 2009;45:S173–86. doi:10.1016/j.neuroimage.2008.10.055

23 Smith SM, Jenkinson M, Woolrich MW, *et al.* Advances in functional and structural MR image analysis and implementation as FSL. *Neuroimage* 2004;23 Suppl 1:S208–19. doi:10.1016/j.neuroimage.2004.07.051

24 Smith SM. Fast robust automated brain extraction. *Hum Brain Mapp* 2002;17:143–55. doi:10.1002/hbm.10062

25 Duering M, Gonik M, Malik R, *et al.* Identification of a strategic brain network underlying processing speed deficits in vascular cognitive impairment. *Neuroimage* 2013;66:177–83. doi:10.1016/j.neuroimage.2012.10.084

26 Torso M, Serra L, Giulietti G, *et al.* Strategic lesions in the anterior thalamic radiation and apathy in early Alzheimer's disease. *PLoS One* 2015;10:e0124998. doi:10.1371/journal.pone.0124998

27 Tartaglia MC, Zhang Y, Racine C, *et al.* Executive dysfunction in frontotemporal dementia is related to abnormalities in frontal white matter tracts. *J Neurol* 2012;259:1071–80. doi:10.1007/s00415-011-6300-x

28 Staff RT, Murray AD, Deary IJ, *et al.* Generality and specificity in cognitive aging: a volumetric brain analysis. *Neuroimage* 2006;30:1433–40. doi:10.1016/j.neuroimage.2005.11.004

29 Hornberger M, Geng J, Hodges JR. Convergent grey and white matter evidence of orbitofrontal cortex changes related to disinhibition in behavioural variant frontotemporal dementia. *Brain* 2011;134:2502–12. doi:10.1093/brain/awr173

30 Shollenbarger SG, Price J, Wieser J, *et al.* Poorer frontolimbic white matter integrity is associated with chronic cannabis use, FAAH genotype, and increased depressive and apathy symptoms in adolescents and young adults. *NeuroImage Clin* 2015;8:117–25. doi:10.1016/j.nicl.2015.03.024

31 Epstein KA, Cullen KR, Mueller BA, *et al.* White matter abnormalities and cognitive impairment in early-onset schizophrenia-spectrum disorders. *J Am Acad Child Adolesc Psychiatry* 2014;53:362–72.e1–2. doi:10.1016/j.jaac.2013.12.007

32 Gold BT, Johnson NF, Powell DK, *et al.* White matter integrity and vulnerability to Alzheimer's disease: preliminary findings and future directions. *Biochim Biophys Acta* 2012;1822:416–22. doi:10.1016/j.bbadis.2011.07.009

33 Mike A, Strammer E, Aradi M, *et al.* Disconnection mechanism and regional cortical atrophy contribute to impaired processing of facial expressions and theory of mind in multiple sclerosis: a structural MRI study. *PLoS One* 2013;8:e82422. doi:10.1371/journal.pone.0082422

34 Sarubbo S, De Benedictis A, Merler S, *et al.* Towards a functional atlas of human white matter. *Hum Brain Mapp* 2015;36:3117–36. doi:10.1002/hbm.22832

35 Borroni B, Brambati SM, Agosti C, *et al.* Evidence of white matter changes on diffusion tensor imaging in frontotemporal dementia. *Arch Neurol* 2007;64:246–51. doi:10.1001/archneur.64.2.246

36 de Groot M, Vernooij MW, Klein S, *et al.* Improving alignment in Tract-based spatial statistics: evaluation and optimization of image registration. *Neuroimage* 2013;76:400–11. doi:10.1016/j.neuroimage.2013.03.015

37 Behrens TEJ, Woolrich MW, Jenkinson M, *et al.* Characterization and propagation of uncertainty in diffusion-weighted MR imaging. *Magn Reson Med* 2003;50:1077–88. doi:10.1002/mrm.10609

38 Behrens TEJ, Berg HJ, Jbabdi S, *et al.* Probabilistic diffusion tractography with multiple fibre orientations: What can we gain? *Neuroimage* 2007;34:144–55. doi:10.1016/j.neuroimage.2006.09.018

39 Hammers A, Allom R, Koepp MJ, *et al.* Three-dimensional maximum probability atlas of the human brain, with particular reference to the temporal lobe. *Hum Brain Mapp* 2003;19:224–47. doi:10.1002/hbm.10123

40 Ebisch SJH, Gallese V, Willems RM, *et al.* Altered intrinsic functional connectivity of anterior and posterior insula regions in high-functioning participants with autism spectrum disorder. *Hum Brain Mapp* 2011;32:1013–28. doi:10.1002/hbm.21085

41 Verly M, Verhoeven J, Zink I, *et al.* Altered functional connectivity of the language network in ASD: Role of classical language areas and cerebellum. *NeuroImage Clin* 2014;4:374–82. doi:10.1016/j.nicl.2014.01.008

42 Rascovsky K, Hodges JR, Knopman D, *et al.* Sensitivity of revised diagnostic criteria for the behavioural variant of frontotemporal dementia. *Brain* 2011;134:2456–77. doi:10.1093/brain/awr179

43 Pérez-Iglesias R, Tordesillas-Gutiérrez D, McGuire PK, *et al.* White Matter Integrity and Cognitive Impairment in First-Episode Psychosis. *Am J Psychiatry* 2010;167:451–8. doi:10.1176/appi.ajp.2009.09050716

44 Li W, Muftuler LT, Chen G, *et al.* Effects of the coexistence of late-life depression and mild cognitive impairment on white matter microstructure. *J Neurol Sci* 2014;338:46–56. doi:10.1016/j.jns.2013.12.016

45 Irish M, Hornberger M, El Wahsh S, *et al.* Grey and white matter correlates of recent and remote autobiographical memory retrieval--insights from the dementias. *PLoS One* 2014;9:e113081. doi:10.1371/journal.pone.0113081

46 Santiago C, Herrmann N, Swardfager W, *et al.* White Matter Microstructural Integrity Is Associated with Executive Function and Processing Speed in Older Adults with Coronary Artery Disease. *Am J Geriatr Psychiatry* 2015;23:754–63. doi:10.1016/j.jagp.2014.09.008

47 Metzler-Baddeley C, Jones DK, Steventon J, *et al.* Cingulum microstructure predicts cognitive control in older age and mild cognitive impairment. *J Neurosci* 2012;32:17612–9. doi:10.1523/JNEUROSCI.3299-12.2012

48 Jalbrzikowski M, Villalon-Reina JE, Karlsgodt KH, *et al.* Altered white matter microstructure is associated with social cognition and psychotic symptoms in 22q11.2 microdeletion syndrome. *Front Behav Neurosci* 2014;8:393. doi:10.3389/fnbeh.2014.00393

49 Schmidt AT, Hanten G, Li X, *et al.* Emotional prosody and diffusion tensor imaging in children after traumatic brain injury. *Brain Inj* 2013;27:1528–35. doi:10.3109/02699052.2013.828851

50 Taddei M, Tettamanti M, Zanoni A, *et al.* Brain white matter organisation in adolescence is related to childhood cerebral responses to facial expressions and harm avoidance. *Neuroimage* 2012;61:1394–401. doi:10.1016/j.neuroimage.2012.03.062

51 Crespi C, Cerami C, Dodich A, *et al.* Microstructural white matter correlates of emotion recognition impairment in Amyotrophic Lateral Sclerosis. *Cortex* 2014;53:1–8. doi:10.1016/j.cortex.2014.01.002

52 Powers JP, Massimo L, McMillan CT, *et al.* White Matter Disease Contributes to Apathy and Disinhibition in Behavioral Variant Frontotemporal Dementia. *Cogn Behav Neurol* 2014;27:206–14. doi:10.1097/WNN.0000000000000044

53 Agosta F, Henry RG, Migliaccio R, *et al.* Language networks in semantic dementia. *Brain* 2010;133:286–99. doi:10.1093/brain/awp233

54 Whitwell JL, Avula R, Senjem ML, *et al.* Gray and white matter water diffusion in the syndromic variants of frontotemporal dementia. *Neurology* 2010;74:1279–87. doi:10.1212/WNL.0b013e3181d9edde

55 Laukka EJ, Lövdén M, Kalpouzos G, *et al.* Microstructural White Matter Properties Mediate the Association between APOE and Perceptual Speed in Very Old Persons without Dementia. *PLoS One* 2015;10:e0134766. doi:10.1371/journal.pone.0134766

56 Tamura I, Kitagawa M, Otsuki M, *et al.* Pure Topographical Disorientation Following a Right Forceps Major of the Splenium Lesion: A Case Study. *Neurocase* 2007;13:178–84. doi:10.1080/13554790701448812

57 Floris G, Borghero G, Cannas A, *et al.* Constructional apraxia in frontotemporal dementia associated with the C9orf72 mutation: broadening the clinical and neuropsychological phenotype. *Amyotroph Lateral Scler Frontotemporal Degener* 2015;16:8–15. doi:10.3109/21678421.2014.959450

58 Laforce R. Behavioral and language variants of frontotemporal dementia: a review of key symptoms. *Clin Neurol Neurosurg* 2013;115:2405–10.http://www.ncbi.nlm.nih.gov/pubmed/24446563

59 Bozzali M, Giulietti G, Basile B, *et al.* Damage to the cingulum contributes to Alzheimer's disease pathophysiology by deafferentation mechanism. *Hum Brain Mapp* 2012;33:1295–308. doi:10.1002/hbm.21287

60 Dubois B, Feldman HH, Jacova C, *et al.* Revising the definition of Alzheimer's disease: a new lexicon. *Lancet Neurol* 2010;9:1118–27. doi:10.1016/S1474-4422(10)70223-4

61 Mahoney CJ, Simpson IJA, Nicholas JM, *et al.* Longitudinal diffusion tensor imaging in frontotemporal dementia. *Ann Neurol* 2015;77:33–46. doi:10.1002/ana.24296

62 Wilde N, Strauss E. Functional equivalence of WAIS-III/WMS-III digit and spatial span under forward and backward recall conditions. *Clin Neuropsychol* 2002;16:322–30. doi:10.1076/clin.16.3.322.13858

63 Schmahmann JD, Smith EE, Eichler FS, *et al.* Cerebral White Matter. *Ann N Y Acad Sci* 2008;1142:266–309. doi:10.1196/annals.1444.017

64 Sun X, Liang Y, Wang J, *et al.* Early frontal structural and functional changes in mild white matter lesions relevant to cognitive decline. *J Alzheimers Dis* 2014;40:123–34. doi:10.3233/JAD-131709

65 DeRosse P, Nitzburg GC, Ikuta T, *et al.* Evidence from structural and diffusion tensor imaging for frontotemporal deficits in psychometric schizotypy. *Schizophr Bull* 2015;41:104–14. doi:10.1093/schbul/sbu150

66 Almairac F, Herbet G, Moritz-Gasser S, *et al.* The left inferior fronto-occipital fasciculus subserves language semantics: a multilevel lesion study. *Brain Struct Funct* 2015;220:1983–95. doi:10.1007/s00429-014-0773-1

67 Liu X, Lai Y, Wang X, *et al.* Reduced white matter integrity and cognitive deficit in never-medicated chronic schizophrenia: a diffusion tensor study using TBSS. *Behav Brain Res* 2013;252:157–63. doi:10.1016/j.bbr.2013.05.061

68 Walterfang M, McGuire PK, Yung AR, *et al.* White matter volume changes in people who develop psychosis. *Br J Psychiatry* 2008;193:210–5. doi:10.1192/bjp.bp.107.043463

69 Tartaglia MC, Zhang Y, Racine C, *et al.* Executive dysfunction in frontotemporal dementia is related to abnormalities in frontal white matter tracts. *J Neurol* 2012;259:1071–80. doi:10.1007/s00415-011-6300-x

70 Balconi M, Cotelli M, Brambilla M, *et al.* Understanding Emotions in Frontotemporal Dementia: The Explicit and Implicit Emotional Cue Mismatch. *J Alzheimers Dis* 2015;46:211–25. doi:10.3233/JAD-142826

71 Block NR, Sha SJ, Karydas AM, *et al.* Frontotemporal Dementia and Psychiatric Illness: Emerging Clinical and Biological Links in Gene Carriers. *Am J Geriatr Psychiatry* 2016;24:107–16. doi:10.1016/j.jagp.2015.04.007

72 Hiyoshi-Taniguchi K, Oishi N, Namiki C, *et al.* The Uncinate Fasciculus as a Predictor of Conversion from Amnestic Mild Cognitive Impairment to Alzheimer Disease. *J Neuroimaging*;25:748–53. doi:10.1111/jon.12196

73 Genc S, Steward CE, Malpas CB, *et al.* Short-term white matter alterations in Alzheimer's disease characterized by diffusion tensor imaging. *J Magn Reson Imaging* 2016;43:627–34. doi:10.1002/jmri.25017

74 Nowrangi MA, Lyketsos CG, Leoutsakos J-MS, *et al.* Longitudinal, region-specific course of diffusion tensor imaging measures in mild cognitive impairment and Alzheimer's disease. *Alzheimers Dement* 2013;9:519–28. doi:10.1016/j.jalz.2012.05.2186

75 Keihaninejad S, Zhang H, Ryan NS, *et al.* An unbiased longitudinal analysis framework for tracking white matter changes using diffusion tensor imaging with application to Alzheimer's disease. *Neuroimage* 2013;72:153–63. doi:10.1016/j.neuroimage.2013.01.044

76 Braak H, Braak E. Neuropathological stageing of Alzheimer-related changes. *Acta Neuropathol* 1991;82:239–59.http://www.ncbi.nlm.nih.gov/pubmed/1759558

77 Broe M, Hodges JR, Schofield E, *et al.* Staging disease severity in pathologically confirmed cases of frontotemporal dementia. *Neurology* 2003;60:1005–11. doi:10.1212/01.WNL.0000052685.09194.39

78 Song S-K, Sun S-W, Ramsbottom MJ, *et al.* Dysmyelination Revealed through MRI as Increased Radial (but Unchanged Axial) Diffusion of Water. *Neuroimage* 2002;17:1429–36. doi:10.1006/nimg.2002.1267

79 Song S-K, Sun S-W, Ju W-K, *et al.* Diffusion tensor imaging detects and differentiates axon and myelin degeneration in mouse optic nerve after retinal ischemia. *Neuroimage* 2003;20:1714–22. doi:10.1016/j.neuroimage.2003.07.005

80 Hafkemeijer A, Möller C, Dopper EGP, *et al.* Differences in structural covariance brain networks between behavioral variant frontotemporal dementia and Alzheimer's disease. *Hum Brain Mapp* 2016;37:978–88. doi:10.1002/hbm.23081

81 Hafkemeijer A, Möller C, Dopper EGP, *et al.* Resting state functional connectivity differences between behavioral variant frontotemporal dementia and Alzheimer's disease. *Front Hum Neurosci* 2015;9:474. doi:10.3389/fnhum.2015.00474

82 Filippi M, Agosta F, Scola E, *et al.* Functional network connectivity in the behavioral variant of frontotemporal dementia. *Cortex* 2013;49:2389–401. doi:10.1016/j.cortex.2012.09.017

83 Ikram MA, van der Lugt A, Niessen WJ, *et al.* The Rotterdam Scan Study: design update 2016 and main findings. *Eur J Epidemiol* 2015;30:1299–315. doi:10.1007/s10654-015-0105-7

84 de Groot M, Ikram MA, Akoudad S, *et al*. Tract-specific white matter degeneration in aging: The Rotterdam Study. *Alzheimer's Dement* 2015;11:321–30. doi:10.1016/j.jalz.2014.06.011

SUPPLEMENT

Supplemental Table 1. Tractography tract thresholds based on De Groot et al. (2015), but multiplied with a factor of eight due to the resolution difference.

White matter tract	Tractography threshold
Anterior thalamic radiation (ATR)	0.016
Cingulum (cingulate gyrus)	0.08
Cingulum (parahippocampal region)	0.16
Forceps major (FMa)	0.04
Forceps minor (FMi)	0.08
Inferior fronto-occipital fasciculus (IFOF)	0.08
Inferior longitudinal fasciculus (ILF)	0.04
Superior longitudinal fasciculus (SLF)	0.008
Uncinate fasciculus (UF)	0.08

Chapter 2.2

Concurrent white and grey matter degeneration of disease-specific networks in early-stage Alzheimer's disease and behavioural variant frontotemporal dementia

Rebecca M.E. Steketee*
Rozanna Meijboom*
Marius de Groot
Esther E. Bron
Wiro J. Niessen
Aad van der Lugt
John C. van Swieten
Marion Smits
** These authors contributed equally to this work*

Neurobiol Aging. 2016;43:119-28.

ABSTRACT

This study investigates regional coherence between white matter (WM) microstructure and grey matter (GM) volume and perfusion measures in Alzheimer's disease (AD) and behavioural variant frontotemporal dementia (bvFTD) using a correlational approach.

WM-GM coherence, compared with controls, was stronger between cingulum WM and frontotemporal GM in AD, and temporoparietal GM in bvFTD. Additionally, in AD compared with controls, coherence was stronger between inferior fronto-occipital fasciculus WM microstructure and occipital GM perfusion.

In this first study assessing regional WM-GM coherence in AD and bvFTD we show that WM microstructure and GM volume and perfusion measures are coherent, particularly in regions implicated in AD and bvFTD pathology. This indicates concurrent degeneration in disease-specific networks. Our methodology allows for the detection of incipient abnormalities that go undetected in conventional between-group analyses.

1. INTRODUCTION

Alzheimer's disease (AD) and behavioural variant frontotemporal dementia (bvFTD) are two common types of presenile dementia (onset ≤ 65 years) [1]. These diseases are characterised by distinct abnormalities in grey matter (GM) and white matter (WM), as measured with magnetic resonance imaging (MRI) [2–6]. Although regional relationships between GM volume and perfusion have been widely studied in AD and bvFTD [7–14], it is still largely unclear whether and how WM and GM abnormalities are related. One hypothesis is that WM and GM abnormalities develop in a Wallerian-like degenerative manner, in which GM cell death leads to degeneration of WM tracts connecting affected GM regions. Another possible mechanism is that WM degeneration occurs independently from GM volume loss and/or hypoperfusion [15]. However, since both diseases are characterised by specific WM and GM abnormalities, it is conceivable that these abnormalities do not occur in isolation, but that they co-occur in the context of a common disease process. Regionally concurrent degeneration would then be reflected in regional coherence of abnormalities in WM and GM.

Thus far, relationships between abnormalities in WM microstructure and GM volume have been found to be inconsistent in AD [16–20], whereas in bvFTD WM microstructural abnormalities have been consistently found to exceed GM volume loss [21–24]. One study looked at the relationship between WM microstructure, GM volume, and GM perfusion in AD and bvFTD [25], and confirmed that WM microstructure is more severely affected in bvFTD than in AD. Additionally, they confirmed that GM volume loss and WM microstructural abnormalities in bvFTD exceed GM hypoperfusion, whereas in AD the degree of (micro)structural abnormalities and GM hypoperfusion is similar. However, this study did not assess the spatial relationships between WM microstructure and GM measures. This precludes the demonstration of possible regional relationships between WM and GM abnormalities, which is of particular interest given their disease-specific regional distribution. One study [26] investigated the regional relationship between WM and GM abnormalities, but limited their investigation to temporoparietal WM-GM relationships in AD, hence leaving whole-brain regional coherence in both AD and bvFTD unexplored. In this study we aimed to establish whether there is coherence between regional abnormalities of WM microstructure and GM volume and perfusion in AD and in bvFTD. First, we assessed abnormalities of WM microstructure, GM volume and GM perfusion for each measure separately. Second, we correlated WM measures in affected tracts with volume and perfusion in the GM regions at either end of the tract.

2. METHODS

2.1 Participants

Patients were recruited at the Alzheimer Centre Southwest Netherlands and included in the analysis if they were clinically diagnosed with AD [27] or bvFTD [28], had an age of 45 to 70 years, and a Mini-Mental State Examination (MMSE [29]) score of ≥ 20. In our memory clinic it is common practice to screen for genetic mutations only in case of a positive family history for dementia. In the clinical sample of this study consisting of nine bvFTD patients, three patients were known to have a genetic mutation (two MAPT, one C9orf72).

Patient exclusion criteria were other causes of dementia, other neurological disorders, psychiatric diagnosis, contraindications for MRI, and expected loss to follow up within 1 year.

Healthy age and gender matched controls with an age between 45 and 70 years, and without psychiatric or neurological history, were recruited from patient peers and through advertisement.

Both patients and controls underwent a full neuropsychological assessment evaluating attention and concentration, executive functioning, memory, language, social cognition, and constructive and visuospatial skills and MMSE. The MMSE was assessed in controls after the MRI scan by the researcher.

The study was approved by the local medical ethics committee, and all participants gave written informed consent.

2.2 Image acquisition

Scanning was performed on a 3 tesla Discovery MR750 system (GE Healthcare, Milwaukee, WI, US).

2.2.1 Diffusion imaging

DTI was acquired with 25 non-collinear directions using a spin echo echo planar imaging (EPI) sequence and with full coverage of the supratentorial brain (echo time (TE) set to minimum with range 81.9ms-90.8ms, repetition time (TR) 7.9ms, voxel size 1.9x1.9x2.5mm^3 with a 240mm^2 field of view (FOV), array spatial sensitivity encoding technique (ASSET) acceleration factor 2, flip angle 90°, maximum b-value 1000 s/mm^2, 3 non-diffusion-weighted volumes, 59 axial slices per volume, total acquisition time 3:50min).

2.2.2 Structural imaging

A high-resolution three-dimensional (3D) inversion recovery fast spoiled gradient echo T1-weighted (T1w) image was acquired for GM volumetric assessment with TE 3.06ms, TR 7.90ms, inversion time 450ms, isotropic voxel size 1mm^3 with a 240mm^2 FOV, ASSET acceleration factor 2, flip angle 12°, 176 sagittal slices, total acquisition time 4:41min.

2.2.3 Perfusion imaging

Perfusion images were acquired using whole brain 3D pseudo-continuous ASL (p-CASL), which is currently the recommended sequence for clinical use [30] (interleaved fast spin-echo stack-of-spiral readout of 512 sampling points on 8 spirals, TE 10.5ms, TR 4632ms, isotropic voxel size 3.3mm^3 with a 240mm^2 FOV, 36 axial slices, number of excitations (NEX) 3, total acquisition time 4:29min; with background suppression, post label delay 1525ms, labelling duration 1450ms). The labelling plane was positioned 9cm below the anterior commissure – posterior commissure line.

2.3 Demographical analysis

Using SPSS Statistics, version 20.0 (IBM, New York, USA), gender differences across groups were assessed using chi-square tests and age differences using one-way ANOVA, with Bonferroni correction for multiple comparisons. As MMSE was not normally distributed across groups (Shapiro-Wilk test $p<0.05$) a nonparametric Kruskal-Wallis test was used to assess differences between groups, with Dunn-Bonferroni correction for multiple comparisons ($p<0.05$).

2.4 DTI processing and analysis

Data were analysed using FMRIB Software Library (FSL5, Oxford, UK) [31–33]. Data were corrected for motion and eddy currents using Eddy Correct and then skull-stripped using BET [34]. Two analyses were performed. First, Tract-based spatial statistics (TBSS) was performed to identify affected WM tracts in AD and bvFTD. Second, Tractography was performed to obtain quantitative diffusion metrics per WM tract in order to correlate WM measures with GM measures.

2.4.1 Tract-Based Spatial Statistics (TBSS)

First, diffusion tensors were reconstructed using DTIFIT [35], allowing computation of an FA image for each participant. Second, using whole brain TBSS [36], WM tracts showing fractional anisotropy (FA) abnormalities were identified.

Group differences in FA were tested with Randomise [37], using 5000 non-parametric permutations, threshold-free cluster enhancement (TFCE) [38], and multiple comparison correction. Default settings for skeletonised data were applied.

Using the General Linear Model toolbox, a one-way ANOVA design with three groups (AD≠bvFTD≠controls) was defined. Six post-hoc t-contrasts (AD>controls, controls>AD, bvFTD>controls, controls>bvFTD, AD>bvFTD, bvFTD>AD) were constructed.

In order to identify post-hoc t-test results within the boundaries of the f-test results, common binary masks were created using FSLmaths. First, for the f-test and all t-tests a binary mask was created (p=0.95). Second, each t-test binary mask was multiplied with the f-test binary mask, resulting in a common binary mask for every t-test. Last, cluster size (voxels (k)≥50) was extracted from all t-test common binary masks using the Cluster tool in FSL.

Using FSLview, results were visualised with the implemented JHU White-Matter Tractography Atlas and the JHU ICBM-DTI-81 White-Matter labels. WM tracts showing lower FA in AD and/or bvFTD in the current study and known to be associated with cognition were selected for tractography.

2.4.2 Tractography

From the selected WM tracts, median FA values were extracted. In addition, median values of mean diffusivity (MD) were extracted to obtain a more comprehensive view on how WM measures relate to GM measures. Both FA and mean diffusivity MD are considered as sensitive measures for diffusion changes and reflect different aspects of diffusion. Automated probabilistic tractography (AutoPtx [39]) was used to apply a tensor fit with DTIFIT [35], followed by a FNIRT registration and a BEDPOSTX probabilistic model fit for each participant. Then PROBTRACKX [35,40] was run for all selected WM tracts (Table 1) in each patient and control individually using default space seed, target, stop and exclusion masks available in AutoPtx [39], resulting in a tract density image for each tract in each participant. To ensure a fair comparison of diffusivity measures between subjects with variable brain size and to account for the size of white matter tracts, tract density images were normalised through division by the number of fibres included in each tract-image. These were then binarised for WM tract segmenta-

tion, based on the best-fit segmentation thresholds established by De Groot et al. (2015) [41] (see supplemental Table 1 for thresholds).

Using FSLstats, whole-brain FA and MD images were masked with thresholded tract images to obtain median FA and MD values for each WM tract. Significant effects of age and TE on FA and MD were identified using linear regression and corrected for if necessary.

2.5 Structural imaging and ASL processing and analysis

GM regions of interest (ROIs) were defined for every participant to obtain quantitative values of volume and perfusion to correlate these with WM measures.

2.5.1 Tissue segmentation

The unified tissue segmentation method [42] of SPM8 (Statistical Parametric Mapping, London, UK) was used to segment the T1w image into GM, WM and cerebrospinal fluid maps. Volume and cerebral blood flow (CBF) were derived from GM only.

2.5.2 ASL post-processing

The ASL dataset consisted of a perfusion-weighted and a proton density image. The GM map of each participant was rigidly registered with the proton density image (Elastix registration software [43]). Subsequently, GM maps were transformed to ASL image space to enable partial volume (PV) correction. The ASL images were corrected for PV effects using local linear regression within a 3D kernel based on tissue maps [44]. Then, CBF was quantified using the single-compartment model recommended in Alsop et al., 2015 [30]. CBF maps were transformed to T1w image space to enable region labelling.

2.5.3 ROI labelling

A multi-atlas approach was used to define ROIs for each participant, as registering multiple atlases to an individual T1w scan provides a much more robust registration than a single atlas approach [8,45]. The atlas included 30 labelled T1w images, each containing 83 ROIs [46,47]. These atlas images were registered to the participants' T1w images using a rigid, affine, and non-rigid B-spline transformation model consecutively. For this registration, both the participants' and the labelled T1w images were masked (Brain Extraction Tool [34]) and T1w images

were non-uniformity corrected [48]. ROI labels were fused using a majority voting algorithm [45]. Registration of all ROI labels was visually inspected for every participant.

2.5.4 Regional GM volume and CBF analysis

GM volume and CBF were analysed in the global supratentorial brain and in ROIs. The multi-atlas approach resulted in a parcellation of each participant's T1w image into 83 ROIs. The cerebellum, brainstem, pallidum, substantia nigra, ventricles and WM regions were excluded from analysis. Regions smaller than a single gyrus were combined to constitute an entire gyrus (Supplemental Table 2). To correct for head size, regional GM volumes were normalised using total intracranial volume (ICV). These are referred to as normalised GM (nGM) volumes and reported as percentage of ICV. To obtain a measure of CBF representative of perfusion in remaining grey matter, CBF was then divided by nGM volume, to correct for volume loss independent of interindividual volume differences. This is referred to as cCBF. Significant effects of age on nGM volume and cCBF were identified using linear regression and corrected for if necessary.

As nGM volumes and cCBF values were not normally distributed across groups (Shapiro-Wilk test $p<0.05$), a nonparametric Kruskal-Wallis test with Dunn-Bonferroni correction for multiple comparisons was used to compare measures from the global supratentorial cortex and the ROIs between groups.

2.6 WM and GM correlation analyses

Correlation analyses were performed between FA and MD in WM tracts affected in AD and/or bvFTD (Table 1) and volume and perfusion of regional GM. To determine the GM regions at either end of the tract (ROI1 and ROI2), tracts were visualised in FSLview using the JHU White-Matter Tractography Atlas overlaid on the MNI152 1mm^3 template, and/or the default WM masks available in AutoPtx [39]. For WM tracts that projected to multiple cortical regions, GM measures (nGM volume, cCBF) were averaged over all cortical regions included in ROI1 or ROI2. This resulted in six variables per tract: FA, MD, nGM volume in ROI1 and ROI2, and cCBF in ROI1 and ROI2 (Figure 1). Correlations between WM measures (FA and MD) and GM measures (nGM and cCBF in ROI1 and ROI2) were assessed with Spearman analysis. Correlations exceeding the threshold of $-0.6 \geq rho \geq 0.6$ are reported.

Differences between these within-group correlations were subsequently tested for significance using a Fisher's r to z transformation with Bonferroni correction. As sample sizes were small, uncorrected significant results are also reported.

WM-GM coherence was considered positive when correlations between FA and GM measures were positive, or when correlations between MD and GM measures were negative. WM-GM coherence was considered negative when correlations between FA and GM measures were negative, or correlations between MD and GM measures were positive.

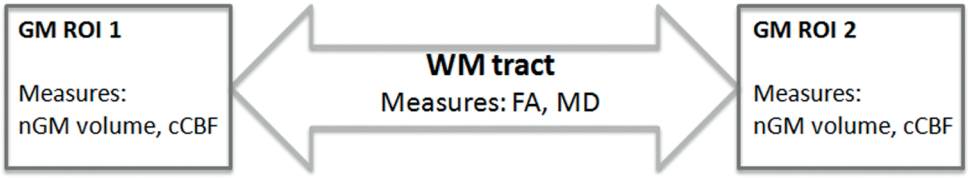

Figure 1. Schematic overview of variables entered into correlation analysis. WM = white matter; FA = fractional anisotropy; MD = mean diffusivity; ROI = region of interest; nGM = grey matter; cCBF = cerebral blood flow.

3. RESULTS

3.1 Participant and disease characteristics

Eleven AD patients, 9 bvFTD patients and 18 controls were included in the study. Gender (χ^2 (2, n=37) = 2.508, p>0.05) and age (F(2,35) = .823, p>0.05) were not different between groups. MMSE differed across groups (H(2) = 19.938, p<0.05), with post-hoc analyses indicating that both patient groups had lower MMSE scores compared to controls, but not to each other (Table 2). One AD patient was excluded from the ASL analysis due to low image quality.

3.2 Separate WM and GM abnormalities

3.2.1 WM abnormalities

AD and bvFTD patients compared with controls showed lower FA (Figure 2, Supplemental Tables 3-4) in WM of the anterior thalamic radiation, cingulum (cin-

Table 1. Affected WM tracts and GM regions at either end of these tracts, and their abbreviations. Affected WM tracts and cortical ROIs were analysed in the left and in the right hemisphere (except for the forceps major and minor).
WM = white matter; ROI = region of interest; GM = grey matter; abbr. = abbreviation.

WM tract	Abbr.	Cortical ROI1	Abbr.	Cortical ROI2	Abbr.
Anterior thalamic radiation	ATR	Inferior frontal gyrus	IFG	Hippocampal formation	HF
		Orbitofrontal gyrus	OFG		
Cingulum (cingulate gyrus)	CGc	Subcallosal area		Posterior cingulate cortex	PCC
		Anterior cingulate cortex	ACC	Precuneus	
Cingulum (hippocampus)	CGh	Posterior cingulate cortex	PCC	Hippocampal formation	HF
		Precuneus		Anterior temporal lobe	ATL
Forceps major	FMa	Left lingual gyrus	Occipital	Right lingual gyrus	Occipital
		Left cuneus		Right cuneus	
		Left lateral occipital lobe		Right lateral occipital lobe	
Forceps minor	FMi	Left superior frontal gyrus	SFG	Right superior frontal gyrus	SFG
		Left straight gyrus		Right straight gyrus	
		Left orbital frontal gyrus	OFG	Right orbital frontal gyrus	OFG
Inferior fronto-occipital fasciculus	IFOF	Inferior frontal gyrus	IFG	Lingual gyrus	Occipital
		Orbitofrontal gyrus	OFG	Cuneus	
				Lateral occipital lobe	
Inferior longitudinal fasciculus	ILF	Inferior temporal gyrus	ITG	Lingual gyrus	Occipital
		Superior temporal gyrus	STG	Cuneus	
		Anterior temporal lobe	ATL	Lateral occipital lobe	

Superior longitudinal fasciculus	SLF	Precentral gyrus		Inferior temporal gyrus	ITG	
		Inferior frontal gyrus	IFG	Posterior temporal lobe	PTL	
Uncinate fasciculus	UF	Inferior frontal gyrus	IFG	Superior temporal gyrus	STG	
		Orbitofrontal gyrus	OFG	Anterior temporal lobe	ATL	

gulate gyrus and hippocampus), forceps major and minor, inferior fronto-occipital fasciculus, inferior and superior longitudinal fasciculus, and uncinate fasciculus.

In all these WM tracts (supplemental Table 5), FA was lower in bvFTD patients than in AD patients. AD patients did not show WM regions of lower FA compared with bvFTD patients.

3.2.2 nGM volume loss

In AD patients compared with controls, nGM volume was lower in the bilateral parietal cortex, left temporal cortex, right occipital regions, right thalamus and left nucleus accumbens. In bvFTD patients compared with controls, global supratentorial nGM volume was lower as were volumes of the bilateral frontal, temporal and parietal cortices and bilateral basal ganglia. There was more extensive volume loss in the frontal lobe in bvFTD than AD patients (Supplemental Table 6, Figure 3).

3.2.3 GM hypoperfusion

AD patients compared with controls showed lower cCBF in the posterior temporal lobe bilaterally, left superior temporal gyrus, bilateral precuneus and left posterior cingulate, and in the lateral remainder of the right occipital lobe. In bvFTD patients, cCBF was not different from controls. AD patients compared with bvFTD patients showed lower cCBF in the bilateral orbitofrontal gyri, right hippocampal formation, left superior and right inferior temporal gyrus, and right fusiform gyrus (Supplemental Table 7, Figure 3).

3.3 Correlations between WM and GM measures

Only WM tracts found to be affected in AD and/or bvFTD (Supplemental Tables 3-5; Table 1), and associated with cognition, were selected for the correlation analysis: anterior thalamic radiation [49,50], cingulum [51], forceps major [49,52] and

Table 2. Participant characteristics

	Controls	BvFTD	AD
N (male)	18 (8)	9 (4)	11 (8)
Mean age ± SD in years	59.8 ± 6.73	62.3 ± 5.68	62.3 ± 5.04
Median MMSE (range)	30 (27-30)	28 (24-30)	25 (22-28)

AD = Alzheimer's disease; bvFTD = behavioural variant frontotemporal dementia; MMSE = Mini-Mental State Examination; SD = standard deviation

minor [49,53,54](representing respectively the splenium and genu of the corpus callosum), inferior fronto-occipital fasciculus [55–57], inferior longitudinal fasciculus [55,58], superior longitudinal fasciculus [58,59] and uncinate fasciculus [51,53,56].

3.3.1 Within-group WM-GM correlations

Within-group correlations (rho ≥ 0.6) between WM and GM measures are shown in Supplemental Table 8. Both patient groups showed more correlations between WM and GM measures than controls.

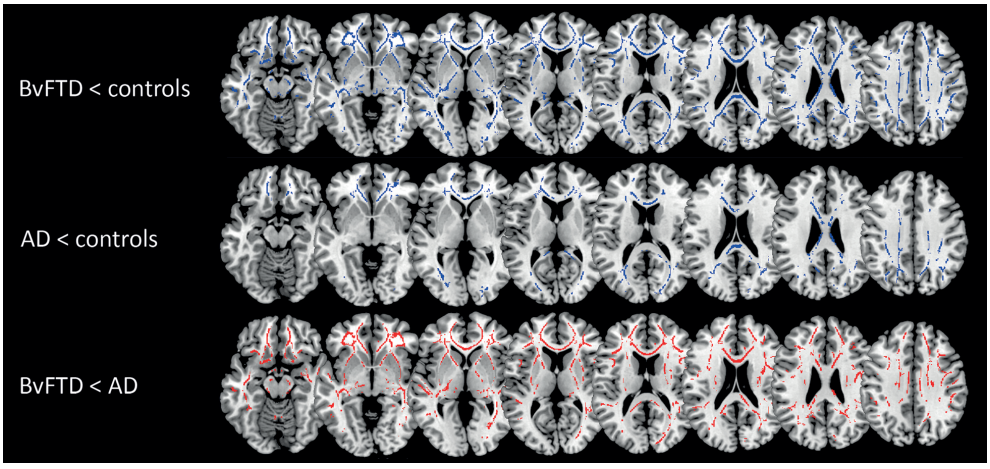

Figure 2. Post-hoc t-test (p<0.05; k=50) white matter FA abnormalities. Lower FA in comparison with controls for bvFTD (top row) and AD (middle row) is shown in blue and lower FA in bvFTD in comparison with AD (bottom row) is shown in red.
FA = fractional anisotropy; AD = Alzheimer's disease; BvFTD = behavioural variant frontotemporal dementia; L = left hemisphere.

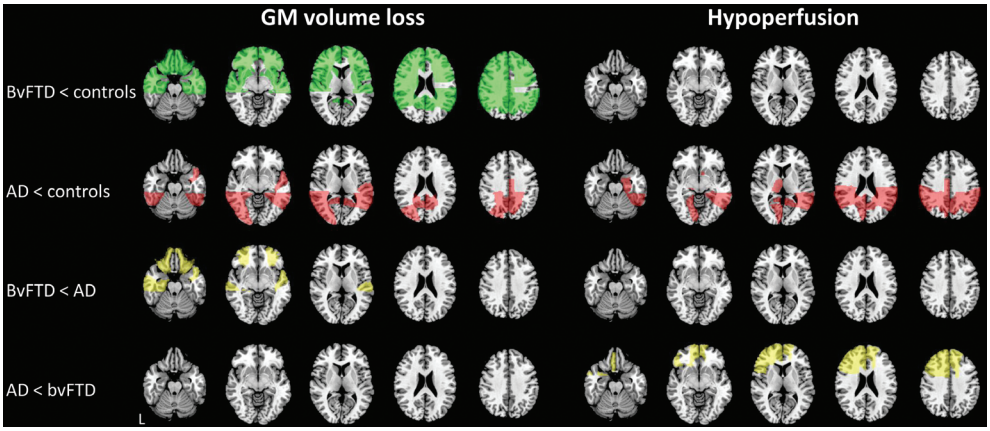

Figure 3. Overview of grey matter (GM) regions showing group differences between normalised GM volume (left) and corrected cerebral blood flow (right). Regions that showed differences between bvFTD and controls are depicted in green, regions showing differences between AD and controls are depicted in red, and regions showing differences between AD and bvFTD in yellow. GM = grey matter; AD = Alzheimer's disease; BvFTD = behavioural variant frontotemporal dementia; L = left hemisphere.

3.3.2 Between-group differences in WM-GM correlations

Group differences detected with Fisher Z testing are shown in Table 3 and visualised in Figure 4. In AD patients compared with controls, strong positive correlations were found between cingulum WM microstructure and frontal GM perfusion and temporal GM volume, and between inferior fronto-occipital fasciculus WM microstructure and occipital GM volume and perfusion.

In bvFTD patients compared with controls, strong positive correlations were found between cingulum WM microstructure and parietal GM perfusion and temporal GM volume.

In bvFTD compared with AD, a strong positive correlation was observed between cingulum WM microstructure and parietal GM perfusion (Figure 5). Not

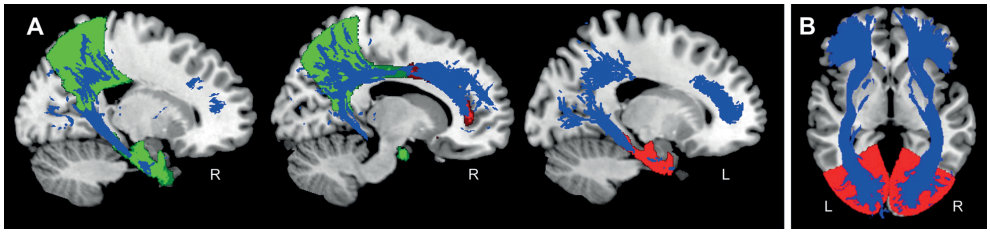

Figure 4. White matter (WM) tracts and grey matter (GM) regions that are correlated in AD and bvFTD. A: Cingulum microstructure (blue) correlated with frontal and temporal GM in AD (red) and temporal and parietal GM in bvFTD (green). B: Inferior fronto-occipital fasciculus microstructure (blue) correlated with occipital GM in AD (red).

a stronger, but negative rather than positive correlation was observed between uncinate fasciculus WM microstructure and frontal GM perfusion.

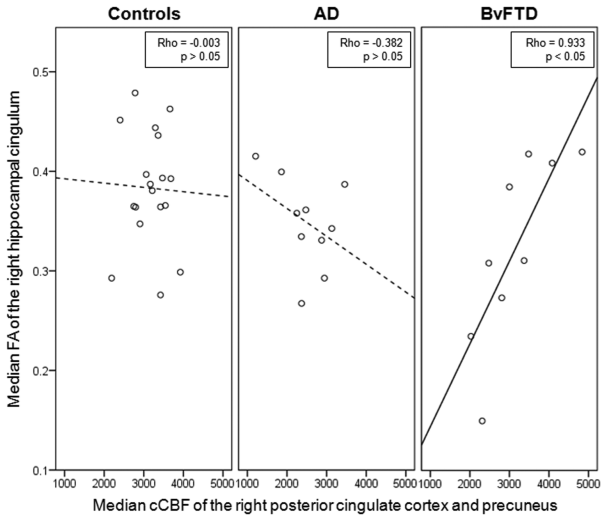

Figure 5. Correlation between median FA of the right hippocampal cingulum and median cCBF in the right PCC and precuneus in controls, AD, and bvFTD patients. Correlations were significantly different between AD and bvFTD patients (solid line). Dashed lines indicate non-significant correlations.
FA = fractional anisotropy; cCBF = cerebral blood flow; PCC = posterior cingulate cortex; AD = Alzheimer's disease; bvFTD = behavioural variant frontotemporal dementia.

Table 3. Between-group differences in regional correlation coefficients for WM tracts and associated GM regions and their respective p-values. Correlations that were significantly different between groups after correcting for multiple comparisons are printed in bold.

Positive WM-GM coherence in AD versus controls

WM tract	GM region	WM-GM correlation coefficient		
		AD	Control	p-value
R_CGC FA	R ACC/subcallosal cCBF	0.648	-0.077	0.05
L CGH MD	L HF/ATL nGM volume	-0.645	0.216	0.02
R IFOF FA	R occipital cCBF	0.636	-0.104	0.05
L IFOF MD	L occipital cCBF	-0.748	0.023	0.02
R IFOF MD	R occipital nGM volume	-0.137	-0.765	0.04

Positive WM-GM coherence in bvFTD versus controls

WM tract	GM region	WM-GM correlation coefficient		
		BvFTD	Control	p-value
R CGC MD	R precuneus/PCC cCBF	**-0.867**	**-0.178**	0.02
R CGH FA	R precuneus/PCC cCBF	**0.933**	**-0.003**	<0.01
R CGH MD	R precuneus/PCC cCBF	-0.650	0.323	0.02
R CGH MD	R HF/ATL nGM volume	-0.767	-0.001	0.04

Positive WM-GM coherence in bvFTD versus AD

WM tract	GM region	WM-GM correlation coefficient		
		BvFTD	AD	p-value
R CGH FA	R precuneus/PCC cCBF	**0.933**	**-0.382**	<0.01

Negative WM-GM coherence in bvFTD versus AD

WM tract	GM region	WM-GM correlation coefficient		
		BvFTD	AD	p-value
L UF MD	L OFG/IFG cCBF	**0.533**	**-0.624**	0.01

WM-GM coherence was considered positive when correlations between FA and GM measures were positive, or when correlations between MD and GM measures were negative. WM-GM coherence was considered negative when correlations between FA and GM measures were negative, or correlations between MD and GM measures were positive.
CGC = cingulum (cingulate gyrus); CGH = cingulum (hippocampal); IFOF = inferior fronto-occipital fasciculus; UF = uncinate fasciculus; OFG = orbitofrontal gyrus; ACC/PCC = anterior/posterior cingulate cortex; HF = hippocampal formation; ATL = anterior temporal lobe; L = left; R = right; cCBF = corrected cerebral blood flow; nGM = normalised grey matter; WM = white matter; FA = fractional anisotropy; MD = mean diffusivity; AD = Alzheimer's disease; bvFTD = behavioural variant frontotemporal dementia.

4. DISCUSSION

In this study we observed a disease-specific dissociation between structural and perfusion abnormalities, specifically more widespread microstructural WM abnormalities and GM atrophy in bvFTD patients, and more widespread hypoperfusion in AD patients. More importantly, we observed coherence between WM microstructure and GM volume and perfusion in both AD and bvFTD, and this coherence was strongly increased compared to controls in regions implicated in AD and bvFTD. We hypothesise that this is due to concurrent degeneration in disease specific networks.

Our findings of WM and GM abnormalities assessed separately are in line with the published literature. Compared to controls, bvFTD showed more extensive structural abnormalities in both WM and GM than AD. In bvFTD, WM abnormalities were observed throughout the entire brain, and GM atrophy in the frontal, temporal, parietal and subcortical regions [5,6,22]. In AD, WM abnormalities were less extensive and found in frontal, parietal and occipital regions, and GM atrophy in temporal, parietal, occipital and subcortical regions [2,5,6]. Only AD showed prominent temporal, parietal and occipital hypoperfusion [7,12,60–62], while there was no significant hypoperfusion in bvFTD.

In this study, we took these – known – findings a step further by assessing the coherence between regional WM and GM measures. In the healthy elderly, only a small number of regions showed positive coherence between WM microstructure and GM volume. Coherence between WM microstructure and GM perfusion was even less pronounced. Conversely, patients showed strong coherence of WM and GM changes in many disease-specific regions, which may thus reflect concurrent degeneration of WM and GM. The strong positive coherence between WM and GM measures in patients was particularly prominent between cingulum WM microstructure and associated temporal GM volume and frontal GM perfusion in AD, and between cingulum WM microstructure and temporal GM volume and parietal GM perfusion in bvFTD.

The cingulum WM is central to the Papez circuit [63], which comprises regions implicated in AD such as the entorhinal cortex, fornix and hippocampal formation. The positive coherence between cingulum WM microstructure and GM volume of the hippocampal formation and anterior temporal lobe can thus be explained by concurrent anterior medial temporal atrophy and cingulum degeneration. Additionally, we observed coherence between the cingulum WM and its associated anterior GM regions, which we hypothesise to be related to the posterior to anterior propagation of AD pathology [64]. This propagation is widely believed to result from Wallerian degeneration in which WM pathology is pre-

sumably secondary to GM pathology. However, there also is increasing evidence that WM pathology is primary to GM pathology in AD [65]. Our cross-sectional correlational study design does not allow for claims on changes over time, but rather shows evidence of concurrent changes in WM and GM. Instead of AD being primarily a WM or GM disease, we speculate that WM microstructural abnormalities and GM abnormalities are dependent in pathophysiology, as changes of the cingulum WM microstructure and associated GM regions seem to co-occur. In support of this, individual WM and GM measures in this study showed a similar degree of WM and GM structural abnormalities in AD.

In bvFTD, positive coherence between cingulum WM microstructure and parietal GM perfusion was not only evident in comparison with controls, but also with AD patients, in whom this regional coherence was absent. On a group level, cingulum WM microstructure in bvFTD was abnormal but parietal perfusion was not. Nevertheless, the strong positive coherence indicates that as cingulum WM deteriorates, perfusion decreases too, implying incipient parietal perfusion abnormalities, as previously reported in bvFTD [62]. Additionally, higher coherence was observed exclusively in the right hemisphere, consistent with the notion of greater right than left hemispheric involvement in bvFTD [66–68].

Of note is that recently different abnormality patterns in bvFTD have been associated with underlying genetic mutations and/or pathology [22,69–71]. The presence of patients with different genetic mutations/pathology may therefore have a differential effect on brain abnormalities across groups. This may also have happened in our study. Importantly, we aimed to investigate coherence in clinical samples of AD and bvFTD patients, i.e. with an AD or bvFTD phenotype. The correlations found here indicate similar brain abnormalities within the bvFTD group that are, given the strength of the correlations, likely to be common to these patients of the bvFTD phenotype.

It may seem counterintuitive that bvFTD showed high coherence in posterior regions and AD in anterior regions, when relating it to propagation of pathology from anterior to posterior in bvFTD [72], and from posterior to anterior in AD [64]. Higher coherence may be expected in more severely affected anterior regions in bvFTD and posterior regions in AD. Instead, this study shows coherence between WM and GM measures in the less rather than the more severely affected regions. We postulate that when abnormalities are incipient, WM and GM changes are concurrent, whereas this coherence may be lost in a more advanced disease stage. This is supported by a recent study reporting correlations between parietal hypoperfusion and cingulate WM in mild cognitive impairment converters, but not

in mild AD patients [26]. Additionally, this postulation is in line with previous findings of changes of functional connectivity in the default mode network (DMN). The DMN consists of a frontal and parietal component, connected through the cingulum. Parallel with our findings, in bvFTD functional connectivity is generally found to be higher in the parietal than in the frontal DMN, whereas in AD functional connectivity is found to be lower in the parietal than in the frontal DMN [73]. The coherence we found between uncinate fasciculus WM and frontal GM perfusion in AD can be similarly interpreted in the context of the salience network (SN), which has previously shown increased frontal functional connectivity in AD [73].

Additionally, in AD coherence was observed between inferior fronto-occipital fasciculus WM microstructure and occipital GM perfusion, but not occipital GM volume. GM abnormalities of the occipital lobe are not consistently implicated in AD pathology [12,61,74] and indeed when we assessed GM measures separately, we found dissimilar perfusion and GM volume abnormalities.

Surprisingly, in bvFTD we observed negative coherence between uncinate fasciculus WM microstructure and frontal GM perfusion, suggesting diverging WM and GM changes. This may seem remarkable as both uncinate fasciculus WM abnormalities and frontal hypoperfusion have been reported in bvFTD [22,75]. In our study we corrected perfusion for GM volume and showed that perfusion was slightly increased in the frontal GM in bvFTD, albeit non-significantly. Slightly increased perfusion may suggest functional compensation for structural damage in the frontal lobe. It was only seen in the frontal lobe, which is indeed the most severely affected brain region structurally in bvFTD. As we found rather extensive frontal WM and GM volume abnormalities, we speculate that the slightly increased perfusion may be the final stage of a compensatory process, prior to the occurrence of hypoperfusion. However, this speculative hypothesis should be verified by longitudinal studies.

Overall, our findings demonstrate that the concurrent changes in WM and GM adhere to the disease-specific distribution of abnormalities, generally propagating from posterior to anterior regions in AD and from anterior to posterior regions in bvFTD. It is of interest that the correlational methodology appears to be sensitive to incipient abnormalities that are not (yet) evident as differences between groups.

This study knows some limitations. First, our patient group sizes were small, which warrants caution with the interpretation of the contradictory findings we observed. Nevertheless, to correct for the sensitivity of small samples to outliers, we used non-parametric testing which is generally more stringent and thus reduces the risk of false positive results but carries the risk of false negative results. A potentially larger problem is the difference in sample size of the patient

groups compared with controls. In a large sample, the threshold for significance of correlations is lower, i.e. relatively low correlation coefficients were significant in our control sample but not in patients. This may have skewed a fair comparison between the groups. We accounted for this by reporting all correlations above the threshold of rho ≥ 0.6. Second, we attribute our findings to the early disease stage of our sample. Measures of disease stage, such as the clinical dementia rating (CDR) scale or frontal rating scale (FRS) were not available for our sample. Instead, MMSE scores were available, which may also be used as a proxy of disease stage. The fact that mean MMSE scores were very high, supports the notion that our patients are at an early stage of dementia. Third, a single FA and MD value was used for each WM tract. In long association fibres this may not be fully representative as it may obscure regional differences within the WM tract. An option would have been to parcellate these tracts into smaller sections. However, as we aimed to study coherence as defined by WM anatomy and its associated GM projections, we chose to look at anatomical connections as a whole rather than at subregions. Similarly, regional heterogeneity may have affected the large GM ROIs. For instance, GM within the occipital lobe was not similarly affected, with the right medial part showing GM volume loss whereas the right lateral part and left occipital ROI did not. Restricting such heterogeneity within an ROI may result in more consistent coherence patterns with associated WM microstructure. Fourth, for acquiring DTI scans we used a number of 25 gradient directions, which is relatively low in comparison with the suggested use of approximately 30 gradient directions [76]. A lower number of gradient directions may bias anisotropy estimation and may therefore influence group differences. As this study was a clinical study, scan time could not be prolonged due to patient care and associated imaging time restrictions. Nevertheless, our group results were in line with previous literature, suggesting fairly limited anisotropy bias.

In conclusion, we observed a disease-specific dissociation between structural degeneration and hypoperfusion. More importantly, we established a framework for assessing coherence between WM microstructure and GM volume and perfusion in AD and bvFTD. Within this framework we showed how that such coherence is mostly absent in healthy elderly controls, but present both in AD and bvFTD. Coherence is particularly strong in regions implicated in AD and bvFTD pathology, indicating concurrent degeneration in disease-specific networks. Moreover, the correlational methodology applied in this framework allows for the detection of incipient abnormalities that would go undetected in comparative group analyses. Our future research is aimed at further defining these relationships at different stages of aging and neurodegeneration.

REFERENCES

1 Koedam ELGE, Lauffer V, van der Vlies AE, *et al.* Early-versus late-onset Alzheimer's disease: more than age alone. *J Alzheimers Dis* 2010;19:1401–8. doi:10.3233/JAD-2010-1337

2 Acosta-Cabronero J, Williams GB, Pengas G, *et al.* Absolute diffusivities define the landscape of white matter degeneration in Alzheimer's disease. *Brain* 2010;133:529–39. doi:10.1093/brain/awp257

3 Du AT, Jahng GH, Hayasaka S, *et al.* Hypoperfusion in frontotemporal dementia and Alzheimer disease by arterial spin labeling MRI. *Neurology* 2006;67:1215–20. doi:10.1212/01.wnl.0000238163.71349.78

4 Hu WT, Wang Z, Lee VM-Y, *et al.* Distinct cerebral perfusion patterns in FTLD and AD. *Neurology* 2010;75:881–8. doi:10.1212/WNL.0b013e3181f11e35

5 Zhang Y, Schuff N, Du A-T, *et al.* White matter damage in frontotemporal dementia and Alzheimer's disease measured by diffusion MRI. *Brain* 2009;132:2579–92. doi:10.1093/brain/awp071

6 Rabinovici GD, Seeley WW, Kim EJ, *et al.* Distinct MRI atrophy patterns in autopsy-proven Alzheimer's disease and frontotemporal lobar degeneration. *Am J Alzheimers Dis Other Demen* 2007;22:474–88. doi:10.1177/1533317507308779

7 Benedictus MR, Binnewijzend MAA, Kuijer JPA, *et al.* Brain volume and white matter hyperintensities as determinants of cerebral blood flow in Alzheimer's disease. *Neurobiol Aging* 2014;35:2665–70. doi:10.1016/j.neurobiolaging.2014.06.001

8 Bron EE, Steketee RME, Houston GC, *et al.* Diagnostic classification of arterial spin labeling and structural MRI in presenile early stage dementia. *Hum Brain Mapp* 2014;35:4916–31. doi:10.1002/hbm.22522

9 Dashjamts T, Yoshiura T, Hiwatashi A, *et al.* Simultaneous arterial spin labeling cerebral blood flow and morphological assessments for detection of Alzheimer's disease. *Acad Radiol* 2011;18:1492–9. doi:10.1016/j.acra.2011.07.015

10 Mak HKF, Chan Q, Zhang Z, *et al.* Quantitative assessment of cerebral hemodynamic parameters by QUASAR arterial spin labeling in Alzheimer's disease and cognitively normal Elderly adults at 3-tesla. *J Alzheimers Dis* 2012;31:33–44. doi:10.3233/JAD-2012-111877

11 Shimizu S, Zhang Y, Laxamana J, *et al.* Concordance and discordance between brain perfusion and atrophy in frontotemporal dementia. *Brain Imaging Behav* 2010;4:46–54. doi:10.1007/s11682-009-9084-1

12 Steketee RME, Bron EE, Meijboom R, *et al.* Early-stage differentiation between presenile Alzheimer's disease and frontotemporal dementia using arterial spin labeling MRI. *Eur Radiol* 2016;26:244–53. doi:10.1007/s00330-015-3789-x

13 Tosun D, Rosen H, Miller BL, *et al.* MRI patterns of atrophy and hypoperfusion associations across brain regions in frontotemporal dementia. *Neuroimage* 2012;59:2098–109. doi:10.1016/j.neuroimage.2011.10.031
14 Wang Z, Das SR, Xie SX, *et al.* Arterial spin labeled MRI in prodromal Alzheimer's disease: A multi-site study. *NeuroImage Clin* 2013;2:630–6. doi:10.1016/j.nicl.2013.04.014
15 Amlien IK, Fjell a M. Diffusion tensor imaging of white matter degeneration in Alzheimer's disease and mild cognitive impairment. *Neuroscience* 2014;276:206–15. doi:10.1016/j.neuroscience.2014.02.017
16 Agosta F, Pievani M, Sala S, *et al.* White matter damage in Alzheimer disease and its relationship to gray matter atrophy. *Radiology* 2011;258:853–63. doi:10.1148/radiol.10101284
17 Alves GS, O'Dwyer L, Jurcoane A, *et al.* Different patterns of white matter degeneration using multiple diffusion indices and volumetric data in mild cognitive impairment and Alzheimer patients. *PLoS One* 2012;7:e52859. doi:10.1371/journal.pone.0052859
18 Lee DY, Fletcher E, Carmichael OT, *et al.* Sub-Regional Hippocampal Injury is Associated with Fornix Degeneration in Alzheimer's Disease. *Front Aging Neurosci* 2012;4:1. doi:10.3389/fnagi.2012.00001
19 Mielke MM, Okonkwo OC, Oishi K, *et al.* Fornix integrity and hippocampal volume predict memory decline and progression to Alzheimer's disease. *Alzheimers Dement* 2012;8:105–13. doi:10.1016/j.jalz.2011.05.2416
20 Wang P-N, Chou K-H, Lirng J-F, *et al.* Multiple diffusivities define white matter degeneration in amnestic mild cognitive impairment and Alzheimer's disease. *J Alzheimers Dis* 2012;30:423–37. doi:10.3233/JAD-2012-111304
21 Avants BB, Cook PA, Ungar L, *et al.* Dementia induces correlated reductions in white matter integrity and cortical thickness: a multivariate neuroimaging study with sparse canonical correlation analysis. *Neuroimage* 2010;50:1004–16. doi:10.1016/j.neuroimage.2010.01.041
22 Mahoney CJ, Ridgway GR, Malone IB, *et al.* Profiles of white matter tract pathology in frontotemporal dementia. *Hum Brain Mapp* 2014;35:4163–79. doi:10.1002/hbm.22468
23 Whitwell JL, Avula R, Senjem ML, *et al.* Gray and white matter water diffusion in the syndromic variants of frontotemporal dementia. *Neurology* 2010;74:1279–87. doi:10.1212/WNL.0b013e3181d9edde
24 Zhang Y, Tartaglia MC, Schuff N, *et al.* MRI signatures of brain macrostructural atrophy and microstructural degradation in frontotemporal lobar degeneration subtypes. *J Alzheimers Dis* 2013;33:431–44. doi:10.3233/JAD-2012-121156
25 Zhang Y, Schuff N, Ching C, *et al.* Joint assessment of structural, perfusion, and diffusion MRI in Alzheimer's disease and frontotemporal dementia. *Int J Alzheimers Dis* 2011;2011:546871. doi:10.4061/2011/546871

26 Lacalle-Aurioles M, Navas-Sánchez FJ, Alemán-Gómez Y, *et al.* The Disconnection Hypothesis in Alzheimer's Disease Studied Through Multimodal Magnetic Resonance Imaging: Structural, Perfusion, and Diffusion Tensor Imaging. *J Alzheimers Dis* 2016;50:1051–64. doi:10.3233/JAD-150288

27 McKhann GM, Knopman DS, Chertkow H, *et al.* The diagnosis of dementia due to Alzheimer's disease: recommendations from the National Institute on Aging-Alzheimer's Association work-groups on diagnostic guidelines for Alzheimer's disease. *Alzheimers Dement* 2011;7:263–9. doi:10.1016/j.jalz.2011.03.005

28 Rascovsky K, Hodges JR, Knopman D, *et al.* Sensitivity of revised diagnostic criteria for the behavioural variant of frontotemporal dementia. *Brain* 2011;134:2456–77. doi:10.1093/brain/awr179

29 Folstein MF, Folstein SE, McHugh PR. 'Mini-mental state'. A practical method for grading the cognitive state of patients for the clinician. *J Psychiatr Res* 1975;12:189–98.http://www.ncbi.nlm.nih.gov/pubmed/1202204.

30 Alsop DC, Detre JA, Golay X, *et al.* Recommended implementation of arterial spin-labeled perfusion MRI for clinical applications: A consensus of the ISMRM perfusion study group and the European consortium for ASL in dementia. *Magn Reson Med* 2015;73:102–16. doi:10.1002/mrm.25197

31 Jenkinson M, Beckmann CF, Behrens TEJ, *et al.* FSL. *Neuroimage* 2012;62:782–90. doi:10.1016/j.neuroimage.2011.09.015

32 Smith SM, Jenkinson M, Woolrich MW, *et al.* Advances in functional and structural MR image analysis and implementation as FSL. *Neuroimage* 2004;23 Suppl 1:S208–19. doi:10.1016/j.neuroimage.2004.07.051

33 Woolrich MW, Jbabdi S, Patenaude B, *et al.* Bayesian analysis of neuroimaging data in FSL. *Neuroimage* 2009;45:S173–86. doi:10.1016/j.neuroimage.2008.10.055

34 Smith SM. Fast robust automated brain extraction. *Hum Brain Mapp* 2002;17:143–55. doi:10.1002/hbm.10062

35 Behrens TEJ, Woolrich MW, Jenkinson M, *et al.* Characterization and propagation of uncertainty in diffusion-weighted MR imaging. *Magn Reson Med* 2003;50:1077–88. doi:10.1002/mrm.10609

36 Smith SM, Jenkinson M, Johansen-Berg H, *et al.* Tract-based spatial statistics: voxelwise analysis of multi-subject diffusion data. *Neuroimage* 2006;31:1487–505. doi:10.1016/j.neuroimage.2006.02.024

37 Winkler AM, Ridgway GR, Webster MA, *et al.* Permutation inference for the general linear model. *Neuroimage* 2014;92:381–97. doi:10.1016/j.neuroimage.2014.01.060

38 Smith SM, Nichols TE. Threshold-free cluster enhancement: addressing problems of smoothing, threshold dependence and localisation in cluster inference. *Neuroimage* 2009;44:83–98. doi:10.1016/j.neuroimage.2008.03.061

39 de Groot M, Vernooij MW, Klein S, *et al.* Improving alignment in Tract-based spatial statistics: evaluation and optimization of image registration. *Neuroimage* 2013;76:400–11. doi:10.1016/j.neuroimage.2013.03.015
40 Behrens TEJ, Berg HJ, Jbabdi S, *et al.* Probabilistic diffusion tractography with multiple fibre orientations: What can we gain? *Neuroimage* 2007;34:144–55. doi:10.1016/j.neuroimage.2006.09.018
41 de Groot M, Ikram MA, Akoudad S, *et al.* Tract-specific white matter degeneration in aging: The Rotterdam Study. *Alzheimer's Dement* 2015;11:321–30. doi:10.1016/j.jalz.2014.06.011
42 Ashburner J, Friston KJ. Unified segmentation. *Neuroimage* 2005;26:839–51. doi:10.1016/j.neuroimage.2005.02.018
43 Klein S, Staring M, Murphy K, *et al.* elastix: a toolbox for intensity-based medical image registration. *IEEE Trans Med Imaging* 2010;29:196–205. doi:10.1109/TMI.2009.2035616
44 Asllani I, Borogovac A, Brown TR. Regression algorithm correcting for partial volume effects in arterial spin labeling MRI. *Magn Reson Med* 2008;60:1362–71. doi:10.1002/mrm.21670
45 Heckemann RA, Hajnal J V, Aljabar P, *et al.* Automatic anatomical brain MRI segmentation combining label propagation and decision fusion. *Neuroimage* 2006;33:115–26. doi:10.1016/j.neuroimage.2006.05.061
46 Gousias IS, Rueckert D, Heckemann RA, *et al.* Automatic segmentation of brain MRIs of 2-year-olds into 83 regions of interest. *Neuroimage* 2008;40:672–84. doi:10.1016/j.neuroimage.2007.11.034
47 Hammers A, Allom R, Koepp MJ, *et al.* Three-dimensional maximum probability atlas of the human brain, with particular reference to the temporal lobe. *Hum Brain Mapp* 2003;19:224–47. doi:10.1002/hbm.10123
48 Tustison NJ, Avants BB, Cook PA, *et al.* N4ITK: improved N3 bias correction. *IEEE Trans Med Imaging* 2010;29:1310–20. doi:10.1109/TMI.2010.2046908
49 Duering M, Gonik M, Malik R, *et al.* Identification of a strategic brain network underlying processing speed deficits in vascular cognitive impairment. *Neuroimage* 2013;66:177–83. doi:10.1016/j.neuroimage.2012.10.084
50 Torso M, Serra L, Giulietti G, *et al.* Strategic lesions in the anterior thalamic radiation and apathy in early Alzheimer's disease. *PLoS One* 2015;10:e0124998. doi:10.1371/journal.pone.0124998
51 Tartaglia MC, Zhang Y, Racine C, *et al.* Executive dysfunction in frontotemporal dementia is related to abnormalities in frontal white matter tracts. *J Neurol* 2012;259:1071–80. doi:10.1007/s00415-011-6300-x
52 Staff RT, Murray AD, Deary IJ, *et al.* Generality and specificity in cognitive aging: a volumetric brain analysis. *Neuroimage* 2006;30:1433–40. doi:10.1016/j.neuroimage.2005.11.004
53 Hornberger M, Geng J, Hodges JR. Convergent grey and white matter evidence of orbitofrontal cortex changes related to disinhibition in behavioural variant frontotemporal dementia. *Brain* 2011;134:2502–12. doi:10.1093/brain/awr173

54 Shollenbarger SG, Price J, Wieser J, *et al.* Poorer frontolimbic white matter integrity is associated with chronic cannabis use, FAAH genotype, and increased depressive and apathy symptoms in adolescents and young adults. *NeuroImage Clin* 2015;8:117–25. doi:10.1016/j.nicl.2015.03.024

55 Epstein KA, Cullen KR, Mueller BA, *et al.* White matter abnormalities and cognitive impairment in early-onset schizophrenia-spectrum disorders. *J Am Acad Child Adolesc Psychiatry* 2014;53:362–72.e1–2. doi:10.1016/j.jaac.2013.12.007

56 Mike A, Strammer E, Aradi M, *et al.* Disconnection mechanism and regional cortical atrophy contribute to impaired processing of facial expressions and theory of mind in multiple sclerosis: a structural MRI study. *PLoS One* 2013;8:e82422. doi:10.1371/journal.pone.0082422

57 Gold BT, Johnson NF, Powell DK, *et al.* White matter integrity and vulnerability to Alzheimer's disease: preliminary findings and future directions. *Biochim Biophys Acta* 2012;1822:416–22. doi:10.1016/j.bbadis.2011.07.009

58 Sarubbo S, De Benedictis A, Merler S, *et al.* Towards a functional atlas of human white matter. *Hum Brain Mapp* 2015;36:3117–36. doi:10.1002/hbm.22832

59 Borroni B, Brambati SM, Agosti C, *et al.* Evidence of white matter changes on diffusion tensor imaging in frontotemporal dementia. *Arch Neurol* 2007;64:246–51. doi:10.1001/archneur.64.2.246

60 Asllani I, Habeck C, Scarmeas N, *et al.* Multivariate and univariate analysis of continuous arterial spin labeling perfusion MRI in Alzheimer's disease. *J Cereb Blood Flow Metab* 2008;28:725–36. doi:10.1038/sj.jcbfm.9600570

61 Binnewijzend MAA, Kuijer JPA, Benedictus MR, *et al.* Cerebral blood flow measured with 3D pseudocontinuous arterial spin-labeling MR imaging in Alzheimer disease and mild cognitive impairment: a marker for disease severity. *Radiology* 2013;267:221–30. doi:10.1148/radiol.12120928

62 Binnewijzend MAA, Kuijer JPA, van der Flier WM, *et al.* Distinct perfusion patterns in Alzheimer's disease, frontotemporal dementia and dementia with Lewy bodies. *Eur Radiol* 2014;24:2326–33. doi:10.1007/s00330-014-3172-3

63 Shah A, Jhawar SS, Goel A. Analysis of the anatomy of the Papez circuit and adjoining limbic system by fiber dissection techniques. *J Clin Neurosci* 2012;19:289–98. doi:10.1016/j.jocn.2011.04.039

64 Braak H, Braak E. Neuropathological stageing of Alzheimer-related changes. *Acta Neuropathol* 1991;82:239–59.http://www.ncbi.nlm.nih.gov/pubmed/1759558

65 Sachdev PS, Zhuang L, Braidy N, *et al.* Is Alzheimer's a disease of the white matter? *Curr Opin Psychiatry* 2013;26:244–51. doi:10.1097/YCO.0b013e32835ed6e8

66 Rosen HJ, Allison SC, Schauer GF, *et al.* Neuroanatomical correlates of behavioural disorders in dementia. *Brain* 2005;128:2612–25. doi:10.1093/brain/awh628

67 Seelaar H, Rohrer JD, Pijnenburg Y a L, *et al.* Clinical, genetic and pathological heterogeneity of frontotemporal dementia: a review. *J Neurol Neurosurg Psychiatry* 2011;82:476–86. doi:10.1136/jnnp.2010.212225

68 Seeley WW, Crawford R, Rascovsky K, *et al.* Frontal paralimbic network atrophy in very mild behavioral variant frontotemporal dementia. *Arch Neurol* 2008;65:249–55. doi:10.1001/archneurol.2007.38

69 Dopper EGP, Rombouts SARB, Jiskoot LC, *et al.* Structural and functional brain connectivity in presymptomatic familial frontotemporal dementia. *Neurology* 2014;83:e19–26. doi:10.1212/WNL.0000000000000583

70 Whitwell JL, Josephs KA. Recent advances in the imaging of frontotemporal dementia. *Curr Neurol Neurosci Rep* 2012;12:715–23. doi:10.1007/s11910-012-0317-0

71 Whitwell JL, Boeve BF, Weigand SD, *et al.* Brain atrophy over time in genetic and sporadic frontotemporal dementia: a study of 198 serial magnetic resonance images. *Eur J Neurol* 2015;22:745–52. doi:10.1111/ene.12675

72 Broe M, Hodges JR, Schofield E, *et al.* Staging disease severity in pathologically confirmed cases of frontotemporal dementia. *Neurology* 2003;60:1005–11. doi:10.1212/01.WNL.0000052685.09194.39

73 Zhou J, Greicius MD, Gennatas ED, *et al.* Divergent network connectivity changes in behavioural variant frontotemporal dementia and Alzheimer's disease. *Brain* 2010;133:1352–67. doi:10.1093/brain/awq075

74 Du A-T, Schuff N, Kramer JH, *et al.* Different regional patterns of cortical thinning in Alzheimer's disease and frontotemporal dementia. *Brain* 2007;130:1159–66. doi:10.1093/brain/awm016

75 Rohrer JD, Ridgway GR, Modat M, *et al.* Distinct profiles of brain atrophy in frontotemporal lobar degeneration caused by progranulin and tau mutations. *Neuroimage* 2010;53:1070–6. doi:10.1016/j.neuroimage.2009.12.088

76 Jones DK. The effect of gradient sampling schemes on measures derived from diffusion tensor MRI: a Monte Carlo study. *Magn Reson Med* 2004;51:807–15. doi:10.1002/mrm.20033

SUPPLEMENT

Supplemental Table 1. White matter tracts affected in Alzheimer's disease (AD) and/or behavioural variant frontotemporal dementia (bvFTD) based on the tract-based spatial statistics (TBSS) ($p<0.05$) analysis of fractional anisotropy (FA). Tractography tract thresholds based on De Groot et al. (2015), multiplied with a factor of eight to correct for the difference in resolution.

White matter tract	Tractography threshold
Anterior thalamic radiation (ATR)	0.016
Cingulum (cingulate gyrus)	0.08
Cingulum (parahippocampal region)	0.16
Forceps major (FMa)	0.04
Forceps minor (FMi)	0.08
Inferior fronto-occipital fasciculus (IFOF)	0.08
Inferior longitudinal fasciculus (ILF)	0.04
Superior longitudinal fasciculus (SLF)	0.008
Uncinate fasciculus (UF)	0.08

Supplemental Table 2. Grey matter regions of interest (ROIs) and their abbreviations.

Lobe	Gyrus	Abbr.	Consisting of:
Frontal	Superior frontal gyrus	SFG	Central superior frontal gyrus Anterior superior frontal gyrus
	Middle frontal gyrus	MFG	
	Inferior frontal gyrus	IFG	
	Straight gyrus		
	Orbitofrontal gyrus	OFG	Anterior orbital gyrus Medial orbital gyrus Lateral orbital gyrus Posterior orbital gyrus
	Subcallosal area		
	Anterior cingulate cortex	ACC	
	Insula		
	Precentral gyrus		
Temporal	Anterior temporal lobe	ATL	Medial anterior temporal lobe Lateral anterior temporal lobe
	Posterior temporal lobe	PTL	
	Amygdala		
	Hippocampal formation	HF	Hippocampus Parahippocampal gyrus
	Superior temporal gyrus	STG	
	Inferior temporal gyrus	ITG	
	Fusiform gyrus		
Parietal	Postcentral gyrus		
	Posterior cingulate cortex	PCC	
	Precuneus		
	Remainder of parietal lobe		
Occipital	Lingual gyrus		
	Cuneus		
	Lateral remainder of occipital lobe		
Subcortical	Thalamus		
	Putamen		
	Caudate		
	Nucleus accumbens		

Regions of interest (ROIs) assessed for grey matter volume and cerebral flood flow. Parcellated gyri (according to (Gousias et al., 2008; Hammers et al., 2003), right column) were combined (middle column) for analysis.

Supplemental Table 3. Post-hoc two sample t-test for FA investigating AD < controls (n=29; $p_{corrected}$<0.05; k=50). k= voxel; L = left; R = right.

Cluster size (k)	White matter tracts within cluster
8687	L, R anterior thalamic radiation L, R body of the corpus callosum L, R cingulum L corticospinal tract
	L forceps major L, R forceps minor L, R genu of the corpus callosum
	L, R inferior fronto-occipital fasciculus
	L inferior longitudinal fasciculus
	L posterior corona radiata
	L splenium of the corpus callosum L, R superior corona radiata
	L, R superior longitudinal fasciculus
	L, R uncinate fasciculus
1691	R cingulum R corticospinal tract R forceps major R inferior fronto-occipital fasciculus R inferior longitudinal fasciculus R posterior corona radiata R splenium of the corpus callosum
	R superior longitudinal fasciculus
1469	R cingulum R forceps major R inferior fronto-occipital fasciculus R inferior longitudinal fasciculus
1313	L anterior thalamic radiation
	L cingulum L forceps major L inferior fronto-occipital fasciculus L inferior longitudinal fasciculus
	L splenium of the corpus callosum
	L superior longitudinal fasciculus
92	L forceps major L splenium of the corpus callosum
51	R superior longitudinal fasciculus

Supplemental Table 4. Post-hoc two sample t-test for FA investigating bvFTD < controls (n=20; $p_{corrected}$<0.05; k=50). k = voxel; L = left; R = right.

Cluster size (k)	White matter tracts within cluster
55201	L, R anterior corona radiata L, R anterior thalamic radiation L, R body of the corpus callosum L, R cingulum L, R corticospinal tract L, R Genu of the corpus callosum
	L, R forceps major
	L, R forceps minor
	L, R inferior fronto-occipital fasciculus
	L, R inferior longitudinal fasciculus L, R splenium of the corpus callosum L, R superior corona radiata L, R superior longitudinal fasciculus
691	R anterior thalamic radiation
	R inferior fronto-occipital fasciculus
204	R anterior corona radiata
161	L superior longitudinal fasciculus
105	L forceps major L inferior fronto-occipital fasciculus L inferior longitudinal fasciculus
93	L forceps major L inferior fronto-occipital fasciculus
	L inferior longitudinal fasciculus
59	R inferior fronto-occipital fasciculus R inferior longitudinal fasciculus
55	R corticospinal tract
52	L forceps major
	L inferior fronto-occipital fasciculus
	L inferior longitudinal fasciculus

Supplemental Table 5. Post-hoc two sample t-test for FA investigating bvFTD < AD (n=27; $p_{corrected}$<0.05; k=50). k = voxel; L = left; R = right.

Cluster size (k)	White matter tracts within cluster
36853	L, R anterior corona radiata
	L, R anterior thalamic radiation
	L, R body of the corpus callosum
	L, R cingulum
	L, R corticospinal tract
	L, R Genu of the corpus callosum
	R forceps major
	L, R forceps minor
	L, R inferior fronto-occipital fasciculus
	L, R inferior longitudinal fasciculus
	R splenium of the corpus callosum
	R superior corona radiata
	L, R superior longitudinal fasciculus
	L, R Uncinate fasciculus
1488	L cingulum
	L forceps major
	L posterior corona radiata
	L splenium of the corpus callosum
854	R cingulum
	R splenium of the corpus callosum
683	L superior longitudinal fasciculus
280	R corticospinal tract
146	L inferior longitudinal fasciculus
136	L posterior thalamic radiation
	L inferior longitudinal fasciculus
121	R anterior thalamic radiation
117	R cingulum
	R forceps major
102	L superior longitudinal fasciculus
100	L corticospinal tract
95	R cingulum
95	R superior longitudinal fasciculus
85	L superior longitudinal fasciculus
61	L superior longitudinal fasciculus
53	L superior longitudinal fasciculus

Supplemental Table 6. ROIs that showed significant differences in GM volume between controls, bvFTD and AD patients. Shown are median nGM volume [% ICV] and 25th and 75th percentile (in parentheses).

	Region of interest Median (25th-75th %ile)	Controls		BvFTD		AD	
		Mean rank	Median (25th-75th %ile)	Mean rank	Median (25th-75th %ile)	Mean rank	
Supratentorial cortex		35.9 (34.6-38.2)	26	28.0 (26.3-32.1)	8[a]	33.1 (31.6-35.4)	17
L	Superior frontal gyrus	1.68 (1.59-1.78)	24	1.10 (0.95-1.47)	7[a]	1.60 (1.57-1.80)	22[c]
R	Superior frontal gyrus	1.65 (1.55-1.80)	25	1.15 (0.97-1.35)	8[a]	1.61 (1.44-1.74)	21[c]
L	Middle frontal gyrus	1.35 (1.23-1.42)	25	0.90 (0.76-1.17)	8[a]	1.21 (1.19-1.34)	20
R	Middle frontal gyrus	1.37 (1.23-1.47)	26	0.96 (0.69-1.13)	7[a]	1.24 (1.12-1.41)	20[c]
L	Inferior frontal gyrus	0.63 (0.58-0.69)	25	0.40 (0.38-0.56)	8[a]	0.59 (0.52-0.62)	19
R	Inferior frontal gyrus	0.59 (0.55-0.62)	24	0.42 (0.34-0.46)	7[a]	0.56 (0.45-0.63)	22[c]
L	Straight gyrus	0.17 (0.14-0.18)	26	0.10 (0.08-0.14)	9[a]	0.14 (0.13-0.16)	17
R	Straight gyrus	0.19 (0.16-0.20)	25	0.12 (0.090.13)	7[a]	0.17 (0.14-0.19)	20[c]
L	Orbitofrontal gyrus	0.81 (0.73-0.86)	25	0.46 (0.36-0.74)	10[a]	0.77 (0.70-0.80)	18
R	Orbitofrontal gyrus	0.82 (0.76-0.88)	24	0.49 (0.42-0.65)	8[a]	0.78 (0.70-0.84)	19
R	Anterior cingulate cortex	0.35 (0.31-0.39)	25	0.26 (0.20-0.29)	7[a]	0.32 (0.28-0.40)	21[c]
L	Insula	0.54 (0.52-0.56)	25	0.39 (0.35-0.50)	9[a]	0.50 (0.46-0.52)	18
R	Insula	0.50 (0.49-0.52)	26	0.37 (0.34-0.45)	9[a]	0.46 (0.45-0.49)	18
L	Precentral gyrus	0.94 (0.89-1.04)	24	0.87 (0.76-0.88)	10[a]	0.97 (0.85-1.01)	20

R	Precentral gyrus	0.93 (0.85-1.01)	23	0.82 (0.72-0.88)	11[a]	0.91 (0.78-1.00)	21
L	Anterior temporal lobe	0.47 (0.42-0.55)	26	0.35 (0.30-0.40)	9[a]	0.42 (0.35-0.47)	18
R	Anterior temporal lobe	0.49 (0.44-0.55)	25	0.34 (0.25-0.39)	7[a]	0.44 (0.43-0.49)	20[c]
L	Posterior temporal lobe	1.72 (1.64-1.88)	25	1.60 (1.46-1.68)	15	1.57 (1.47-1.58)	14[b]
L	Amygdala	0.09 (0.08-0.10)	26	0.08 (0.07-0.09)	14	0.08 (0.07-0.09)	14[b]
L	Hippocampal formation	0.39 (0.37-0.43)	27	0.32 (0.28-0.36)	11[a]	0.36 (0.29-0.38)	15[b]
R	Hippocampal formation	0.39 (0.36-0.42)	26	0.28 (0.27-0.37)	9[a]	0.37 (0.33-0.39)	18
L	Superior temporal gyrus	0.73 (0.69-0.77)	23	0.59 (0.55-0.68)	11[a]	0.72 (0.65-0.78)	21
R	Superior temporal gyrus	0.78 (0.70-0.82)	25	0.60 (0.50-0.69)	10[a]	0.70 (0.64-0.79)	18
L	Inferior temporal gyrus	0.71 (0.65-0.77)	26	0.58 (0.39-0.63)	10[a]	0.66 (0.50-0.70)	17
R	Inferior temporal gyrus	0.76 (0.67-0.82)	26	0.50 (0.38-0.58)	8[a]	0.64 (0.56-0.76)	18
L	Fusiform gyrus	0.22 (0.19-0.24)	25	0.17 (0.15-0.19)	9[a]	0.21 (0.17-0.24)	19
R	Fusiform gyrus	0.22 (0.18-0.23)	23	0.16 (0.12-0.19)	11[a]	0.22 (0.15-0.24)	21
R	Postcentral gyrus	0.78 (0.73-0.85)	25	0.67 (0.56-0.76)	12[a]	0.73 (0.66-0.78)	17
L	Posterior cingulate cortex	0.34 (0.30-0.35)	24	0.27 (0.24-0.32)	12[a]	0.31 (0.27-0.34)	18
R	Posterior cingulate cortex	0.34 (0.32-0.36)	26	0.27 (0.23-0.32)	12[a]	0.28 (0.27-0.31)	15[b]
L	Precuneus	1.27 (1.17-1.31)	26	1.06 (1.03-1.13)	10[a]	1.15 (1.05-1.20)	16[b]
R	Precuneus	1.28 (1.17-1.39)	27	1.01 (0.88-1.12)	9[a]	1.15 (0.99-1.19)	16[b]
L	Remainder of parietal lobe	1.35 (1.28-1.46)	27	1.10 (1.02-1.23)	11[a]	1.14 (1.09-1.26)	13[b]
R	Remainder of parietal lobe	1.33 (1.27-1.46)	26	1.14 (0.88-1.29)	13[a]	1.17 (0.98-1.30)	13[b]

R	Lingual gyrus	0.53 (0.51-0.57)	25	0.51 (0.47-0.51)	16	0.48 (0.45-0.52)	13[b]
R	Cuneus	0.38 (0.35-0.40)	24	0.34 (0.32-0.39)	18	0.31 (0.27-0.36)	12[b]
R	Lateral remainder of occipital lobe	1.54 (1.43-1.63)	24	1.38 (1.12-1.48)	14	1.38 (1.36-1.51)	17
R	Thalamus	0.17 (0.16-0.18)	25	0.14 (0.11-0.18)	15	0.15 (0.13-0.16)	14[b]
L	Caudate	0.20 (0.17-0.21)	23	0.15 (0.12-0.18)	11	0.18 (0.17-0.22)	21
R	Caudate	0.21 (0.18-0.23)	24	0.15 (0.13-0.19)	10[a]	0.19 (0.17-0.21)	19
L	Nucleus accumbens	0.022 (0.021-0.027)	27	0.017 (0.014-0.019)	11[a]	0.018 (0.016-0.021)	15[b]
L	Putamen	0.17 (0.17-0.20)	24	0.15 (0.11-0.17)	13[a]	0.15 (0.13-.19)	17
R	Putamen	0.15 (0.13-0.17)	24	0.12 (0.09-0.15)	12[a]	0.13 (0.12-.15)	19

Median nGM volumes [% ICV] and 25th and 75th percentile in ROIs for which post hoc pairwise comparisons showed significant differences between controls, bvFTD and AD patients. The mean ranks represent the group means of the rank-ordered nGM data in that particular ROI. These mean ranks were compared to assess differences between groups rather than the median because group distributions were not similarly shaped.
nGM = normalised gray matter; ICV = intracranial volume; ROIs = regions of interest; bvFTD = behavioural variant frontotemporal dementia; AD = Alzheimer's disease; L = left; R = right.
[a] mean ranks controls>bvFTD, $p<0.05$
[b] mean ranks controls>AD, $p<0.05$
[c] mean ranks AD>bvFTD, $p<0.05$

Supplemental Table 7. ROIs that showed significant differences in cCBF (ml/100g GM/min) between controls, bvFTD and AD patients. Shown are median cCBF and 25th and 75th percentile (in parentheses).

Region of interest Median (25th-75th %ile)		Controls		BvFTD		AD	
		Mean rank	Median (25th-75th %ile)	Mean rank	Median (25th-75th %ile)	Mean rank	
L	Orbitofrontal gyrus	6.34 (5.58-6.85)	19	7.07 (5.93-8.68)	26[a]	5.11 (4.63-6.56)	12
R	Orbitofrontal gyrus	5.91 (4.93-6.34)	19	6.50 (5.96-8.06)	27[a]	5.19 (4.53-5.93)	12
L	Posterior temporal lobe	2.56 (2.27-2.71)	22	2.60 (1.84-2.92)	21	1.90 (1.79-2.30)	12[b]
R	Posterior temporal lobe	2.49 (2.08-2.27)	23	2.20 (1.89-2.62)	19	1.89 (1.78-2.08)	12[b]
R	Hippocampal formation	10.00 (9.25-10.84)	18	12.09 (10.48-13.21)	28[a]	9.17 (8.71-10.02)	12
L	Superior temporal gyrus	6.70 (6.00-7.32)	22	7.31 (5.34-8.00)	24[a]	5.47 (4.52-6.63)	10[b]
R	Inferior temporal gyrus	6.01 (5.27-7.13)	19	6.98 (5.98-8.37)	26[a]	4.83 (4.59-7.00)	13
R	Fusiform gyrus	16.90 (13.26-20.75)	26	19.13 (17.18-19.97)	20[a]	14.35 (9.71-16.20)	11
L	Posterior cingulate cortex	18.38 (15.53-19.05)	23	15.55 (14.19-19.00)	19	14.49 (12.18-16.08)	11[b]
L	Precuneus	3.21 (2.92-3.84)	23	3.06 (2.46-4.25)	20	2.44 (1.98-3.19)	11[b]

R	Precuneus	3.51 (3.02-3.77)	23	3.37 (2.47-4.33)	21	2.49 (2.11-3.04)	11[b]
R	Lateral remainder of occipital lobe	2.77 (2.18-2.99)	23	2.16 (1.57-2.93)	18	2.11 (1.31-2.31)	12[b]

cCBF and 25th and 75th percentile (values divided by 1000). ROIs for which post-hoc pairwise comparisons showed significant different mean ranks between controls, bvFTD and AD patients are shown. The mean ranks represent the group means of the rank-ordered CBF data in that particular ROI. These mean ranks were compared to assess differences between groups rather than the median because group distributions were not similarly shaped.

cCBF = corrected cerebral blood flow; ROIs = regions of interest; bvFTD = behavioural variant frontotemporal dementia; AD = Alzheimer's disease; L = left; R = right.

[a] mean ranks bvFTD>AD, $p<0.05$

[b] mean ranks controls>AD, $p<0.05$

Supplemental Table 8. Within-group correlations between WM microstructure and nGM volume or cCBF exceeding rho≥0.6 for either AD, bvFTD or controls. Significant correlations are printed in bold.

WM tract	GM region	WM-GM correlation coefficient		
		Controls	BvFTD	AD
R ATR FA	R HF nGM volume	0.150	0.142	**0.694**
R ATR MD	R HF nGM volume	0.127	-0.335	**-0.607**
R CGc FA	R ACC/subcallosal area cCBF	-0.077	0.283	**0.648**
R CGc FA	R precuneus/PCC cCBF	0.257	**0.750**	0.527
L CGc MD	L ACC/subcallosal area nGM volume	-0.006	**-0.683**	0.009
R CGc MD	R precuneus/PCC cCBF	-0.178	**-0.867**	**-0.648**
R CGh FA	R precuneus/PCC cCBF	-0.003	**0.933**	-0.382
L CGh MD	L HF/ATL nGM volume	0.216	-0.517	**-0.645**
R CGh MD	R HF/ATL nGM volume	-0.001	**-0.767**	-0.445
L CGh MD	L precuneus/PCC cCBF	-0.394	-0.050	-0.600
R CGh MD	R precuneus/PCC cCBF	0.323	-0.650	-0.091
R FMa FA	R occipital cCBF	0.100	-0.617	-0.164
R IFOF FA	R occipital cCBF	-0.104	0.400	**0.636**
L IFOF MD	L occipital cCBF	0.023	-0.350	**-0.748**
R IFOF MD	R occipital cCBF	-0.020	-0.600	-0.438
R IFOF MD	R occipital nGM volume	**-0.765**	-0.200	-0.137
L IFOF MD	L OFG/IFG nGM volume	-0.200	**-0.717**	-0.273
R IFOF MD	R OFG/IFG nGM volume	**-0.546**	-0.517	**-0.761**
R ILF MD	R occipital nGM volume	**-0.765**	-0.617	-0.318
R ILF MD	R ITG/STG/ATL nGM volume	**-0.577**	**-0.767**	**-0.827**
R SLF MD	R ITG/PTL nGM volume	-0.182	**-0.683**	-0.182
L SLF MD	L precentral/IFG nGM volume	**-1.000**	**-1.000**	**-1.000**
R SLF MD	R precentral/IFG nGM volume	-0.452	**-0.700**	-0.582
L UF MD	L IFG/OFG cCBF	0.026	0.533	-0.624
L UF MD	L IFG/OFG nGM volume	-0.189	**-0.733**	-0.027
L UF MD	L STG/ATL nGM volume	-0.219	**-0.750**	-0.227

WM = white matter; nGM = normalised grey matter, cCBF = corrected cerebral blood flow; bvFTD = behavioural variant frontotemporal dementia; AD = Alzheimer's disease; FA = fractional anisotropy; L = left; R = right; MD = mean diffusivity; ATR = anterior thalamic radiation; CGc = cingulum (cingulate gyrus); CGh = cingulum (hippocampus); FMa = forceps major; IFOF = inferior fronto-occipital fasciculus; ILF = inferior longitudinal fasciculus; SLF = superior longitudinal fasciculus; UF = uncinate fasciculus; HF = hippocampal formation; = OFG = orbitofrontal gyrus; IFG = inferior frontal gyrus; ACC = anterior cingulate cortex; PCC = posterior cingulate cortex; ATL = anterior temporal lobe; ITG = inferior temporal gyrus; STG = superior temporal gyrus; PTL = posterior temporal lobe.

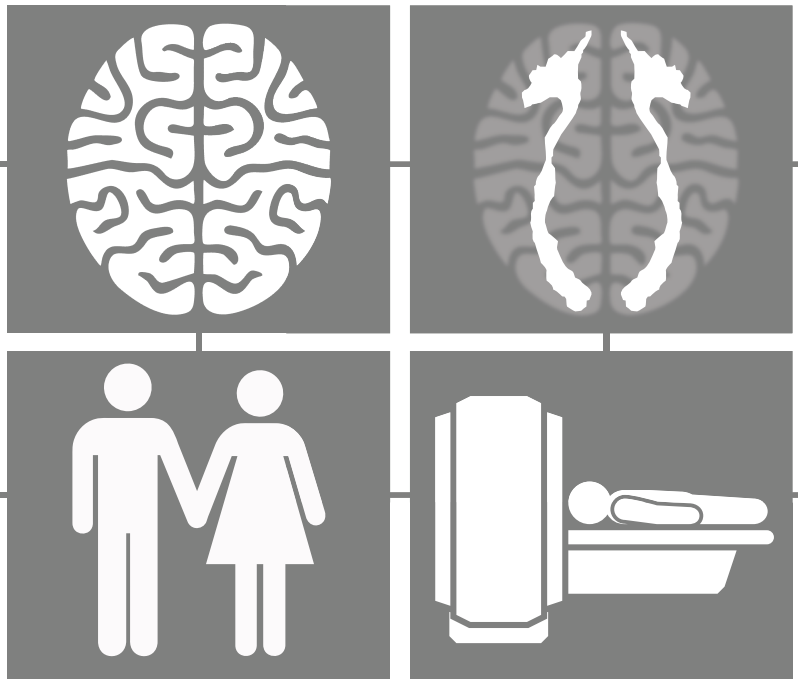

Section 3

Advanced MRI in early-stage dementia symptomatology

Chapter 3.1

Microstructural white matter is associated with specific cognitive domains in early-stage behavioural variant frontotemporal dementia and Alzheimer's disease

Rozanna Meijboom
Rebecca M.E. Steketee
Lize C. Jiskoot
Aad van der Lugt
John C. van Swieten
Marion Smits

Submitted

ABSTRACT

White matter (WM) microstructure has been associated with abnormal and normal cognitive functioning. In behavioural variant frontotemporal dementia (bvFTD) and Alzheimer's disease (AD) abnormalities of WM microstructure are observed. It can be postulated that specific symptomatology in bvFTD and AD is related to specific abnormalities of WM microstructure. This is of interest in early-stage bvFTD and AD, when symptoms may still be mild or unspecific, and microstructural WM abnormalities are already present. We investigated associations between cognition and WM microstructure in early-stage AD and bvFTD, to assess whether different WM tracts play a role in early-stage symptomatology of AD and bvFTD.

Eleven AD and 12 bvFTD early-stage patients, and 18 controls underwent diffusion tensor imaging at 3T. WM tract diffusivity measures and cognitive scores were established, and compared between groups. Correlations between diffusion and cognition were calculated for both AD and bvFTD.

We observed that attention and executive deficits were associated with WM microstructure abnormalities of several WM tracts in bvFTD, and to a lesser extent in AD. Language deficits were associated with WM microstructure abnormality in AD, and to a lesser extent normal language functioning was associated with WM microstructure in bvFTD. Additionally, normal memory functioning in bvFTD, as well as normal visuoconstructive functioning in AD was associated with WM microstructure abnormality. Evident memory deficits were not associated with any WM tract abnormalities in AD.

In conclusion, there is an association between cognitive functioning and WM microstructure of specific WM tracts in early-stage AD and bvFTD patients. This suggests that specific WM tracts play an important role in cognitive functioning, and are not universally involved in all affected cognitive domains in early-stage AD and bvFTD.

1. INTRODUCTION

Behavioural variant frontotemporal dementia (bvFTD) and Alzheimer's disease (AD) are two common diseases underlying presenile dementia (age<65 years). BvFTD is mainly characterised by behavioural symptoms: disinhibition, apathy, loss of sympathy or empathy, stereotypical behaviour and hyperorality [1]. Additionally, these patients present with cognitive abnormalities in executive functioning [1], and, although not a core characteristic, they may also present with memory deficits [2,3]. AD is mainly characterised by cognitive abnormalities, particularly in the domain of learning and retrieving new information. Other cognitive difficulties in AD include impaired reasoning and handling of complex tasks, visuospatial deficits and impaired language functioning. Additionally, some AD patients may present with behavioural changes such as mood fluctuations, social withdrawal and impaired motivation [4].

Brain abnormalities are thought to underlie the specific bvFTD and AD symptomatology, such as frontotemporal grey matter (GM) atrophy in bvFTD and temporoparietal GM atrophy in AD [1,4,5]. White matter (WM) microstructure changes are also observed in both bvFTD and AD, in frontal, temporal and parietal WM tracts [6–9] and have been associated with symptomatology in dementia [6,10]. WM microstructure is also associated with normal cognitive functioning (e.g. executive functioning, language, memory and visuoconstructive functioning) [11]. The superior longitudinal fasciculus for instance is well-known for its role in language functioning [12], and the uncinate fasciculus for its role in behavioural functioning [10,13–15].

Given the functional association of white matter tracts with major cognitive domains it can be postulated that the specific symptomatology in AD and bvFTD is related to specific abnormalities of WM microstructure. This is of particular interest for the early stages of bvFTD and AD, when symptoms may still be mild or unspecific [16], and microstructural WM abnormalities are already present. As such, WM microstructure changes may aid diagnosis of early-stage AD and bvFTD. In this study we investigated the functional associations between early-stage cognition and WM microstructure in both bvFTD and AD, to assess whether different WM tracts play a role in early-stage symptomatology of AD and bvFTD.

2. METHODS

2.1 Participants

Patients were recruited in the Alzheimer Centre Southwest Netherlands. Inclusion criteria were an age between 40 and 70 years, suspected diagnosis of early AD [4] or bvFTD [1], and a Mini-Mental State Examination [17] (MMSE) score of ≥ 20. Exclusion criteria were contraindications for MRI, an expected loss to follow-up within one year; other neurological disorders, a different cause of dementia, alternative psychiatric diagnosis, and past or current substance abuse. Patients were followed for at least one year after initial diagnosis to determine diagnosis certainty of AD or bvFTD. Patients underwent the MMSE as part of their routine clinical diagnostic work-up.

Healthy controls, matched for age and gender, and without neurological or psychiatric history, were recruited through advertisement. Controls underwent neuropsychological testing and the MMSE as part of this study.

The study was approved by the local medical ethics committee. All participants gave written informed consent.

2.2 Image acquisition

An MRI protocol including structural scans was performed on a 3T GE Discovery MR750 system (GE Healthcare, Milwaukee, WI, US). DTI scans with full coverage of the supratentorial brain were acquired using a spin echo echo planar imaging sequence. Acquisition parameters consisted of: 28 total volumes with 59 axial slices each, 3 non-diffusion weighted volumes, 25 diffusion-weighted directions, scan duration 3.50 min, field of view 240mm, echo time (TE) set to minimum with mean 84.6ms (range: 81.9-90.8ms), repetition time 7930ms, array spatial sensitivity encoding technique acceleration factor 2, flip angle 90°, acquisition matrix 128x128mm, slice thickness 2.5mm, and maximum b-value 1000 s/mm^2.

2.3 Neuropsychological data acquisition

Patients underwent a neuropsychological examination performed by an experienced neuropsychologist at the Alzheimer Centre Southwest Netherlands. Cognitive domains assessed were language, memory, attention and executive functioning, and visuoconstructive functioning (Table 1).

Table 1. Cognitive domains and their specific neuropsychological tests used to assess cognitive functioning in patients and controls.

Cognitive domain	Neuropsychological test
Language	Boston Naming Test (60 items)[18]
Memory	15 Words Test[19] Digit Span of the Wechsler Adult Intelligence Scale third edition (WAIS-III)[20] Mini-Mental State Examination (MMSE) orientation questions[17]
Attention / executive functions	Trail Making Test A and B (TMT)[21] Stroop colour-word task[22] Categorical and letter fluency test[23] Modified Wisconsin Card Sorting test (WCST)[24] Letter Digit Substitution Test (LDST)[25]
Visuoconstructive functioning	Clock drawing[26]

2.4 Post-processing and statistical analysis

2.4.1 Demographical analysis

Between-group differences in age were tested using a one-way ANOVA. Between-group differences in MMSE scores were tested using a Welch-ANOVA and post-hoc Games-Howell t-tests, due to unequal variance across groups. Gender was compared across groups using chi-square tests. Analyses were done using IBM SPSS Statistics (version 21.0, New York, USA) with a significance threshold of $p<0.05$.

2.4.2 Microstructural white matter (WM) post-processing

Data were analysed using FMRIB Software Library (FSL5, Oxford, UK) [27–29]. Data were corrected for motion and eddy currents using Eddy Correct and then skull-stripped using BET [30].

Tracts known to be associated with cognitive functioning were selected for tractography: anterior thalamic radiation [31,32], cingulum [10], forceps major [31,33], forceps minor [15,31,34], inferior fronto-occipital fasciculus [35–37], inferior longitudinal fasciculus [35,38], superior longitudinal fasciculus [38,39] and uncinate fasciculus [10,15,37]. The genu and splenium of the corpus callosum were represented by respectively the forceps minor and major.

Automated probabilistic tractography (AutoPtx) [40] was used to apply a tensor fit with DTIFIT [41], followed by a FNIRT registration and a BEDPOSTX probabilistic model fit for each participant. PROBTRACKX [41,42] was then run for all selected WM tracts using default space seed, target, stop and exclusion masks available in AutoPtx [40], resulting in a participant-specific tract density image. Tract density images were normalised by dividing them by the number of fibres included in the tract, and then binarised for WM tract segmentation, based on the best-fit segmentation thresholds established by De Groot et al. (2015) [71] (see supplemental Table 1 for thresholds).

Tensor-fit images were masked with thresholded tract images using FSLstats, to acquire median fractional anisotropy (FA) and mean diffusivity (MD)for each tract.

2.4.3 Neuropsychological post-processing

Neuropsychological test scores were corrected for age and education level using a generalised linear model and then transformed to z-scores based on the average of all groups together. Z-scores were averaged for the tests assessing memory, and attention and executive functioning to establish one score per cognitive domain (a composite score) for each participant (SPSS21.0, New York, USA).

2.4.4 Analysis of cognitive and microstructural WM abnormalities

Effect of age on FA and MD was investigated using linear regression analysis and corrected for if necessary (SPSS21.0, New York, USA). To establish cognitive and microstructural WM abnormalities in patients, cognitive domain scores and WM microstructural values were compared between AD patients and controls, and bvFTD patients and controls. Due to unequal variance across groups, independent non-parametric Mann-Whitney U tests were used with a Bonferroni correction for multiple comparisons (SPSS21.0, New York, USA). Bonferroni threshold was established by dividing the significance level of p=0.05 by the number of comparisons being done: 4 for cognition and 32 for WM (p_{WM}<0.002; $p_{cognition}$<0.0125).

2.4.5 Correlational analysis

FA and MD values uncorrected for age, and z-scores (based on the average of all groups together) uncorrected for age and education were used for correlational analysis. For each left and right WM tract, correlations between the two diffusion values (FA and MD) and z-scores for the four cognitive domains were calculated. Correlational analysis was performed using a non-parametric partial correlation analysis, correcting for age and education level (SPSS21.0, New York, USA). Correlations - uncorrected for multiple comparisons due to low study power - with $p<0.05$ and $r>0.7$ were considered.

3. RESULTS

3.1 Participant and disease characteristics

Eleven AD patients, 12 bvFTD patients and 21 controls were included in the study. Three controls were excluded due to incidental structural imaging findings and one control due to missing neuropsychological data. Two bvFTD patients and one AD patient were excluded from the analyses due to missing cognitive data as their neuropsychological exams were performed elsewhere as part of their routine clinical work-up and could not be repeated for this study. Data from 10 AD patients, 10 bvFTD patients and 17 controls were used for analysis (Table 2).

Participants did not differ in age at ($F(2,34) = .689$, $p>0.05$) or gender at ($\chi^2(2,34) = 1.409$, $p>0.05$). MMSE score was different between AD and controls only ($F(2,34) = 16.123$, $p<0.001$).

Table 2. Demographic characteristics.

Group	N	Mean age (SD)	Mean MMSE (SD)
BvFTD	10 (6 male)	59.5(8.2)	27.4 (2.1)
AD	10 (7 male)	62.8 (5.0)	25.2 (2.0)
Controls	17 (8 male)	60.5 (6.2)	29.1 (1.0)

BvFTD = behavioural variant frontotemporal dementia, AD = Alzheimer's disease, N = sample size.. SD = standard deviation. MMSE = Mini-Mental State Examination.

3.2 Cognitive and microstructural WM abnormalities

In comparison with controls, attention and executive functioning was affected in bvFTD and AD, and language and memory in AD only (Table 3).

In bvFTD in comparison with controls (Table 4), decreased FA and increased MD was observed in all WM tracts bilaterally, except for the left anterior thalamic radiation and the forceps major where FA was normal. In AD in comparison with controls (Table 4), decreased FA was observed in the right inferior longitudinal and superior longitudinal fasciculus, bilateral hippocampal and cingulate cingulum and inferior fronto-occipital fasciculus, forceps major and minor. In AD in comparison with controls, increased MD was observed in nearly all WM tracts, except for the bilateral cingulate cingulum and superior longitudinal fasciculus.

Table 3. Mean cognitive domain z-scores for bvFTD, AD and controls. Scores are corrected for age and education level.

	BvFTD	**AD**	**Controls**
Language	-0.22	**-0.64**	0.60
Attention and executive functioning	**-0.42**	**-0.46**	0.50
Memory	-0.13	**-0.65**	0.57
Visuoconstructive functioning	-0.48	-0.09	0.43

bvFTD = behavioural variant frontotemporal dementia , AD=Alzheimer's disease.
Vs controls, $p_{bonferroni}$<0.0125

3.3 Correlations between cognition and microstructural WM

In bvFTD (Table 5, Figure 1), normal language functioning correlated with normal FA in the left anterior thalamic radiation. Attention and executive deficits correlated with FA abnormalities in the right cingulate cingulum, right inferior fronto-occipital fasciculus, right inferior and superior longitudinal fasciculus, and with MD abnormalities in the left cingulate cingulum, left hippocampal cingulum, left inferior fronto-occipital fasciculus and forceps minor, and with both abnormal FA and MD in the left uncinate fasciculus. Normal memory functioning correlated with abnormal MD in the left cingulate cingulum.

Table 4. Mean FA ($x10^{-3}$), and MD ($x10^{-3}$) for bvFTD, AD and controls for WM tracts associated with cognition.

WM tract	L/R	FA			MD		
		BvFTD	AD	Controls	BvFTD	AD	Controls
ATR	L	324.29	330.01	326.80	**0.90***	**0.83***	0.82
	R	**317.96***	319.82	321.64	**0.94***	**0.84***	0.82
CGC	L	**395.61***	**421.47***	435.99	**0.87***	0.80	0.81
	R	**349.37***	**381.22***	402.68	**0.88***	0.81	0.81
CGH	L	**225.18***	**258.71***	265.98	**0.96***	**0.88***	0.85
	R	**214.96***	**250.00***	267.64	**1.04***	**0.87***	0.84
IFOF	L	**378.17***	**406.50***	413.75	**0.89***	**0.83***	0.83
	R	**378.87***	**407.13***	423.97	**0.90***	**0.84***	0.82
ILF	L	**371.79***	386.73	386.45	**0.87***	**0.83***	0.83
	R	**383.24***	**391.74***	402.46	**0.87***	**0.83***	0.82
SLF	L	**309.20***	324.83	329.22	**0.84***	0.80	0.80
	R	**309.07***	**325.62***	330.37	**0.85***	0.79	0.80
UF	L	**289.85***	330.61	354.94	**0.96***	**0.84***	0.82
	R	**275.48***	325.35	336.64	**1.01***	**0.85***	0.84
FMi	n/a	**311.75***	**386.05***	418.34	**0.98***	**0.85***	0.82
FMa	n/a	381.67	**380.62***	397.56	**0.83***	**0.82***	0.81

FA = fractional anisotropy, MD = mean diffusivity, WM=white matter, bvFTD = behavioural variant frontotemporal dementia , AD=Alzheimer's disease, ATR = anterior thalamic radiation, CGC = cingulum (cingulate), CGH = cingulum (hippocampal), IFOF = inferior fronto-occipital fasciculus, ILF = inferior longitudinal fasciculus, SLF = superior longitudinal fasciculus, UF = uncinate fasciculus, FMi = forceps minor, FMa = forceps major, L= left, R=right.

***Vs controls, $p_{bonferroni}$<0.002**

Figure 1. Functional associations between white matter (WM) microstructure and cognitive domains in Alzheimer's disease (AD) and behavioural variant frontotemporal dementia (bvFTD).

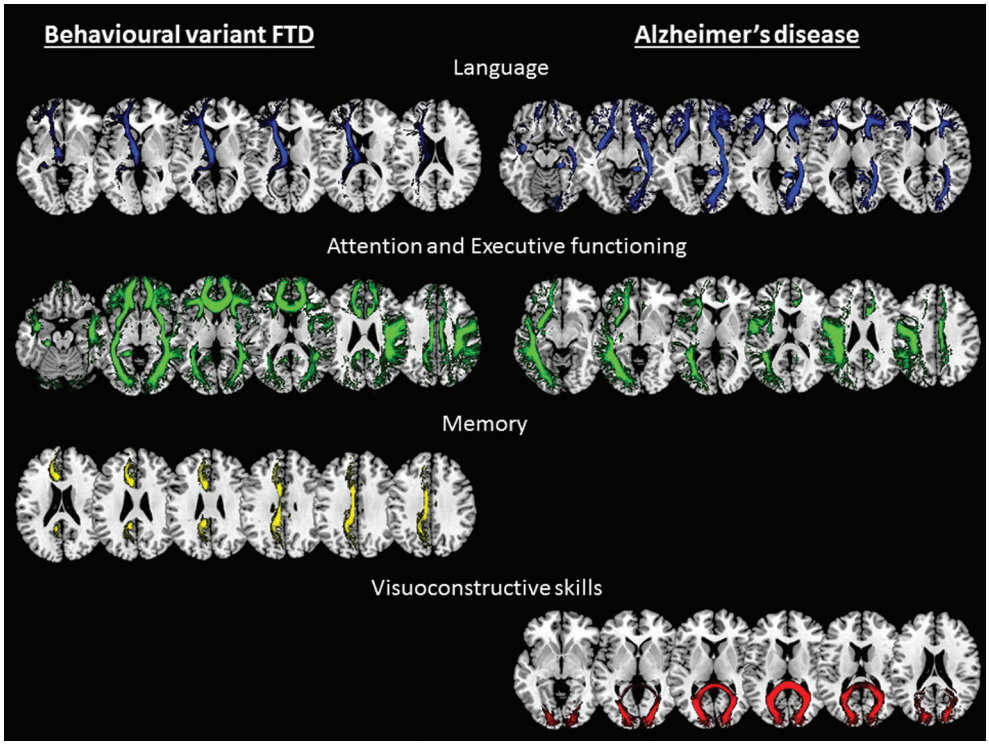

In AD (Table 5, Figure 1), language deficits correlated with FA abnormalities in the right inferior fronto-occipital fasciculus, and with MD abnormalities in the right hippocampal cingulum. Language deficits also correlated with FA in the uncinate fasciculus, where FA was normal. Attention and executive deficits correlated with normal MD in the right cingulate cingulum and superior longitudinal fasciculus, and with MD abnormalities in the left uncinate and inferior longitudinal fasciculus. Visuoconstructive functioning in AD correlated with abnormal MD in the forceps major.

Table 5. Correlations between abnormal cognitive domains and affected WM microstructure (FA, MD) in AD and bvFTD.

			BvFTD				AD			
			Language	**Attention and Executive functioning**	**Memory**	**Visuoconstructive functioning**	**Language**	**Attentio and Executive functioning**	**Memory**	**Visuoconstructive functioning**
ATR	L	FA	**.754**	.255	.445	.395	.610	.072	.088	.531
		MD	.121	.651	-.479	.087	.513	.636	.504	.096
ATR	R	FA	.369	-.059	.161	-.009	.384	-.453	-.365	.216
		MD	.475	-.085	.310	-.457	.517	.527	.650	.103
CGC	L	FA	.209	-.078	.051	-.299	.207	.102	-.055	.494
		MD	-.140	**.796**	**-.820**	-.047	.349	.669	.612	-.007
CGC	R	FA	.489	**.726**	-.165	.276	.547	-.175	.400	.091
		MD	-.176	-.172	-.227	-.680	.473	**.763**	.324	.452
CGH	L	FA	.098	-.477	.317	-.691	.578	.267	.482	.512
		MD	-.072	**.738**	-.619	.183	-.165	.545	-.202	.258
CGH	R	FA	.030	-.113	.139	-.137	.534	.061	.072	.387
		MD	-.292	.251	-.597	-.461	**.845**	.514	.218	.165
IFOF	L	FA	.203	-.346	.217	-.529	.668	.011	.225	.167
		MD	.171	**.851**	-.517	.094	.106	.705	.623	-.144
IFOF	R	FA	.271	**.793**	-.222	.580	**.773**	-.030	-.058	-.073

		MD	.240	-.008	-.037	-.523	.052	.343	.347	-.436
ILF	L	FA	.568	-.282	.585	.202	.299	-.576	-.366	.595
		MD	-.018	.530	-.502	-.309	.128	**.825**	.075	-.032
ILF	R	FA	.269	**.885**	-.348	.289	.062	-.134	-.166	.642
		MD	.162	-.173	.023	-.610	.067	.276	.297	-.197
SLF	L	FA	.316	.630	-.163	.071	.178	-.593	-.415	.631
		MD	-.209	-.019	-.326	-.500	.236	**.789**	.019	-.197
SLF	R	FA	.334	**.934**	-.403	.352	.239	-.320	-.563	.510
		MD	.159	-.296	.149	-.579	.129	.514	.412	-.424
UF	L	FA	-.186	**-.846**	.426	-.356	**.740**	.424	.102	.314
		MD	.195	**.935**	-.545	.266	-.354	**.721**	.444	-.300
	R	FA	-.068	-.322	.427	.484	.431	-.536	-.181	.201
		MD	.061	.275	-.398	-.483	.296	.469	-.125	-.030
FMi		FA	-.184	-.328	.299	.232	.421	-.559	-.242	.499
		MD	.291	**.782**	-.434	.073	-.051	.258	.209	-.301
FMa		FA	.245	.696	-.254	.028	.259	-.117	-.260	.701
		MD	-.324	.016	-.366	-.696	-.261	.224	.364	**-.759**

bvFTD = behavioural variant frontotemporal dementia; AD = Alzheimer's disease; FA = fractional anisotropy; MD = mean diffusivity.
Significant ($p<0.05$) correlations are grey highlighted in bold.

4. DISCUSSION

In this study we investigated functional associations between WM microstructure and cognitive domains in bvFTD and AD separately to assess whether different WM tracts play a role in early-stage symptomatology of bvFTD and AD. We observed that attention and executive deficits were associated with WM microstructure of several WM tracts in bvFTD, and to a lesser extent in AD. WM microstructure was associated with language deficits in AD, and to a lesser extent with language functioning in bvFTD. Additionally, WM microstructure was associated with memory functioning in bvFTD, as well as with visuoconstructive functioning in AD.

WM microstructure was abnormal in all WM tracts in both early-stage AD and bvFTD but with more diffusion measures being affected in bvFTD than in AD. Among the least affected tracts were the forceps major and anterior thalamic radiation in bvFTD, and the superior longitudinal fasciculus in AD. On a neurocognitive level, we observed that attention and executive functioning was abnormal in both early-stage bvFTD and AD, and language and memory in early-stage AD.

Of all domains, attention and executive functioning shows most functional associations with WM microstructure. More associations were observed in bvFTD than in AD, which may be explained by this domain being severely affected in bvFTD , perhaps in combination with the more pronounced WM microstructure abnormalities in bvFTD than in AD [7]. In bvFTD, attention and executive functioning deficits were associated with microstructural abnormalities of the cingulate cingulum, left hippocampal cingulum, forceps minor, inferior fronto-occipital, right superior and inferior longitudinal fasciculus and left uncinate fasciculus. This is in line with previous findings linking attention and executive functioning to these particular WM tracts in various disease and/or healthy populations [10,13–15,43–52].

In AD, attention and executive deficits were associated with microstructural abnormalities of the left uncinate fasciculus and with normal WM microstructure in the right cingulate cingulum, and the left inferior and superior longitudinal fasciculus. The observed functional associations between these WM tracts and attention and executive functioning have been previously suggested in other populations [47,52–59]. Interestingly, a strong association was observed between WM microstructure not different from controls and attention and executive deficits. A possible explanation is that changes in these diffusion measures are too subtle and variable to be detected on a group level [7], but are nonetheless functionally associated with attention and executive deficits.

Language – as assessed with an object naming task - showed several functional associations with WM microstructure in AD, whereas in bvFTD only one functional association was observed. This is in line with the language deficits found in AD and not in bvFTD.

Language deficits in AD were associated with normal WM microstructure in the uncinate fasciculus and abnormal WM microstructure in the right inferior fronto-occipital fasciculus and right hippocampal cingulum in AD. The inferior fronto-occipital and uncinate fasciculi are known for their role in semantic processing [12,60,61]. However, to our knowledge, the hippocampal cingulum has not specifically been implicated with language functioning. One study has reported cingulum involvement in a syndrome with altered language functioning [62], but evident hippocampal cingulum involvement in language functioning has not been reported previously.

Normal language functioning in bvFTD was associated with WM microstructure in the left anterior thalamic radiation. Previous research has observed a similar functional relationship between the left anterior thalamic radiation and several semantic language tasks, including an object naming task [63]. It is unclear why the anterior thalamic radiation plays a role in language functioning in bvFTD specifically, but these results may suggest that the anterior thalamic radiation may be important for early language deficits in bvFTD.

Visuoconstructive functioning in AD was associated with microstructural abnormalities of the forceps major. Such a functional association has been previously reported in patients with a lesion in the forceps major/splenium [64–67]. Other WM tracts that have been previously associated with the visuoconstructive domain, for instance the superior longitudinal and inferior fronto-occipital fasciculus, were not found to be significantly associated with visuoconstructive deficits in AD [68]. This suggests that in this early stage of AD particularly microstructural abnormalities of the forceps major play an important role in visuoconstructive functioning.

Although memory is a prominently affected domain in AD [4], it was not associated with any WM tract abnormalities. This may suggest that known GM abnormalities, such as of the hippocampus, are more involved in memory than those of WM microstructure. On the other hand, when exploring the correlations without regard for significance, it was observed that most WM tracts have moderate correlations with memory, although this was more evident for bvFTD than for AD. This suggests that WM tracts may be involved in memory processes, which may become apparent in a larger sample with greater statistical power. Alternatively,

the use of composite scores may have obscured specific memory processes and their associations with WM tracts.

In bvFTD, the memory domain was not affected, but did show an association with abnormal WM microstructure of the left cingulate cingulum. This suggests a role for the affected cingulum in memory functioning in bvFTD. Such an association is supported by similar observations in previous literature, for instance in traumatic brain injury and healthy elderly [69,70].

This study knows some limitations. First, visuoconstructive functioning and language were assessed with a single neuropsychological test, which may not be representative for all aspects of these domains. However, these are validated tests, which are routinely used in clinic practice to assess these domains. Memory and attention and executive functioning were assessed with several neuropsychological tests and individual scores were transformed to one composite score for each domain. Here it could be argued that smaller and more specific effects may have become obscured, but that the cognitive domain overall is better represented. Second, sample sizes of patients were small. This is not desirable, but unfortunately inherent to clinical studies where patients are carefully selected for inclusion to establish clinically homogenous groups. Due to this underpowered sample, results were not corrected for multiple comparisons to avoid the risk of false negative results. Consequently the risk of false positives is present, but somewhat reduced by only reporting strong correlations ($r > 0.7$).

In conclusion, we found an association between cognitive deficits and specific WM microstructure abnormalities in early-stage AD and bvFTD patients. This suggests that specific WM tracts play an important role in cognitive functioning, and are not universally involved in all affected cognitive domains in AD and bvFTD.

REFERENCES

1 Rascovsky K, Hodges JR, Knopman D, *et al.* Sensitivity of revised diagnostic criteria for the behavioural variant of frontotemporal dementia. *Brain* 2011;134:2456–77. doi:10.1093/brain/awr179

2 Irish M, Devenney E, Wong S, *et al.* Neural substrates of episodic memory dysfunction in behavioural variant frontotemporal dementia with and without C9ORF72 expansions. *NeuroImage Clin* 2013;2:836–43. doi:10.1016/j.nicl.2013.06.005

3 Smits LL, van Harten AC, Pijnenburg YAL, *et al.* Trajectories of cognitive decline in different types of dementia. *Psychol Med* 2015;45:1051–9. doi:10.1017/S0033291714002153

4 McKhann GM, Knopman DS, Chertkow H, *et al.* The diagnosis of dementia due to Alzheimer's disease: recommendations from the National Institute on Aging-Alzheimer's Association workgroups on diagnostic guidelines for Alzheimer's disease. *Alzheimers Dement* 2011;7:263–9. doi:10.1016/j.jalz.2011.03.005

5 Karas G, Sluimer J, Goekoop R, *et al.* Amnestic Mild Cognitive Impairment: Structural MR Imaging Findings Predictive of Conversion to Alzheimer Disease. *Am J Neuroradiol* 2008;29:944–9. doi:10.3174/ajnr.A0949

6 Mahoney CJ, Ridgway GR, Malone IB, *et al.* Profiles of white matter tract pathology in frontotemporal dementia. *Hum Brain Mapp* 2014;35:4163–79. doi:10.1002/hbm.22468

7 Steketee RME, Meijboom R, de Groot M, *et al.* Concurrent white and gray matter degeneration of disease-specific networks in early-stage Alzheimer's disease and behavioral variant frontotemporal dementia. *Neurobiol Aging* 2016;43:119–28. doi:10.1016/j.neurobiolaging.2016.03.031

8 Bozzali M, Falini A, Franceschi M, *et al.* White matter damage in Alzheimer's disease assessed in vivo using diffusion tensor magnetic resonance imaging. 2002;:742–6.

9 Acosta-Cabronero J, Alley S, Williams GB, *et al.* Diffusion tensor metrics as biomarkers in Alzheimer's disease. *PLoS One* 2012;7:e49072. doi:10.1371/journal.pone.0049072

10 Tartaglia MC, Zhang Y, Racine C, *et al.* Executive dysfunction in frontotemporal dementia is related to abnormalities in frontal white matter tracts. *J Neurol* 2012;259:1071–80. doi:10.1007/s00415-011-6300-x

11 Cremers LGM, de Groot M, Hofman A, *et al.* Altered tract-specific white matter microstructure is related to poorer cognitive performance: The Rotterdam Study. *Neurobiol Aging* 2016;39:108–17. doi:10.1016/j.neurobiolaging.2015.11.021

12 Dick AS, Bernal B, Tremblay P. The language connectome: new pathways, new concepts. *Neuroscientist* 2014;20:453–67. doi:10.1177/1073858413513502

13 Whitwell JL, Avula R, Senjem ML, *et al.* Gray and white matter water diffusion in the syndromic variants of frontotemporal dementia. *Neurology* 2010;74:1279–87. doi:10.1212/WNL.0b013e3181d9edde

14 Agosta F, Henry RG, Migliaccio R, *et al.* Language networks in semantic dementia. *Brain* 2010;133:286–99. doi:10.1093/brain/awp233
15 Hornberger M, Geng J, Hodges JR. Convergent grey and white matter evidence of orbitofrontal cortex changes related to disinhibition in behavioural variant frontotemporal dementia. *Brain* 2011;134:2502–12. doi:10.1093/brain/awr173
16 Varma AR, Snowden JS, Lloyd JJ, *et al.* Evaluation of the NINCDS-ADRDA criteria in the differentiation of Alzheimer's disease and frontotemporal dementia. *J Neurol Neurosurg Psychiatry* 1999;66:184–8.http://www.ncbi.nlm.nih.gov/pubmed/10071097
17 Folstein MF, Folstein SE, McHugh PR. 'Mini-mental state'. A practical method for grading the cognitive state of patients for the clinician. *J Psychiatr Res* 1975;12:189–98.http://www.ncbi.nlm.nih.gov/pubmed/1202204.
18 Kaplan E, Goodglass H, Weintraub S. *The Boston Naming Test*. Philadelphia: : Lea & Febiger 1978.
19 Rey A. *L'examen clinique en psychologie*. Paris, France: : Presses Universitaires de France 1958.
20 Wechsler D. *WAIS-II Nederlandse Bewerking. Technische handleiding.* Lisse: : Harcourt Test Publishers 2005.
21 *Army Individual Test Battery. Manual of directions and scoring.* Washington, DC: : War Department, Adjutant General's office 1994.
22 Stroop J. Studies of interference in serial verbal reactions. *J Exp Psychol* 1935;18:643–62.
23 Thurstone L, Thurstone T. *Primary mental abilities*. Chigago: : Science Research Associates 1962.
24 Nelson HE. A modified card sorting test sensitive to frontal lobe defects. *Cortex* 1976;12:313–24.
25 Jolles J, Houx PJ, Van Boxtel MPJ. *Maastricht Aging Study: determinants of cognitive aging*. Maastricht, The Netherlands: : Neuropsych publishers 1995.
26 Royall DR, Cordes JA, Polk M. Clox: an executive clock drawing task. *J Neurol Neurosurg Psychiatry* 1998;64:588–94.
27 Jenkinson M, Beckmann CF, Behrens TEJ, *et al.* FSL. *Neuroimage* 2012;62:782–90. doi:10.1016/j.neuroimage.2011.09.015
28 Woolrich MW, Jbabdi S, Patenaude B, *et al.* Bayesian analysis of neuroimaging data in FSL. *Neuroimage* 2009;45:S173–86. doi:10.1016/j.neuroimage.2008.10.055
29 Smith SM, Jenkinson M, Woolrich MW, *et al.* Advances in functional and structural MR image analysis and implementation as FSL. *Neuroimage* 2004;23 Suppl 1:S208–19. doi:10.1016/j.neuroimage.2004.07.051
30 Smith SM. Fast robust automated brain extraction. *Hum Brain Mapp* 2002;17:143–55. doi:10.1002/hbm.10062

31 Duering M, Gonik M, Malik R, *et al.* Identification of a strategic brain network underlying processing speed deficits in vascular cognitive impairment. *Neuroimage* 2013;66:177–83. doi:10.1016/j.neuroimage.2012.10.084

32 Torso M, Serra L, Giulietti G, *et al.* Strategic lesions in the anterior thalamic radiation and apathy in early Alzheimer's disease. *PLoS One* 2015;10:e0124998. doi:10.1371/journal.pone.0124998

33 Staff RT, Murray AD, Deary IJ, *et al.* Generality and specificity in cognitive aging: a volumetric brain analysis. *Neuroimage* 2006;30:1433–40. doi:10.1016/j.neuroimage.2005.11.004

34 Shollenbarger SG, Price J, Wieser J, *et al.* Poorer frontolimbic white matter integrity is associated with chronic cannabis use, FAAH genotype, and increased depressive and apathy symptoms in adolescents and young adults. *NeuroImage Clin* 2015;8:117–25. doi:10.1016/j.nicl.2015.03.024

35 Epstein KA, Cullen KR, Mueller BA, *et al.* White matter abnormalities and cognitive impairment in early-onset schizophrenia-spectrum disorders. *J Am Acad Child Adolesc Psychiatry* 2014;53:362–72.e1–2. doi:10.1016/j.jaac.2013.12.007

36 Gold BT, Johnson NF, Powell DK, *et al.* White matter integrity and vulnerability to Alzheimer's disease: preliminary findings and future directions. *Biochim Biophys Acta* 2012;1822:416–22. doi:10.1016/j.bbadis.2011.07.009

37 Mike A, Strammer E, Aradi M, *et al.* Disconnection mechanism and regional cortical atrophy contribute to impaired processing of facial expressions and theory of mind in multiple sclerosis: a structural MRI study. *PLoS One* 2013;8:e82422. doi:10.1371/journal.pone.0082422

38 Sarubbo S, De Benedictis A, Merler S, *et al.* Towards a functional atlas of human white matter. *Hum Brain Mapp* 2015;36:3117–36. doi:10.1002/hbm.22832

39 Borroni B, Brambati SM, Agosti C, *et al.* Evidence of white matter changes on diffusion tensor imaging in frontotemporal dementia. *Arch Neurol* 2007;64:246–51. doi:10.1001/archneur.64.2.246

40 de Groot M, Vernooij MW, Klein S, *et al.* Improving alignment in Tract-based spatial statistics: evaluation and optimization of image registration. *Neuroimage* 2013;76:400–11. doi:10.1016/j.neuroimage.2013.03.015

41 Behrens TEJ, Woolrich MW, Jenkinson M, *et al.* Characterization and propagation of uncertainty in diffusion-weighted MR imaging. *Magn Reson Med* 2003;50:1077–88. doi:10.1002/mrm.10609

42 Behrens TEJ, Berg HJ, Jbabdi S, *et al.* Probabilistic diffusion tractography with multiple fibre orientations: What can we gain? *Neuroimage* 2007;34:144–55. doi:10.1016/j.neuroimage.2006.09.018

43 Powers JP, Massimo L, McMillan CT, *et al.* White Matter Disease Contributes to Apathy and Disinhibition in Behavioral Variant Frontotemporal Dementia. *Cogn Behav Neurol* 2014;27:206–14. doi:10.1097/WNN.0000000000000044

44 Zheng Z, Shemmassian S, Wijekoon C, *et al.* DTI correlates of distinct cognitive impairments in Parkinson's disease. *Hum Brain Mapp* 2014;35:1325–33. doi:10.1002/hbm.22256
45 Liu X, Lai Y, Wang X, *et al.* Reduced white matter integrity and cognitive deficit in never-medicated chronic schizophrenia: a diffusion tensor study using TBSS. *Behav Brain Res* 2013;252:157–63. doi:10.1016/j.bbr.2013.05.061
46 Santiago C, Herrmann N, Swardfager W, *et al.* White Matter Microstructural Integrity Is Associated with Executive Function and Processing Speed in Older Adults with Coronary Artery Disease. *Am J Geriatr Psychiatry* 2015;23:754–63. doi:10.1016/j.jagp.2014.09.008
47 Sun X, Liang Y, Wang J, *et al.* Early frontal structural and functional changes in mild white matter lesions relevant to cognitive decline. *J Alzheimers Dis* 2014;40:123–34. doi:10.3233/JAD-131709
48 Pérez-Iglesias R, Tordesillas-Gutiérrez D, McGuire PK, *et al.* White Matter Integrity and Cognitive Impairment in First-Episode Psychosis. *Am J Psychiatry* 2010;167:451–8. doi:10.1176/appi.ajp.2009.09050716
49 Downey LE, Mahoney CJ, Buckley AH, *et al.* White matter tract signatures of impaired social cognition in frontotemporal lobar degeneration. *NeuroImage Clin* 2015;8:640–51. doi:10.1016/j.nicl.2015.06.005
50 Sasson E, Doniger GM, Pasternak O, *et al.* Structural correlates of cognitive domains in normal aging with diffusion tensor imaging. *Brain Struct Funct* 2012;217:503–15. doi:10.1007/s00429-011-0344-7
51 Hatton SN, Lagopoulos J, Hermens DF, *et al.* White matter tractography in early psychosis: clinical and neurocognitive associations. *J Psychiatry Neurosci* 2014;39:417–27.http://www.ncbi.nlm.nih.gov/pubmed/25111788
52 Poletti S, Bollettini I, Mazza E, *et al.* Cognitive performances associate with measures of white matter integrity in bipolar disorder. *J Affect Disord* 2015;174:342–52. doi:10.1016/j.jad.2014.12.030
53 Murray AL, Thompson DK, Pascoe L, *et al.* White matter abnormalities and impaired attention abilities in children born very preterm. *Neuroimage* 2016;124:75–84. doi:10.1016/j.neuroimage.2015.08.044
54 Chiang H-L, Chen Y-J, Lo Y-C, *et al.* Altered white matter tract property related to impaired focused attention, sustained attention, cognitive impulsivity and vigilance in attention-deficit/hyperactivity disorder. *J Psychiatry Neurosci* 2015;40:325–35.http://www.ncbi.nlm.nih.gov/pubmed/25871496
55 Peters BD, Ikuta T, DeRosse P, *et al.* Age-Related Differences in White Matter Tract Microstructure Are Associated with Cognitive Performance from Childhood to Adulthood. *Biol Psychiatry* 2014;75:248–56. doi:10.1016/j.biopsych.2013.05.020

56 Ikuta T, Shafritz KM, Bregman J, *et al.* Abnormal cingulum bundle development in autism: a probabilistic tractography study. *Psychiatry Res* 2014;221:63–8. doi:10.1016/j.pscychresns.2013.08.002

57 Hummer TA, Wang Y, Kronenberger WG, *et al.* The relationship of brain structure to age and executive functioning in adolescent disruptive behavior disorder. *Psychiatry Res Neuroimaging* 2015;231:210–7. doi:10.1016/j.pscychresns.2014.11.009

58 Serra L, Cercignani M, Basile B, *et al.* White matter damage along the uncinate fasciculus contributes to cognitive decline in AD and DLB. *Curr Alzheimer Res* 2012;9:326–33.http://www.ncbi.nlm.nih.gov/pubmed/22272613

59 Diao L, Yu H, Zheng J, *et al.* Abnormalities of the uncinate fasciculus correlate with executive dysfunction in patients with left temporal lobe epilepsy. *Magn Reson Imaging* 2015;33:544–50. doi:10.1016/j.mri.2015.02.011

60 Ivanova M V., Isaev DY, Dragoy O V., *et al.* Diffusion-tensor imaging of major white matter tracts and their role in language processing in aphasia. *Cortex* Published Online First: May 2016. doi:10.1016/j.cortex.2016.04.019

61 Mirman D, Zhang Y, Wang Z, *et al.* The ins and outs of meaning: Behavioral and neuroanatomical dissociation of semantically-driven word retrieval and multimodal semantic recognition in aphasia. *Neuropsychologia* 2015;76:208–19. doi:10.1016/j.neuropsychologia.2015.02.014

62 Faria AV, Landau B, O'Hearn KM, *et al.* Quantitative analysis of gray and white matter in Williams syndrome. *Neuroreport* 2012;23:283–9. doi:10.1097/WNR.0b013e3283505b62

63 Han Z, Ma Y, Gong G, *et al.* White matter structural connectivity underlying semantic processing: evidence from brain damaged patients. *Brain* 2013;136:2952–65. doi:10.1093/brain/awt205

64 Tamura I, Kitagawa M, Otsuki M, *et al.* Pure Topographical Disorientation Following a Right Forceps Major of the Splenium Lesion: A Case Study. *Neurocase* 2007;13:178–84. doi:10.1080/13554790701448812

65 Putnam MC, Steven MS, Doron KW, *et al.* Cortical Projection Topography of the Human Splenium: Hemispheric Asymmetry and Individual Differences. *J Cogn Neurosci* 2010;22:1662–9. doi:10.1162/jocn.2009.21290

66 Aralasmak A, Ulmer JL, Kocak M, *et al.* Association, Commissural, and Projection Pathways and Their Functional Deficit Reported in Literature. *J Comput Assist Tomogr* 2006;30:695–715. doi:10.1097/01.rct.0000226397.43235.8b

67 Verlinden VJA, de Groot M, Cremers LGM, *et al.* Tract-specific white matter microstructure and gait in humans. *Neurobiol Aging* 2016;43:164–73. doi:10.1016/j.neurobiolaging.2016.04.005

68 Chechlacz M, Gillebert CR, Vangkilde SA, *et al.* Structural Variability within Frontoparietal Networks and Individual Differences in Attentional Functions: An Approach Using the Theory of Visual Attention. *J Neurosci* 2015;35:10647–58. doi:10.1523/JNEUROSCI.0210-15.2015

69 Wu TC, Wilde EA, Bigler ED, *et al.* Evaluating the Relationship between Memory Functioning and Cingulum Bundles in Acute Mild Traumatic Brain Injury Using Diffusion Tensor Imaging. *J Neurotrauma* 2010;27:303–7. doi:10.1089/neu.2009.1110

70 Kantarci K, Senjem ML, Avula R, *et al.* Diffusion tensor imaging and cognitive function in older adults with no dementia. *Neurology* 2011;77:26–34. doi:10.1212/WNL.0b013e31822313dc

71 de Groot M, Ikram MA, Akoudad S, et al. Tract-specific white matter degeneration in aging: The Rotterdam Study. Alzheimer's Dement 2015;11:321–30. doi:10.1016/j.jalz.2014.06.011

SUPPLEMENT

Supplemental Table 1. Tractography tract thresholds based on De Groot et al. (2015), but multiplied with a factor of eight due to the resolution difference.

White matter tract	Tractography threshold
Anterior thalamic radiation (ATR)	0.016
Cingulum (cingulate gyrus)	0.08
Cingulum (parahippocampal region)	0.16
Forceps major (FMa)	0.04
Forceps minor (FMi)	0.08
Inferior fronto-occipital fasciculus (IFOF)	0.08
Inferior longitudinal fasciculus (ILF)	0.04
Superior longitudinal fasciculus (SLF)	0.008
Uncinate fasciculus (UF)	0.08

3.1

Chapter 3.2

Hemispheric dissociation of microstructural white matter and functional connectivity abnormalities in semantic and behavioural variant frontotemporal dementia

Rozanna Meijboom
Rebecca M.E. Steketee
Leontine S. Ham
Aad van der Lugt
John C. van Swieten
Marion Smits

Accepted in Journal of Alzheimer's Disease after revision (2016)

ABSTRACT

Semantic dementia (SD) and behavioural variant frontotemporal dementia (bvFTD), subtypes of FTD, are characterised by distinct clinical symptoms and distinct neuroimaging features, with predominant *left* temporal grey matter (GM) atrophy in SD and bilateral or *right* frontal GM atrophy in bvFTD. Such different hemispheric predilection may also be reflected by other neuroimaging features, such as in brain connectivity. This study investigated white matter (WM) microstructure and functional connectivity differences between SD and bvFTD, specifically focusing on the hemispheric predilection of these differences.

Eight SD and 12 bvFTD early-stage patients, and 17 controls underwent diffusion tensor imaging and resting state functional magnetic resonance imaging at 3T. Whole-brain WM microstructure was assessed to determine distinct WM tracts affected in SD and bvFTD. For these WM tracts, diffusivity measures and lateralization indices were calculated. Functional connectivity was established for grey matter (GM) regions affected in early stage SD or bvFTD.

Whole-brain WM microstructure abnormalities were more pronounced in the left hemisphere in SD and in the right hemisphere in bvFTD. Lateralisation of tract-specific WM abnormalities was seen in SD only, towards the left hemisphere. Functional connectivity of disease-specific regions was mainly decreased in both hemispheres in SD and in the right hemisphere in bvFTD.

In conclusion, SD and bvFTD show WM microstructural and functional connectivity abnormalities in different brain regions, that are overall more pronounced in the left hemisphere in SD and in the right hemisphere in bvFTD. This indicates a hemispheric dissociation of abnormalities in brain connectivity between SD and bvFTD.

1. INTRODUCTION

Frontotemporal dementia (FTD) is a common cause of dementia in relatively young patients (<65 years). FTD is the umbrella term for several dementia subtypes affecting the frontal and/or temporal lobes. Two main subtypes of FTD are semantic dementia (SD) and behavioural variant FTD (bvFTD) [1]. Although both SD and bvFTD affect the frontotemporal regions, they are clinically different. SD is characterised by a language disorder, with core features of impaired confrontation naming and impaired single-word comprehension, and shows predominantly left anterior temporal lobe (ATL) atrophy [2–4]. In contrast, bvFTD is characterised by behavioural symptoms, such as apathy and disinhibition, and shows predominantly bilateral or right frontal lobe atrophy [3–5]. As the left hemisphere is important for language functioning [6] and the bilateral frontal lobes for behaviour [7,8], the left lateralised atrophy pattern in SD and the right-lateralised/bilateral atrophy pattern in bvFTD are likely to underlie the differences in symptomatology. It can be hypothesised that other brain abnormalities, such as brain connectivity, may also be differentially lateralised between SD and bvFTD.

Brain connectivity changes in frontotemporal networks have been suggested to play an important role in both bvFTD and language variants of dementia [9,10]. Brain connectivity can be assessed in terms of WM microstructure and functional connectivity, which have been suggested to be interrelated [11–13]. Both have been found to be abnormal in SD and bvFTD. Previous studies have observed WM microstructure abnormalities in SD mainly in the uncinate, arcuate and inferior longitudinal fasciculus - more pronounced in the left hemisphere [14–19] -, and in bvFTD mainly in the bilateral uncinate fasciculus, cingulum and forceps minor/genu of the corpus callosum [20,21]. Only a few studies looked at WM microstructural differences between SD and bvFTD [15,22,23], and mainly indicated severe *left* inferior longitudinal fasciculus abnormalities in SD, and increased forceps minor abnormalities in bvFTD. To the best of our knowledge none of these studies looked specifically at differences in lateralisation towards a particular hemisphere.

Similarly, functional connectivity changes have been observed in both SD and bvFTD within known functional networks and within regions implicated in SD and bvFTD [9,24–29], but only one study [26] reported functional network differences between SD and bvFTD in the default-mode, executive and salience network. Other functional connectivity differences between SD and bvFTD, such as in regions that are affected early in the disease process or between regions connected by affected WM tracts, and importantly the possible hemispheric predilection of these abnormalities, remain non-investigated.

As differences in brain connectivity - and in particular their hemispheric lateralisation - between SD and bvFTD are not yet clarified, this study investigates differences in WM microstructure and functional connectivity between SD and bvFTD, specifically focusing on the hemispheric predilection of these differences.

2. METHODS

2.1 Participants

Patients were recruited in the Alzheimer Centre Southwest Netherlands. Inclusion criteria were: age between 40 and 70 years; diagnosis of SD [2] or bvFTD [30]; a Mini-Mental State Examination [31] (MMSE) score of ≥ 20. Exclusion criteria were contraindications for MRI; other neurological disorders; a different cause of dementia; alternative psychiatric diagnosis; past or current substance abuse. SD patients were classified as left or right variant SD patients.

Healthy controls, matched for age and gender, and without neurological or psychiatric diagnosis, were recruited through advertisement.

The study was approved by the local medical ethics committee. All participants gave written informed consent.

2.2 Image acquisition

Scanning was performed on a 3T GE Discovery MR750 system (GE Healthcare, Milwaukee, WI, US). See Table 1 for acquisition parameters.

A high-resolution three-dimensional (3D) inversion recovery (IR) fast spoiled gradient echo (FSPGR) T1-weighted (T1w) image was acquired for anatomical reference. DTI scans with a spin echo echo planar imaging (EPI) sequence and functional scans with a gradient echo EPI sequence were acquired with full coverage of the supratentorial brain. For functional scans participants were instructed to focus on a fixation cross, to think of nothing in particular and to remain awake.

Table I. Acquisition parameters.

	T1w	fMRI	DTI
FOV (mm)	240	240	240
TE (ms)	3.06	30	84.7
TR (ms)	7904	3000	7.93
ASSET factor	2	2	2
Flip angle	12°	90°	90°
Acquisition matrix	240x240	96x96	128x128
Slice thickness (mm)	1	3	2.5
Volumes (slices per volume)	1 (176)	200 (44)	28 (59)
Duration (min)	4.41	10.00	3.50
Diffusion-weighted directions	n/a	n/a	25
Maximum b-value (s/ mm2)	n/a	n/a	1000
TI (ms)	450	n/a	n/a

T1w = T1-weighted, fMRI = functional magnetic resonance imaging, DTI = diffusion tensor imaging, FOV= field of view, TE = echo time, TR = repetition time, ASSET = array spatial sensitivity encoding technique, TI = inversion time.

2.3 Demographical analysis

Age was compared across groups using a one-way ANOVA, and gender differences using chi-square tests. Variance of MMSE scores was not equal across groups, hence between-group differences in MMSE score were tested using a Welch-ANOVA and post-hoc Games-Howell t-tests. Analyses were done using SPSS Statistics, version 21.0 (New York, USA) with the threshold for significance set at $p<0.05$.

2.4 Grey matter (GM) volume analysis

Whole-brain GM volumes were calculated according to the methods described in Bron et al. (2014) [32]. GM volumes were obtained from the T1w image using the unified tissue segmentation method of SPM8 (Statistical Parametric Mapping, London, UK), and divided by intracranial volume (ICV) to correct for head size. This normalised GM volume (nGM) was compared between all groups using a one-way ANOVA and post-hoc Bonferroni tests (IBM SPSS Statistics, version 21.0, New York, USA).

2.5 Microstructural white matter (WM) analysis

Data were analysed using FMRIB Software Library (FSL5, Oxford, UK) [33–35]. Data were corrected for motion and eddy currents using Eddy Correct and then skull-stripped using BET [36].

2.5.1 Tract-Based Spatial Statistics (TBSS)

Diffusion tensors were reconstructed using DTIFIT [37], resulting in participant images for fractional anisotropy (FA), mean diffusivity (MD), axial diffusivity (AxD), and the second and third eigenvalues. The latter were averaged using FSLmaths to calculate radial diffusivity (RD) images.

Using TBSS [38], registration of DTI images was performed and participant-specific skeletons for each of the diffusivity measures were created.

For all diffusivity measures, group differences were tested with Randomise [39] using 5000 nonparametric permutations and threshold-free cluster enhancement (TFCE) [40]. Using the General Linear Model (GLM) toolbox, a one-way ANOVA design was defined with three groups (SD≠bvFTD≠controls) and six t-contrasts (SD>controls, SD<controls, bvFTD>controls, bvFTD<controls, SD>bvFTD, SD<bvFTD) assessing post-hoc between-group differences. Results were family wise error (FWE) corrected for multiple comparisons.

Post-hoc t-tests results ($p_{FWE\_corrected}<0.05$) were identified within the boundaries of the f-test results using FSLmaths. First, for the f-test and all t-tests a binary mask was created ($p_{threshold}=0.95$). Second, each t-test binary mask was multiplied with the f-test binary mask, resulting in a common binary mask for every t-test. Clusters were extracted for each t-test using the Cluster toolbox ($p_{threshold}=0.95$; k (cluster size)≥50).

Results ($p_{FWE\_corrected}$<0.05; k=50) were visualised and anatomically identified in FSLview with the implemented JHU White-Matter Tractography Atlas and the JHU ICBM-DTI-81 White-Matter labels.

WM tracts showing diffusivity abnormalities between patient groups were selected for further tractography analysis.

2.5.2 Tractography

Median diffusivity values were extracted from those WM tracts that were different between SD and bvFTD. First, automated probabilistic tractography (AutoPtx) [41] was used to apply a tensor fit with DTIFIT [37], followed by FNIRT registration and a BEDPOSTX probabilistic model fit for each participant. Second, PROBTRACKX [37,42] was run for all selected WM tracts using default space seed, target, stop and exclusion masks available in AutoPtx [41], resulting in a participant-specific tract density image. Tract density images were normalised by dividing them by the number of fibres included in the tract-image and then binarised for WM tract segmentation, based on the best-fit segmentation thresholds established by De Groot et al. (2015) [43] (see supplemental (suppl) Table 1 for thresholds).

Tensor-fit established diffusivity images were masked with thresholded tract images using FSLstats, to acquire median FA, MD, RD and AxD values for each tract. For each diffusivity measure a lateralisation index was calculated in each tract that differed between SD and bvFTD, except for the forceps minor, being a midline structure. The following formula was used:

(1) Lateralisation index=(L−R)/(L+R).

Left lateralisation of abnormalities is indicated by a *negative* lateralisation index for FA, and a *positive* lateralisation index for MD, RD and AxD. Lateralisation indices were corrected – if necessary - for age and TE using linear regression. Between-group differences for all lateralisation indices were compared using a one-way ANOVA. Analyses were done using SPSS Statistics, version 21.0 (New York, USA).

2.6 Functional connectivity analysis

2.6.2 Hypothesis driven method

The anterior temporal lobe (ATL) and medial posterior orbitofrontal cortex (OFC), known to be affected in SD and bvFTD respectively, were selected as seed regions of interest (ROIs) for analysis. Left and right were assessed separately.

Data were analysed using FMRIB Software Library (FSL5, Oxford, UK) [33–35]. Anatomical images were reoriented to establish standard template orientation and then skull-stripped using the Brain Extraction Tool (BET) [36]. Preprocessing was done using the FMRI Expert Analysis Tool (FEAT) with a high pass filter set to 120s, MCFLIRT [44] motion correction to correct for linear motion, and spatial smoothing with a Gaussian kernel of 5 FWHM. Functional data were then linearly registered (normal search, 7 degrees of freedom (DOF)) to the corresponding T1w images, followed by both linear (full search, 12 DOF) and nonlinear registration (10mm warp resolution) to a standard MNI152 1mm brain template.

The medial, lateral and posterior orbital gyrus (left and right), and the medial and lateral anterior temporal lobe (left and right) were taken from the Hammers atlas [45]. Using FSLmaths, these individual ROIs were merged to construct four ROIs, namely the left and right ATL, and left and right OFC. Timeseries for each ROI were extracted using FSLmeans. Additionally, timeseries were extracted for subject-specific WM and cerebral spinal fluid (CSF) using predefined templates[46], and for a subject-specific brain mask.

Within-subject analysis was performed using a first-level FEAT with a lenient threshold ($p_{uncorrected}<0.05$) in order to establish functional connectivity of each ROI with the remainder of the brain. Motion parameters and timeseries of WM, CSF and global brain signal were considered confound regressors.

Between-group functional connectivity differences for each ROI were established using a higher-level FEAT. Modelling and estimation of functional connectivity was done using FEATs Bayesian statistics tool, FMRIBs local analysis of mixed effects 1 (FLAME1). With the Bayesian statistics model correction for multiple comparisons is not required [47]. An ANCOVA GLM was then defined with three groups (SD≠bvFTD≠controls), and six t-contrasts (SD>controls, SD<controls, bvFTD>controls, bvFTD<controls, SD>bvFTD, SD<bvFTD) assessing post-hoc between-group differences, with GM volume added as covariate. Both the f-test and all t-tests were assessed with FEAT Cluster thresholding ($p<0.05$, $z=2.3$) after which all t-tests were masked with f-test results to investigate within f-test boundaries results only.

Results were visualised in FSLview and anatomically identified using the Harvard-Oxford structural cortical and subcortic alatlases implemented in FSLview.

2.6.1 Exploratory method

Functional connectivity between GM regions on either end of the WM tracts that were different between SD and bvFTD was assessed in an exploratory analysis, using functional connectivity methods previously described in Ebisch et al. (2011) [48] and Verly et al. (2014) [49]. This was done to observe whether affected WM tracts were related to functional connectivity of adjoining GM regions and as different WM tracts may be affected between groups, whether this was also different between groups.

Between-group differences were however not observed.

3. RESULTS

3.1 Participant characteristics

Eight SD patients, 12 bvFTD patients and 17 controls were included (Table 2). Seven SD patients were classified as left and one as a right variant SD. One SD patient and three bvFTD patients were excluded from the functional connectivity analysis due to missing rs-fMRI data. Age ($F(2, 34) = .704$, $p>0.05$) and gender ($\chi^2(2, 34) = 1.003$, $p>0.05$) were not different between groups; this was also the case for the functional connectivity analysis. MMSE score was different across groups ($F(2, 12.82) = 7.79$, $p < 0.05$) and was lower in both SD ($p=0.049$) and bvFTD ($p=0.025$) patients than in controls, but was not different between SD and bvFTD patients ($p>0.05$). For the functional connectivity analysis MMSE score was different between groups ($F(2,30) = 6.6$, $p<0.05$), and was lower in bvFTD than in controls ($p=0.046$).

Table 2. Demographic characteristics of participants included in the diffusion tensor imaging analysis.

Group	N (male)	Mean age in years (Std dev)	Mean MMSE (Std Dev)
SD	8 (5)	62.9 (3.5)	25.6 (3.3)
BvFTD	12 (6)	60.3 (7.7)	26.6 (2.8)
Controls	17 (7)	59.5 (6.8)	29.1 (1.1)

SD = semantic dementia, BvFTD = behavioural frontotemporal dementia, N = sample size. Values given as Mean (standard deviation). MMSE = Mini-Mental State Examination.

3.2 GM volume

The three groups showed a difference in whole-brain GM volume corrected for ICV ($F(2, 34) = 15.92$, $p<0.05$), with a mean of 0.32% (standard deviation (Std Dev)0.03) for SD, 0.30% (Std Dev 0.04) for bvFTD and 0.36% (Std Dev 0.03) for controls. Lower GM volume was observed in both SD patients ($p<0.01$) and bvFTD patients ($p<0.001$) than in controls. GM volume was not different between the patient groups.

3.3 Microstructural WM

3.3.1 Whole-brain WM abnormalities

SD and bvFTD patients in comparison with controls showed decreased FA and increased MD, RD and AxD in the bilateral forceps minor and major, corpus cal-

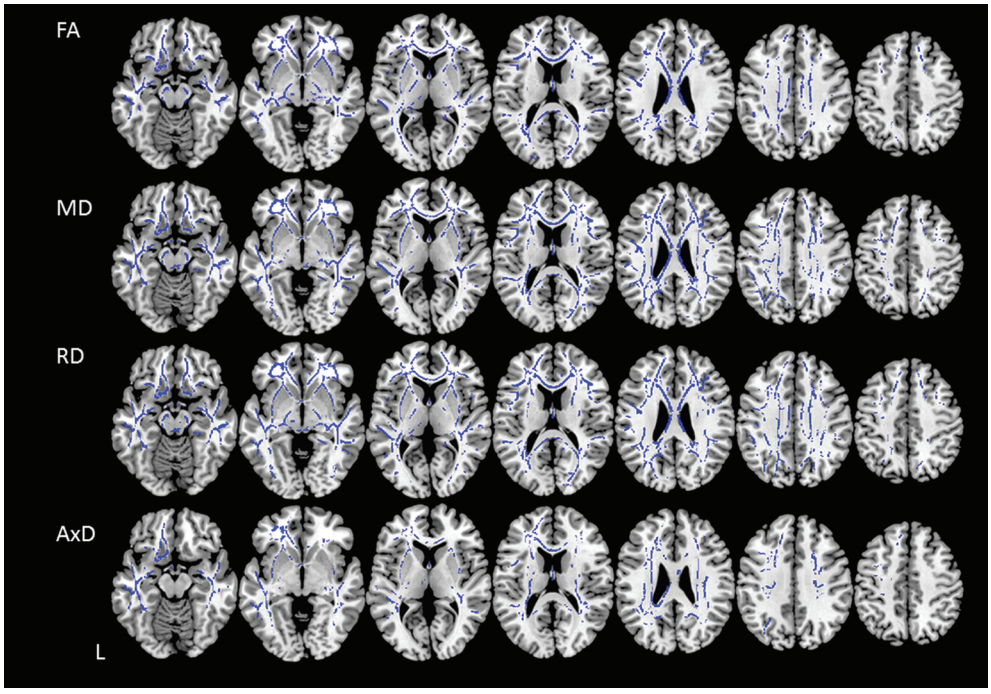

Figure 1. White matter microstructure abnormalities for semantic dementia (SD) compared with controls (SD<controls for FA; SD>controls for MD, RD and AxD).. FA = fractional anisotropy, MD = mean diffusivity, RD = radial diffusivity, AxD = axial diffusivity.

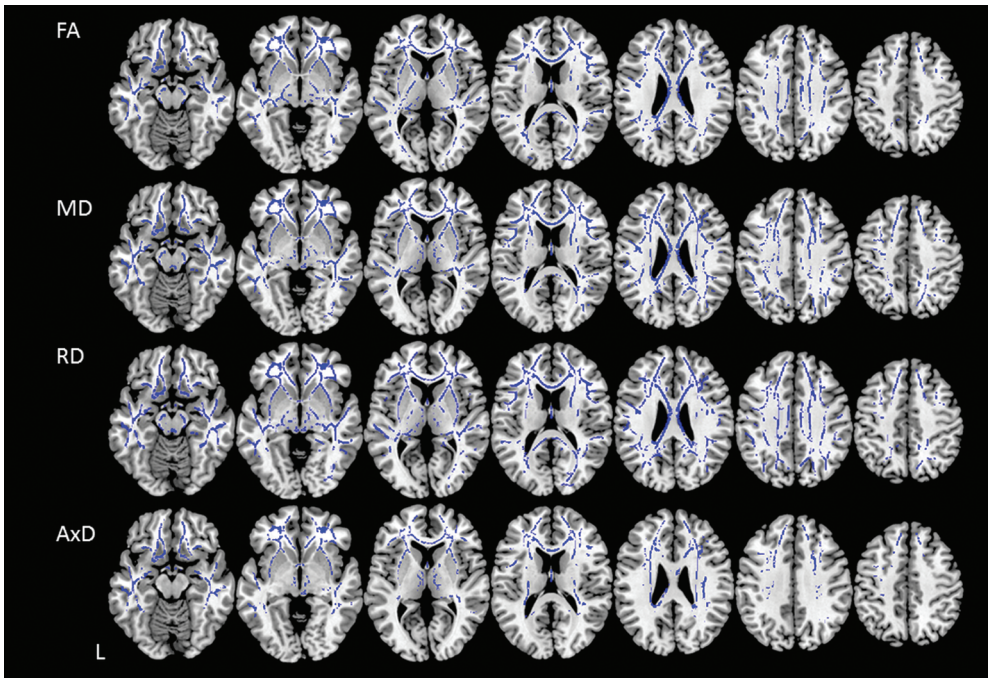

Figure 2. White matter microstructure abnormalities for behavioural variant frontotemporal dementia (bvFTD) compared with controls (bvFTD<controls for FA; bvFTD>controls for MD, RD and AxD). FA = fractional anisotropy, MD = mean diffusivity, RD = radial diffusivity, AxD = axial diffusivity.

losum, inferior fronto-occipital fasciculus, anterior thalamic radiation, cingulum, uncinate fasciculus, and inferior and superior longitudinal fasciculi (Figures 1 and 2, suppl Tables 2A-D).

Direct comparison between SD and bvFTD patients showed WM microstructure abnormalities in the left hemisphere in SD patients, and mostly in the right hemisphere in bvFTD patients. Specifically, SD patients compared with bvFTD patients (Figure 3, suppl Tables 2B-D) showed increased MD, RD and AxD in the *left* inferior fronto-occipital fasciculus, uncinate fasciculus, and inferior longitudinal fasciculus. Additionally, increased MD and RD, but not AxD, was observed in the left superior longitudinal fasciculus. Decreased FA was not observed. On the other hand, bvFTD patients compared with SD patients (Figure 4, suppl Tables 2A-D) showed decreased FA in the forceps minor and cingulum, and in the *right* inferior fronto-occipital fasciculus, anterior thalamic radiation, and uncinate fasciculus. In the latter three WM tracts AxD was also found to be increased. Increased MD and RD were observed in these tracts bilaterally.

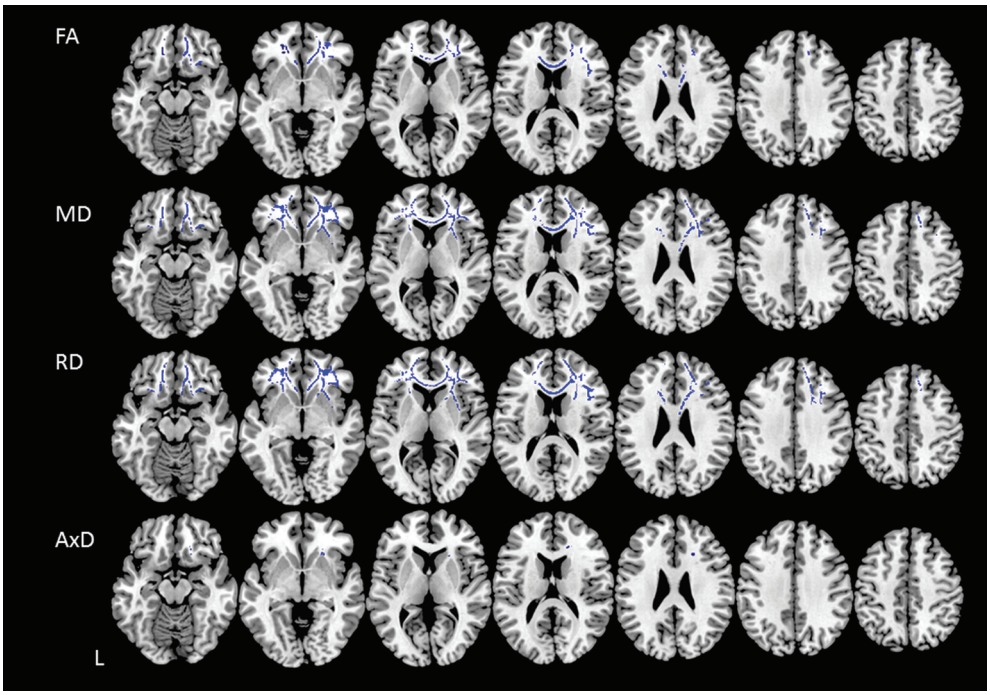

Figure 3. White matter microstructure abnormalities for semantic dementia (SD) in comparison with behavioural variant frontotemporal dementia (bvFTD) (SD>bvFTD). MD = mean diffusivity, RD = radial diffusivity, AxD = axial diffusivity.

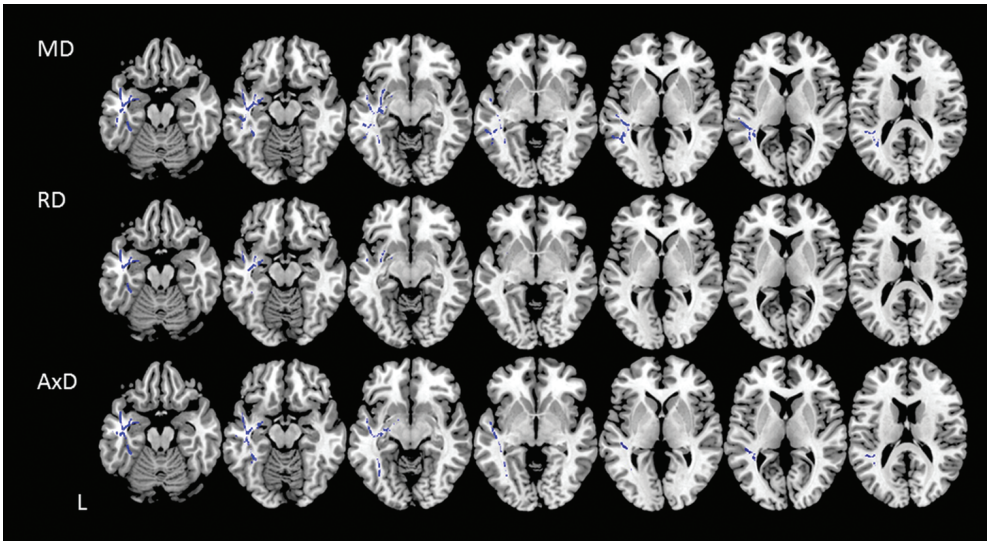

Figure 4. White matter microstructure abnormalities for behavioural variant frontotemporal dementia (bvFTD) in comparison with semantic dementia (SD) (bvFTD<SD for FA; bvFTD>SD for MD, RD and AxD). FA = fractional anisotropy, MD = mean diffusivity, RD = radial diffusivity, AxD = axial diffusivity.

Table 3. Between-group differences for WM measures lateralisation indices. Left lateralisation is indicated by a positive value for MD, RD and AxD, and a negative value for FA.

	Lateralisation index											
WM	**FA**			**MD**			**RD**			**AxD**		
Tract	**Mean BvFTD**	**Mean SD**	**Mean HC**	**Mean BvFTD**	**Mean SD**	**Mean HC**	**Mean BvFTD**	**Mean SD**	**Mean HC**	**Mean BvFTD**	**Mean SD**	**Mean HC**
ATR	.0103	.0141	.0044	-.0182	.0004	-.0056	-.0172	-.0012	-.0053	-.0212	**.0037**	-.0077
CGH	.0429	-.0807	-.0036	-.0291	**.066**	.0082	-,0204	.0046	-.0182	-.0279	**.0423**	<.001
IFOF	.0099	-.0247	-.0028	-.004	**.0156**	-.0031	-,0122	**.0252**	-.0009	-0.002	.0074	-.0073
ILF	-.0062	-.0188	-.0135	-.0001	.0257	.0044	.0023	.0303	.0077	-.0075	**.0234**	-.0028
SLF	.0133	**-.0265**	<-.001	-.0041	.0199	.0022	-,0055	**.0256**	.0024	-0.003	0.0111	<.001
UF	.0187	-.0563	.0153	-.0217	**.0484**	-.0136	-,0256	**.0607**	-.0213	-.0145	**.0306**	-.005

WM=white matter, FA=fractional anisotropy, MD=mean diffusivity, RD=radial diffusivity, AxD=axial diffusivity, BvFTD=behavioural variant frontotemporal dementia, SD=semantic dementia, ATR=anterior thalamic radiation, CGH=cingulum (hippocampus), IFOF=inferior fronto-occipital fasciculus, ILF=inferior longitudinal fasciculus, SLF=superior longitudinal fasciculus, UF=uncinate fasciculus.

SD≠controls p<0.05

SD≠bvFTD p<0.05

3.3.2 Lateralisation of WM abnormalities

Lateralisation of WM abnormalities was investigated for the anterior thalamic radiation, hippocampal and cingulate part of the cingulum, inferior fronto-occipital, inferior and superior longitudinal and uncinate fasciculus (Table 3).

Significantly different lateralisation indices showed a left-ward lateralisation in SD patients compared with controls for MD and RD in the uncinate and inferior fronto-occipital fasciculus, for MD and AxD in the hippocampal cingulum, for RD and FA in the superior longitudinal fasciculus, and for AxD in the uncinate fasciculus, inferior longitudinal fasciculus and anterior thalamic radiation.

Lateralisation indices of diffusivity measures were not significantly different between bvFTD patients and controls.

Significantly different lateralisation indices between SD and bvFTD showed a left-ward lateralisation in SD patients and a right-ward lateralisation in bvFTD patients for MD, RD and AxD in the hippocampal cingulum and uncinate fasciculus, for MD in the superior longitudinal fasciculus, for RD in the inferior fronto-occipital fasciculus, and for AxD in the inferior longitudinal fasciculus. These lateralisation differences were likely induced by SD lateralisation and not by bvFTD

3.4 Functional connectivity

3.4.1 Left anterior temporal lobe (ATL)

SD patients in comparison with controls showed *in*creased functional connectivity between the *left* ATL and the *left* hippocampus, amygdala, fusiform gyrus, parahippocampal gyrus, and inferior and middle temporal gyrus. SD patient compared both with controls and bvFTD patients showed *de*creased functional connectivity between the *left* ATL and the *bilateral* middle frontal gyrus, superior frontal gyrus and anterior cingulate cortex.

BvFTD patients in comparison with controls showed *in*creased connectivity between the *left* ATL and the bilateral cuneus, calcarine cortex, occipital pole and lateral occipital cortex. BvFTD patients in comparison with controls showed *de*creased functional connectivity between the *left* ATL and the *right* precentral gyrus, middle frontal gyrus, superior frontal gyrus and supplementary motor area. In comparison with SD patients there was decreased functional connectivity between the *left* ATL and the *right* precentral gyrus and *left* hippocampus, amygdala, fusiform gyrus, parahippocampal gyrus, inferior temporal gyrus and middle temporal gyrus.

Results are shown in figure 5 and supplemental table 3.

3.4.2 Right anterior temporal lobe (ATL)

Both SD and bvFTD patients in comparison with controls showed *de*creased functional connectivity between the *right* ATL and the *left* inferior temporal gyrus, middle temporal gyrus and superior temporal gyrus (Figure 6, suppl Table 3). No differences were observed between SD and bvFTD patients.

Between-group differences for *in*creased functional connectivity of the *right* ATL were not observed.

3.4.3 Left orbitofrontal cortex (OFC)

SD patients in comparison with controls showed *de*creased functional connectivity between the *left* OFC and the *right* posterior cingulate cortex and central

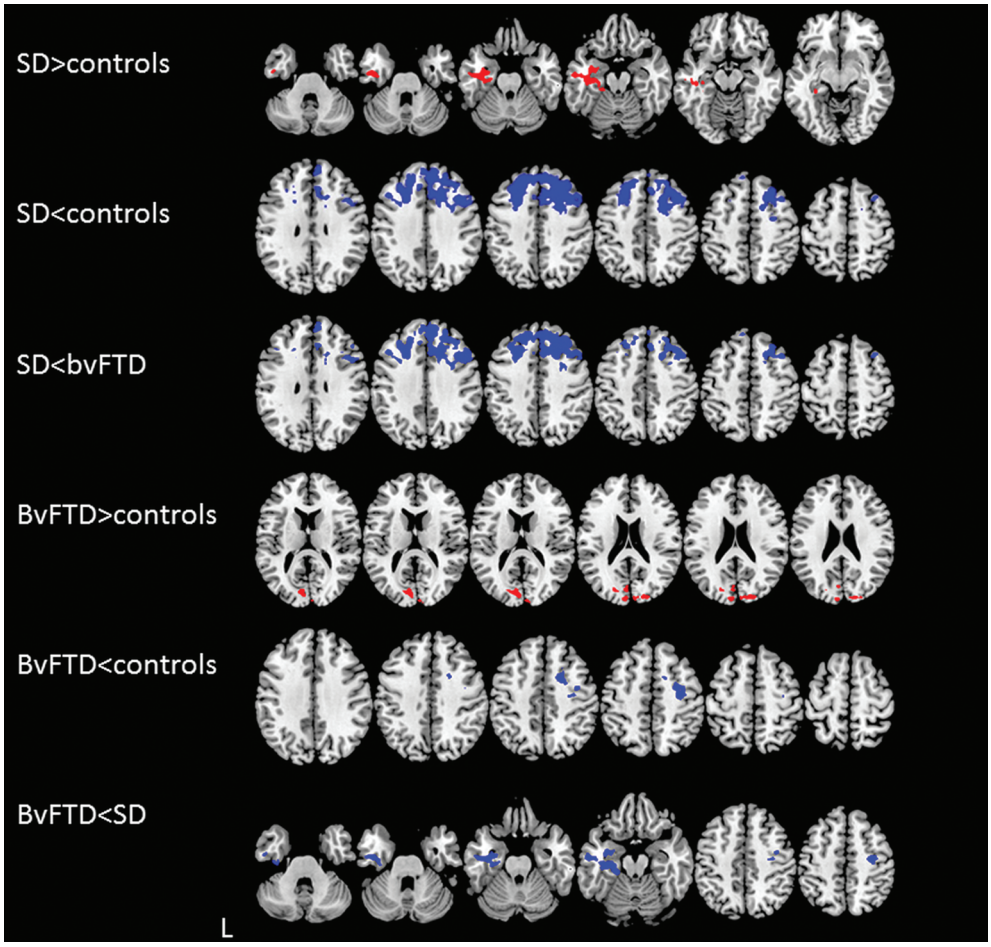

Figure 5. Functional connectivity increase (red) and decrease (blue) of the left anterior temporal lobe (ATL). SD = semantic dementia, BvFTD = behavioural variant frontotemporal dementia.

operculum, and *bilateral* postcentral gyrus and parietal operculum. SD patients in comparison with bvFTD patients showed *de*creased functional connectivity between the *left* OFC and the *bilateral* posterior cingulate cortex, central operculum, postcentral gyrus and parietal operculum.

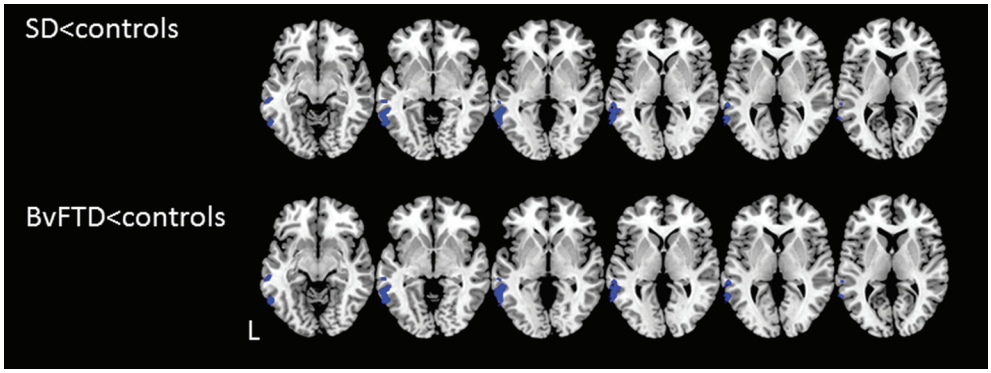

Figure 6. Functional connectivity decrease of the right anterior temporal lobe (ATL). SD = semantic dementia, BvFTD = behavioural variant frontotemporal dementia.

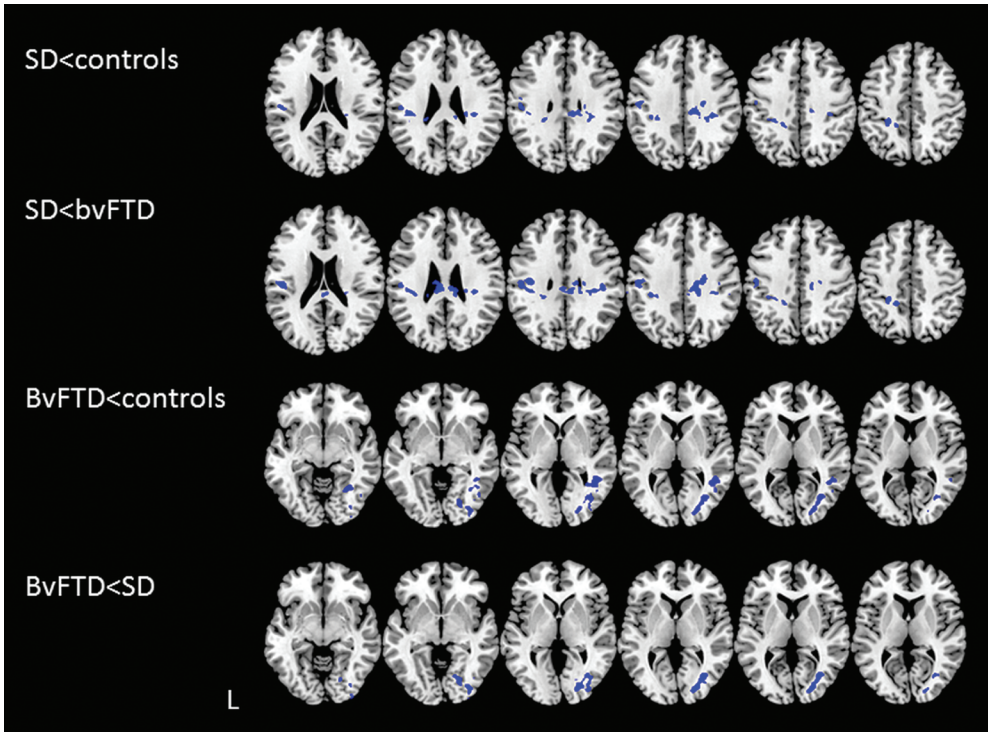

Figure 7. Functional connectivity decrease of the left orbitofrontal cortex (OFC). SD = semantic dementia, BvFTD = behavioural variant frontotemporal dementia.

BvFTD patients in comparison with both controls and SD patients showed *de*creased functional connectivity between the *left* OFC and the *right* lingual gyrus, occipital fusiform gyrus, lateral occipital lobe, inferior temporal gyrus and middle temporal gyrus.

Between-group differences for *in*creased functional connectivity of the *left* OFC were not observed. Results are shown in figure 7 and supplemental table 3.

3.4.3 Right orbitofrontal cortex (OFC)

Between-group differences were not observed for functional connectivity of the *right* OFC.

4. DISCUSSION

This study observed a left-right differentiation of WM microstructure and functional connectivity abnormalities in SD and bvFTD. Whole-brain WM microstructure abnormalities were more pronounced in the left hemisphere in SD and in the right hemisphere in bvFTD. Lateralisation of tract-specific WM abnormalities was seen in SD only, towards the left hemisphere. Functional connectivity of disease-specific regions was mainly decreased with both hemispheres in SD and with the right hemisphere in bvFTD.

Differences in WM microstructure abnormalities were most prominent in the left temporal lobe in SD and in the right frontal lobe in bvFTD, and can be related to disease-specific symptoms, namely the language disorders in SD [2,6] and the behavioural disturbances in bvFTD [8,30].

In SD, changes of WM microstructure were observed in language-specific WM tracts that were lateralised toward the *left* hemisphere. These abnormalities (increased MD, RD and AxD) were most pronounced in the left ventral language stream (uncinate, inferior longitudinal and inferior fronto-occipital fasciculus) and only subtly in the dorsal language stream (superior longitudinal fasciculus). The ventral stream is thought to be associated with semantic processing [50,51], and its predominant involvement in SD is in line with SD symptomatology, i.e. impaired single-word comprehension and confrontation naming [2]. Conversely, the relative sparing of the dorsal stream, which is associated with phonological speech processing [51], is reflected by the preserved language production in SD.

In bvFTD, changes of WM microstructure were observed in behaviour-associated WM tracts in the bilateral – more pronounced in the right - frontal WM. These changes (mainly decreased FA and increased RD and MD) were most evident in the *right* inferior fronto-occipital and uncinate fasciculus, and in the *right* part of the forceps minor. Uncinate fasciculus abnormalities [52] have been associated with the typical bvFTD symptoms of behavioural dyscontrol [15], disinhibiton [53,54], executive dysfunctioning [55], and apathy [54]. Implication of the inferior fronto-occipital fasciculus in bvFTD is not as clear, but an association with impaired emotion recognition in bvFTD [56] and involvement in emotional responses [57] and emotional prosody [58] has been suggested. The function of the forceps minor in relation to bvFTD has not been extensively studied, but its involvement in disinhibition [53] and executive functioning [59] has been proposed.

Not all diffusivity measures were affected equally in both diseases, possibly indicating specific neuropathological processes occurring at specific disease stages. In particular, AxD abnormalities (reflecting axonal injury or loss [60]) were less extensive in both SD and bvFTD than those of the other diffusivity measures. It may be that there was only mild axonal injury or loss at this early stage of SD and bvFTD, while myelin loss (reflected by changes in RD [61]) was already very prominent at this stage. Additionally, FA abnormalities (reflecting WM directionality) were more or less equally distributed across the two hemispheres in both SD and bvFTD. A possible explanation may be that FA, being a composite measure of AxD and RD, has higher sensitivity to WM microstructural abnormalities. It can be hypothesised that FA changes are already present to such an extent that a hemispheric difference can no longer be appreciated. Interestingly, whereas more pronounced FA abnormalities seem to obscure hemispheric differences, these hemispheric differences become clear when looking at AxD abnormalities. This indicates that whereas a sensitive measure such as FA already shows diffuse abnormalities in early stage dementia, AxD may be specifically sensitive to hemispheric lateralization in regions typical for these early stages.

A hemispheric dissociation between the two FTD subtypes was further indicated by functional connectivity abnormalities of the ATL and OFC, which were present in both hemispheres in SD (albeit more pronounced in the left hemisphere) and mainly in the right hemisphere in bvFTD.

The *left* ATL showed an extensive functional connectivity decrease in the bilateral frontal GM in SD in comparison with both healthy controls and bvFTD, whereas bvFTD showed a less widespread decrease in the *right* frontal GM. This more prominent role of the *left* ATL in SD is in line with known pronounced GM

atrophy of the *left* ATL [2] and may be explained by its role in semantic processing [62,63], a cognitive domain affected in SD but not in bvFTD. Despite a less obvious role of the *left* ATL in bvFTD than in SD, the literature does also report GM volume loss of the *left* ATL [64] in bvFTD, possibly explaining its less extensive decrease in functional connectivity observed here. Additionally, the involvement of the frontal lobe may on the one hand be explained by the frontal lobe's rich connections with the ATL [62], and on the other hand by its involvement in both SD and bvFTD pathology [64,65].

The *left* ATL also showed an *increase* in functional connectivity in SD with left temporal regions that are well-connected with the ATL [62,66] and are also implicated in language processing [67,68]. Such increased functional connectivity has been suggested to be indicative of a compensatory mechanism [69,70], which may be highly important in the early stages of dementia to counteract the effects of inicipient neuronal dysfunctioning. In this study, increased functional connectivity between the ATL and temporal regions may thus suggest an upregulation of the posterior part of the language network to compensate for the functional language deterioration of the *left* ATL. In bvFTD a similar mechanism was seen to be activated between the *left* ATL and the bilateral - but mainly *left* - medial occipital lobe. The temporal lobe and occipital lobe may be part of a functional network involving visual aspects of language [71], but why this network showed a compensatory process in bvFTD is unclear.

Surprisingly, the *right* ATL showed a *de*crease in functional connectivity only with the *left* posterior temporal lobe (PTL) in both SD and bvFTD, and not with the frontal lobes. In general, the PTL has been suggested to be involved in naming [68,72], lexical and semantic processing [73], and also in memory processing [74], which possibly explains its involvement in SD. However, the nature of its connection with the *right* ATL, which is not necessarily involved in language, remains unclear. For bvFTD, as the left PTL is important for memory processing [74] and the right ATL for social knowledge [62], this finding may explain the social impairment typical of bvFTD, i.e. patients forget how to behave in a socially appropriate manner.

Functional connectivity changes of the OFC were limited to the *left* OFC in both SD and bvFTD. In SD, this finding is in line with its left-hemispheric predilection, leaving the *right* OFC functionally unaffected. In bvFTD however, right OFC abnormalities would have been expected. However, previous studies of bvFTD have also occasionally reported only left GM atrophy of the OFC [75], as well as only right [76], or bilateral involvement [53,75], all of which have been associated with behavioural dysfunctioning [53,75–77]. In SD, *left* OFC functional connectivity was decreased with the bilateral parietal lobe. Previous studies have asso-

ciated parietal regions with theory of mind, memory functioning and language processing [78–83]; cognitive functions that are also affected in SD [2,84]. The relationship between the parietal lobe and OFC may be specifically explained by the role of the OFC in language processing [81].

In bvFTD, the *left* OFC showed decreased connectivity with the right temporal and occipital lobe. Together with these regions, the OFC has been shown to form a network that is involved in visual and socio-emotional functioning [76,77,85–89]. It is possible that decreased functional connectivity in this network is related to the specific behavioural symptoms in bvFTD. Functional connectivity between the *left* OFC and right occipito-temporal regions was also decreased in bvFTD when compared with SD, again indicating that distinct functional connectivity differences may underlie specific bvFTD behavioural symptomatology.

Taken together, we find support for the hypothesis that changes of WM microstructure and functional connectivity are related [11–13]. Direct association between functional connectivity on either side of affected WM tracts was not observed, but regional overlap of WM microstructural and functional connectivity abnormalities was present. We found WM microstructure abnormalities in temporal and frontal WM tracts, and functional connectivity abnormalities in the temporal and frontal lobes, as well as in adjacent GM regions connected by the affected WM tracts. Specifically, these concerned the *left* inferior longitudinal fasciculus and uncinate fasciculus connecting frontal, temporal and parietal lobes in SD, and the *right* inferior fronto-occipital fasciculus and uncinate fasciculus connecting the frontal, temporal and occipital lobes in bvFTD.

This study has some limitations. First, samples sizes of SD and bvFTD patients were small. This is unfortunate but inherent to research of relatively rare conditions in combination with well-defined inclusion criteria. Despite our small sample size we observed pronounced abnormalities, surviving stringent statistical thresholding, that are in line with the current literature. Second, due to the small sample size we were not able to perform further rs-fMRI analyses, e.g. whole-brain analysis, which may leave possible further differences unexplored.

In conclusion, SD and bvFTD show WM microstructural and functional connectivity abnormalities, affecting different structures, that were overall more pronounced in the left hemisphere in SD and in the right hemisphere in bvFTD. This indicates a hemispheric dissociation of abnormalities in brain connectivity between SD and bvFTD.

REFERENCES

1 Neary D, Snowden JS, Gustafson L, *et al.* Frontotemporal lobar degeneration: A consensus on clinical diagnostic criteria. *Neurology* 1998;51:1546–54. doi:10.1212/WNL.51.6.1546

2 Gorno-Tempini ML, Hillis a E, Weintraub S, *et al.* Classification of primary progressive aphasia and its variants. *Neurology* 2011;76:1006–14. doi:10.1212/WNL.0b013e31821103e6

3 Karageorgiou E, Miller BL. Frontotemporal lobar degeneration: a clinical approach. *Semin Neurol* 2014;34:189–201. doi:10.1055/s-0034-1381735

4 Bocti C, Rockel C, Roy P, *et al.* Topographical patterns of lobar atrophy in frontotemporal dementia and Alzheimer's disease. *Dement Geriatr Cogn Disord* 2006;21:364–72. doi:10.1159/000091838

5 Rascovsky K, Hodges JR, Knopman D, *et al.* Sensitivity of revised diagnostic criteria for the behavioural variant of frontotemporal dementia. *Brain* 2011;134:2456–77. doi:10.1093/brain/awr179

6 Ocklenburg S, Beste C, Arning L, *et al.* The ontogenesis of language lateralization and its relation to handedness. *Neurosci Biobehav Rev* 2014;43:191–8. doi:10.1016/j.neubiorev.2014.04.008

7 Cummings JL. Frontal-subcortical circuits and human behavior. *Arch Neurol* 1993;50:873–80. http://www.ncbi.nlm.nih.gov/pubmed/8352676.

8 Bonelli RM, Cummings JL. Frontal-subcortical circuitry and behavior. *Dialogues Clin Neurosci* 2007;9:141–51.http://www.pubmedcentral.nih.gov/articlerender.fcgi?artid=3181854&tool=pmcentrez&rendertype=abstract.

9 Zhou J, Greicius MD, Gennatas ED, *et al.* Divergent network connectivity changes in behavioural variant frontotemporal dementia and Alzheimer's disease. *Brain* 2010;133:1352–67. doi:10.1093/brain/awq075

10 D'Anna L, Mesulam MM, Thiebaut de Schotten M, *et al.* Frontotemporal networks and behavioral symptoms in primary progressive aphasia. *Neurology* 2016;86:1393–9. doi:10.1212/WNL.0000000000002579

11 Damoiseaux JS, Greicius MD. Greater than the sum of its parts: a review of studies combining structural connectivity and resting-state functional connectivity. *Brain Struct Funct* 2009;213:525–33. doi:10.1007/s00429-009-0208-6

12 Greicius MD, Supekar K, Menon V, *et al.* Resting-state functional connectivity reflects structural connectivity in the default mode network. *Cereb Cortex* 2009;19:72–8. doi:10.1093/cercor/bhn059

13 Honey CJ, Sporns O, Cammoun L, *et al.* Predicting human resting-state functional connectivity. 2009;106:1–6.

14 Zhang S, Arfanakis K. White matter segmentation based on a skeletonized atlas: Effects on diffusion tensor imaging studies of regions of interest. *J Magn Reson Imaging* 2013;00:1–10. doi:10.1002/jmri.24445

15 Whitwell JL, Avula R, Senjem ML, *et al.* Gray and white matter water diffusion in the syndromic variants of frontotemporal dementia. *Neurology* 2010;74:1279–87. doi:10.1212/WNL.0b013e3181d9edde

16 Sajjadi S a, Acosta-Cabronero J, Patterson K, *et al.* Diffusion tensor magnetic resonance imaging for single subject diagnosis in neurodegenerative diseases. *Brain* 2013;136:2253–61. doi:10.1093/brain/awt118

17 Botha H, Duffy JR, Whitwell JL, *et al.* Classification and clinicoradiologic features of primary progressive aphasia (PPA) and apraxia of speech. *Cortex* 2015;69:220–36. doi:10.1016/j.cortex.2015.05.013

18 Agosta F, Henry RG, Migliaccio R, *et al.* Language networks in semantic dementia. *Brain* 2010;133:286–99. doi:10.1093/brain/awp233

19 Acosta-Cabronero J, Patterson K, Fryer TD, *et al.* Atrophy, hypometabolism and white matter abnormalities in semantic dementia tell a coherent story. *Brain* 2011;134:2025–35. doi:10.1093/brain/awr119

20 Tovar-Moll F, de Oliveira-Souza R, Bramati IE, *et al.* White matter tract damage in the behavioral variant of frontotemporal and corticobasal dementia syndromes. *PLoS One* 2014;9:e102656. doi:10.1371/journal.pone.0102656

21 Mahoney CJ, Ridgway GR, Malone IB, *et al.* Profiles of white matter tract pathology in frontotemporal dementia. *Hum Brain Mapp* 2014;35:4163–79. doi:10.1002/hbm.22468

22 Zhang Y, Tartaglia MC, Schuff N, *et al.* MRI signatures of brain macrostructural atrophy and microstructural degradation in frontotemporal lobar degeneration subtypes. *J Alzheimers Dis* 2013;33:431–44. doi:10.3233/JAD-2012-121156

23 Agosta F, Scola E, Canu E, *et al.* White matter damage in frontotemporal lobar degeneration spectrum. *Cereb Cortex* 2012;22:2705–14. doi:10.1093/cercor/bhr288

24 Guo CC, Gorno-Tempini ML, Gesierich B, *et al.* Anterior temporal lobe degeneration produces widespread network-driven dysfunction. *Brain* 2013;136:2979–91. doi:10.1093/brain/awt222

25 Yang Q, Guo Q-H, Bi Y-C. The brain connectivity basis of semantic dementia: a selective review. *CNS Neurosci Ther* 2015;21:784–92. doi:10.1111/cns.12449

26 Farb NA, Grady CL, Strother S, *et al.* Abnormal network connectivity in frontotemporal dementia: evidence for prefrontal isolation. *Cortex* 2013;49:1856–73. doi:10.1016/j.cortex.2012.09.008

27 Filippi M, Agosta F, Scola E, *et al.* Functional network connectivity in the behavioral variant of frontotemporal dementia. *Cortex* 2013;49:2389–401. doi:10.1016/j.cortex.2012.09.017

28 Whitwell JL, Josephs KA, Avula R, *et al.* Altered functional connectivity in asymptomatic MAPT subjects: a comparison to bvFTD. *Neurology* 2011;77:866–74. doi:10.1212/WNL.0b013e31822c61f2

29 Caminiti SP, Canessa N, Cerami C, *et al.* Affective mentalizing and brain activity at rest in the behavioral variant of frontotemporal dementia. *NeuroImage Clin* 2015;9:484–97. doi:10.1016/j.nicl.2015.08.012

30 Rascovsky K, Hodges JR, Knopman D, *et al.* Sensitivity of revised diagnostic criteria for the behavioural variant of frontotemporal dementia. *Brain* 2011;134:2456–77. doi:10.1093/brain/awr179
31 Folstein MF, Folstein SE, McHugh PR. 'Mini-mental state'. A practical method for grading the cognitive state of patients for the clinician. *J Psychiatr Res* 1975;12:189–98.http://www.ncbi.nlm.nih.gov/pubmed/1202204.
32 Bron EE, Steketee RME, Houston GC, *et al.* Diagnostic classification of arterial spin labeling and structural MRI in presenile early stage dementia. *Hum Brain Mapp* 2014;35:4916–31. doi:10.1002/hbm.22522
33 Jenkinson M, Beckmann CF, Behrens TEJ, *et al.* FSL. *Neuroimage* 2012;62:782–90. doi:10.1016/j.neuroimage.2011.09.015
34 Woolrich MW, Jbabdi S, Patenaude B, *et al.* Bayesian analysis of neuroimaging data in FSL. *Neuroimage* 2009;45:S173–86. doi:10.1016/j.neuroimage.2008.10.055
35 Smith SM, Jenkinson M, Woolrich MW, *et al.* Advances in functional and structural MR image analysis and implementation as FSL. *Neuroimage* 2004;23 Suppl 1:S208–19. doi:10.1016/j.neuroimage.2004.07.051
36 Smith SM. Fast robust automated brain extraction. *Hum Brain Mapp* 2002;17:143–55. doi:10.1002/hbm.10062
37 Behrens TEJ, Woolrich MW, Jenkinson M, *et al.* Characterization and propagation of uncertainty in diffusion-weighted MR imaging. *Magn Reson Med* 2003;50:1077–88. doi:10.1002/mrm.10609
38 Smith SM, Jenkinson M, Johansen-Berg H, *et al.* Tract-based spatial statistics: voxelwise analysis of multi-subject diffusion data. *Neuroimage* 2006;31:1487–505. doi:10.1016/j.neuroimage.2006.02.024
39 Winkler AM, Ridgway GR, Webster MA, *et al.* Permutation inference for the general linear model. *Neuroimage* 2014;92:381–97. doi:10.1016/j.neuroimage.2014.01.060
40 Smith SM, Nichols TE. Threshold-free cluster enhancement: addressing problems of smoothing, threshold dependence and localisation in cluster inference. *Neuroimage* 2009;44:83–98. doi:10.1016/j.neuroimage.2008.03.061
41 de Groot M, Vernooij MW, Klein S, *et al.* Improving alignment in Tract-based spatial statistics: evaluation and optimization of image registration. *Neuroimage* 2013;76:400–11. doi:10.1016/j.neuroimage.2013.03.015
42 Behrens TEJ, Berg HJ, Jbabdi S, *et al.* Probabilistic diffusion tractography with multiple fibre orientations: What can we gain? *Neuroimage* 2007;34:144–55. doi:10.1016/j.neuroimage.2006.09.018
43 de Groot M, Ikram MA, Akoudad S, *et al.* Tract-specific white matter degeneration in aging: The Rotterdam Study. *Alzheimer's Dement* 2015;11:321–30. doi:10.1016/j.jalz.2014.06.011

44 Jenkinson M, Bannister P, Brady M, *et al.* Improved optimization for the robust and accurate linear registration and motion correction of brain images. *Neuroimage* 2002;17:825–41.http://www.ncbi.nlm.nih.gov/pubmed/12377157.

45 Hammers A, Allom R, Koepp MJ, *et al.* Three-dimensional maximum probability atlas of the human brain, with particular reference to the temporal lobe. *Hum Brain Mapp* 2003;19:224–47. doi:10.1002/hbm.10123

46 Beckmann CF, DeLuca M, Devlin JT, *et al.* Investigations into resting-state connectivity using independent component analysis. *Philos Trans R Soc L B Biol Sci* 2005;360:1001–13. doi:10.1098/rstb.2005.1634

47 Gelman A, Hill J, Yajima M. Why We (Usually) Don't Have to Worry About Multiple Comparisons. *J Res Educ Eff* 2012;5:189–211. doi:10.1080/19345747.2011.618213

48 Ebisch SJH, Gallese V, Willems RM, *et al.* Altered intrinsic functional connectivity of anterior and posterior insula regions in high-functioning participants with autism spectrum disorder. *Hum Brain Mapp* 2011;32:1013–28. doi:10.1002/hbm.21085

49 Verly M, Verhoeven J, Zink I, *et al.* Altered functional connectivity of the language network in ASD: Role of classical language areas and cerebellum. *NeuroImage Clin* 2014;4:374–82. doi:10.1016/j.nicl.2014.01.008

50 Dick AS, Bernal B, Tremblay P. The language connectome: new pathways, new concepts. *Neuroscientist* 2014;20:453–67. doi:10.1177/1073858413513502

51 Saur D, Kreher BW, Schnell S, *et al.* Ventral and dorsal pathways for language. *Proc Natl Acad Sci U S A* 2008;105:18035–40. doi:10.1073/pnas.0805234105

52 Von Der Heide RJ, Skipper LM, Klobusicky E, *et al.* Dissecting the uncinate fasciculus: disorders, controversies and a hypothesis. *Brain* 2013;136:1692–707. doi:10.1093/brain/awt094

53 Hornberger M, Geng J, Hodges JR. Convergent grey and white matter evidence of orbitofrontal cortex changes related to disinhibition in behavioural variant frontotemporal dementia. *Brain* 2011;134:2502–12. doi:10.1093/brain/awr173

54 Powers JP, Massimo L, McMillan CT, *et al.* White Matter Disease Contributes to Apathy and Disinhibition in Behavioral Variant Frontotemporal Dementia. *Cogn Behav Neurol* 2014;27:206–14. doi:10.1097/WNN.0000000000000044

55 Tartaglia MC, Zhang Y, Racine C, *et al.* Executive dysfunction in frontotemporal dementia is related to abnormalities in frontal white matter tracts. *J Neurol* 2012;259:1071–80. doi:10.1007/s00415-011-6300-x

56 Crespi C, Cerami C, Dodich A, *et al.* Microstructural white matter correlates of emotion recognition impairment in Amyotrophic Lateral Sclerosis. *Cortex* 2014;53:1–8. doi:10.1016/j.cortex.2014.01.002

57 Taddei M, Tettamanti M, Zanoni A, *et al.* Brain white matter organisation in adolescence is related to childhood cerebral responses to facial expressions and harm avoidance. *Neuroimage* 2012;61:1394–401. doi:10.1016/j.neuroimage.2012.03.062

58 Schmidt AT, Hanten G, Li X, *et al.* Emotional prosody and diffusion tensor imaging in children after traumatic brain injury. *Brain Inj* 2013;27:1528–35. doi:10.3109/02699052.2013.828851
59 Pérez-Iglesias R, Tordesillas-Gutiérrez D, McGuire PK, *et al.* White Matter Integrity and Cognitive Impairment in First-Episode Psychosis. *Am J Psychiatry* 2010;167:451–8. doi:10.1176/appi.ajp.2009.09050716
60 Song S-K, Sun S-W, Ju W-K, *et al.* Diffusion tensor imaging detects and differentiates axon and myelin degeneration in mouse optic nerve after retinal ischemia. *Neuroimage* 2003;20:1714–22. doi:10.1016/j.neuroimage.2003.07.005
61 Song S-K, Sun S-W, Ramsbottom MJ, *et al.* Dysmyelination Revealed through MRI as Increased Radial (but Unchanged Axial) Diffusion of Water. *Neuroimage* 2002;17:1429–36. doi:10.1006/nimg.2002.1267
62 Wong C, Gallate J. The function of the anterior temporal lobe: a review of the empirical evidence. *Brain Res* 2012;1449:94–116. doi:10.1016/j.brainres.2012.02.017
63 Gainotti G. Is the difference between right and left ATLs due to the distinction between general and social cognition or between verbal and non-verbal representations? *Neurosci Biobehav Rev* 2015;51:296–312. doi:10.1016/j.neubiorev.2015.02.004
64 Broe M, Hodges JR, Schofield E, *et al.* Staging disease severity in pathologically confirmed cases of frontotemporal dementia. *Neurology* 2003;60:1005–11. doi:10.1212/01.WNL.0000052685.09194.39
65 Mummery CJ, Patterson K, Price CJ, *et al.* A voxel-based morphometry study of semantic dementia: relationship between temporal lobe atrophy and semantic memory. *Ann Neurol* 2000;47:36–45.http://www.ncbi.nlm.nih.gov/pubmed/10632099
66 Olson IR, McCoy D, Klobusicky E, *et al.* Social cognition and the anterior temporal lobes: a review and theoretical framework. *Soc Cogn Affect Neurosci* 2013;8:123–33. doi:10.1093/scan/nss119
67 Cabeza R, Nyberg L. Imaging cognition II: An empirical review of 275 PET and fMRI studies. *J Cogn Neurosci* 2000;12:1–47.http://www.ncbi.nlm.nih.gov/pubmed/10769304
68 Harvey DY, Schnur TT. Distinct loci of lexical and semantic access deficits in aphasia: Evidence from voxel-based lesion-symptom mapping and diffusion tensor imaging. *Cortex* 2015;67:37–58. doi:10.1016/j.cortex.2015.03.004
69 Bookheimer SY, Strojwas MH, Cohen MS, *et al.* Patterns of brain activation in people at risk for Alzheimer's disease. *N Engl J Med* 2000;343:450–6. doi:10.1056/NEJM200008173430701
70 Borroni B, Alberici A, Cercignani M, *et al.* Granulin mutation drives brain damage and reorganization from preclinical to symptomatic FTLD. *Neurobiol Aging* 2012;33:2506–20. doi:10.1016/j.neurobiolaging.2011.10.031
71 Allison T, McCarthy G, Nobre A, *et al.* Human extrastriate visual cortex and the perception of faces, words, numbers, and colors. *Cereb Cortex*;4:544–54.http://www.ncbi.nlm.nih.gov/pubmed/7833655

72 Büchel C, Price C, Friston K. A multimodal language region in the ventral visual pathway. *Nature* 1998;394:274–7. doi:10.1038/28389

73 Axelrod V, Bar M, Rees G, *et al.* Neural Correlates of Subliminal Language Processing. *Cereb Cortex* 2015;25:2160–9. doi:10.1093/cercor/bhu022

74 Söderlund H, Black SE, Miller BL, *et al.* Episodic memory and regional atrophy in frontotemporal lobar degeneration. *Neuropsychologia* 2008;46:127–36. doi:10.1016/j.neuropsychologia.2007.08.003

75 O'Callaghan C, Bertoux M, Irish M, *et al.* Fair play: social norm compliance failures in behavioural variant frontotemporal dementia. *Brain* 2016;139:204–16. doi:10.1093/brain/awv315

76 Kipps CM, Nestor PJ, Acosta-Cabronero J, *et al.* Understanding social dysfunction in the behavioural variant of frontotemporal dementia: the role of emotion and sarcasm processing. *Brain* 2009;132:592–603. doi:10.1093/brain/awn314

77 Hutchings R, Hodges JR, Piguet O, *et al.* Why Should I Care? Dimensions of Socio-Emotional Cognition in Younger-Onset Dementia. *J Alzheimers Dis* 2015;48:135–47. doi:10.3233/JAD-150245

78 Jefferies E. The neural basis of semantic cognition: converging evidence from neuropsychology, neuroimaging and TMS. *Cortex* 2013;49:611–25. doi:10.1016/j.cortex.2012.10.008

79 Wirth M, Jann K, Dierks T, *et al.* Semantic memory involvement in the default mode network: a functional neuroimaging study using independent component analysis. *Neuroimage* 2011;54:3057–66. doi:10.1016/j.neuroimage.2010.10.039

80 Chan Y-C, Lavallee JP. Temporo-parietal and fronto-parietal lobe contributions to theory of mind and executive control: an fMRI study of verbal jokes. *Front Psychol* 2015;6. doi:10.3389/fpsyg.2015.01285

81 Sans-Sansa B, McKenna PJ, Canales-Rodríguez EJ, *et al.* Association of formal thought disorder in schizophrenia with structural brain abnormalities in language-related cortical regions. *Schizophr Res* 2013;146:308–13. doi:10.1016/j.schres.2013.02.032

82 Awad M, Warren JE, Scott SK, *et al.* A common system for the comprehension and production of narrative speech. *J Neurosci* 2007;27:11455–64. doi:10.1523/JNEUROSCI.5257-06.2007

83 Graff-Radford J, Jones DT, Graff-Radford NR. Pathophysiology of language, speech and emotions in neurodegenerative disease. *Parkinsonism Relat Disord* 2014;20 Suppl 1:S49–53. doi:10.1016/S1353-8020(13)70014-2

84 Duval C, Bejanin A, Piolino P, *et al.* Theory of mind impairments in patients with semantic dementia. *Brain* 2012;135:228–41. doi:10.1093/brain/awr309

85 Kumfor F, Piguet O. Disturbance of emotion processing in frontotemporal dementia: a synthesis of cognitive and neuroimaging findings. *Neuropsychol Rev* 2012;22:280–97. doi:10.1007/s11065-012-9201-6

86 Goodkind MS, Sturm VE, Ascher EA, *et al.* Emotion recognition in frontotemporal dementia and Alzheimer's disease: A new film-based assessment. *Emotion* 2015;15:416–27. doi:10.1037/a0039261
87 Vuilleumier P, Pourtois G. Distributed and interactive brain mechanisms during emotion face perception: evidence from functional neuroimaging. *Neuropsychologia* 2007;45:174–94. doi:10.1016/j.neuropsychologia.2006.06.003
88 Cerami C, Crespi C, Della Rosa PA, *et al.* Brain changes within the visuo-spatial attentional network in posterior cortical atrophy. *J Alzheimers Dis* 2015;43:385–95. doi:10.3233/JAD-141275
89 Damoiseaux JS, Rombouts SA, Barkhof F, *et al.* Consistent resting-state networks across healthy subjects. *Proc Natl Acad Sci U S A* 2006;103:13848–53. doi:10.1073/pnas.0601417103

SUPPLEMENT

Supplemental Table 1. White matter tracts different between semantic dementia (SD) and behavioural variant frontotemporal dementia (bvFTD) based on the tract-based spatial statistics (TBSS) ($p<0.05$) analysis of diffusivity measures. Tractography tract thresholds are based on De Groot et al. (2015), but multiplied with a factor of eight due to the resolution difference.

White matter tract	Tractography threshold
Anterior thalamic radiation (ATR)	0.016
Cingulum (cingulate gyrus)	0.08
Cingulum (parahippocampal region)	0.16
Inferior fronto-occipital fasciculus (IFOF)	0.08
Inferior longitudinal fasciculus (ILF)	0.04
Superior longitudinal fasciculus (SLF)	0.008
Uncinate fasciculus (UF)	0.08

Supplemental Table 2A. Post-hoc two sample t-tests ($p_{corrected}$<0.05; k≥50) for FA investigating group differences between SD, bvFTD and controls.
FA = fractional anisotropy, SD = semantic dementia, bvFTD = behavioural variant frontotemporal dementia, L = left, R = right.

T-stat	Number of clusters	Total number of voxels	Number of voxels within largest cluster	Anatomical regions within largest cluster
SD<controls	16	41.147	38.759	L,R Forceps minor L,R Forceps major L,R Genu of the corpus callosum L,R Body of the corpus callosum L,R Splenium of the corpus callosum L,R Inferior fronto-occipital fasciculus L,R Anterior thalamic radiation L,R Cingulum L,R Uncinate fasciculus L,R Inferior longitudinal fasciculus L,R Superior longitudinal fasciculus
bvFTD<controls	11	48.453	47.210	L,R Forceps minor L,R Forceps major L,R Genu of the corpus callosum L,R Body of the corpus callosum L,R Splenium of the corpus callosum L,R Inferior fronto-occipital fasciculus L,R Anterior thalamic radiation L,R Cingulum L,R Uncinate fasciculus L,R Inferior longitudinal fasciculus L,R Superior longitudinal fasciculus
bvFTD<SD	2	5.550	4.968	L,R Forceps minor L,R Genu of the corpus callosum L,R Body of the corpus callosum R Inferior fronto-occipital fasciculus R Anterior thalamic radiation L,R Cingulum R Uncinate fasciculus

Supplemental Table 2B. Post-hoc two sample t-tests ($p_{corrected}$<0.05; k≥50) for MD investigating group differences between SD, bvFTD and controls.
MD = mean diffusivity, SD = semantic dementia, bvFTD = behavioural variant frontotemporal dementia, L = left, R = right.

T-stat	Number of clusters	Total number of voxels	Number of voxels within largest cluster	Anatomical regions within largest cluster
SD>controls	9	59.192	58.050	L,R Forceps minor L,R Forceps major L,R Genu of the corpus callosum L,R Body of the corpus callosum L,R Splenium of the corpus callosum L,R Inferior fronto-occipital fasciculus L,R Anterior thalamic radiation L,R Cingulum L,R Uncinate fasciculus L,R Inferior longitudinal fasciculus L,R Superior longitudinal fasciculus
bvFTD>controls	8	62.862	61.229	L,R Forceps minor L,R Forceps major L,R Genu of the corpus callosum L,R Body of the corpus callosum L,R Splenium of the corpus callosum L,R Inferior fronto-occipital fasciculus L,R Anterior thalamic radiation L,R Cingulum L,R Uncinate fasciculus L,R Inferior longitudinal fasciculus L,R Superior longitudinal fasciculus
bvFTD>SD	1	12.229	12.229	L,R Forceps minor L,R Genu of the corpus callosum L,R Body of the corpus callosum L,R Inferior fronto-occipital fasciculus L,R Anterior thalamic radiation L,R Cingulum L,R Uncinate fasciculus
SD>bvFTD	1	4.331	4.331	L Inferior fronto-occipital fasciculus L Uncinate fasciculus L Inferior longitudinal fasciculus L Superior longitudinal fasciculus

Supplemental Table 2C. Post-hoc two sample t-tests ($p_{corrected}$<0.05; k≥50) for RD investigating group differences between SD, bvFTD and controls.
RD = radial diffusivity, SD = semantic dementia, bvFTD = behavioural variant frontotemporal dementia, L = left, R = right.

T-stat	Number of clusters	Total number of voxels	Number of voxels within largest cluster	Anatomical regions within largest cluster
SD>controls	8	59.248	55.938	L,R Forceps minor L,R Forceps major L,R Genu of the corpus callosum L,R Body of the corpus callosum L,R Splenium of the corpus callosum L,R Inferior fronto-occipital fasciculus L,R Anterior thalamic radiation L,R Cingulum L,R Uncinate fasciculus L,R Inferior longitudinal fasciculus L,R Superior longitudinal fasciculus
bvFTD>controls	4	66.140	65.518	L,R Forceps minor L,R Forceps major L,R Genu of the corpus callosum L,R Body of the corpus callosum L,R Splenium of the corpus callosum L,R Inferior fronto-occipital fasciculus L,R Anterior thalamic radiation L,R Cingulum L,R Uncinate fasciculus L,R Inferior longitudinal fasciculus L,R Superior longitudinal fasciculus
bvFTD>SD	1	13.120	13.120	L,R Forceps minor L,R Genu of the corpus callosum L,R Body of the corpus callosum L,R Inferior fronto-occipital fasciculus L,R Anterior thalamic radiation L,R Cingulum L,R Uncinate fasciculus
SD>bvFTD	1	1.823	1.823	L Inferior fronto-occipital fasciculus L Uncinate fasciculus L Inferior longitudinal fasciculus L Superior longitudinal fasciculus

Supplemental Table 2D. Post-hoc two sample t-tests ($p_{corrected}$<0.05; k≥50) for AxD investigating group differences between SD, bvFTD and controls.
AxD = axial diffusivity, SD = semantic dementia, bvFTD = behavioural variant frontotemporal dementia, L = left, R = right.

T-stat	Number of clusters	Total number of voxels	Number of voxels within largest cluster	Anatomical regions within largest cluster
SD>controls	9	25.059	16.848	L Forceps minor L Forceps major L Genu of the corpus callosum L Body of the corpus callosum L Splenium of the corpus callosum L Inferior fronto-occipital fasciculus L Anterior thalamic radiation L Cingulum L Uncinate fasciculus L Inferior longitudinal fasciculus L Superior longitudinal fasciculus
bvFTD>controls	5	30.230	26.332	L,R Forceps minor L,R Forceps major L,R Genu of the corpus callosum L,R Body of the corpus callosum L,R Inferior fronto-occipital fasciculus L,R Anterior thalamic radiation L,R Cingulum L,R Uncinate fasciculus L,R Inferior longitudinal fasciculus L,R Superior longitudinal fasciculus
bvFTD>SD	2	557	347	R Inferior fronto-occipital fasciculus R Anterior thalamic radiation R Uncinate fasciculus
SD>bvFTD	2	3.605	2.862	L Inferior fronto-occipital fasciculus L Uncinate fasciculus L Inferior longitudinal fasciculus

Supplemental Table 3. Functional connectivity ($p<0.05_{FWE\_corrected}$) of affected GM regions in SD or bvFTD with the rest of the brain. GM = grey matter, SD = semantic dementia, bvFTD = behavioural variant frontotemporal dementia, ATL = anterior temporal lobe, OFC = orbitofrontal cortex, L = left, R= right, P = posterior, A = anterior.

		SD>HC	SD<HC	SD<bvFTD	bvFTD<HC	bvFTD>HC	bvFTD<SD
ATL L	**Number of clusters**	1	2	6	1	4	4
	Total number of voxels	5.120	26.128	29.500	2.199	2.159	6.585
	Number of voxels within largest cluster	n/a	26.070	19.471	n/a	1.261	5.442
	Anatomical regions within largest cluster	L Hippocampus L Amygdala L Fusiform gyrus L Parahippocampal gyrus (P,A) L Inferior temporal gyrus (P,A) L Middle temporal gyrus (P,A)	L,R Middle frontal gyrus L,R Superior frontal gyrus L,R Anterior cingulate cortex	L,R Middle frontal gyrus L,R Superior frontal gyrus R Anterior cingulate cortex	R Precentral gyrus R Middle frontal gyrus R Superior frontal gyrus R Supplemental motor area	L,R Cuneus L,R Calcarine cortex L R Occipital pole L,R lateral occipital cortex	L Hippocampus L Amygdala L Fusiform gyrus L Parahippocampal gyrus (P,A) L Inferior temporal gyrus (P,A) L Middle temporal gyrus (P,A) R Precentral gyrus

ATL R	**Number of clusters**		1		1		
	Total number of voxels		3.084		3.045		
	Number of voxels within largest cluster		n/a		n/a		
	Anatomical regions within largest cluster		L Superior temporal gyrus (P) L Middle temporal gyrus (P) L Inferior temporal gyrus (P)		L Superior temporal gyrus (P) L Middle temporal gyrus (P) L Inferior temporal gyrus (P)		

OFC L	**Number of clusters**		6	5	2		3
	Total number of voxels		6.015	8.253	3.808		4.055
	Number of voxels within largest cluster		1.762	3.402	3.806		2.650
	Anatomical regions within largest cluster		R Posterior cingulate cortex L, R Postcentral gyrus L, R Parietal operculum cortex L Central operculum cortex	R Posterior cingulate cortex L, R Post central gyrus L,RParietal operculum L,R Central operculum cortex	R Lingual R Occipital fusiform gyrus R Lateral occipital lobe R Inferior temporal gyrus (P) R Middle temporal gyrus (P)		R Lingual R Occipital fusiform gyrus R Lateral occipital lobe R Inferior temporal gyrus (P) R Middle temporal gyrus (P)

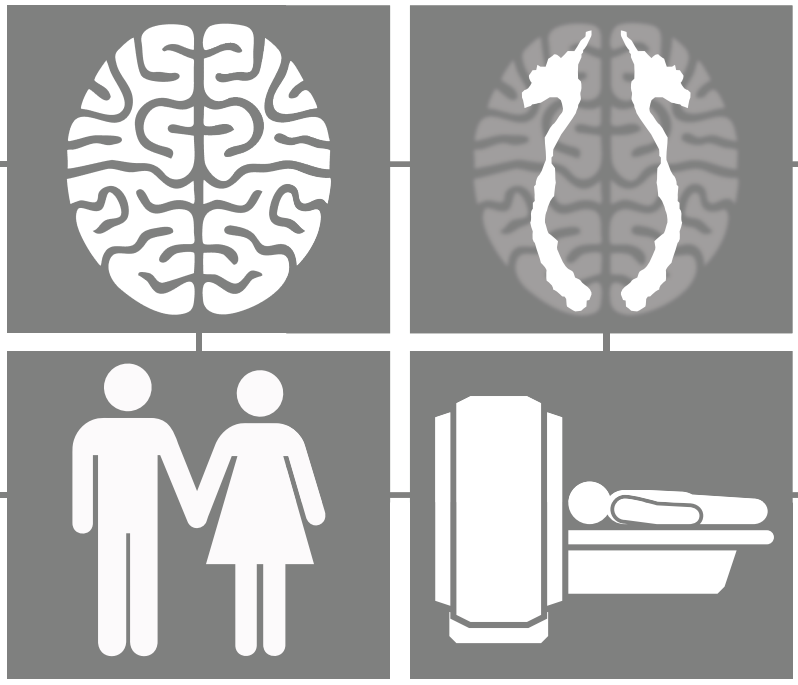

Section 4

Advanced MRI in phenocopy frontotemporal dementia

Chapter 4.1

Functional connectivity and microstructural white matter changes in phenocopy frontotemporal dementia

Rozanna Meijboom
Rebecca M.E. Steketee
Inge de Koning
Robert J. Osse
Lize C. Jiskoot
Frank J. de Jong
Aad van der Lugt
John C. van Swieten
Marion Smits

Eur Radiol. 2016 Jul 19. [Epub ahead of print]

ABSTRACT

Phenocopy frontotemporal dementia (phFTD) is a rare and poorly understood clinical syndrome. PhFTD shows core behavioural variant FTD (bvFTD) symptoms, without associated cognitive deficits and brain abnormalities on conventional MRI, and without progression. In contrast with phFTD, functional connectivity and white matter (WM) microstructural abnormalities have been observed in bvFTD. We hypothesise that phFTD belongs to the same disease spectrum as bvFTD, and investigated whether functional connectivity and microstructural WM changes similar to bvFTD are present in phFTD.

Seven phFTD patients without progression or alternative psychiatric diagnosis, twelve bvFTD patients and seventeen controls underwent resting state functional MRI (rs-fMRI) and diffusion tensor imaging (DTI). Default mode network (DMN) connectivity and WM measures were compared between groups.

PhFTD showed subtle increased DMN connectivity, and subtle microstructural changes in frontal WM tracts. BvFTD showed abnormalities in similar regions as phFTD, but had lower increased DMN connectivity, and more extensive microstructural WM changes.

Our findings can be interpreted as neuropathological changes in phFTD and are in support of the hypothesis that phFTD and bvFTD may belong to the same disease spectrum. Advanced MRI techniques, objectively identifying brain abnormalities, would therefore be potentially suited to improve diagnosis of phFTD.

1. INTRODUCTION

Phenocopy (or nonprogressive) frontotemporal dementia (phFTD) is a rare and poorly understood syndrome, which was only recently described by Davies et al. 2006 [1] in a subgroup of behavioural variant FTD (bvFTD) patients who had a better prognosis than expected.

PhFTD symptomatology is very similar to that of bvFTD, but some aspects of phFTD are essentially different. In phFTD, core bvFTD symptoms, such as apathy, behavioural disinhibition, and loss of insight[2], are generally not accompanied by cognitive and brain abnormalities as is the case in bvFTD. PhFTD patients show a cognitive profile that ranges from normal to suggesting FTD [3–6] and have a relatively intact performance of daily living activities (ADL)[2,6]. These clinical features in phFTD appear stable over time, whereas in bvFTD patients rapid progression of cognitive deficits is evident [1,6–8]. On conventional (structural) magnetic resonance imaging (MRI), phFTD patients show no or only borderline abnormalities [1,8] in the frontal and temporal regions that are typically affected in bvFTD[9]. Positron emission tomography (PET) does not show the frontal hypometabolism that is observed in bvFTD [10]. As bvFTD patients may initially also present without structural MRI abnormalities, early-stage distinction between phFTD and bvFTD may be difficult.

A pathophysiological explanation for phFTD symptomatology is currently unavailable. Patients often remain undiagnosed or receive an alternative psychiatric diagnosis. Additionally, they are occasionally found to be C9orf72 mutation carriers [11]. It is therefore of importance to investigate the presence of possible brain abnormalities underlying their symptoms using more advanced MRI techniques such as resting state functional MRI (rs-fMRI) and diffusion tensor imaging (DTI). These techniques measure subtle brain changes so far left unexplored, by looking at functional connectivity and microstructural white matter (WM). A well-defined network showing functional abnormalities in bvFTD is the default mode network (DMN). In bvFTD, parietal regions of the DMN show increased connectivity [12,13]. Frontal DMN connectivity changes are more ambiguous, found to be either increased [14] or decreased [12]. Such functional changes are thought to precede grey matter atrophy appearing at the later stages of bvFTD [12,15]. WM abnormalities in bvFTD are found mainly in frontal and temporal areas such as the uncinate fasciculus (UF), cingulum and the genu of the corpus callosum (CC) [16]. Similar regions are found to be already affected in asymptomatic-FTD mutation-carriers [15].

As phFTD patients present with behavioural symptoms similar to bvFTD, we hypothesise that phFTD and bvFTD may belong to the same disease spectrum.

This study investigates whether phFTD patients have underlying brain abnormalities that are similar to those seen in bvFTD patients: functional brain abnormalities expressed as DMN connectivity changes and microstructural WM abnormalities expressed as diffusion changes.

2. METHODS

2.1 Participants

All patients were recruited in the Alzheimer Centre Southwest Netherlands. PhFTD patients (aged 40-75 years) with prominent behavioural changes interfering with social functioning, consisting of disinhibition and/or apathy and/or stereotypy; no reported progression one year after initial routine diagnostic workup, and bvFTD patients (aged 45-70 years) with a diagnosis of bvFTD [17]; a clinical dementia rating scale score of ≤ 1; a Mini-Mental State Examination [18] (MMSE) score of ≥ 20, were included in the study.

Patients with other neurological disorders, past or current substance abuse or other psychiatric diagnosis were excluded. PhFTD patients with a diagnosis of dementia and missing heteroamnesis, and bvFTD patients with a different cause of dementia, were also excluded.

Healthy controls (aged 60-70 years), without neurological or psychiatric history, were recruited through advertisement. They were matched for gender with phFTD patients and for age with all patients.

The study was approved by the local medical ethics committee. All participants gave written informed consent.

2.2 Psychiatric, neuropsychological and genetic mutation assessment

PhFTD patients underwent full psychiatric assessment as part of this study to exclude alternative diagnoses. Additionally, their DNA was tested for the C9orf72 mutation.

All participants underwent a full neuropsychological assessment and an MMSE [18]. Six phFTD patients had a cognitive profile suggestive of FTD, but

showed no progression relative to previous neuropsychological testing consistent with the phFTD criteria. One phFTD patient had a normal cognitive profile. Mean interval between current and first neuropsychological testing was 36 months (range: 8-71 months). The cognitive profile was consistent with bvFTD for bvFTD patients and normal for controls.

2.3 Image acquisition

Scanning was performed on two 3T GE Discovery MR750 systems (GE Healthcare, Milwaukee, WI, US) with identical protocols. PhFTD patients and twelve controls were scanned on one, and bvFTD patients and eight controls on the other scanner. All participants underwent a high-resolution three-dimensional (3D) inversion recovery (IR) fast spoiled gradient echo (FSPGR) T1-weighted image for anatomical reference, and a functional gradient echo echo planar imaging (EPI) and

Table 1. Acquisition parameters.

	T1w	fMRI	DTI
FOV (mm)	240	240	240
TE (ms)	3.06	30	84.2*
TR (ms)	7.90	3000	7925
ASSET factor	2	2	2
Flip angle	12°	90°	90°
Acquisition matrix	240x240	96x96	128x128
Slice thickness (mm)	1	3	2.5
Volumes (slices per volume)	1 (176)	200 (44)	28 (59)
Duration (min)	4.41	10.00	3.50
Diffusion-weighted directions	n/a	n/a	25
Maximum b-value (s/ mm2)	n/a	n/a	1000
TI (ms)	450	n/a	n/a

T1w = T1-weighted, fMRI = functional magnetic resonance imaging, DTI = diffusion tensor imaging, FOV= field of view, TE = echo time, TR = repetition time, ASSET = array spatial sensitivity encoding technique, TI = inversion time.
*TE for DTI was set to minimum. This number represents the average TE. The range of TE was 81.9-90.8 ms.

DTI spin echo EPI with full coverage of the supratentorial brain (Table 1). During the functional scan participants were instructed to focus on a fixation cross, to think of nothing in particular, and to stay awake.

2.4 Structural MRI analysis

Whole brain grey matter (GM) volume was calculated for each participant according to the methods described in Bron et al. 2014 [19]. For each participant, whole brain GM volume was divided by their individual intracranial volume (ICV) to correct for head size (expressed as % ICV)[20–22], and referred to as normalised GM (nGM). These values (%ICV) were then averaged per group, resulting in a mean nGM volume expressed as %ICV. These group means were then compared between groups using a one-way ANOVA and post-hoc Bonferroni tests (SPSS21, USA).

2.5 Rs-fMRI analysis

Rs-fMRI data were analysed using FMRIB Software library (FSL4.1.9, UK) (see supplement section 1 for more detail). The brain was extracted using the Brain Extraction Tool (BET) [23]. Then, MELODIC independent component analysis was used for pre-processing of the functional data and establishing the DMN component. Due to small sample size, only one network of interest could be investigated. The DMN was chosen as it is a well-defined functional network showing functional abnormalities in bvFTD, allowing for meaningful comparison between phFTD and bvFTD. Hereafter, the participant-specific DMN was identified using Dual regression [24]. Subsequently, Randomise [25] was used to assess between-group DMN connectivity differences using a one-way ANCOVA with three groups (phFTD≠bvFTD≠controls) and GM volume as covariate. Main effects were investigated and six t-contrasts (phFTD>HC, HC>phFTD, bvFTD>HC, HC>bvFTD, phFTD>bvFTD, bvFTD>phFTD) were constructed to assess post-hoc between-group differences.

Cluster was used to extract cluster information. Results ($p_{corrected}$<0.05, cluster size (k) ≥1; $p_{uncorrected}$ <0.05, k≥20) were visualised using FSLview. Structural atlases implemented in FSLView were used to anatomically identify the DMN regions.

2.6 DTI analysis

Data were corrected for motion, eddy currents and EPI distortions using ExploreDTI [26]. Further analyses were performed with FSL (5.0.2.2, UK) (see supplement section 1 for more detail). BET [23] was used to create skull-stripped binary-masks, after which DTIFIT [27] was used to reconstruct diffusion tensors and to create subject images for all WM measures, i.e. fractional anisotropy (FA), mean diffusivity (MD), axial diffusivity (AxD) and radial diffusivity (RD). Then, registration was performed using Tract-Based Spatial Statistics (TBSS) [28], resulting in subject-specific WM skeletons for each WM measure. Subsequently, Randomise [25] was used to assess between-group WM measure differences using a one-way ANOVA with the same groups and post-hoc t-tests as in the rs-fMRI analysis.

Cluster was used to extract cluster information. Results ($p_{corrected}<0.05$, $k\geq20$) were visualised using FSLView. The WM atlases implemented in FSLView were used to anatomically identify the WM regions.

3. RESULTS

3.1 Participant and disease characteristics

Data of 7 phFTD patients, 12 bvFTD patients (9 for rs-fMRI analysis) and 17 controls were used for the current analyses (Table 2). In total, nine phFTD patients (all male), 12 bvFTD patients (seven male) and 20 healthy controls (all male) were originally included in the study. Two phFTD patients and three controls were excluded from the analysis (see supplement section 2). Three bvFTD patients had missing rs-fMRI data. One phFTD patient's follow-up was just under one year (11 months), for logistical reasons. The clinical diagnosis phFTD was established based on the clinical profile and lack of disease progression.

Table 2. Demographic characteristics.

Group	N	Mean age	Mean MMSE
PhFTD	7 (all male)	63.4 (4.8)	26.6 (1.4)
BvFTD	12 (7 male)	60.2 (7.6)	26.6 (2.8)
Controls	17 (all male)	64.1 (3.3)	28.2 (1.5)

PhFTD = phenocopy FTD. BvFTD = behavioural FTD. N = sample size. Values given as Mean (SD). MMSE = Mini-Mental State Examination.

Age (H (2) = 2,23 p>0.05, Table 2) and MMSE score did not differ between groups (H (2) = 5,93, p>0.05, Table 2).

None of the phFTD patients received an alternative psychiatric diagnosis that could explain their behavioural symptoms. Additionally, none carried the C9orf72 mutation.

3.2 Structural MRI

The three groups showed a difference in nGM (H (2) = 16.38, p<0.05), with a mean of 0.32 %ICV (SD 0.02) for phFTD, 0.29 %ICV (SD 0.04) for bvFTD, and 0.35 %ICV (SD 0.02) for controls. Compared with controls, both phFTD patients (p=0.013) and bvFTD patients (p<0.001) had lower nGM volume. nGM volume was not different between phFTD and bvFTD patients (p=0.359).

3.3 Functional connectivity

PhFTD and bvFTD patients (Figure 1, supplement Table 1A) showed connectivity in all regions of the DMN. Controls showed connectivity in all DMN regions except the right lateral temporal cortex (LTC) (Figure 1, supplement Table 1A).

PhFTD patients compared with controls showed increased DMN connectivity in the bilateral medial prefrontal cortex (mPFC), LTC, and inferior parietal lobule (IPL), and in the left posterior cingulate cortex (PCC)/precuneus (Figure 2, supplement Table 1B).

BvFTD patients compared with controls showed increased DMN connectivity in the bilateral mPFC, and right LTC and IPL (Figure 2, supplement Table 1B), and decreased DMN connectivity in the more posterior right IPL.

PhFTD patients compared with bvFTD patients showed increased DMN connectivity in the bilateral mPFC and LTC, and right IPL (Figure 2, supplement Table 1B).

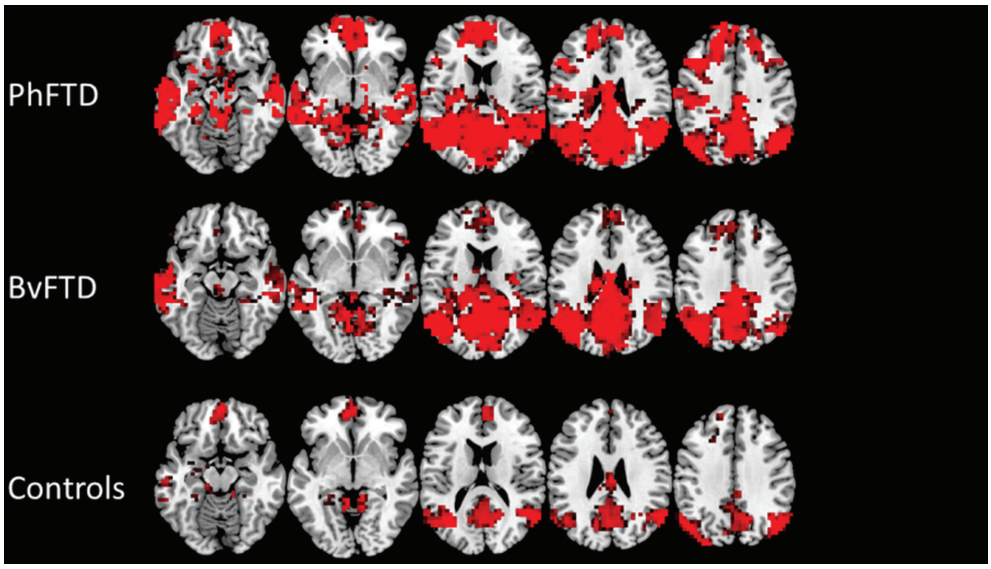

Figure 1. Mean default mode network (DMN) connectivity ($p<0.05$, not corrected for multiple comparisons, but Bonferroni corrected ($p<0.05$) for multiple contrasts; $k\geq20$) in phenocopy frontotemporal dementia (phFTD), behavioural variant FTD (bvFTD) and controls.

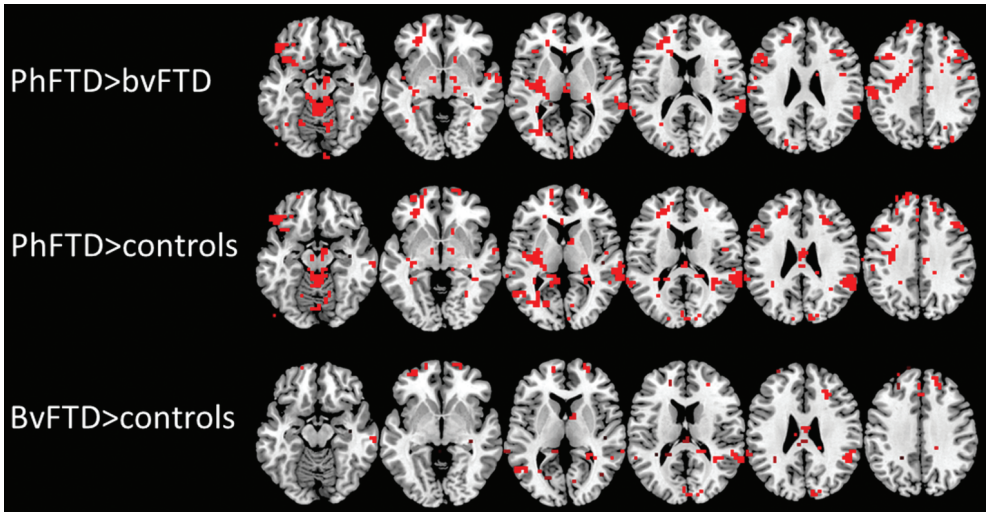

Figure 2. Post-hoc t-test comparisons (phFTD>bvFTD, phFTD>controls, bvFTD>controls) showing between-group DMN connectivity differences ($p<0.05$, not corrected for multiple comparisons, but within the constraints of the omnibus f-test ($p<0.05$, Bonferroni corrected for multiple contrasts); $k\geq20$).
DMN = default mode network, phFTD = phenocopy frontotemporal dementia, bvFTD = behavioural variant FTD.

3.4 Microstructural WM

PhFTD and bvFTD patients compared with controls showed decreased FA and increased RD and MD mainly in the frontal and temporoparietal WM (Figure 3, supplement Tables 2A-C), such as the cingulum (both cingulate and hippocampus portion), inferior fronto-occipital fasciculus (IFOF), superior longitudinal fasciculus (SLF), corpus callosum and uncinate fasciculus. In bvFTD patients in comparison with controls increased AxD was observed in these regions as well (Figure 3, supplement Table 2D).

BvFTD patients compared with phFTD patients showed decreased FA and increased AxD in frontal WM, and increased MD and RD in frontotemporal WM, mainly in the cingulum (cingulate portion), IFOF, SLF, corpus callosum and uncinate fasciculus (Figure 4, supplement Tables 2A-D).

Figure 4. Post-hoc t-test microstructural white matter changes for bvFTD in comparison with phFTD ($p_{corrected}$<0.05; k≥20). Lower FA and higher MD, RD and AxD in bvFTD are shown in blue. PhFTD = phenocopy frontotemporal dementia, bvFTD = behavioural variant FTD, FA = fractional anisotropy, MD = mean diffusivity, RD = radial diffusivity, AxD = axial diffusivity.

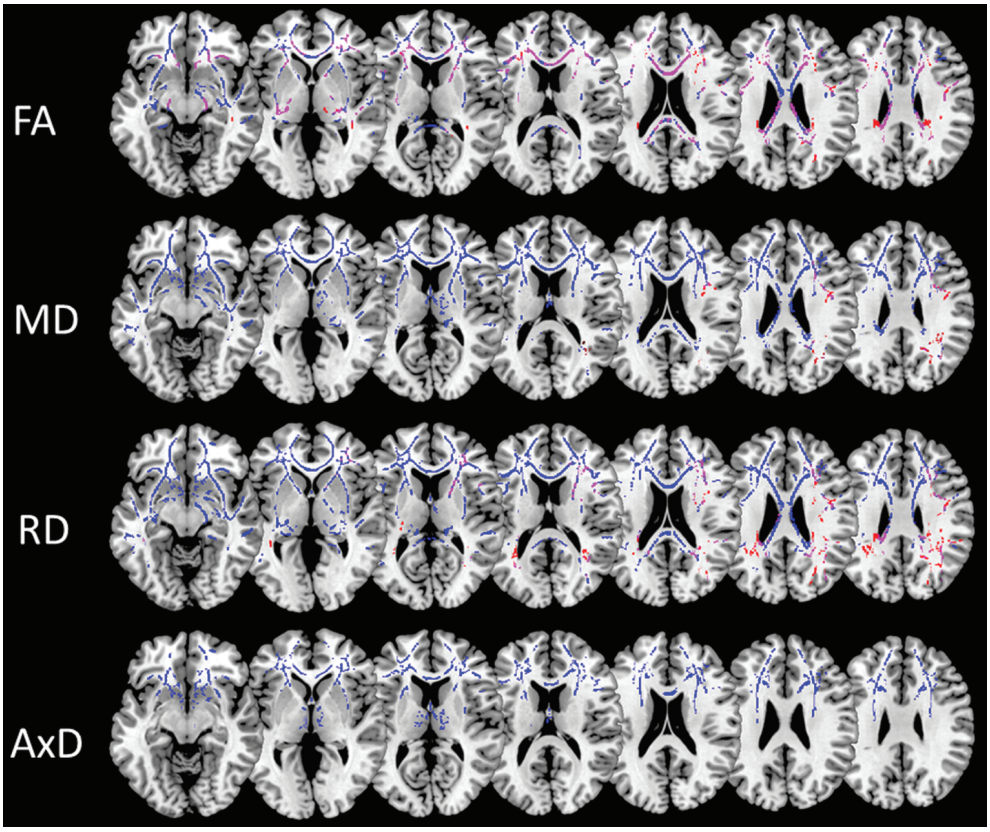

Figure 3. Post-hoc t-test of microstructural white matter changes for phFTD ($p_{corrected}$<0.05; k≥20) and bvFTD ($p_{corrected}$<0.05; k≥20) in comparison with controls. Lower FA and higher MD, RD and AxD in comparison with controls is shown in phFTD in red and in bvFTD in blue. WM regions showing overlapping abnormalities in phFTD and bvFTD are shown in pink.
PhFTD = phenocopy frontotemporal dementia, bvFTD = behavioural variant frontotemporal dementia, FA = fractional anisotropy, MD = mean diffusivity, RD = radial diffusivity, AxD = axial diffusivity.

4. DISCUSSION

To the best of our knowledge, this is the first study demonstrating functional connectivity changes and microstructural WM abnormalities in phFTD. There was increased DMN connectivity in nearly all regions of the DMN, and abnormal microstructural WM in frontal and temporoparietal lobes. These changes were similar to the changes observed in bvFTD, supporting our hypothesis that phFTD may belong to the same disease spectrum as bvFTD. Specifically, bvFTD also showed higher connectivity in DMN regions, but to a lesser extent than in phFTD, and microstructural WM abnormalities in the frontal and temporoparietal lobes, but more pronounced than in phFTD.

DMN connectivity was increased, albeit to a moderate extent, in both phFTD and bvFTD. As there are overt behavioural symptoms in phFTD, as well as frequent neuropsychological abnormalities, it is not surprising to observe functional brain abnormalities. Increased functional connectivity reflects changes in neuronal activity becoming more congruent between regions. This may point to a brain mechanism compensating for early diminished neuronal functioning [29,30]. The degree of increased connectivity may reflect the brain's remaining ability of compensation, and in case of advanced neuronal dysfunctioning, this ability may no longer present, resulting in decreased connectivity. This theory may explain why we observe higher connectivity in phFTD than in bvFTD. As pronounced cortical atrophy is evident in bvFTD but not in phFTD [1,8,9,31], neuronal dysfunctioning is likely much more prominent in bvFTD. This means that more relatively preserved neurons in phFTD may be able to provide a better functioning compensational mechanism than in bvFTD. The observation that the inferior parietal lobule showed both increased and decreased (depending on its subregion) functional connectivity in bvFTD in comparison with controls, is in line with this view. It is plausible that the various subregions of the inferior parietal lobule are not affected to the same extent in bvFTD, resulting in decreased functional connectivity in the more affected subregion and in increased functional connectivity in the less affected subregion. Future studies consisting of a larger patient sample could shed further light on whether other resting state networks show similar functional connectivity changes to the DMN. A network of particular interest would be the salience network, which is a frontal functional network known to be affected in bvFTD [13]. This would allow for further meaningful comparisons between phFTD and bvFTD.

Frontotemporal and parietal microstructural WM abnormalities were observed in both phFTD and bvFTD. In phFTD, FA was decreased (i.e. there was less directional diffusion) and RD and MD were increased (i.e. there was more diffu-

sion, particularly perpendicular to the tract's axis) in multiple WM tracts, including the cingulum, UF, IFOF, genu of the CC and SLF. Damage to these WM tracts has been linked to the various cognitive functions typically affected in bvFTD. Loss of behavioural control (e.g. disinhibition) has been related to diffusion changes in the UF, forceps minor and cingulum [32,33]. Additionally, abnormalities in executive functioning, visuo-spatial attention, working memory and apathy have also been linked with diffusivity changes in the cingulum [34,35]. Interestingly, RD changes in these tracts were less pronounced than FA changes, which may be explained by FA being a composite measure of both RD and AxD (i.e. diffusion along the tract's main axis), and therefore more sensitive to subtle myelin and/or axonal changes, reflected by changes in RD [36] and AxD [37] respectively. In phFTD, AxD abnormalities were not observed, which may be explained by myelin damage only, without axonal injury. In bvFTD, WM changes were more pronounced and widespread, with lower FA, and higher MD, RD and AxD than in phFTD. Hence, here we show an association in phFTD, similar to bvFTD, between symptomatology and damage to the frontotemporal and parietal WM tracts. Additionally, we show differences possibly reflecting neuropathological changes between phFTD and bvFTD, with phFTD suggesting myelin damage only, and bvFTD showing more pronounced myelin and axonal damage.

Previous literature has shown a relationship between microstructural WM changes and functional connectivity changes [38–40], and proposes that microstructural WM predicts, or is reflected by, functional connectivity [39,40]. For example, the medial prefrontal cortex and posterior cingulate cortex, core regions of the DMN, are connected through the cingulum [39]. Cingulum abnormalities such as observed in this study may have – to a certain extent – disconnected these regions, reducing functional connectivity between anterior and posterior DMN regions. In support of this idea, there were more pronounced anterior WM abnormalities in bvFTD that extended more posteriorly than in phFTD, and both frontal and parietal functional connectivity were seen to be correspondingly lower. A recent study by Weiler et al. (2014) [41] observed that higher RD in the cingulum and parahippocampal bundle (both connecting DMN regions) predicted reduced performance on measures related to DMN cognitive functions. We therefore hypothesise that more advanced abnormalities of WM tracts of the DMN may eventually lead to a functional decrease in the associated DMN areas and result in reduced cognitive functioning. As we did not aim to directly explore such a mechanism, our study design does not allow for any firm conclusions concerning this mechanism. A longitudinal design employing correlational analyses is needed to verify this hypothesis.

Overall, phFTD showed functional connectivity and subtle WM changes, whereas bvFTD showed fewer functional connectivity and more extensive WM changes. Lower overall cortical GM volume in phFTD patients was observed in this study using a quantitative method, but was not observed in the regular clinical diagnostic work-up. This suggests that GM volume loss is also present in phFTD patients, but at such a limited degree that it is not clinically detected. These findings are indicative of incipient degeneration in phFTD. In order to investigate phFTD without the interference of an alternative diagnosis we ruled out alternative psychiatric disorders, neuropsychological progression and presence of the C9orf72 mutation. The observed incipient brain changes in this well-defined population are in favour of the controversial notion that phFTD and bvFTD may belong to the same disease spectrum. PhFTD presents with behavioural, neuropsychological and, as shown here, also neurodegenerative changes that are all similar to those observed in bvFTD.

This study has some limitations. First, we were only able to investigate a small number of phFTD and bvFTD patients, limiting statistical power. As a result, rs-fMRI effects, already expected to be subtle, were only detectable using a relatively lenient statistical threshold, and could only be investigated in one functional network.The sample size is inherent to the rarity of the phFTD syndrome, together with the application of strict inclusion and exclusion criteria to avoid inadvertent inclusion of patients with bvFTD or alternative psychiatric disorders. Second, the bvFTD group was not fully matched for gender with the phFTD and control group. There is no conclusive evidence on gender differences in functional connectivity [42] or microstructural WM. Both higher and lower FA was measured in the cingulum and in the WM underlying the frontal cortex in men and in women compared with the opposite gender [43]. Given these findings it is not likely that the FA decreases observed in this study were driven by gender differences. Third, the bvFTD group and part of the control group were scanned on a different scanner, although of identical type and field strength, and with identical protocols. While a scanner effect cannot be excluded, both rs-fMRI and DTI have been shown to be highly reproducible in terms of DMN functional connectivity and TBSS respectively, even across different scanner platforms and vendors [44,45]. Moreover, the fact that our findings in bvFTD are consistent with the previous literature suggest that the effect of scanner is likely to be minimal.

In conclusion, our findings are in support of the hypothesis that phFTD and bvFTD may belong to the same disease spectrum. In phFTD, there are changes in functional connectivity and microstructural WM that are similar to those found in

bvFTD. Advanced MRI techniques, such as rs-fMRI and DTI, are therefore potentially suited to improve diagnosis of phFTD by identifying such incipient changes. Naturally, the hypothesis that phFTD and bvFTD may belong to the same disease spectrum would require confirmation with other diagnostic tools, such as histopathology. Also, further assessment in a longitudinal study to assess changes over time would be required, at which our future efforts are aimed. Our findings could provide a direction for further development of MR - or other - diagnostic tools.

REFERENCES

1 Davies RR, Kipps CM, Mitchell J, *et al.* Progression in frontotemporal dementia: identifying a benign behavioral variant by magnetic resonance imaging. *Arch Neurol* 2006;63:1627–31. doi:10.1001/archneur.63.11.1627

2 Hornberger M, Shelley BP, Kipps CM, *et al.* Can progressive and non-progressive behavioural variant frontotemporal dementia be distinguished at presentation? *J Neurol Neurosurg Psychiatry* 2009;80:591–3. doi:10.1136/jnnp.2008.163873

3 Bertoux M, de Souza LC, Corlier F, *et al.* Two Distinct Amnesic Profiles in Behavioral Variant Frontotemporal Dementia. *Biol Psychiatry* Published Online First: 2013. doi:10.1016/j.biopsych.2013.08.017

4 Hornberger M, Piguet O, Kipps C, *et al.* Executive function in progressive and nonprogressive behavioral variant frontotemporal dementia. *Neurology* 2008;71:1481–8. doi:10.1212/01.wnl.0000334299.72023.c8

5 Irish M, Graham A, Graham KS, *et al.* Differential impairment of source memory in progressive versus non-progressive behavioral variant frontotemporal dementia. *Arch Clin Neuropsychol* 2012;27:338–47. doi:10.1093/arclin/acs033

6 Mioshi E, Hodges JR. Rate of change of functional abilities in frontotemporal dementia. *Dement Geriatr Cogn Disord* 2009;28:419–26. doi:10.1159/000255652

7 Garcin B, Lillo P, Hornberger M, *et al.* Determinants of survival in behavioral variant frontotemporal dementia. *Neurology* 2009;73:1656–61. doi:10.1212/WNL.0b013e3181c1dee7

8 Kipps CM, Davies RR, Mitchell J, *et al.* Clinical significance of lobar atrophy in frontotemporal dementia: application of an MRI visual rating scale. *Dement Geriatr Cogn Disord* 2007;23:334–42. doi:10.1159/000100973

9 Rosen HJ, Gorno-Tempini ML, Goldman WP, *et al.* Patterns of brain atrophy in frontotemporal dementia and semantic dementia. *Neurology* 2002;58:198–208.http://www.ncbi.nlm.nih.gov/pubmed/11805245

10 Kipps CM, Hodges JR, Fryer TD, *et al.* Combined magnetic resonance imaging and positron emission tomography brain imaging in behavioural variant frontotemporal degeneration: refining the clinical phenotype. *Brain* 2009;132:2566–78. doi:10.1093/brain/awp077

11 Khan BK, Yokoyama JS, Takada LT, *et al.* Atypical, slowly progressive behavioural variant frontotemporal dementia associated with C9ORF72 hexanucleotide expansion. *J Neurol Neurosurg Psychiatry* 2012;83:358–64. doi:10.1136/jnnp-2011-301883

12 Whitwell JL, Josephs KA, Avula R, *et al.* Altered functional connectivity in asymptomatic MAPT subjects: a comparison to bvFTD. *Neurology* 2011;77:866–74. doi:10.1212/WNL.0b013e31822c61f2

13 Zhou J, Greicius MD, Gennatas ED, *et al.* Divergent network connectivity changes in behavioural variant frontotemporal dementia and Alzheimer's disease. *Brain* 2010;133:1352–67. doi:10.1093/brain/awq075
14 Rytty R, Nikkinen J, Paavola L, *et al.* GroupICA dual regression analysis of resting state networks in a behavioral variant of frontotemporal dementia. *Front Hum Neurosci* 2013;7:461. doi:10.3389/fnhum.2013.00461
15 Dopper EGP, Rombouts SARB, Jiskoot LC, *et al.* Structural and functional brain connectivity in presymptomatic familial frontotemporal dementia. *Neurology* 2014;83:e19–26. doi:10.1212/WNL.0000000000000583
16 Mahoney CJ, Ridgway GR, Malone IB, *et al.* Profiles of white matter tract pathology in frontotemporal dementia. *Hum Brain Mapp* 2014;35:4163–79. doi:10.1002/hbm.22468
17 Rascovsky K, Hodges JR, Knopman D, *et al.* Sensitivity of revised diagnostic criteria for the behavioural variant of frontotemporal dementia. *Brain* 2011;134:2456–77. doi:10.1093/brain/awr179
18 Folstein MF, Folstein SE, McHugh PR. 'Mini-mental state'. A practical method for grading the cognitive state of patients for the clinician. *J Psychiatr Res* 1975;12:189–98.http://www.ncbi.nlm.nih.gov/pubmed/1202204.
19 Bron EE, Steketee RME, Houston GC, *et al.* Diagnostic classification of arterial spin labeling and structural MRI in presenile early stage dementia. *Hum Brain Mapp* 2014;35:4916–31. doi:10.1002/hbm.22522
20 Arvanitakis Z, Fleischman DA, Arfanakis K, *et al.* Association of white matter hyperintensities and gray matter volume with cognition in older individuals without cognitive impairment. *Brain Struct Funct* 2015;:2135–46. doi:10.1007/s00429-015-1034-7
21 Van Elderen SSGC, Zhang Q, Sigurdsson S, *et al.* Brain Volume as an Integrated Marker for the Risk of Death in a Community-Based Sample: Age Gene/Environment Susceptibility-Reykjavik Study. *Journals Gerontol - Ser A Biol Sci Med Sci* 2015;71:131–7. doi:10.1093/gerona/glu192
22 Dalton CM, Chard DT, Davies GR, *et al.* Early development of multiple sclerosis is associated with progressive grey matter atrophy in patients presenting with clinically isolated syndromes. *Brain* 2004;127:1101–7. doi:10.1093/brain/awh126
23 Smith SM. Fast robust automated brain extraction. *Hum Brain Mapp* 2002;17:143–55. doi:10.1002/hbm.10062
24 Filippini N, MacIntosh BJ, Hough MG, *et al.* Distinct patterns of brain activity in young carriers of the APOE-epsilon4 allele. *Proc Natl Acad Sci U S A* 2009;106:7209–14. doi:10.1073/pnas.0811879106
25 Winkler AM, Ridgway GR, Webster MA, *et al.* Permutation inference for the general linear model. *Neuroimage* 2014;92:381–97. doi:10.1016/j.neuroimage.2014.01.060

26 Leemans A, Jeurissen B, Sijbers J, *et al.* ExploreDTI: a graphical toolbox for processing, analyzing, and visualizing diffusion MR data. In: *Proceedings 17th Scientific Meeting, International Society for Magnetic Resonance in Medicine*. 2009. 3537.http://www.mendeley.com/research/exploredti-a-graphical-toolbox-for-processing-analyzing-and-visualizing-diffusion-mr-data/\nhttp://www.exploredti.com/ref/ExploreDTI_ISMRM_2009.pdf

27 Behrens TEJ, Woolrich MW, Jenkinson M, *et al.* Characterization and propagation of uncertainty in diffusion-weighted MR imaging. *Magn Reson Med* 2003;50:1077–88. doi:10.1002/mrm.10609

28 Smith SM, Jenkinson M, Johansen-Berg H, *et al.* Tract-based spatial statistics: voxelwise analysis of multi-subject diffusion data. *Neuroimage* 2006;31:1487–505. doi:10.1016/j.neuroimage.2006.02.024

29 Borroni B, Alberici A, Cercignani M, *et al.* Granulin mutation drives brain damage and reorganization from preclinical to symptomatic FTLD. *Neurobiol Aging* 2012;33:2506–20. doi:10.1016/j.neurobiolaging.2011.10.031

30 Bookheimer SY, Strojwas MH, Cohen MS, *et al.* Patterns of brain activation in people at risk for Alzheimer's disease. *N Engl J Med* 2000;343:450–6. doi:10.1056/NEJM200008173430701

31 Seeley WW, Crawford R, Rascovsky K, *et al.* Frontal paralimbic network atrophy in very mild behavioral variant frontotemporal dementia. *Arch Neurol* 2008;65:249–55. doi:10.1001/archneurol.2007.38

32 Hornberger M, Geng J, Hodges JR. Convergent grey and white matter evidence of orbitofrontal cortex changes related to disinhibition in behavioural variant frontotemporal dementia. *Brain* 2011;134:2502–12. doi:10.1093/brain/awr173

33 Whitwell JL, Avula R, Senjem ML, *et al.* Gray and white matter water diffusion in the syndromic variants of frontotemporal dementia. *Neurology* 2010;74:1279–87. doi:10.1212/WNL.0b013e3181d9edde

34 Lu PH, Lee GJ, Shapira J, *et al.* Regional differences in white matter breakdown between frontotemporal dementia and early-onset Alzheimer's disease. *J Alzheimers Dis* 2014;39:261–9. doi:10.3233/JAD-131481

35 Tartaglia MC, Zhang Y, Racine C, *et al.* Executive dysfunction in frontotemporal dementia is related to abnormalities in frontal white matter tracts. *J Neurol* 2012;259:1071–80. doi:10.1007/s00415-011-6300-x

36 Song S-K, Sun S-W, Ramsbottom MJ, *et al.* Dysmyelination Revealed through MRI as Increased Radial (but Unchanged Axial) Diffusion of Water. *Neuroimage* 2002;17:1429–36. doi:10.1006/nimg.2002.1267

37 Song S-K, Sun S-W, Ju W-K, *et al.* Diffusion tensor imaging detects and differentiates axon and myelin degeneration in mouse optic nerve after retinal ischemia. *Neuroimage* 2003;20:1714–22. doi:10.1016/j.neuroimage.2003.07.005

38 Damoiseaux JS, Greicius MD. Greater than the sum of its parts: a review of studies combining structural connectivity and resting-state functional connectivity. *Brain Struct Funct* 2009;213:525–33. doi:10.1007/s00429-009-0208-6

39 Greicius MD, Supekar K, Menon V, *et al.* Resting-state functional connectivity reflects structural connectivity in the default mode network. *Cereb Cortex* 2009;19:72–8. doi:10.1093/cercor/bhn059

40 Honey CJ, Sporns O, Cammoun L, *et al.* Predicting human resting-state functional connectivity. 2009;106:1–6.

41 Weiler M, de Campos BM, Nogueira MH, *et al.* Structural connectivity of the default mode network and cognition in Alzheimer's disease. *Psychiatry Res* 2014;223:15–22. doi:10.1016/j.pscychresns.2014.04.008

42 Weissman-Fogel I, Moayedi M, Taylor KS, *et al.* Cognitive and default-mode resting state networks: do male and female brains 'rest' differently? *Hum Brain Mapp* 2010;31:1713–26. doi:10.1002/hbm.20968

43 Gong G, He Y, Evans AC. Brain connectivity: gender makes a difference. *Neuroscientist* 2011;17:575–91. doi:10.1177/1073858410386492

44 Choe AS, Jones CK, Joel SE, *et al.* Reproducibility and Temporal Structure in Weekly Resting-State fMRI over a Period of 3.5 Years. *PLoS One* 2015;10:e0140134. doi:10.1371/journal.pone.0140134

45 Jovicich J, Marizzoni M, Bosch B, *et al.* Multisite longitudinal reliability of tract-based spatial statistics in diffusion tensor imaging of healthy elderly subjects. *Neuroimage* 2014;101:390–403. doi:10.1016/j.neuroimage.2014.06.075

SUPPLEMENT

Supplement section 1

Rs-fMRI analysis

Resting state data were analysed using FMRIB Software library (FSL4.1.9, Oxford, UK)[1–3]. T1w images were first reoriented to ensure the same orientation as the standard template T1 images. The skull was stripped using the Brain Extraction Tool (BET)[4].

The Multivariate Exploratory Linear Optimised Decomposition into Independent Components (MELODIC) toolbox was used to preprocess the data and to perform independent component analysis (ICA). Preprocessing consisted of several steps. First the high pass filter was set to remove low-frequency drifts (cut-off 120s). Then MCFLIRT[5] motion correction was applied to correct for linear motion followed by spatial smoothing performed with a Gaussian kernel of 5 FWHM. During registration, functional data were first linearly registered to the corresponding T1w images (full search, 7 degrees of freedom (DOF)). This was followed by both linear and nonlinear registration to a standard template brain (full search, 12 DOF) with a warp resolution of 10mm and a resampling resolution of 4mm. Resting state networks were identified by performing a multi-session temporal concatenation ICA. Component output was limited to 30. Dual regression[6] was used to identify the group components in the functional data of each participant. The component representing the DMN was identified. The DMN was chosen because it is an anatomically clearly defined network and shows pronounced abnormalities in bvFTD patients [7,8]. Only one network was investigated because of the small sample size of the study and thus reduced statistical power. FSLcc was used to identify the component showing the highest correlation between a DMN template[9] and ICA output.

The Randomise[10] tool was used to assess between-group differences in DMN network connectivity. The design was constructed using the general linear model (GLM) toolbox. A one-way ANCOVA with three groups (phFTD≠bvFTD≠controls) was performed to assess which regions showed different connectivity between groups. Effects per group were investigated and six t-contrasts (phFTD>HC, HC>phFTD, bvFTD>HC, HC>bvFTD, phFTD>bvFTD, bvFTD>phFTD) were constructed to assess post-hoc between-group differences. Grey matter volume was added as covariate to account for grey matter atrophy. Threshold-free cluster enhancement (TFCE) [11] and nonparametric permutation testing with 5000 permutations was applied. Results were not family-wise

error corrected for multiple comparisons on a voxel level. However, the f-test resulting from the one-way ANOVA and the group effects (phFTD, bvFTD, controls) were Bonferroni corrected for the number of contrasts, thus using an effective threshold of $p<0.0125$. Subsequent Bonferroni correction for the number of post-hoc t-tests was considered unnecessary as their results were assessed within the constraints of the omnibus f-test. This was done by creating common binary masks to identify post-hoc t-tests results within the omnibus f-test positive connectivity regions. Using the FSLmaths tool, first binary masks were created for the f-test and for every t-test. Second, the binary mask of each t-test was multiplied with binary mask of the f-test, resulting in common binary masks for each t-test.

All t-test common binary masks ($p<0.05$, not corrected for multiple comparisons), the f-test and the three group effects ($p<0.05$, Bonferroni corrected for multiple contrasts) were evaluated using the Cluster tool to extract cluster size with a cluster threshold of $k\geq20$ voxels.

Results were visualised using FSLview. The Harvard-Oxford Cortical Structural Atlas and the Harvard-Oxford Subcortical Structural Atlas implemented in FSLView were used to anatomically identify the DMN regions.

DTI analysis

Data were corrected for motion, eddy currents and EPI distortions using ExploreDTI[12]. Further analyses were performed with FSL (5.0.2.2, Oxford, UK) [1–3]. BET[4] was used to create skull-stripped binary-masks. Using DTIFIT, as implemented in FMRIB's Diffusion Toolbox (FDT)[13], the diffusion tensors were reconstructed. Then DTIFIT created subject images for fractional anisotropy (FA), mean diffusivity (MD), the first eigenvalue/axial diffusivity (AxD) and the second and third eigenvalues. FSLmaths was used to calculate subject radial diffusivity (RD) images by averaging the second and third eigenvalue images.

Registration of diffusivity measure images was executed by Tract-Based Spatial Statistics (TBSS) [14]. First, subject FA image outliers from DTIFIT were excluded by removing brain-end artefacts and end slices. Second, non-linear registration of all subject FA images to the FMRIB58 FA template was performed. Third, all subject FA images were normalised to the Montreal Neurological Institute (MNI) template. Then the mean of all normalised subject FA images was taken to create a mean FA skeleton. Fifth, the mean FA skeleton was binarised. Then each subject's FA image was projected onto this binary FA skeleton. TBSS was repeated for AxD, MD and RD images. FA nonlinear registration parameters were applied to subject AxD, MD and RD images creating nonlinearly registered images for each

of them. For each measure all subject images were projected onto the FA skeleton, creating a new skeleton for each diffusivity measure.

Randomise[10] was run to test for between-group differences in all described diffusivity measures. TFCE[11] nonparametric permutation testing with 5000 permutations was applied. Results were family-wise error (FWE) corrected for multiple comparisons.

WM microstructure differences between phFTD, bvFTD and controls were assessed using the same design defined for the rs-fMRI analysis, but now only the f-test and subsequent post-hoc t-tests were investigated. As group effects were not investigated, additional Bonferroni correction for the number of contrast was unnecessary. Again, common binary masks were created to assess t-test results within the constraints of the omnibus f-test results by multiplying binary masks of each t-test with the binary mask of the f-test. All t-test common binary masks ($p<0.05$, FWE corrected for multiple comparisons) were evaluated using Cluster to extract cluster size with a cluster threshold of $k\geq20$.

Results were visualised using FSLView. The JHU White-Matter Tractography Atlas and the JHU ICBM-DTI-81 White-Matter labels implemented in FSLView were used to anatomically identify the white matter regions.

References

1 Jenkinson M, Beckmann CF, Behrens TEJ, *et al.* FSL. *Neuroimage* 2012;62:782–90.

2 Woolrich MW, Jbabdi S, Patenaude B, *et al.* Bayesian analysis of neuroimaging data in FSL. *Neuroimage* 2009;45:S173–86.

3 Smith SM, Jenkinson M, Woolrich MW, *et al.* Advances in functional and structural MR image analysis and implementation as FSL. *Neuroimage* 2004;23 Suppl 1:S208–19.

4 Smith SM. Fast robust automated brain extraction. *Hum Brain Mapp* 2002;17:143–55.

5 Jenkinson M, Bannister P, Brady M, *et al.* Improved optimization for the robust and accurate linear registration and motion correction of brain images. *Neuroimage* 2002;17:825–41.

6 Filippini N, MacIntosh BJ, Hough MG, *et al.* Distinct patterns of brain activity in young carriers of the APOE-epsilon4 allele. *Proc Natl Acad Sci U S A* 2009;106:7209–14.

7 Zhou J, Greicius MD, Gennatas ED, *et al.* Divergent network connectivity changes in behavioural variant frontotemporal dementia and Alzheimer's disease. *Brain* 2010;133:1352–67.

8 Buckner RL, Andrews-Hanna JR, Schacter DL. The brain's default network: anatomy, function, and relevance to disease. *Ann N Y Acad Sci* 2008;1124:1–38.

9 Beckmann CF, DeLuca M, Devlin JT, *et al.* Investigations into resting-state connectivity using independent component analysis. *Philos Trans R Soc L B Biol Sci* 2005;360:1001–13.

10 Winkler AM, Ridgway GR, Webster MA, *et al.* Permutation inference for the general linear model. *Neuroimage* 2014;92:381–97.

11 Smith SM, Nichols TE. Threshold-free cluster enhancement: addressing problems of smoothing, threshold dependence and localisation in cluster inference. *Neuroimage* 2009;44:83–98.

12 Leemans A, Jeurissen B, Sijbers J, *et al.* ExploreDTI: a graphical toolbox for processing, analyzing, and visualizing diffusion MR data. In: *Proceedings 17th Scientific Meeting, International Society for Magnetic Resonance in Medicine*. 2009. 3537.http://www.mendeley.com/research/exploredti-a-graphical-toolbox-for-processing-analyzing-and-visualizing-diffusion-mr-data/\nhttp://www.exploredti.com/ref/ExploreDTI_ISMRM_2009.pdf

13 Behrens TEJ, Woolrich MW, Jenkinson M, *et al.* Characterization and propagation of uncertainty in diffusion-weighted MR imaging. *Magn Reson Med* 2003;50:1077–88.

14 Smith SM, Jenkinson M, Johansen-Berg H, *et al.* Tract-based spatial statistics: voxelwise analysis of multi-subject diffusion data. *Neuroimage* 2006;31:1487–505.

Supplement section 2 – Participant exclusion after inclusion

Nine phFTD patients (all male), 12 bvFTD patients (seven male) and 20 healthy controls (all male) were included in the study. Two phFTD patients were excluded from the analysis: one refused neuropsychological testing and one showed disease progression on neuropsychological testing. One phFTD patient showed a cortical infarct in the right parietal lobe on the structural MRI scan, but reported no residual clinical symptoms and his neuropsychological profile was rated as normal; he was therefore retained in the analysis. Three controls were excluded from the analysis: one due to a below average score on a neuropsychological domain typically affected in FTD; the second due to an incidental scanner artefact observed in the MR images; the third because of missing DTI data. Three bvFTD patients had missing rs-fMRI data.

Supplement Table 1A. Group effects (p<0.05, not corrected for multiple comparisons, but Bonferroni corrected (p<0.05) for multiple contrasts; k≥20) of DMN connectivity in phFTD, bvFTD and controls.

Group effect	Number of DMN clusters	Total number of voxels	Number of voxels within largest DMN cluster	Anatomical regions within largest DMN cluster
phFTD	2	7,852	7,827	Medial prefrontal cortex L, R Lateral temporal cortex L, R Inferior parietal lobule L, R Precuneus/posterior cingulate cortex L, R
bvFTD	2	4,848	4,458	Lateral temporal cortex L, R Inferior parietal lobule L, R Precuneus/posterior cingulate cortex L, R
HC	5	1,635	1,015	Inferior parietal lobule R Precuneus/posterior cingulate cortex L, R

DMN = default mode network, phFTD = phenocopy frontotemporal dementia, bvFTD = behavioural variant frontotemporal dementia, HC = healthy controls, L = left, R = right.

Supplement Table 1B. Post-hoc two sample t-tests (p<0.05, not corrected for multiple comparisons, but within the constraints of the omnibus f-test (p<0.05, Bonferroni corrected for multiple contrasts); k≥20) of group differences in DMN connectivity between phFTD, bvFTD and controls.

T-stat	Number of DMN clusters	Total number of voxels	Number of voxels within largest DMN cluster	Anatomical regions within largest DMN cluster
phFTD>HC	7	635	162	Lateral temporal cortex R Inferior parietal lobule R
bvFTD>HC	3	104	43	Lateral temporal cortex R Inferior parietal lobule R
HC>bvFTD	1	44	44	Inferior parietal lobule R
phFTD>bvFTD	7	852	374	Lateral temporal cortex L Subcortical and cerebellar regions L

DMN = default mode network, phFTD = phenocopy frontotemporal dementia, bvFTD = behavioural variant frontotemporal dementia, HC = healthy controls, L = left, R = right.

Supplement Table 2A. Post-hoc two sample t-tests ($p_{corrected}$<0.05; k≥20) of group differences in FA between phFTD, bvFTD and controls.

T-stat	Number of clusters	Total number of voxels	Number of voxels within largest cluster	Anatomical regions within largest cluster
phFTD<HC	28	14,084	4,644	Forceps minor Genu of the corpus callosum L, R Body of the corpus callosum L, R Inferior fronto-occipital fasciculus L, R Anterior thalamic radiation L, R Cingulum L, R Uncinate fasciculus L, R
bvFTD<HC	12	31,220	29,598	Forceps minor Forceps major Genu of the corpus callosum L, R Body of the corpus callosum L, R Splenium of the corpus callosum L, R Inferior fronto-occipital fasciculus L, R Anterior thalamic radiation L, R Cingulum L, R Uncinate fasciculus L, R Inferior longitudinal fasciculus L, R Superior longitudinal fasciculus L, R
bvFTD<phFTD	4	8,025	7,777	Forceps minor Genu of the corpus callosum L, R Body of the corpus callosum L, R Inferior fronto-occipital fasciculus L, R Anterior thalamic radiation L, R Cingulum L, R Uncinate fasciculus L, R

FA = fractional anisotropy, phFTD = phenocopy frontotemporal dementia, bvFTD = behavioural variant frontotemporal dementia, HC = healthy controls, L = left, R = right.

Supplement Table 2B. Post-hoc two sample t-tests ($p_{corrected}$<0.05; k≥20) of group differences in MD between phFTD, bvFTD and controls.

T-stat	Number of clusters	Total number of voxels	Number of voxels within largest cluster	Anatomical regions within largest cluster
phFTD>HC	5	1,686	883	Anterior thalamic radiation L, R Inferio fronto-occipital fasciculus L, R Superior longitudinal fasciculus L, R
bvFTD>HC	14	39,036	37,066	Forceps minor Forceps major Genu of the corpus callosum L, R Body of the corpus callosum L, R Splenium of the corpus callosum L, R Inferior fronto-occipital fasciculus L, R Anterior thalamic radiation L, R Cingulum L, R Uncinate fasciculus L, R Inferior longitudinal fasciculus L, R Superior longitudinal fasciculus L, R
bvFTD>phFTD	4	19,769	19,586	Forceps minor Genu of the corpus callosum L, R Body of the corpus callosum L, R Inferior fronto-occipital fasciculus L, R Anterior thalamic radiation L, R Cingulum L, R Uncinate fasciculus L, R Inferior longitudinal fasciculus L Superior longitudinal fasciculus L, R

MD = mean diffusivity, phFTD = phenocopy frontotemporal dementia, bvFTD = behavioural variant frontotemporal dementia, HC = healthy controls, L = left, R = right.

Supplement Table 2C. Post-hoc two sample t-tests ($p_{corrected}$<0.05; k≥20) of group differences in RD between phFTD, bvFTD and controls.

T-stat	Number of clusters	Total number of voxels	Number of voxels within largest cluster	Anatomical regions within largest cluster
phFTD>HC	9	7,963	6,137	Forceps minor Forceps major Inferior fronto-occipital fasciculus R Anterior thalamic radiation R Cingulum R Uncinate fasciculus R Inferior longitudinal fasciculus R Superior longitudinal fasciculus R
bvFTD>HC	16	46,485	45,111	Forceps minor Forceps major Genu of the corpus callosum L, R Body of the corpus callosum L, R Splenium of the corpus callosum L, R Inferior fronto-occipital fasciculus L, R Anterior thalamic radiation L, R Cingulum L, R Uncinate fasciculus L, R Inferior longitudinal fasciculus L, R Superior longitudinal fasciculus L, R
bvFTD>phFTD	6	22,230	21,946	Forceps minor Genu of the corpus callosum L, R Body of the corpus callosum L, R Inferior fronto-occipital fasciculus L, R Anterior thalamic radiation L, R Cingulum L, R Uncinate fasciculus L, R Inferior longitudinal fasciculus L, R Superior longitudinal fasciculus L, R

RD = radial diffusivity, phFTD = phenocopy frontotemporal dementia, bvFTD = behavioural variant frontotemporal dementia, HC = healthy controls, L = left, R = right.

Supplement Table 2D. Post-hoc two sample t-tests ($p_{corrected}$<0.05; k≥20) of group differences in AxD between phFTD, bvFTD and controls.

T-stat	Number of clusters	Total number of voxels	Number of voxels within largest cluster	Anatomical regions within largest cluster
phFTD>HC	0	n/a	n/a	n/a
bvFTD>HC	3	18,269	17,552	Forceps minor Genu of the corpus callosum L, R Body of the corpus callosum L, R Inferior fronto-occipital fasciculus L, R Anterior thalamic radiation L, R Cingulum L Uncinate fasciculus L, R Superior longitudinal fasciculus L, R
bvFTD>phFTD	8	11,202	10,396	Forceps minor Genu of the corpus callosum L, R Body of the corpus callosum L, R Inferior fronto-occipital fasciculus L, R Anterior thalamic radiation L, R Uncinate fasciculus L, R Superior longitudinal fasciculus L, R

AxD = axial diffusivity, phFTD = phenocopy frontotemporal dementia, bvFTD = behavioural variant frontotemporal dementia, HC = healthy controls, L = left, R = right.

Chapter 4.2

Structural and functional brain abnormalities place phenocopy frontotemporal dementia (FTD) in the FTD spectrum

Rebecca M.E. Steketee
Rozanna Meijboom
Esther E. Bron
Robert J. Osse
Inge de Koning
Lize C. Jiskoot
Stefan Klein
Frank J. de Jong
Aad van der Lugt
John C. van Swieten
Marion Smits

NeuroImage: Clinical 2016;11:595-605

ABSTRACT

'Phenocopy' frontotemporal dementia (phFTD) patients may clinically mimic the behavioural variant of FTD (bvFTD), but do not show functional decline or abnormalities upon visual inspection of routine neuroimaging. We aimed to identify abnormalities in grey matter (GM) volume and perfusion in phFTD and to assess whether phFTD belongs to the FTD spectrum. We compared phFTD patients with both healthy controls and bvFTD patients.

Seven phFTD and 11 bvFTD patients, and 20 age-matched controls underwent structural T1-weighted magnetic resonance imaging (MRI) and 3D pseudo-continuous arterial spin labelling (pCASL) at 3T. Normalised GM (nGM) volumes and perfusion, corrected for partial volume effects, were quantified regionally as well as in the entire supratentorial cortex, and compared between groups taking into account potential confounding effects of gender and scanner.

PhFTD patients showed cortical atrophy, most prominently in the right temporal lobe. Regional GM volume was otherwise generally not different from either controls or from bvFTD, despite the fact that bvFTD showed extensive frontotemporal atrophy. Perfusion was increased in the left prefrontal cortex compared to bvFTD and to a lesser extent to controls.

PhFTD and bvFTD show overlapping cortical structural abnormalities indicating a continuum of changes especially in the frontotemporal regions. Together with functional changes suggestive of a compensatory response to incipient pathology in the left prefrontal regions, these findings are the first to support a possible neuropathological aetiology of phFTD and suggest that phFTD may be a neurodegenerative disease on the FTD spectrum.

1. INTRODUCTION

FTD is a presenile neurodegenerative disorder affecting the frontal and temporal lobes, with the behavioural variant (bvFTD) as its most common subtype. BvFTD is characterised by progressive deterioration in social and personal conduct [1]. Core clinical features are behavioural disinhibition, apathy, loss of empathy, and perseverative, stereotypical or compulsive behaviour. In addition to these symptoms, the diagnosis of probable bvFTD requires frontotemporal changes on neuroimaging and a gradual decline in functional abilities [2]. A subset (reports range from 7% up to 37% [3,4]) of predominantly male patients presents with behavioural changes characteristic of bvFTD, but without abnormalities on structural magnetic resonance imaging (MRI) or fluorodeoxyglucose-positron emission tomography (FDG-PET) [5-8]. In addition, these patients have a more benign disease course [7] and do not show a decline in activities of daily living [9]. This clinical syndrome is referred to as 'phenocopy' FTD (phFTD) [10].

Because normal neuroimaging features and no cognitive decline over time are reported in these patients, a neurodegenerative aetiology is disputed. Autopsy findings are sparse, but have not shown features of neurodegeneration [11,12], Very recently, repeat expansion in the C9ORF72 gene has been associated with very slowly progressive FTD, resembling phFTD. Some patients with this mutation have initially been diagnosed with phFTD [3,13], but currently, phFTD is still defined as a clinical syndrome. An alternative notion is that phFTD patients might have a pre-existent psychiatric disorder and decompensate during mid-life [14-16].

In the present study we used advanced quantitative MRI techniques and analyses to investigate both structural and functional abnormalities in phFTD in more detail, as the typical behavioural changes in phFTD imply neurophysiological changes which may be detected with these advanced methods [3]. We used arterial spin labelling (ASL)-MRI to quantify brain perfusion with higher spatial resolution than thus far achieved with PET [17]. Focal atrophy can be detected by regional quantification of grey matter volume on structural imaging. Grey matter volume and perfusion in phFTD patients were compared with both healthy controls and bvFTD patients in order to assess whether phFTD belongs to the FTD spectrum.

2. METHODS

2.1 Participant selection

PhFTD and bvFTD patients were recruited from the Alzheimer Centre Southwest Netherlands at Erasmus MC, Rotterdam, The Netherlands, which is a tertiary referral centre with special focus on FTD. Exclusion criteria for both phFTD and bvFTD patients were contraindications for MR imaging and lack of hetero-anamnestic information. In addition, phFTD patients were excluded when there was a diagnosis of dementia, or when other neurological or psychiatric disorders were suspected.

Of the fifteen patients that fulfilled the criteria for phFTD, i.e. behavioural features but no imaging findings consistent with bvFTD, and no progression for at least one year after initial diagnostic work-up, six patients declined to participate; one was excluded due to refusal of neuropsychological assessment; and one eventually showed progressive cognitive impairment at neuropsychological follow-up, resulting in the analysis of seven phFTD patients. One patient showing an asymptomatic cortical infarct in the right parietal lobe on MRI was retained in the analyses, as no residual clinical symptoms were reported and the infarct was not in a region of interest for FTD. Image processing results were visually checked and did not show any effect of the infarct on segmentation or registration procedures. All phFTD patients were screened for the presence of the repeat expansion of the C9ORF72 gene.

Twelve bvFTD patients with possible bvFTD [2] with an onset before 65 years and a Mini Mental State Examination (MMSE) score ≥ 20 were prospectively recruited as part of a larger ongoing study on advanced MR neuroimaging in the early stage of presenile dementia. If the diagnosis at the initial visit was uncertain, definitive diagnosis was confirmed after sufficient follow-up. One patient was excluded from analysis due to poor perfusion data quality, resulting in the analysis of 11 bvFTD patients.

Healthy age-matched controls were recruited through advertisement and from the patients' peers. They were matched for gender with the phFTD patients. Exclusion criteria were history of neurological or psychiatric disorders and contraindications for MRI. Of the twenty-three controls, two were excluded due to missing data and one because of below-average scores on neuropsychological assessment, resulting in the analysis of twenty healthy controls.

The study was approved by the medical ethics committee of Erasmus MC. All participants gave written informed consent.

2.2 Neuropsychological and psychiatric assessment

All participants underwent extensive neuropsychological examination as part of routine diagnostic work-up, assessing language and speech, attention and mental processing speed, executive functions, memory, and social cognition. PhFTD patients had an additional assessment to verify whether they fulfilled the criterion of no progression for at least one year. Additionally, they were assessed by an experienced psychiatrist to rule out major psychiatric disorders other than dementia. Psychiatric assessment was based on interviews with the patients and their caregivers, the Brief Psychiatric Rating Scale (BPRS [18]; Dutch translation [19]), and the psychiatrist's observations.

2.3 Image acquisition

Patients underwent MR imaging on two identical 3T scanners (Discovery MR750 system GE Healthcare, USA) with identical protocols. Seven healthy controls and all phFTD patients were scanned on one, and 13 healthy controls and all bvFTD patients on the other scanner.

2.3.1 Structural imaging

For grey matter volumetric assessment and anatomical reference, a high-resolution three-dimensional (3D) inversion recovery (IR) fast spoiled gradient-echo (FSPGR) T1-weighted (T1w) image was acquired (inversion time (TI) 450ms, echo time (TE) 3.06ms, repetition time (TR) 7.904s, flip angle 12°, ASSET factor 2, isotropic resolution 1mm^3 in a 240mm field of view (FOV), 176 sagittal slices, total acquisition time 4.41 min).

2.3.2 Perfusion imaging

Perfusion images were acquired using whole brain 3D pseudo-continuous ASL (p-CASL), currently the recommended sequence for clinical use [20] (interleaved fast spin-echo stack-of-spiral readout of 512 sampling points on 8 spirals, background suppressed, post labelling delay 1525ms, labelling duration 1450ms, TE 10.5ms, TR 4632ms, isotropic resolution 3.3mm^3 in a 240mm FOV, 36 axial slices, number of excitations (NEX) 3, total acquisition time 4.29 min). The labelling plane was positioned 9 cm below the anterior commissure – posterior commissure line.

2.4 Image data processing

We processed imaging data according to the methods described in detail by Bron et al., 2014 [21].

2.4.1 Tissue segmentation

Using the unified tissue segmentation method in SPM8 (Statistical Parametric Mapping, London, UK), we segmented T1w images into grey matter (GM), white matter and cerebrospinal fluid maps. The GM maps were subsequently used to derive GM volumes and cerebral blood flow (CBF).

2.4.2 ASL post-processing

The ASL data consisted of a difference image and a control image. GM maps were rigidly registered with the difference image (Elastix registration software [22]) and registrations were checked visually. Tissue maps were transformed to ASL image space to perform partial volume (PV) correction, and PV effects in ASL difference and control images were subsequently corrected using local linear regression within a 3D kernel based on tissue maps [23]. We quantified PV-corrected ASL images as CBF maps using the single-compartment model [20]. CBF maps were transformed to T1w image space for further analysis.

2.4.3 ROI labelling

We defined regions of interest (ROIs) for each participant using a multi-atlas approach. This involved registration of 30 labelled T1w images, each containing 83 cortical and subcortical ROIs [24,25], to the participants' T1w images. The labels of the 30 atlas images were fused by means of majority voting to obtain a final ROI labelling [26]. Rigid, affine, and non-rigid B-spline transformation models were applied successively for registration to the participants' nonuniformity-corrected T1w images [27]. Both the participants' and the labelled T1w images were masked for this registration using the Brain Extraction Tool [28].

2.4.4 ROI analysis

For all ROIs, we derived GM volumes and mean GM CBF values. The subcortical ROIs, cerebellum, brainstem, ventricles and white matter were excluded from analysis. ROIs that parcellated gyri in multiple sections were combined to constitute entire gyri (supplementary table 1). GM volumes and mean GM CBF values were subsequently obtained for the left and right hemisphere separately. Region-

al GM volumes were divided by the total intracranial volume to correct for head size and are referred to as normalised GM (nGM) volumes.

2.5 Data analysis

Using SPSS Statistics, version 20.0 (New York, USA) we first analysed differences in gender and scanner across groups with Fisher's exact test. As these were significantly different between groups ($p<0.05$), we then used hierarchical regression to sequentially assess the effects of scanner, gender, and group on nGM and CBF. Only the nGM and regional CBF ROIs that showed a significant effect of group but did not show significant effects of scanner and/or gender were further tested for differences between groups. This was done using a nonparametric Kruskal-Wallis test with Dunn-Bonferroni correction for multiple comparisons as nGM, CBF, age and MMSE were not normally distributed across groups (Shapiro-Wilk test $p<0.05$). The findings were visually represented in boxplots of nGM and CBF for each of the brain lobes. Statistical thresholds were set at $p<0.05$.

3. RESULTS

3.1 Participant characteristics

Age was not different between groups ($H(2) = 1.129$, $p>.05$, Kruskal-Wallis test) (table 1). MMSE was significantly different between groups ($F(2) = 10.182$, $p<.05$, Kruskal-Wallis test): both phFTD and bvFTD patients had significantly lower MMSE scores than controls.

Table 1: participant characteristics

	Controls	phFTD	bvFTD
N (male)	20 (20)	7 (7)	11 (5)
Median age in years (25^{th}-75^{th} %ile)	64 (62-66)	61 (60-70)	63 (57-66)
Median MMSE (25^{th}-75^{th} %ile)	28 (28-30)	27 (26-28)	27 (24-28)

bvFTD = behavioural variant frontotemporal dementia; IQR = interquartile range; MMSE = Mini Mental State Examination; phFTD = phenocopy frontotemporal dementia; SD = standard deviation

None of the phFTD patients had a C9ORF72 mutation, nor could their behavioural disturbances be attributed to an underlying psychiatric disorder. Neuropsychological assessment was normal in one and suggestive of FTD in six phFTD patients, but did not demonstrate progressive decline.

Median follow-up to establish definitive diagnosis of bvFTD was 1.4 years (range 1.7 months - 2.4 years).

3.2 Grey matter volumetric changes

There were significant differences in nGM volume between groups mostly in frontal and temporal regions (Figure 1A, Table 2). PhFTD patients had lower supratentorial nGM volume than controls which was most pronounced in the right posterior temporal lobe, right superior temporal gyrus and bilateral fusiform gyrus. BvFTD showed extensive bilateral frontotemporal nGM volume loss compared to controls. Compared to phFTD, bvFTD showed lower nGM volume in the right hippocampal formation and the right amygdala. Other nGM volumes were not significantly different between bvFTD and phFTD. This spectrum of findings, with mean nGM volumes being highest in controls, lowest in bvFTD and in-between in phFTD, was particularly apparent in the frontal and temporal lobes (Figure 2A).

3.3 Perfusion changes in the grey matter

There were significant differences in CBF between groups in frontal regions (Figure 1B, Table 3). CBF in the bilateral subcallosal area was higher in phFTD than both in bvFTD and controls, as illustrated in Figure 2B. CBF in bvFTD was lower than in phFTD in the left superior and inferior frontal gyrus, the left orbitofrontal gyrus, and in the bilateral straight gyrus. bvFTD showed lower CBF than controls in the left inferior frontal and straight gyrus, and the left orbitofrontal gyrus.

Table 2: median nGM volume [% ICV] and 25th and 75th percentile (in parentheses) for healthy controls (HC), phFTD and bvFTD patients.

	Region of interest	Healthy controls		PhFTD		BvFTD	
	Median (25th-75th %ile)	Mean rank	Median (25th-75th %ile)	Mean rank	Median (25th-75th %ile)	Mean rank	
	Supratentorial cortex	35.3 (33.3-36.1)	26	31.6 (30.0-33.6)	13[a]	29.1 (27.2-34.1)	11[c]
L	Superior frontal gyrus	1.62 (1.56-1.68)	26	1.50 (1.41-1.56)	15	1.21 (1.00-1.59)	11[c]
R	Superior frontal gyrus	1.62 (1.48-1.75)	25	1.55 (1.40-1.60)	18	1.17 (1.02-1.51)	11[c]
L	Middle frontal gyrus	1.29 (1.14-1.41)	23	1.20 (1.17-1.35)	20	0.95 (0.82-1.27)	12[c]
R	Middle frontal gyrus	1.27 (1.18-1.35)	25	1.17 (1.13-1.24)	17	0.98 (0.75-1.27)	12[c]
R	Inferior frontal gyrus	0.57 (0.54-0.62)	24	0.54 (0.50-0.59)	19	0.44 (0.40-0.52)	11[c]
L	Straight gyrus	0.15 (0.14-0.18)	25	0.15 (0.11-0.17)	20	0.10 (0.09-0.13)	10[c]
R	Straight gyrus	0.17 (0.15-0.19)	26	0.14 (0.12-0.19)	18	0.12 (0.09-0.13)	9[c]
L	Orbitofrontal gyrus	0.79 (0.73-0.84)	25	0.74 (0.60-0.76)	15	0.47 (0.39-0.76)	12[c]
R	Orbitofrontal gyrus	0.80 (0.76-0.85)	25	0.67 (0.64-0.78)	14	0.53 (0.44-0.77)	12[c]
R	Anterior cingulate gyrus	0.33 (0.29-0.39)	25	0.31 (0.28-0.32)	18	0.26 (0.20-0.29)	11[c]
L	Insula	0.54 (0.51-0.55)	25	0.51 (0.46-0.53)	19	0.39 (0.36-0.49)	9[c]
R	Insula	0.50 (0.49-0.53)	26	0.47 (0.46-0.50)	19	0.37 (0.34-0.42)	8[c]
L	Anterior temporal lobe	0.44 (0.41-0.49)	25	0.44 (0.38-0.46)	21	0.34 (0.27-0.37)	9[c]
R	Anterior temporal lobe	0.48 (0.44-0.52)	26	0.45 (0.39-0.49)	19	0.34 (0.26-0.38)	9[c]
L	Posterior temporal lobe	1.70 (1.66-1.74)	24	1.69 (1.50-1.74)	18	1.58 (1.43-1.65)	12[c]

R	Posterior temporal lobe	1.82 (1.75-1.89)	26	1.60 (1.53-1.63)	11[a]	1.57 (1.44-1.76)	13[c]
L	Hippocampal formation	0.39 (0.35-0.41)	24	0.37 (0.32-0.42)	21	0.29 (0.24-0.34)	10[c]
R	Hippocampal formation	0.38 (0.36-0.40)	24	0.37 (0.32-0.42)	22[b]	0.28 (0.26-0.37)	9[c]
L	Amygdala	0.09 (0.08-0.09)	24	0.09 (0.07-0.09)	20	0.07 (0.07-0.08)	12[c]
R	Amygdala	0.08 (0.07-0.08)	22	0.08 (0.07-0.09)	26[b]	0.07 (0.05-0.08)	11[c]
L	Superior temporal gyrus	0.71 (0.70-0.78)	25	0.63 (0.55-0.71)	15	0.59 (0.58-0.66)	12[c]
R	Superior temporal gyrus	0.72 (0.68-0.79)	26	0.65 (0.58-0.70)	13[a]	0.64 (0.51-0.71)	12[c]
L	Inferior temporal gyrus	0.70 (0.62-0.74)	26	0.66 (0.54-0.67)	17	0.50 (0.38-0.60)	9[c]
R	Inferior temporal gyrus	0.72 (0.62-0.76)	26	0.65 (0.54-0.67)	18	0.50 (0.35-0.59)	9[c]
L	Fusiform gyrus	0.22 (0.19-0.22)	26	0.16 (0.15-0.19)	14[a]	0.17 (0.11-0.18)	11[c]
R	Fusiform gyrus	0.21 (0.19-0.24)	26	0.16 (0.14-0.19)	12[a]	0.15 (0.13-0.18)	11[c]
L	Remainder of parietal lobe	1.33 (1.25-1.42)	25	1.24 (1.17-1.31)	15	1.16 (1.05-1.32)	13[c]

Median nGM volumes and 25th and 75th percentile in ROIs for which post hoc pairwise comparisons showed significant different ***mean ranks*** between healthy controls, phFTD and bvFTD patients. The mean ranks (italics) represent the group means of the rank-ordered nGM data in that particular ROI. The mean ranks rather than the medians of the nGM volume distributions were compared to assess differences between groups because group distributions were not similarly shaped. The shading indicates the relative order of mean ranks between groups, with light grey indicating the highest and dark grey indicating the lowest rank.

[a] phFTD < controls; $p \leq .05$.

[b] bvFTD < phFTD; $p \leq .05$.

[c] bvFTD < controls; $p \leq .05$.

nGM = normalised grey matter; ICV = intracranial volume; ROIs = regions of interest; PhFTD = phenocopy frontotemporal dementia; bvFTD = behavioural variant frontotemporal dementia; HC = healthy controls; L = left; R = right.

Table 3: Median CBF and 25th and 75th percentile (in parentheses) for healthy controls (HC), phFTD and bvFTD patients.

	Region of interest	Healthy controls		PhFTD		BvFTD	
	Median (25th-75th %ile)	Mean rank	Median (25th-75th %ile)	Mean rank	Median (25th-75th %ile)	Mean rank	
L	Superior frontal gyrus	38.1 (34.5-45.4)	19	46.0 (39.0-65.0)	28[b]	35.0 (29.6-43.8)	15
L	Inferior frontal gyrus	48.6 (40.5-51.1)	22	50.7 (43.8-60.7)	27[b,c]	38.1 (31.1-42.3)	11[b]
L	Straight gyrus	49.8 (44.6-54.3)	22	55.1 (46.4-63.7)	27[b,c]	38.1 (35.2-46.6)	11[b]
R	Straight gyrus	47.0 (43.6-50.1)	21	51.7 (44.0-62.6)	28[b]	38.7 (32.5-45.0)	11
L	Orbitofrontal gyrus	44.1 (40.3-48.8)	23	43.0 (38.5-62.6)	25[b,c]	35.9 (30.3-38.7)	10[b]
L	Subcallosal area	31.6 (25.3-42.4)	19	45.0 (40.1-50.8)	32[a,b]	23.8 (20.4-32.4)	12
R	Subcallosal area	27.8 (22.4-41.8)	19	42.8 (41.3-48.2)	31[a,b]	29.5 (17.9-34.6)	13

Median CBF and 25th and 75th percentile in ROIs for which post hoc pairwise comparisons showed significant different *mean ranks* between healthy controls, phFTD and bvFTD patients. The mean ranks (italics) represent the group means of the rank-ordered CBF data in that particular ROI. The mean ranks rather than the medians of the CBF value distributions were compared to assess differences between groups because group distributions were not similarly shaped. The shading indicates the relative order of mean ranks between groups, with light grey indicating the highest and dark grey indicating the lowest rank.

[a] phFTD > controls; $p \leq .05$.

[b] bvFTD < phFTD; $p \leq .05$.

[c] bvFTD < controls; $p \leq .05$.

CBF = cerebral blood flow; ROIs = regions of interest; phFTD = phenocopy frontotemporal dementia; bvFTD = behavioural variant frontotemporal dementia; HC = healthy controls; L = left; R = right.

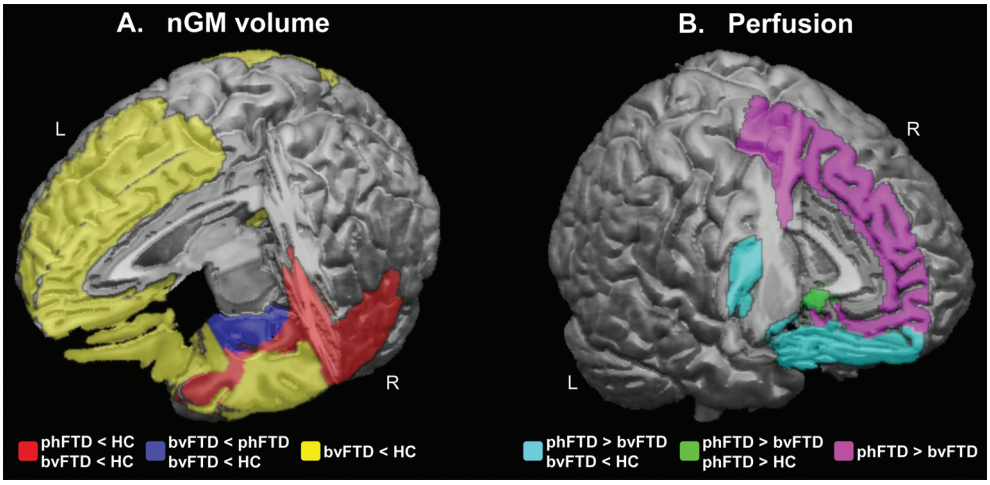

Figure 1. Schematic overview of cortical regions showing (A) normalised GM volume and (B) perfusion abnormalities. Figure 1A shows in red regional nGM atrophy present in both phFTD and bvFTD; in blue regional nGM volume loss in bvFTD compared to both phFTD and controls; and in yellow regional nGM volume loss in in bvFTD when compared to controls, but not compared to phFTD. Figure 1B shows in cyan hyperperfusion in phFTD compared to bvFTD in regions that show hypoperfusion in bvFTD compared to controls; in green regional hyperperfusion in phFTD compared to both bvFTD and controls; and in violet regional hyperperfusion in phFTD compared to bvFTD.
HC = healthy controls; phFTD = phenocopy frontotemporal dementia; bvFTD = behavioural variant frontotemporal dementia; nGM = normalised grey matter.

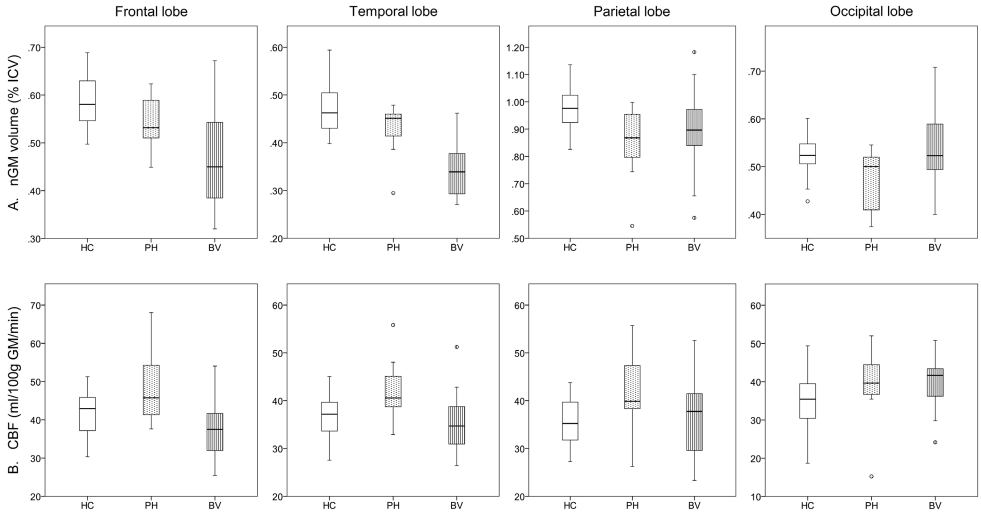

Figure 2. A) Normalised GM (% ICV) and B) CBF (ml/100g GM/min) in the different lobes for healthy controls (HC), phFTD (PH) and bvFTD (BV) patients. The central box represents values from lower to upper quartile (25-75th percentile), the middle line represents the median, and vertical bars extend from minimum to maximum value. Spheres outside the bars indicate extreme values (value ≥ 1.5 x interquartile range). Note that GM volumes in phFTD are generally in-between those of HC and bvFTD, and that perfusion in phFTD is generally higher than in bvFTD and controls.
HC = healthy controls; phFTD = phenocopy frontotemporal dementia; bvFTD = behavioural variant frontotemporal dementia; nGM = normalised grey matter; ICV = intracranial volume; CBF = cerebral blood flow.

4. DISCUSSION

To the best of our knowledge, our study is the first to show cortical brain abnormalities in phFTD. We found cortical atrophy in phFTD, most prominently in the right superior and posterior temporal lobe, and the fusiform gyrus bilaterally. Furthermore, we found left frontal hyperperfusion in phFTD compared to bvFTD and to a lesser extent to controls, which may reflect functional compensation for incipient pathology.

Regional right temporal atrophy was not only seen in phFTD but also present in bvFTD, suggesting similar underlying pathophysiology. Atrophy in right temporal regions has been linked to impaired emotion recognition and empathy in neurodegenerative disease [29,30], and more specifically to emotional blunting in bvFTD [31]. In addition, frontotemporal atrophy lateralised to the right hemisphere is more often associated with socially undesirable behaviour in FTD than

when lateralised to the left [32]. The fact that we found atrophy in this specific region may explain why symptoms in phFTD patients are mostly isolated to the behavioural domain, in contrast to bvFTD patients who show a more widespread frontotemporal atrophy and additional cognitive and functional decline.

Our findings are in contrast to previous studies, in which no atrophy in phFTD was found using semi-quantitative ratings [7,33]. One possible explanation might be that such semi-quantitative rating was not sufficiently sensitive. However, other studies using the potentially more sensitive VBM method did not show any abnormalities either [5,34], except for one case study reporting non-specific parieto-occipital, thalamic and subtle frontoinsular atrophy [3]. The discrepancy with the present study may lie in the fact that we used highly specific patient selection criteria, i.e. behavioural features consistent with bvFTD, without progression for at least one year, without psychiatric disorders and without C9ORF72 mutations. It may also be due to methodological differences between voxel-wise and ROI analyses. ROI analysis circumvents the problem of inter-individual anatomical variability, as well as subsequent corrections for such variability that may compromise resolution (such as smoothing). Additionally, statistical power of ROI analysis is hampered less by corrections for multiple comparisons than voxel-wise testing.

Apart from the focal right temporal atrophy, nGM volumes in phFTD were generally not different from neither bvFTD nor from controls. Only the right hippocampal formation and amygdala showed more atrophy in bvFTD compared with phFTD, suggesting preservation of those regions in phFTD, whereas these were severely affected in bvFTD [35]. Of note is that otherwise, nGM volumes were similar between phFTD and bvFTD, despite widespread GM loss in bvFTD compared to controls. These findings suggest that there is a continuum in nGM volumes ranging from normal on the one end to clearly abnormal in bvFTD on the other, with phFTD in-between. Together with the overlapping finding in both phFTD and bvFTD of right temporal lobe atrophy, this suggests that phFTD may be a disease on the FTD spectrum.

Our study was the first to use ASL-MRI in phFTD to assess perfusion. ASL is tightly coupled to brain metabolism and function as measured with FDG-PET, but previous PET studies failed to find any abnormalities in phFTD [5,8]. We found higher perfusion in phFTD in the bilateral straight gyrus and left superior, inferior and orbital frontal gyrus compared to bvFTD, and to a lesser extent compared to controls. Some of these regions, i.e. in the left inferior frontal gyrus, correspond to those showing hypoperfusion in bvFTD compared to controls. Such hyperperfusion in phFTD relative to bvFTD may reflect a compensatory process of increased activity to compensate for incipient pathology in regions affected in bvFTD [36]. A

similar pattern could be observed in the right straight gyrus, where perfusion was increased in phFTD compared to bvFTD, while there was a trend (p=0.06) towards hypoperfusion in bvFTD compared to controls. The other hyperperfused regions in phFTD relative to bvFTD, namely the superior frontal gyrus and subcallosal region, did not show hypoperfusion in bvFTD. Although not observed in our bvFTD sample, left superior frontal hypoperfusion has been found in FTD in previous ASL studies [37-39]. Similarly, PET studies have reported subcallosal hypometabolism in FTD [40-42]. Therefore, a compensatory process may still be hypothesised.

Taken together, our findings in phFTD suggest functional compensation as well as focal structural abnormalities overlapping with those found in bvFTD. Overlapping focal cortical atrophy was limited to the right temporal lobe, consistent with the disease-specific prominent behavioural changes of phFTD, while cortical volumes in the remaining frontotemporal regions were in-between normal and those in bvFTD. These findings support the idea that phFTD is a disease of the FTD spectrum. One could even wonder whether phFTD is not simply an early manifestation of bvFTD. The notion of phFTD as a neurodegenerative disease is however still disputed due to the absence of disease progression in these patients. Psychiatric disorders have been proposed as an alternative or contributory aetiology [14-16,43]. In support of this view, imaging findings show substantial overlap between FTD and disorders such as schizophrenia [44,45] and depression [46,47]. In addition, phFTD patients may carry a C9ORF72 mutation [3,13] which is not only associated with bvFTD, but also with psychotic symptoms [48]. Yet in our patients, alternative psychiatric diagnoses were ruled out, which renders interpretation in the context of neurodegenerative disease more likely. In addition, none of the phFTD patients had a mutation of the C9ORF72 gene. Therefore, as of yet, phFTD still seems to be described best as a clinical syndrome. As such, our phFTD population comprised patients with a distinct clinical profile: behavioural features consistent with bvFTD, without progression for at least one year, without psychiatric disorders and without the C9ORF72 mutation. This well-defined clinical profile may have enabled a first link between the typical behavioural changes in phFTD and potential neurophysiological changes as detected with imaging.

The present study has some limitations. Firstly, the sample size was small. This is inherent to phFTD being a rare disease, with only 17 documented cases in a large tertiary referral centre as ours. Nevertheless, we studied a very well-defined phFTD sample, by strictly controlling for disease progression and alternative psychiatric aetiology. One patient did have an asymptomatic cortical infarct in the right parietal lobe, but as this did not affect image processing results we expect

it did not influence our findings. Secondly, groups were not fully gender-matched and were scanned on two - albeit identical - scanners. We used hierarchical regression analysis to account for potential confounding effects of gender and scanner. Although this stringent analysis limited the number of regions that were eventually analysed between groups and carries the risk of false negative results, it decreased the probability of false positives, and as such strengthens the validity of our findings. Finally, despite a one year follow-up to ensure the absence of progression, longer follow-up in a longitudinal study will be even better suited to assess whether patients show no or very slow progression. Therefore, follow-up of our phFTD sample is currently ongoing. Ultimately, post-mortem examination is essential to determine whether neuropathology is present and if so, what type. Hence, studies investigating both neurodegenerative aetiology and neuropsychiatric presentation of behavioural changes later in life [49] may further elucidate the relationship between behaviour and neurophysiology.

In conclusion, in addition to overlapping focal right temporal lobe atrophy in phFTD and bvFTD, we found a continuum of frontotemporal cortical volumes ranging from normal on the one end to clearly abnormal in bvFTD on the other, with phFTD in-between. Furthermore, we observed left frontal hyperperfusion in phFTD, suggestive of a compensatory process in response to incipient pathology in regions affected in FTD. To the best of our knowledge, our findings are the first evidence of a neuropathological substrate of phFTD and to possibly place it in an FTD spectrum. This may serve as the basis for further assessment in larger patient samples with longitudinal clinical and pathological follow-up.

REFERENCES

1. Neary D, Snowden JS, Gustafson L, Passant U, Stuss D, Black S, et al. Frontotemporal lobar degeneration: a consensus on clinical diagnostic criteria. Neurology. 1998;51: 1546-1554.
2. Rascovsky K, Hodges JR, Knopman D, Mendez MF, Kramer JH, Neuhaus J, et al. Sensitivity of revised diagnostic criteria for the behavioural variant of frontotemporal dementia. Brain. 2011;134: 2456-2477.
3. Khan BK, Yokoyama JS, Takada LT, Sha SJ, Rutherford NJ, Fong JC, et al. Atypical, slowly progressive behavioural variant frontotemporal dementia associated with C9ORF72 hexanucleotide expansion. J Neurol Neurosurg Psychiatry. 2012;83: 358-364.
4. Hornberger M, Shelley BP, Kipps CM, Piguet O, Hodges JR. Can progressive and non-progressive behavioural variant frontotemporal dementia be distinguished at presentation? J Neurol Neurosurg Psychiatr. 2009;80: 591-593.
5. Kipps CM, Hodges JR, Fryer TD, Nestor PJ. Combined magnetic resonance imaging and positron emission tomography brain imaging in behavioural variant frontotemporal degeneration: refining the clinical phenotype. Brain. 2009;132: 2566-2578.
6. Kipps CM, Davies RR, Mitchell J, Kril JJ, Halliday GM, Hodges JR. Clinical significance of lobar atrophy in frontotemporal dementia: application of an MRI visual rating scale. Dement Geriatr Cogn Disord. 2007;23: 334-342.
7. Davies RR, Kipps CM, Mitchell J, Kril JJ, Halliday GM, Hodges JR. Progression in frontotemporal dementia: identifying a benign behavioral variant by magnetic resonance imaging. Arch Neurol. 2006;63: 1627-1631.
8. Kerklaan BJ, Berckel BN, Herholz K, Dols A, Flier WM, Scheltens P, et al. The Added Value of 18-Fluorodeoxyglucose-Positron Emission Tomography in the Diagnosis of the Behavioral Variant of Frontotemporal Dementia. Am J Alzheimers Dis Other Demen. 2014.
9. Mioshi E, Hodges JR. Rate of change of functional abilities in frontotemporal dementia. Dement Geriatr Cogn Disord. 2009;28: 419-426.
10. Hornberger M, Piguet O, Kipps C, Hodges JR. Executive function in progressive and nonprogressive behavioral variant frontotemporal dementia. Neurology. 2008;71: 1481-1488.
11. Diehl-Schmid J, Grimmer T, Drzezga A, Bornschein S, Riemenschneider M, Forstl H, et al. Decline of cerebral glucose metabolism in frontotemporal dementia: a longitudinal 18F-FDG-PET-study. Neurobiol Aging. 2007;28: 42-50.
12. Kertesz A, McMonagle P, Blair M, Davidson W, Munoz DG. The evolution and pathology of frontotemporal dementia. Brain. 2005;128: 1996-2005.
13. Gomez-Tortosa E, Serrano S, de Toledo M, Perez-Perez J, Sainz MJ. Familial benign frontotemporal deterioration with C9ORF72 hexanucleotide expansion. Alzheimers Dement. 2014.

14. Kipps CM, Hodges JR, Hornberger M. Nonprogressive behavioural frontotemporal dementia: recent developments and clinical implications of the 'bvFTD phenocopy syndrome'. Curr Opin Neurol. 2010;23: 628-632.
15. Piguet O, Hornberger M, Mioshi E, Hodges JR. Behavioural-variant frontotemporal dementia: diagnosis, clinical staging, and management. Lancet Neurol. 2011;10: 162-172.
16. Manes F. Psychiatric conditions that can mimic early behavioral variant frontotemporal dementia: the importance of the new diagnostic criteria. Curr Psychiatry Rep. 2012;14: 450-452.
17. Wong EC, Buxton RB, Frank LR. Quantitative perfusion imaging using arterial spin labeling. Neuroimaging Clin N Am. 1999;9: 333-342.
18. Overall JE, Gorham DR. The brief psychiatric rating scale. Psychol Rep. 1962;10: 799-812.
19. Dingemans P. Vertaling en bewerking: Uitgebreide BPRS handleiding, Los Angeles Project. Amsterdam: Psychiatrisch Centrum AZUA; 1986.
20. Alsop DC, Detre JA, Golay X, Günther M, Hendrikse J, Hernandez-Garcia L, et al. Recommended implementation of arterial spin-labeled perfusion MRI for clinical applications: A consensus of the ISMRM perfusion study group and the European consortium for ASL in dementia. . 2015;73: 102-116.
21. Bron EE, Steketee RME, Houston GC, Oliver RA, Achterberg HC, Loog M, et al. Diagnostic classification of arterial spin labeling and structural MRI in presenile early stage dementia. Hum Brain Mapp. 2014;35: 4916-4931.
22. Klein S, Staring M, Murphy K, Viergever MA, Pluim JP. Elastix: a Toolbox for Intensity-Based Medical Image Registration. IEEE Trans Med Imaging. 2010;29: 196-205.
23. Asllani I, Borogovac A, Brown TR. Regression algorithm correcting for partial volume effects in arterial spin labeling MRI. Magn Reson Med. 2008;60: 1362-1371.
24. Hammers A, Allom R, Koepp MJ, Free SL, Myers R, Lemieux L, et al. Three-dimensional maximum probability atlas of the human brain, with particular reference to the temporal lobe. Hum Brain Mapp. 2003;19: 224-247.
25. Gousias IS, Rueckert D, Heckemann RA, Dyet LE, Boardman JP, Edwards AD, et al. Automatic segmentation of brain MRIs of 2-year-olds into 83 regions of interest. Neuroimage. 2008;40: 672-684.
26. Heckemann RA, Hajnal JV, Aljabar P, Rueckert D, Hammers A. Automatic anatomical brain MRI segmentation combining label propagation and decision fusion. Neuroimage. 2006;33: 115-126.
27. Tustison NJ, Avants BB, Cook PA, Zheng Y, Egan A, Yushkevich PA, et al. N4ITK: improved N3 bias correction. IEEE Trans Med Imaging. 2010;29: 1310-1320.
28. Smith SM. Fast robust automated brain extraction. Hum Brain Mapp. 2002;17: 143-155.
29. Rosen HJ, Wilson MR, Schauer GF, Allison S, Gorno-Tempini ML, Pace-Savitsky C, et al. Neuroanatomical correlates of impaired recognition of emotion in dementia. Neuropsychologia. 2006;44: 365-373.

30. Rankin KP, Gorno-Tempini ML, Allison SC, Stanley CM, Glenn S, Weiner MW, et al. Structural anatomy of empathy in neurodegenerative disease. Brain. 2006;129: 2945-2956.
31. Lee GJ, Lu PH, Mather MJ, Shapira J, Jimenez E, Leow AD, et al. Neuroanatomical correlates of emotional blunting in behavioral variant frontotemporal dementia and early-onset Alzheimer's disease. J Alzheimers Dis. 2014;41: 793-800.
32. Mychack P, Kramer JH, Boone KB, Miller BL. The influence of right frontotemporal dysfunction on social behavior in frontotemporal dementia. Neurology. 2001;56: S11-5.
33. Pennington C, Hodges JR, Hornberger M. Neural correlates of episodic memory in behavioral variant frontotemporal dementia. J Alzheimers Dis. 2011;24: 261-268.
34. Kipps CM, Nestor PJ, Acosta-Cabronero J, Arnold R, Hodges JR. Understanding social dysfunction in the behavioural variant of frontotemporal dementia: the role of emotion and sarcasm processing. Brain. 2009;132: 592-603.
35. Barnes J, Whitwell JL, Frost C, Josephs KA, Rossor M, Fox NC. Measurements of the amygdala and hippocampus in pathologically confirmed Alzheimer disease and frontotemporal lobar degeneration. Arch Neurol. 2006;63: 1434-1439.
36. Hu WT, Wang Z, Lee VM, Trojanowski JQ, Detre JA, Grossman M. Distinct cerebral perfusion patterns in FTLD and AD. Neurology. 2010;75: 881-888.
37. Tosun D, Rosen H, Miller BL, Weiner MW, Schuff N. MRI patterns of atrophy and hypoperfusion associations across brain regions in frontotemporal dementia. Neuroimage. 2012;59: 2098-2109.
38. Zhang Y, Schuff N, Ching C, Tosun D, Zhan W, Nezamzadeh M, et al. Joint assessment of structural, perfusion, and diffusion MRI in Alzheimer's disease and frontotemporal dementia. Int J Alzheimers Dis. 2011;2011: 546871.
39. Du AT, Jahng GH, Hayasaka S, Kramer JH, Rosen HJ, Gorno-Tempini ML, et al. Hypoperfusion in frontotemporal dementia and Alzheimer disease by arterial spin labeling MRI. Neurology. 2006;67: 1215-1220.
40. Salmon E, Garraux G, Delbeuck X, Collette F, Kalbe E, Zuendorf G, et al. Predominant ventromedial frontopolar metabolic impairment in frontotemporal dementia. Neuroimage. 2003;20: 435-440.
41. Schroeter ML, Raczka K, Neumann J, Yves von Cramon D. Towards a nosology for frontotemporal lobar degenerations-a meta-analysis involving 267 subjects. Neuroimage. 2007;36: 497-510.
42. Kanda T, Ishii K, Uemura T, Miyamoto N, Yoshikawa T, Kono AK, et al. Comparison of grey matter and metabolic reductions in frontotemporal dementia using FDG-PET and voxel-based morphometric MR studies. Eur J Nucl Med Mol Imaging. 2008;35: 2227-2234.
43. Gossink FT, Dols A, Kerssens CJ, Krudop WA, Kerklaan BJ, Scheltens P, et al. Psychiatric diagnoses underlying the phenocopy syndrome of behavioural variant frontotemporal dementia. J Neurol Neurosurg Psychiatry. 2015.

44. Andreasen NC, O'Leary DS, Flaum M, Nopoulos P, Watkins GL, Boles Ponto LL, et al. Hypofrontality in schizophrenia: distributed dysfunctional circuits in neuroleptic-naive patients. Lancet. 1997;349: 1730-1734.
45. Olabi B, Ellison-Wright I, McIntosh AM, Wood SJ, Bullmore E, Lawrie SM. Are there progressive brain changes in schizophrenia? A meta-analysis of structural magnetic resonance imaging studies. Biol Psychiatry. 2011;70: 88-96.
46. Drevets WC, Price JL, Simpson JR,Jr, Todd RD, Reich T, Vannier M, et al. Subgenual prefrontal cortex abnormalities in mood disorders. Nature. 1997;386: 824-827.
47. Dotson VM, Davatzikos C, Kraut MA, Resnick SM. Depressive symptoms and brain volumes in older adults: a longitudinal magnetic resonance imaging study. J Psychiatry Neurosci. 2009;34: 367-375.
48. Snowden JS, Rollinson S, Thompson JC, Harris JM, Stopford CL, Richardson AM, et al. Distinct clinical and pathological characteristics of frontotemporal dementia associated with C9ORF72 mutations. Brain. 2012;135: 693-708.
49. Krudop WA, Kerssens CJ, Dols A, Prins ND, Moller C, Schouws S, et al. Building a new paradigm for the early recognition of behavioral variant frontotemporal dementia: Late Onset Frontal Lobe Syndrome study. Am J Geriatr Psychiatry. 2014;22: 735-740.

SUPPLEMENT

Supplementary Table 1. regions of interest (ROIs)

Lobe	Gyrus	Consisting of:
Frontal	Superior frontal gyrus	
	Middle frontal gyrus	
	Inferior frontal gyrus	
	Straight gyrus	
	Orbitofrontal gyrus	Anterior orbital gyrus Medial orbital gyrus Lateral orbital gyrus Posterior orbital gyrus
	Subcallosal area	
	Anterior cingulate gyrus	
	Insula	
	Precentral gyrus	
Temporal	Anterior temporal lobe	Medial anterior temporal lobe Lateral anterior temporal lobe
	Posterior temporal lobe	
	Amygdala	
	Hippocampal formation	Hippocampus Parahippocampal gyrus
	Superior temporal gyrus	
	Inferior temporal gyrus	
	Fusiform gyrus	
Parietal	Postcentral gyrus	
	Posterior cingulate gyrus	
	Precuneus	
	Remainder of parietal lobe	
Occipital	Lingual gyrus	
	Cuneus	
	Lateral remainder of occipital lobe	

Regions of interest (ROIs) assessed for grey matter volume and cerebral flood flow. Parcellated gyri (according to [24,25], right column) were combined (middle column) for analysis.

Chapter 4.3

Longitudinal changes in phenocopy frontotemporal dementia: a case series

Paper in preparation

ABSTRACT

Phenocopy frontotemporal dementia (phFTD) is a syndrome of much debate, as it shares core characteristics with bvFTD yet without associated cognitive deficits and brain abnormalities on conventional magnetic resonance imaging (MRI), and without progression. Using advanced MRI techniques, subtle structural and functional brain changes in phFTD similar to bvFTD were recently observed, and it was hypothesised that phFTD and bvFTD may belong to the same disease spectrum. The aim of the current study was to gain more insight into longitudinal brain changes in phFTD.

Six (5 for MRI) phFTD patients at 3-year follow-up were qualitatively compared with baseline measures, and with 9 bvFTD patients and 17 controls. Qualitative comparison was performed for measures of cognition, grey matter volume, cerebral blood flow and fractional anisotropy. Additionally, the clinical profile at follow-up for each phFTD case was described.

PhFTD patients showed symptomatology similar to bvFTD, but with a relatively stable clinical profile. Qualitative comparison showed progression of language and memory deficits and a stable pattern of structural brain abnormalities, with cognitive scores and structural values generally in between the normal and bvFTD, and functional changes in the sense of increased perfusion.

These findings are still in support of the notion that phFTD and bvFTD may belong to the same disease spectrum. These findings may be used as motivation and a basis for further longitudinal studies in phFTD, specifically exploring the structural versus functional brain changes.

1. INTRODUCTION

The clinical syndrome phenocopy frontotemporal dementia (phFTD) is the subject of much debate. It shares behavioural changes as core features with bvFTD but does not follow the same disease course. Apathy, behavioural disinhibition, and loss of insight occur in both phFTD and bvFTD [1]. However, phFTD does not show the cognitive and brain abnormalities that are typical for bvFTD. Their cognitive profile may range from normal to suggesting bvFTD [2–5] but they appear stable over time, whereas in bvFTD rapid progression of cognitive deficits is evident [5–8]. On conventional (structural) magnetic resonance imaging (MRI), phFTD shows no or only mild abnormalities [6,8] in the frontotemporal brain regions typically affected in bvFTD [9]. Consequently, as a pathophysiological explanation is not yet available, phFTD patients often remain undiagnosed or may receive an uncertain psychiatric diagnosis. Additionally, C9orf72 repeat expansions may occasionally mimic phFTD, as cognitive deficits remain stable over years [10]. In our recent work [11,12] we aimed to address this diagnostic concern and lack of neurological explanation by using advanced MRI techniques to investigate the possible presence of more subtle brain abnormalities.

Using diffusion tensor imaging (DTI) we observed white matter (WM) microstructure abnormalities in the frontal and temporoparietal lobes in phFTD similar to bvFTD, but less pronounced than in bvFTD [11]. Using an advanced post-processing method of structural imaging to explore grey matter (GM) volumes, we observed loss of GM volume in the right temporal lobe [12]. Additionally, we observed a continuum with - especially - frontotemporal GM volumes ranging from the normal in healthy to abnormal in bvFTD, and phFTD in between with scores not significantly different from either [12]. Using resting state functional MRI (rs-fMRI) we observed increased default mode network (DMN) functional connectivity in phFTD in nearly all regions of the DMN, similar to bvFTD but more pronounced [11]. Using arterial spin labelling (ASL) we observed left frontal hyperperfusion [12].

These findings indicate that more subtle brain abnormalities are evident in phFTD. As these abnormalities are similar to bvFTD - in addition to their similar symptomatology - we concluded with the notion that phFTD and bvFTD may belong to the same disease spectrum. In the current study we aimed to gain more insight into longitudinal brain changes in phFTD by means of a case series exploring advanced MRI and neuropsychological examination in phFTD patients at 3-year follow-up.

2. METHODS

2.1 Participants

All patients were recruited in the Alzheimer Centre Southwest Netherlands. PhFTD patients (aged 40-75 years) with prominent behavioural changes interfering with social functioning, consisting of disinhibition and/or apathy and/or stereotypy; without reported progression one year after initial routine diagnostic workup; and bvFTD patients (aged 45-70 years) with a diagnosis of bvFTD [13]; a clinical dementia rating scale score of ≤ 1; a Mini-Mental State Examination [14] (MMSE) score of ≥ 20, were included in the study.

Patients with other neurological disorders, past or current substance abuse or other psychiatric diagnosis were excluded. PhFTD patients with a diagnosis of dementia or missing heteroamnesis, and bvFTD patients with a different cause of dementia, were also excluded.

Healthy controls (aged 60-70 years), without neurological or psychiatric history, were recruited through advertisement. They were matched for gender with phFTD patients and for age with all patients.

The study was approved by the local medical ethics committee. All participants gave written informed consent.

2.2 Participant assessment

PhFTD patients received an MRI scan, neuropsychological examination, MMSE, psychiatric assessment and genetic testing of the C9orf72 mutation at baseline. For convenience we will refer to this group as baseline phFTD. At 3-year follow-up, the phFTD patients received an MRI scan, neuropsychological examination and MMSE.

BvFTD patients and controls underwent an MRI scan, neuropsychological examination and MMSE at baseline only.

2.3 Image acquisition and assessment

Scanning was performed on two 3T GE Discovery MR750 systems (GE Healthcare, Milwaukee, WI, US) with identical protocols. PhFTD patients and nine controls

were scanned on one, and bvFTD patients and eight controls on the other scanner.

For clinical radiological assessment, GM volumetric assessment and anatomical reference, a high-resolution three-dimensional (3D) inversion recovery (IR) fast spoiled gradient-echo (FSPGR) T1-weighted (T1w) scan was acquired. T1w parameters were a scan duration of 4.41 min, field of view (FOV) of 240mm, inversion time (TI) of 450ms, echo time (TE) of 3.06ms, repetition time (TR) of 7904ms, array spatial sensitivity encoding technique acceleration (ASSET) factor of 2, a flip angle of 12°, an acquisition matrix of 240x240mm, and a slice thickness of 1mm.

DTI scans with full coverage of the supratentorial brain were acquired using a spin echo echo planar imaging (EPI) sequence. Acquisition parameters consisted of: 28 total volumes with 59 axial slices each, 3 non-diffusion weighted volumes, 25 diffusion-weighted directions, scan duration 3.50 min, FOV 240mm, TE set to minimum with mean 84.04ms (range: 81.9-90.8ms; TE mean and range based on baseline scans), TR 7925ms, ASSET factor of 2, flip angle 90°, acquisition matrix 128x128mm, slice thickness 2.5mm, and maximum b-value 1000 s/mm^2.

ASL scans were acquired using whole brain 3D pseudocontinuous ASL (p-CASL), which is currently the recommended sequence for clinical use [15]. Perfusion scans were acquired using the recommended parameters (interleaved fast spin-echo stackof-spiral readout of 512 sampling points on 8 spirals, background suppressed, labelling duration 1450 ms, TE 10.5 ms, TR 4632 ms, isotropic resolution 3.3 mm3, FOV 240 mm, 36 axial slices, number of excitations (NEX) 3, total acquisition time 4.29 min), with exception of the post labelling delay which was 1525 ms in the current study. The labelling plane was positioned 9 cm below the anterior commissure–posterior commissure line.

Structural (conventional) imaging at baseline and follow-up was clinically assessed and reported upon by a neuroradiologist at Alzheimer Centre Southwest Netherlands.

DTI scans (baseline and follow-up) were post-processed using Tractography according to the methods previously described in Steketee & Meijboom et al. 2016 [16]. Median fractional anisotropy (FA) values were established for the following (bilateral) WM tracts: anterior thalamic radiation, cingulate and hippocampal cingulum, inferior fronto-occipital fasciculus, inferior and superior longitudinal fasciculus, uncinate fasciculus, and forceps minor and major.

GM volumes and CBF (baseline and follow-up) were post-processed according to the methods previously described in Steketee et al. 2016 [12]. Whole-brain GM volumes expressed as percentage of intracranial volume (%ICV), and whole-

brain and regional mean CBF were established. For each brain lobe we then averaged the appropriate regional CBF values to establish mean CBF for the frontal, temporal, parietal and occipital lobe.

2.4 Neuropsychological data acquisition and assessment

Patients received a neuropsychological examination performed by a neuropsychologist at Alzheimer Centre Southwest Netherlands. Cognitive domains assessed were attention and executive functioning, language, memory, and visuoconstructive functioning (Table 1).

Baseline and follow-up neuropsychological scores were assessed and reported upon by the neuropsychologist.

Baseline and follow-up neuropsychological test scores were transformed to z-scores using the mean and standard deviation of controls as a reference. For the tests assessing attention and executive functioning, and memory, these z-scores were averaged to establish one score per cognitive domain (a composite score) for each participant (SPSS21.0, New York, USA).

Table 1. Cognitive domains and their specific neuropsychological tests used to assess cognitive functioning in patients and controls.

Cognitive domain	Neuropsychological test
Attention and concentration / executive functions	Trail Making Test (TMT)[17] Stroop colour-word task[18] Categorical and letter fluency test[19] Modified Wisconsin Card Sorting test (WCST)[20] Letter Digit Substitution Test (LDST)[21]
Language	Boston Naming Test (60 items)[22]
Memory	15 Words Test[23] Digit Span of the Wechsler Adult Intelligence Scale third edition (WAIS-III)[24] Mini-Mental State Examination (MMSE) orientation questions[14]
Visuoconstructive functioning	Clock drawing[25]

2.5 Qualitative analysis

Seven phFTD patients, 12 bvFTD patients and 17 controls were included in the study. One phFTD patient was excluded due to missing follow-up data. Six phFTD patients underwent follow-up assessment, one of whom did not undergo an MRI due to a pacemaker. Only neuropsychological examination was performed in this patient. Three bvFTD patients were excluded due to incomplete data: two had missing neuropsychological data and one had ASL scans of unusable quality. Cognitive, DTI, ASL and structural imaging data of 6 phFTD patients (5 for MRI data), 9 bvFTD patients and all controls were used for qualitative comparisons (Table 2).

Age did not differ between groups (F (2) = 0,856 p>0.05; Welch-ANOVA test). The ANOVA test for MMSE score was significant (F (2) = 4.035, p=0.028); post-hoc between-group comparisons showed MMSE score was lower in phFTD than in controls (p=0.041) (SPSS21.0, New York, USA). See Table 2 for an overview of the demographics. For frequency of education levels per group see Table 3.

Table 2. Demographic characteristics of reference groups

Group	N	Mean age	Mean MMSE
PhFTD	6 (6 male)	63.8 (5.1)	26.3 (1.4)
BvFTD	9 (4 male)	60.1 (8.4)	27.1 (2.0)
Controls	17 (17 male)	64.1 (3.3)	28.3 (1.4)

PhFTD = phenocopy FTD, BvFTD = behavioural variant frontotemporal dementia, N = sample size. Values given as Mean (standard deviation). MMSE = Mini-Mental State Examination.

Table 3. Education level frequencies per group

Education level	PhFTD	BvFTD	Controls
1	0	0	0
2	0	0	0
3	1	2	0
4	4	3	1
5	1	1	9
6	1	3	4
7	0	0	3

PhFTD = phenocopy FTD, BvFTD = behavioural variant frontotemporal dementia.
Education levels reported using the dutch Verhage education scale (1964): with a score of 1 representing less than primary education and a score of 7 representing university education.

None of the phFTD patients received an alternative psychiatric diagnosis that could explain their behavioural symptoms. Additionally, none carried the C9orf72 mutation.

For each group (phFTD baseline, phFTD follow-up, bvFTD and controls) cognitive domain scores, WM tract FA, whole-brain GM volume (%ICV) and whole-brain and regional CBF, were averaged (SPSS21.0, New York, USA).

3. RESULTS

3.1 Summary of qualitative comparison of advanced MRI measures

Patients with phFTD generally performed worse on follow-up for language and memory in comparison with baseline, and similarly for visuoconstructive functioning and attention and executive functioning. Follow-up phFTD scores for all domains were in between scores for bvFTD patients and controls (Figure 1, Table 1).

Whole-brain GM volume in phFTD upon follow-up was similar to baseline and in between volumes of bvFTD and controls (Figure 2, Table 2). Whole brain

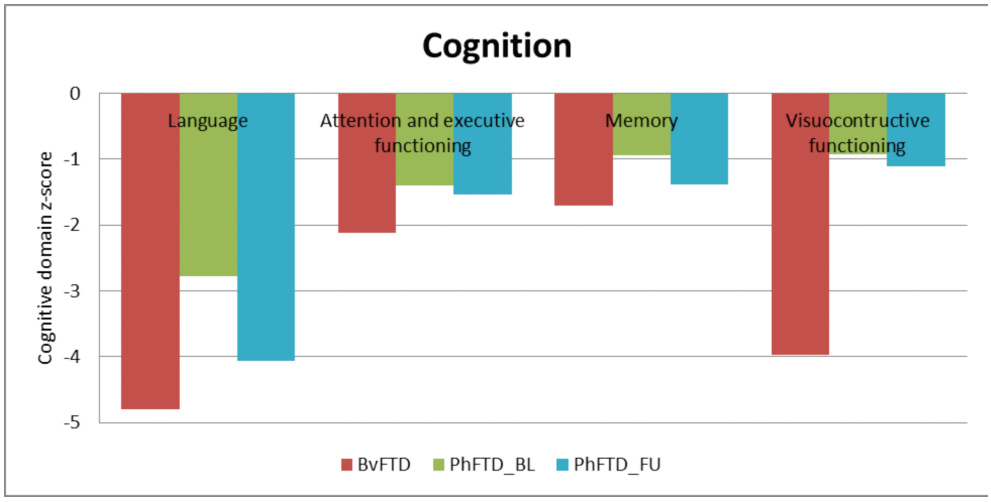

Figure 1. Cognitive domain z-scores for each group (bvFTD, baseline phFTD, follow-up phFTD). Z-scores are calculated using means of controls as a reference (i.e. control mean = 0). Domains assessed are language, attention and executive functioning, memory and visuoconstructive functioning.
bvFTD = behavioural variant frontotemporal dementia, phFTD = phenocopy frontotemporal dementia, BL = baseline, FU = follow-up.

and regional perfusion in follow-up phFTD was increased in comparison with baseline phFTD (Figure 3, Table 3). WM tract FA in follow-up phFTD was similar to baseline phFTD (Figure 4, Table 4), and generally in between bvFTD and controls.

Cognitive test results , GM volume, CBF and FA values for each phFTD case at baseline and follow-up, are listed in Tables 1-4.

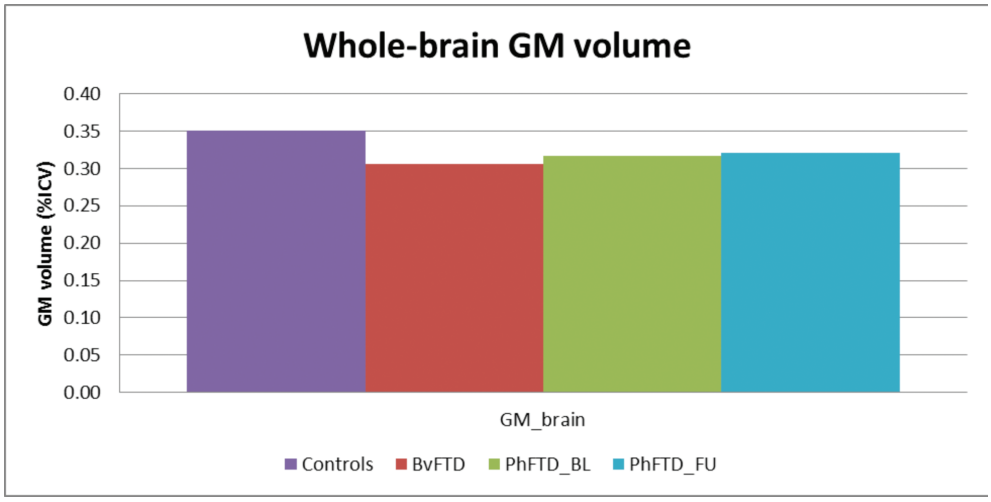

Figure 2. Whole-brain grey matter (GM) volume expressed in intracranial volume (ICV) shown for each group (bvFTD, baseline phFTD, follow-up phFTD, controls). bvFTD = behavioural variant frontotemporal dementia, phFTD = phenocopy frontotemporal dementia, BL = baseline, FU = follow-up.

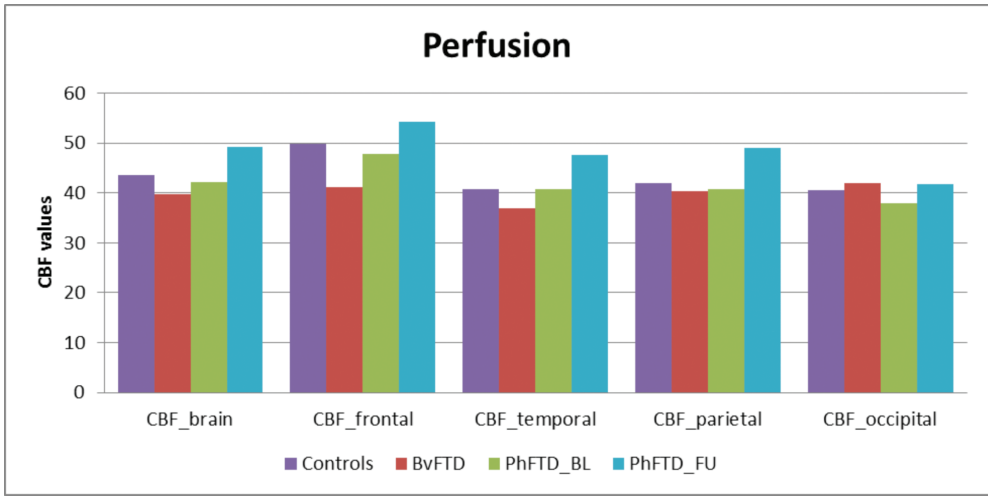

Figure 3. Whole-brain perfusion and brain-lobe perfusion shown for each group (bvFTD, baseline phFTD, follow-up phFTD, controls). bvFTD = behavioural variant frontotemporal dementia, phFTD = phenocopy frontotemporal dementia, BL = baseline, FU = follow-up.

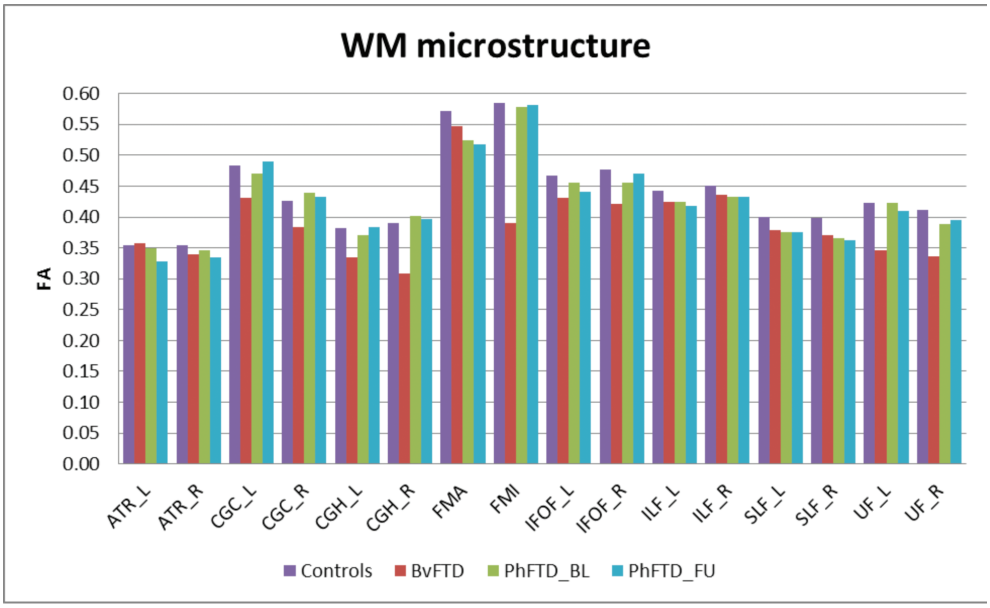

Figure 4. White matter (WM) microstructure represented by fractional anisotropy (FA) per WM tract shown for each group (bvFTD, baseline phFTD, follow-up phFTD, controls). WM tracts included are the left and right anterior thalamic radiation (ATR_L and ATR_R), left and right cingulate cingulum (CGC_L and CGC_R), left and right hippocampal cingulum (CGH_L and CGH_R), forceps major (FMA), forceps minor (FMI), left and right inferior fronto-occipital fasciculus (IFOF_L and IFOF_R), left and right inferior longitudinal fasciculus (ILF_L and ILF_R), left and right superior longitudinal fasciculus (SLF_L and SLF_R), and left and right uncinate fasciculus (UF_L and UF_R). bvFTD = behavioural variant frontotemporal dementia, phFTD = phenocopy frontotemporal dementia, BL = baseline, FU = follow-up.

Table 1. Cognitive domain z-scores for phenocopy frontotemporal dementia (phFTD) cases at baseline and follow-up.

		Case 1	Case 2	Case 3	Case 4	Case 5	Case 6
Language	Baseline	-2.90	-8.33	-0.96	-2.12	-0.57	-1.73
	Follow-up	-5.62	-8.72	-1.73	-4.06	-2.12	-2.12
Attention and executive functioning	Baseline	-1.80	-2.55	-0.92	-1.09	0.26	-2.28
	Follow-up	-1.64	-2.98	-0.68	-0.78	0.07	-3.22
Memory	Baseline	-0.88	0.35	-1.12	-0.87	-0.14	-3.01
	Follow-up	-1.77	-0.89	-1.60	-0.07	-0.56	-3.43
Visuoconstructive functioning	Baseline	-0.54	-0.54	0.61	-0.54	-1.68	-2.83
	Follow-up	0.61	-0.54	-0.54	0.61	-1.68	-5.11

Table 2. Whole brain grey matter (GM) volume (% intracranial volume) for phenocopy frontotemporal dementia (phFTD) cases at baseline and follow-up.

		Case 1	Case 2	Case 3	Case 5	Case 6
Whole-brain GM volume (%ICV)	Baseline	0.3491	0.2759	0.3368	0.3165	0.3083
	Follow-up	0.3432	0.2589	0.3373	0.3215	0.3408

Table 3. Whole brain and regional cerebral blood flow (CBF) for phenocopy frontotemporal dementia (phFTD) cases at baseline and follow-up.

		Case 1	Case 2	Case 3	Case 5	Case 6
Whole-brain CBF	Baseline	37.49	59.88	28.36	42.60	42.19
	Follow-up	54.45	60.86	36.18	44.14	50.54
Frontal CBF	Baseline	39.49	68.45	35.28	49.22	46.96
	Follow-up	55.86	70.78	47.81	44.22	52.26
Temporal CBF	Baseline	36.93	55.39	30.30	40.44	40.70
	Follow-up	57.48	60.44	34.24	42.13	43.52
Parietal CBF	Baseline	37.82	55.83	28.68	39.30	42.54
	Follow-up	53.20	56.27	38.17	41.71	56.14
Occipital CBF	Baseline	35.18	51.49	17.11	47.56	38.22
	Follow-up	46.49	47.71	19.75	48.61	46.78

Table 4. White matter (WM) tract fractional anisotropy (FA) for phenocopy frontotemporal dementia (phFTD) cases at baseline and follow-up. L= left, R=right.

		Case 1	Case 2	Case 3	Case 5	Case 6
Anterior thalamic radiation L	Baseline	0.3541	0.3201	0.3662	0.3465	0.3592
	Follow-up	0.3407	0.3008	0.3641	0.3391	0.2965
Anterior thalamic radiation R	Baseline	0.3336	0.3480	0.3803	0.3260	0.3428
	Follow-up	0.3161	0.3223	0.3665	0.3407	0.3266
Cingulate cingulum L	Baseline	0.5052	0.4491	0.4825	0.4090	0.5019
	Follow-up	0.5179	0.4527	0.5384	0.4183	0.5214
Cingulate cingulum R	Baseline	0.4420	0.3750	0.5104	0.3768	0.4958
	Follow-up	0.4559	0.3885	0.5044	0.3824	0.4334

Hippocampal cingulum L	Baseline	0.4199	0.3505	0.3499	0.3573	0.3777
	Follow-up	0.4318	0.3105	0.3825	0.3908	0.3995
Hippocampal cingulum R	Baseline	0.4296	0.3619	0.4049	0.3985	0.4162
	Follow-up	0.3975	0.3843	0.3976	0.4323	0.3712
Forceps major	Baseline	0.5719	0.4507	0.6411	0.4990	0.4561
	Follow-up	0.5214	0.4376	0.6366	0.4994	0.4947
Forceps minor	Baseline	0.6663	0.5138	0.6446	0.5522	0.5117
	Follow-up	0.6613	0.4763	0.6846	0.5605	0.5225
Inferior fronto-occipital fasciculus L	Baseline	0.4499	0.4099	0.5251	0.4643	0.4261
	Follow-up	0.4630	0.3940	0.4632	0.4818	0.4028
Inferior fronto-occipital fasciculus R	Baseline	0.4735	0.4159	0.4733	0.4978	0.4154
	Follow-up	0.4794	0.4105	0.4855	0.5242	0.4480
Inferior longitudinal fasciculus L	Baseline	0.4526	0.3619	0.4910	0.4104	0.4052
	Follow-up	0.4422	0.3593	0.4732	0.4164	0.3970
Inferior longitudinal fasciculus R	Baseline	0.4718	0.3656	0.5011	0.4138	0.4113
	Follow-up	0.4439	0.3778	0.5054	0.4316	0.4015
Superior longitudinal fasciculus L	Baseline	0.3991	0.3126	0.4226	0.3709	0.3710
	Follow-up	0.3912	0.3175	0.4218	0.3775	0.3657
Superior longitudinal fasciculus R	Baseline	0.3948	0.3209	0.4297	0.3220	0.3573
	Follow-up	0.3932	0.3204	0.4238	0.3208	0.3509
Uncinate fasciculus L	Baseline	0.4561	0.3864	0.4923	0.3966	0.3794
	Follow-up	0.4226	0.3883	0.4797	0.3691	0.3919
Uncinate fasciculus R	Baseline	0.4266	0.3498	0.4217	0.3814	0.3642
	Follow-up	0.4033	0.3545	0.4254	0.3900	0.4051

3.2 Case descriptions

Case 1

Patient 1 was a 64 year old male who reported first noticing behavioural changes 15 years previously. His major complaints involved loss of empathy, increased and uncontrolled anger, loss of initiative, compulsivity, irritability, increased talking and moving.

The neuropsychological report at follow-up stated disorders of language (naming), divided attention and social cognition. Additionally, mild abnormalities in the executive functions and working memory/memory were observed. In comparison with the neuropsychological report at baseline the patient showed a very mild progression of language, memory and divided attention abnormalities. Although the clinical and neuropsychological profile suggested bvFTD, the protracted disease course and lack of evident progression of cognitive dysfunctioning did not support the clinical diagnosis of probable bvFTD.

The radiological report at follow-up stated that GM atrophy or WM abnormalities were not observed on conventional (structural) MRI.

Case 2

Patient 2 was a 73 year old male who reported first noticing behavioural changes at least 12 years previously. His major complaints included increased dependency on his partner, loss of initiative, apathy, increase of food intake, and the inability to cope with changes.

The neuropsychological report at follow-up stated disorders of naming, task-switching, visuo-associative memory and emotion recognition. In comparison with baseline neuropsychological examination there was a decrease in memory functioning and inhibition.

The radiological report of conventional (structural) imaging at follow-up stated a mild increase of global GM atrophy (global cortical atrophy scale 1 (GCA)), and no regional GM atrophy. Additionally, it stated that already known WM lesions were observed (Fazekas 3), which were most likely of vascular origin.

Case 3

Patient 3 was a 74 year old male who reported first noticing behavioural changes at least 8 years previously. Major complaints included angry and aggressive behaviour, impulsivity, decreased empathy, sexual disinhibition, speech disinhibition, compulsive information gathering, and no symptom insight.

The neuropsychological report at follow-up stated weak scores on verbal memory and emotion recognition. Other domains showed average or just-below average scores. In comparison with baseline neuropsychological examination, emotion recognition was more abnormal, but in contrast, scores for a complex executive task were higher. Scores on the other domains showed no changes.

The radiological report of conventional (structural) imaging at follow-up stated no regional atrophy, and very mild global atrophy (GCA 1). No changes were observed in comparison with baseline MRI.

Case 4

Patient 4 was a 62 year old male who reported first noticing behavioural changes at least 10 years previously. His main complaints included severe forgetfulness, switching letters during speech, incorrect use of words, disinhibition in general, and disinhibition of speech specifically.

The neuropsychological report at follow-up stated weak performance of divided attention, and below-average performance on language, processing speed and working memory. The other domains, among which memory and social cognition, were of average score. In comparison with baseline neuropsychological examination there was progression in one attention and one processing speed task, while other scores remained stable.

The patient did not receive a follow-up MRI due to placement of a pacemaker during follow-up. The radiological report of conventional (structural) imaging at baseline stated global atrophy (GCA 1), which was somewhat more pronounced in the parietal lobe. There were some WM lesions (Fazekas 1). Importantly, as the patient reported memory problems, the report stated that no hippocampal atrophy was observed.

Case 5

Patient 5 was a 67 year old male who reported first noticing behavioural changes 10 years previously. Major complaints included loss of empathy, impulsive purchases, increased intake of food, isolated behaviour, unhappiness, increased anger triggered by minor events, loss of initiative, reduced vocabulary and forgetfulness.

The neuropsychological report at follow-up stated average and above-average performance on cognitive domains, with the exception of weak performance on emotion recognition. The report concluded that no cognitive disorders were objectified, and that there were no changes in comparison with neuropsychological examination at baseline.

The radiological report of conventional (structural) imaging at follow-up stated no cortical atrophy or WM lesions, other than known lacunar infarcts in the brainstem and a cortical infarct in the right parietal lobe. This profile was not different from MRI at baseline.

Case 6

Patient 6 was a 63 year old male who reported first noticing behavioural changes 20 years previously. Major complaints included short term memory loss, reduced personal hygiene, verbal aggressiveness, inappropriate, a.o. sexual, remarks, word finding problems, loss of control concerning drinking and eating.

The neuropsychological report at follow-up stated disorders of executive functioning, attention and social cognition. Weak memory performance is observed for encoding of new material, retaining and recall. Visuoconstruction and praxis were abnormal. There were no evident disorders of language and orientation. In comparison with baseline neuropsychological examination, minimal progression was observed for executive functioning, social cognition and processing speed. However, overall the cognitive profile was stable in comparison with neuropsychological examination performed in 2003.

The radiological report of conventional (structural) imaging at follow-up stated minimal frontal atrophy, which did not show evident progression in comparison with baseline MRI. Additionally, three microbleeds were observed, and a hypertensive origin was suggested.

4. DISCUSSION

The aim of this case series was a qualitative description of brain and cognitive changes in phFTD patients after a 3-year time period. No evident clinical progression was observed in phFTD cases with disease durations ranging from 8 to 20 years. Neuropsychological examination showed that cognitive profiles may be normal, may be suggestive of bvFTD, and be stable or show some progression. Conventional (structural) MRI showed no or unspecific atrophy patterns, which did not or only mildly progressed. Qualitative comparison of cognitive performance at baseline and follow-up showed some progression in the language and memory domains, yet all cognitive domain scores were still in between those of bvFTD and controls. Qualitative comparison of advanced MRI measures showed that structural brain abnormalities in phFTD showed no evident progression and

were generally in between bvFTD and controls. Additionally, it showed that functional brain abnormalities, i.e. hyperperfusion, progressed over time and were more pronounced than in bvFTD and controls.

This case series illustrates that clinically phFTD does not show clear longitudinal changes, except for some progression in language and memory deficits; this may suggest that progression of these domains clinically may become apparent before that of other cognitive domains, although their scores were still in between bvFTD and controls.

Importantly, this case series also suggests that structural abnormalities, such as GM volume and WM microstructure, appear to be both relatively stable and in between bvFTD and controls, whereas functional abnormalities show longitudinal changes. Higher perfusion was observed for the whole brain and for each lobe, which is in line with our previous findings [12]. Naturally, a firm conclusion cannot be drawn as we could not perform any formal comparisons with controls and baseline measurements due to the small study sample. However, we can speculate on this interesting finding, as previous literature has hypothesised that functional changes may be related to a mechanism compensating for subtle neuronal dysfunctioning [26,27]. Our hypothesis is that deterioration of neuronal functioning over time in phFTD is associated with compensatory changes in perfusion, in the absence of unchanged GM volume.

This case series also points out the diversity of the clinical profile in phFTD cases and the difficulties with phFTD diagnosis. For instance, disease duration, behavioural profiles, cognitive profiles and conventional (structural) MRI were similar amongst all cases, but were not the same. A specific example is case 2 who showed lower GM volumes, lower neuropsychological scores, higher perfusion and lower FA in WM tracts, in comparison with the other cases. Together with mild progression clinically, we could speculate that these findings suggest that this patient is in a slightly more advanced disease stage than the other cases. However, disease duration is 12 years, which is still highly unlike bvFTD. This emphasises the need for long-term follow-up with repeat assessments to understand disease development in this particular case, and in phFTD in general.

This study knows some limitations, specifically its qualitative nature and a small sample size. However, as phFTD is a rare and relatively unknown syndrome, more information is of great value for its understanding and diagnosis. This case series adds to the increasing knowledge of longitudinal changes in phFTD [1,4–6,28].

In conclusion, phFTD patients assessed at 3-year follow-up show symptomatology similar to bvFTD, but with a relatively stable clinical profile. They show progression of language and memory deficits and a stable pattern of structural brain abnormalities, with cognitive scores and structural values generally in between normal and bvFTD, and functional changes in the sense of increased perfusion. Overall, these observations are still in support of the notion that phFTD and bvFTD may belong to the same disease spectrum. Despite the fact that a descriptive case series does not allow for strong conclusions, we may use these observations as motivation and a basis for further longitudinal studies in phFTD, specifically exploring the structural versus functional brain changes.

REFERENCES

1 Hornberger M, Shelley BP, Kipps CM, *et al.* Can progressive and non-progressive behavioural variant frontotemporal dementia be distinguished at presentation? *J Neurol Neurosurg Psychiatry* 2009;80:591–3. doi:10.1136/jnnp.2008.163873

2 Bertoux M, de Souza LC, Corlier F, *et al.* Two Distinct Amnesic Profiles in Behavioral Variant Frontotemporal Dementia. *Biol Psychiatry* Published Online First: 2013. doi:10.1016/j.biopsych.2013.08.017

3 Hornberger M, Piguet O, Kipps C, *et al.* Executive function in progressive and nonprogressive behavioral variant frontotemporal dementia. *Neurology* 2008;71:1481–8. doi:10.1212/01.wnl.0000334299.72023.c8

4 Irish M, Graham A, Graham KS, *et al.* Differential impairment of source memory in progressive versus non-progressive behavioral variant frontotemporal dementia. *Arch Clin Neuropsychol* 2012;27:338–47. doi:10.1093/arclin/acs033

5 Mioshi E, Hodges JR. Rate of change of functional abilities in frontotemporal dementia. *Dement Geriatr Cogn Disord* 2009;28:419–26. doi:10.1159/000255652

6 Davies RR, Kipps CM, Mitchell J, *et al.* Progression in frontotemporal dementia: identifying a benign behavioral variant by magnetic resonance imaging. *Arch Neurol* 2006;63:1627–31. doi:10.1001/archneur.63.11.1627

7 Garcin B, Lillo P, Hornberger M, *et al.* Determinants of survival in behavioral variant frontotemporal dementia. *Neurology* 2009;73:1656–61. doi:10.1212/WNL.0b013e3181c1dee7

8 Kipps CM, Davies RR, Mitchell J, *et al.* Clinical significance of lobar atrophy in frontotemporal dementia: application of an MRI visual rating scale. *Dement Geriatr Cogn Disord* 2007;23:334–42. doi:10.1159/000100973

9 Rosen HJ, Gorno-Tempini ML, Goldman WP, *et al.* Patterns of brain atrophy in frontotemporal dementia and semantic dementia. *Neurology* 2002;58:198–208.http://www.ncbi.nlm.nih.gov/pubmed/11805245

10 Khan BK, Yokoyama JS, Takada LT, *et al.* Atypical, slowly progressive behavioural variant frontotemporal dementia associated with C9ORF72 hexanucleotide expansion. *J Neurol Neurosurg Psychiatry* 2012;83:358–64. doi:10.1136/jnnp-2011-301883

11 Meijboom R, Steketee RME, de Koning I, *et al.* Functional connectivity and microstructural white matter changes in phenocopy frontotemporal dementia. *Eur Radiol* Published Online First: 19 July 2016. doi:10.1007/s00330-016-4490-4

12 Steketee RME, Meijboom R, Bron EE, *et al.* Structural and functional brain abnormalities place phenocopy frontotemporal dementia (FTD) in the FTD spectrum. *NeuroImage Clin* 2016;11:595–605. doi:10.1016/j.nicl.2016.03.019

13 Rascovsky K, Hodges JR, Knopman D, *et al.* Sensitivity of revised diagnostic criteria for the behavioural variant of frontotemporal dementia. *Brain* 2011;134:2456–77. doi:10.1093/brain/awr179
14 Folstein MF, Folstein SE, McHugh PR. 'Mini-mental state'. A practical method for grading the cognitive state of patients for the clinician. *J Psychiatr Res* 1975;12:189–98.http://www.ncbi.nlm.nih.gov/pubmed/1202204.
15 Alsop DC, Detre JA, Golay X, *et al.* Recommended implementation of arterial spin-labeled perfusion MRI for clinical applications: A consensus of the ISMRM perfusion study group and the European consortium for ASL in dementia. *Magn Reson Med* 2015;73:102–16. doi:10.1002/mrm.25197
16 Steketee RME, Meijboom R, de Groot M, *et al.* Concurrent white and gray matter degeneration of disease-specific networks in early-stage Alzheimer's disease and behavioral variant frontotemporal dementia. *Neurobiol Aging* 2016;43:119–28. doi:10.1016/j.neurobiolaging.2016.03.031
17 *Army Individual Test Battery. Manual of directions and scoring.* Washington, DC: : War Department, Adjutant General's office 1994.
18 Stroop J. Studies of interference in serial verbal reactions. *J Exp Psychol* 1935;18:643–62.
19 Thurstone L, Thurstone T. *Primary mental abilities*. Chigago: : Science Research Associates 1962.
20 Nelson HE. A modified card sorting test sensitive to frontal lobe defects. *Cortex* 1976;12:313–24.
21 Jolles J, Houx PJ, Van Boxtel MPJ. *Maastricht Aging Study: determinants of cognitive aging*. Maastricht, The Netherlands: : Neuropsych publishers 1995.
22 Kaplan E, Goodglass H, Weintraub S. *The Boston Naming Test*. Philadelphia: : Lea & Febiger 1978.
23 Rey A. *L'examen clinique en psychologie*. Paris, France: : Presses Universitaires de France 1958.
24 Wechsler D. *WAIS-II Nederlandse Bewerking. Technische handleiding.* Lisse: : Harcourt Test Publishers 2005.
25 Royall DR, Cordes JA, Polk M. Clox: an executive clock drawing task. *J Neurol Neurosurg Psychiatry* 1998;64:588–94.
26 Bookheimer SY, Strojwas MH, Cohen MS, *et al.* Patterns of brain activation in people at risk for Alzheimer's disease. *N Engl J Med* 2000;343:450–6. doi:10.1056/NEJM200008173430701
27 Borroni B, Alberici A, Cercignani M, *et al.* Granulin mutation drives brain damage and reorganization from preclinical to symptomatic FTLD. *Neurobiol Aging* 2012;33:2506–20. doi:10.1016/j.neurobiolaging.2011.10.031
28 Garcin B, Lillo P, Hornberger M, *et al.* Determinants of survival in behavioral variant frontotemporal dementia. *Neurology* 2009;73:1656–61. doi:10.1212/WNL.0b013e3181c1dee7

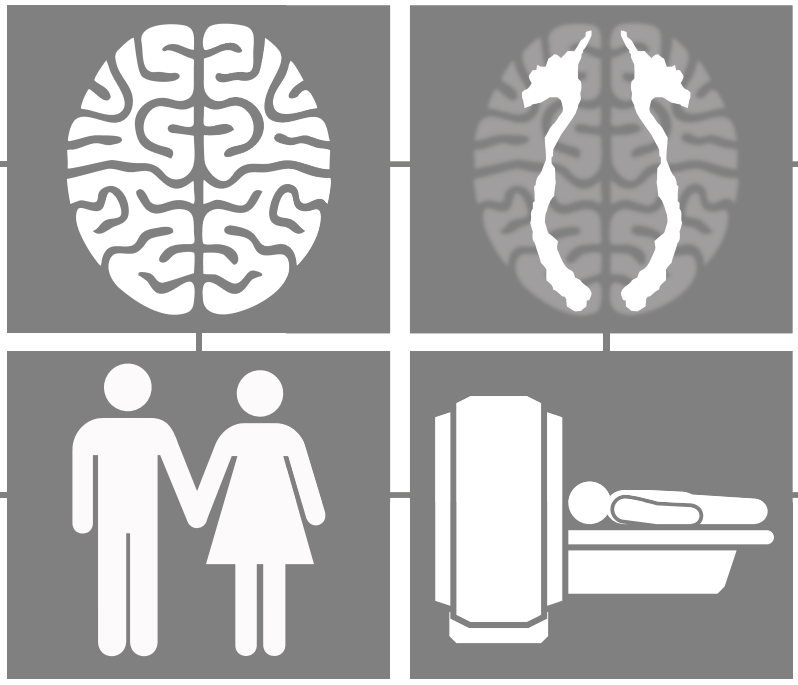

Chapter 5

General Discussion

In this thesis, I investigated the use of advanced magnetic resonance imaging (MRI) techniques, i.e. diffusion tensor imaging (DTI), resting state functional MRI (rs-fMRI) and arterial spin labelling (ASL), in underlying diseases of dementia: behavioural variant frontotemporal dementia (bvFTD), phenocopy frontotemporal dementia (phFTD), semantic dementia (SD) and Alzheimer's disease (AD). I investigated the use of these techniques in identifying subtle brain abnormalities, associating subtle brain abnormalities with disease symptomatology and improving early (differential) diagnosis. In this section I will provide an overview of the main findings and discuss the methodological considerations, clinical implications and future perspectives.

Main findings

Alzheimer's disease (AD) and behavioural variant frontotemporal dementia (bvFTD)

BvFTD and AD are two of the most common underlying disorders of presenile dementia (age<65 years) [1]. BvFTD is mainly characterized by behavioural problems such as disinhibition and apathy [2]. In contrast, AD is mainly characterized by a memory disturbance for recently learned material as well as for learning new material [3]. This disease-specific clinical profile usually predominates in later stages of AD and bvFTD, but in earlier stages symptoms may still be mild and unspecific. This complicates differential diagnosis of AD and bvFTD and may lead to inconclusive diagnosis or misdiagnosed patients. With the use of conventional MRI, diagnosis of AD or bvFTD can be supported. However, in early disease stages, conventional (structural) MRI may still appear normal or show diffuse brain abnormalities unspecific for AD or bvFTD [4–6]. More advanced MRI techniques, such as DTI, rs-fMRI and ASL can potentially aid the diagnostic process by looking at more subtle brain abnormalities: DTI assesses white matter (WM) microstructure, rs-fMRI assesses functional connectivity and ASL assesses grey matter (GM) perfusion. These techniques provide the following advantages over conventional imaging: quantification of subtle brain abnormalities (chapter 2.1) and combination of subtle brain abnormality measures (chapter 2.2).

Early-stage and long-term clinical differentiation of AD and bvFTD may especially benefit from objective quantitative measures (chapter 2.1), because these allow for establishing reference values in a healthy population, with which patients can be compared. To this end, we explored the diagnostic utility of quantitative mea-

sures of tract-specific WM microstructure and functional connectivity of the default mode network (DMN), using DTI and rs-fMRI respectively. Despite the DMN being a well-defined resting state network showing functional abnormalities in dementia, quantitative assessment of its functional connectivity did not aid differential diagnosis of AD and bvFTD. In contrast, measures of quantitative tract-specific WM microstructure indicated pronounced differences between early-stage AD and bvFTD, with WM microstructural abnormalities being widely observed in bvFTD, and only regionally in the hippocampal cingulum in AD. The extent of these differences was smaller after 1-year follow-up, but WM microstructural abnormalities were still more pronounced in bvFTD than in AD, specifically in the cingulate cingulum and inferior fronto-occipital fasciculus. This indicates that differential diagnosis of AD and bvFTD will benefit from using tract-specific WM microstructure, especially in the early stages, as diagnostic tool.

An important advantage of these quantitative advanced MRI techniques, such as DTI and ASL, is that the measures they provide may also be used in combination (chapter 2.2). This combination provides the unique opportunity to gain insight into the relationship between WM microstructure (DTI) and GM perfusion (ASL) changes in AD and bvFTD. It should be noted that the use of structural MRI may be improved by quantifying GM volumes, and additionally, by combining these measures with WM microstructure and GM perfusion. This combination allowed us to observe a disease-specific dissociation of structural and functional abnormalities, with structural degeneration in bvFTD on the one hand and hypoperfusion in AD on the other hand. Importantly, we observed strong coherence between WM and GM changes in regions implicated in later stages of AD and bvFTD pathology, which indicates concurrent WM and GM degeneration in disease-specific networks. Additionally, as coherence was mostly absent in healthy elderly, and WM and GM measures that were not necessarily different between groups did show coherence in AD and bvFTD, the correlational methodology applied here allowed for detection of incipient abnormalities that would otherwise go undetected in conventional comparative group analyses.

As advanced imaging not only allows us to quantify abnormalities, but is also more sensitive to detect more subtle abnormalities, it gives us the possibility to investigate relationships between subtle brain changes and clinical cognitive profiles in the early stages of AD and bvFTD (chapter 3.1). We observed that abnormalities of attention and executive deficits are related to microstructural WM changes in several WM tracts in bvFTD and to a lesser extent in AD. Such a rela-

tionship was also observed for language deficits in AD, and to a lesser extent for normal language functioning and WM microstructure in bvFTD. Additionally, normal memory functioning in bvFTD, as well as normal visuoconstructive functioning in AD was associated with WM microstructure abnormality. Interestingly, no relationship with WM abnormalities was observed for evident memory deficits in AD. This suggests that only certain cognitive domains are functionally related to abnormalities of WM microstructure in AD and bvFTD, and that GM abnormalities may play a more important role for deficits in other cognitive domains.

Frontotemporal dementia (FTD) variants

Frontotemporal dementia (FTD) is an umbrella term for several dementia variants affecting the frontal and temporal lobes, generally with an onset before the age of 65 years (presenile dementia)[7]. Well-known variants of FTD are the behavioural variant (bvFTD), as well as language variants, such as SD [8]. PhFTD, a rare syndrome clinically similar to bvFTD, may also belong to this FTD spectrum.

BvFTD is one of the most common variants, predominantly showing bilateral or right frontal lobe atrophy [2,8,9]. As described previously, it is mainly characterized by behavioural symptoms, and differential diagnosis with AD may be difficult in the early stage. Additionally, differential diagnosis of bvFTD and alternative psychiatric disorders may also be very challenging. This is due to resemblance between the behavioural disorder in bvFTD and psychiatric symptomatology such as psychosis and late onset schizophrenia[10]. This specific differential diagnostic issue is especially applicable to phFTD, which is a poorly understood syndrome, clinically similar to bvFTD but without its typical disease course. PhFTD presents with core bvFTD symptoms, such as apathy and behavioural disinhibition [11], but without the associated cognitive deficits [12–15] and disease progression [5,15–17], and without (or with unspecific borderline) brain abnormalities on conventional (structural) MRI [5,16]. As phFTD presents with a behavioural syndrome without apparent degeneration, its symptomatalogy may be attributed to alternative psychiatric disorders instead. However, in our studies investigating a carefully selected sample of phFTD patients, we established by means of psychiatric examination that phFTD symptomatology was not explained by an alternative psychiatric diagnosis. Instead, using advanced MRI techniques to investigate the more subtle brain changes, we observed brain abnormalities similar to bvFTD underlying phFTD symptomatology. Structurally, we observed abnormal WM microstructure in the frontal and temporoparietal lobes in phFTD also similar to bvFTD but less extensive (chapter 4.1), and cortical atrophy in the right temporal lobe (chapter 4.2). Cortical atrophy over-

lapped with bvFTD and frontotemporal GM volumes showed a continuum ranging from the normal to abnormal in bvFTD with phFTD in between. Functionally, we observed increased DMN functional connectivity in phFTD in nearly all regions of the DMN, similar to bvFTD but more pronounced (chapter 4.1), and left frontal hyperperfusion (chapter 4.2). Such functional increases are thought to reflect a mechanism compensating for incipient diminished neuronal functioning [18]. The ability of this mechanism to compensate is likely to decrease when the abnormalities become more severe, such as in bvFTD.

We extended these findings by qualitatively comparing cognition, brain function and brain structure in phFTD at 3-year follow-up with baseline (chapter 4.3). We observed some progression of language and memory deficits and a stable pattern of structural brain abnormalities, with cognitive scores and structural values generally in between normal and those in bvFTD. Interestingly, higher perfusion was observed for the whole brain and for each lobe, which is in line with the above described theory of compensation (chapter 4.1 and 4.2). Consequently, we hypothesized that deterioration of neuronal functioning over time in phFTD is associated with compensatory changes in perfusion, in the absence of unchanged GM volume.

Taken together, these findings suggest that phFTD may belong to the same disease spectrum as bvFTD, and may also indicate that advanced MRI techniques are potentially suited to detect subtle brain changes in phFTD that may improve diagnosis. Naturally, the hypothesis that phFTD may belong to the bvFTD disease spectrum requires confirmation with other diagnostic tools, such as histopathology. The findings of our studies may provide a direction for further development of such diagnostic - MRI or other - tools. Additionally, the longitudinal findings may be used as motivation and a basis for further longitudinal studies in phFTD, specifically exploring the structural versus functional brain changes.

The SD variant of FTD, in contrast with bvFTD, is characterized by a language disorder and shows predominantly left anterior temporal lobe (ATL) atrophy [8,9,19]. In contrast, bvFTD affects the right or bilateral frontal lobe [2,8,9]. We observed a similar hemispheric dissociation between SD and bvFTD when looking at brain connectivity abnormalities (chapter 3.2). This was especially evident for microstructural abnormalities of WM tracts in the left hemisphere in SD, and functional connectivity in the right hemisphere in bvFTD. Microstructural WM abnormalities were more pronounced in and lateralized towards the left hemisphere in SD compared with bvFTD, particularly in the uncinate, inferior longitudinal and inferior fronto-occipital fasciculus. These WM tracts are part of the ventral language

stream, which is associated with semantic processing [20,21], a domain characteristically affected in SD [19]. In bvFTD compared with SD, microstructural WM abnormalities were also more pronounced in one hemisphere - the right hemisphere - but were less lateralized than in SD. They were most pronounced in WM tracts associated with behavioural symptoms [22–26] which are evident in bvFTD (e.g. executive and emotional functioning): right uncinate and inferior fronto-occipital fasciculus, and the forceps minor. Functional connectivity of disease-specific regions (ATL and orbitofrontal cortex (OFC)) was mainly decreased with both hemispheres in SD compared with bvFTD and with the right hemisphere in bvFTD compared with SD. Explanation of observed functional connectivity by relating it to symptomatology was less straightforward, but generally the observed functional connectivity was found in GM regions previously observed to be associated with language in SD and behaviour in bvFTD. These findings indicate that SD and bvFTD show a hemispheric dissociation of brain connectivity in the frontotemporal regions, which underlies their differential symptomatology.

In conclusion, findings from this thesis have several indications for the use of advanced MRI in AD, bvFTD, SD and phFTD. First, AD and bvFTD findings may indicate that early-stage differential diagnosis of AD and bvFTD will benefit from using tract-specific WM microstructure as diagnostic tool (chapter 2.1); that there may be disease-specific concurrent degeneration of WM and GM structures in AD and bvFTD (chapter 2.2); that combining quantitative WM and GM measures may allow for detection of incipient abnormalities in AD and bvFTD that otherwise remain undetected (chapter 2.2); and that only certain cognitive domains may be functionally related to abnormalities of WM microstructure in AD and/or bvFTD (chapter 3.1). Second, SD and bvFTD findings are suggestive of a hemispheric dissociation of frontotemporal brain connectivity in SD and bvFTD, possibly explaining their differences in symptomatology (chapter 3.2). Third, phFTD findings suggest that phFTD may belong to the same disease spectrum as bvFTD, and they may also indicate that advanced MRI techniques are potentially suited to detect subtle brain changes in phFTD that may improve diagnosis (section 4).

Methodological considerations

Small sample size

The sample size of the studies presented in this thesis are small. A small sample is inherent to clinical studies investigating relatively rare syndromes, such as phFTD, bvFTD, SD and presenile AD. Rare and particularly controversial diseases (such as phFTD) warrant the application of strict inclusion and exclusion criteria to establish disease-homogenous samples allowing for meaningful between-group comparisons. For example, only 15 cases of phFTD were documented in our large referral centre in a five year period. Additionally, not all patients are willing to participate (e.g. only nine out of fifteen in this study) and importantly, clinical diagnosis may turn out to be incorrect upon follow-up. The latter is especially emphasized by our study on early-stage dementia. Overall, only 51 patients diagnosed with probable AD and/or FTD were included in a 3.5-year period. Due to an early disease stage – and therefore possible uncertain diagnosis - twelve patients received a final diagnosis other than dementia upon follow-up and were excluded from the study. Moreover, six patients received a diagnosis of primary progressive aphasia (PPA) without specification of underlying AD or bvFTD pathology, or SD diagnosis. Of the remaining 39 patients, a confirmed diagnosis was established for eleven AD patients, nine bvFTD patients and eight SD patients (the other five cancelled the appointment or terminated the MRI scan prematurely). Overall, this emphasizes the difficulties with sample size in clinical studies, and especially with clinical diagnostics in a rare and early-stage population.

Effect of small sample size on study results

Small sample size limits statistical power and may thus influence our study results and interpretation. It may introduce false positives or lead to underestimation of group differences. Especially in the case of contradictory or unexpected findings caution with result interpretation is warranted. We have addressed the issue of false positives in our studies by applying corrections for multiple comparisons. In some analyses we were unable to apply such corrections and instead used alternative approaches (e.g. higher cluster size threshold, lower p-value threshold, non-parametrical testing) to minimize the occurrence of false positives. As a result, we may have underestimated the group differences, but we have increased certainty about the differences observed.

Rs-fMRI turned out to be especially vulnerable to a low sample size in our studies. Low sample size allowed for investigating a single resting state network only:

the DMN, and the whole-brain DMN results we observed were only detectable using a relatively lenient threshold. Additionally, between-group differences of functional connectivity remained obscured in quantitative region of interest (ROI) analysis. This is worrisome for neuroscientific studies aiming to identify resting state networks in smaller populations. However, it also indicates that rs-fMRI is likely not a useful technique for clinical diagnostics. This indication may be used to guide future efforts of improving MRI diagnostics, which should rather be focused elsewhere, for example on DTI and ASL. Despite the fact that low sample size likely also had some influence on DTI and ASL findings, we observed both within-group and between-group abnormalities that survived stringent statistical thresholds and that were in accordance with previous literature, suggesting meaningful results and less sensitivity of DTI and ASL to small sample size.

Clinical implications and future directives

We observed differential brain abnormalities in AD and FTD subtypes using DTI, ASL and, to a much lesser extent, rs-fMRI, where conventional MRI techniques commonly fail. This indicates diagnostic utility for advanced MRI techniques in detecting more subtle brain abnormalities that may remain undiscovered using conventional (structural) imaging.

For instance, differential diagnosis of AD and bvFTD can be aided by using tract-specific quantitative DTI to detect widespread WM microstructural abnormalities in bvFTD and only regionally in the hippocampal cingulum in AD. Moreover, differential diagnosis of AD and bvFTD may be aided by combining quantitative measures of WM and GM. Correlating such quantitative measures allows for detection of incipient abnormalities that go undetected in regular group analysis. Additionally, diagnosis of phFTD may be aided by using advanced MRI to detect subtle brain changes in phFTD, similar to bvFTD, that have not been observed previously by using conventional MRI.

It should be noted that the findings observed in our studies are based on group analyses. Consequently, results are potentially not directly applicable to an individual patient level. Our work provides an indication of the utility of advanced MRI techniques in dementia and can aid future research focussing on individual patient assessment.

The use of DTI and ASL may be very beneficial for clinical diagnosis of early-stage presenile dementia as both techniques can produce quantitative measures that

detect subtle brain abnormalities. Conventional (structural) MRI does not detect such subtle changes, but its use may be improved by quantifying GM volumes using advanced post-processing pipelines. On the other hand, the use of rs-fMRI for the purpose of clinical diagnosis is debatable. We did not detect functional DMN connectivity differences between a small sample of AD and bvFTD patients, using a quantitative approach. As clinical use warrants sensitivity of measures at an individual patient level; minor differences in quantitative functional DMN connectivity in a small patient group does not seem to make rs-fMRI suitable for individual diagnostics. In contrast, both ASL and DTI were able to detect group-specific differences in the same small samples.

Our findings are especially indicative for the use of DTI as a diagnostic tool, and hence I will elaborate on this technique specifically. DTI has proven sensitive to detecting brain diffusion changes in patient groups where abnormalities are expected to be subtle. Furthermore, despite being established in small groups, these abnormalities are in line with previous research, suggesting sensitivity of DTI on an individual patient level. Additionally, quantification of DTI findings is possible, allowing for tract-specific measures of WM microstructure abnormalities. Importantly, an even more detailed approach is possible by establishing mean diffusion values per WM tract segment rather than for the whole WM tract. Especially in long tracts, such as the inferior fronto-occipital fasciculus, one mean for the whole tract will obscure regional differences. Such regional differences are likely of reasonable extent in dementia, where for example in bvFTD mainly frontotemporal WM is affected. Importantly, as diffusion models are becoming more advanced using high angular resolution diffusion-weighted imaging (HARDI) approaches, diffusion measures will have improved accuracy, will likely have better sensitivity to microstructural WM changes in neurodegeneration, and may become an even better diagnostic tool in the future.

In order to improve diagnostic utility of DTI, or recent diffusion approaches such as HARDI, it is important to investigate sensitivity and specificity of quantitative WM microstructure in larger samples and establish reference values in a healthy population. Reference values have recently been established for GM volume (Vernooij et al., unpublished data) within the initiative of the Rotterdam Scan Study [27], indicating feasibility for establishing reference values for WM microstructure.

Also of note is the contribution of quantitative DTI to computer-aided-diagnosis (CAD) in dementia. A recent CAD study has shown that fractional anisotropy (FA) values improve computer-aided differentiation between AD and bvFTD (Bron

et al., unpublished data). This is important as CAD will likely become more involved as support tool in future radiological diagnosis.

Conclusion

Advanced MRI techniques identify subtle brain abnormalities in dementia subtypes not otherwise detected using conventional (structural) MR imaging. These subtle brain abnormalities aid to the understanding of brain processes in dementia, and especially DTI and ASL may aid clinical diagnosis and differentiation of the dementia subtypes. Future research should especially focus on quantitative MRI by establishing reference values for MRI measures.

REFERENCES

1 Greicius MD, Geschwind MD, Miller BL. Presenile dementia syndromes: an update on taxonomy and diagnosis. *J Neurol Neurosurg Psychiatry* 2002;72:691–700.http://www.ncbi.nlm.nih.gov/pubmed/12023408

2 Rascovsky K, Hodges JR, Knopman D, *et al.* Sensitivity of revised diagnostic criteria for the behavioural variant of frontotemporal dementia. *Brain* 2011;134:2456–77. doi:10.1093/brain/awr179

3 McKhann GM, Knopman DS, Chertkow H, *et al.* The diagnosis of dementia due to Alzheimer's disease: recommendations from the National Institute on Aging-Alzheimer's Association workgroups on diagnostic guidelines for Alzheimer's disease. *Alzheimers Dement* 2011;7:263–9. doi:10.1016/j.jalz.2011.03.005

4 Gregory CA, Serra-Mestres J, Hodges JR. Early diagnosis of the frontal variant of frontotemporal dementia: how sensitive are standard neuroimaging and neuropsychologic tests? *Neuropsychiatry Neuropsychol Behav Neurol* 1999;12:128–35.http://www.ncbi.nlm.nih.gov/pubmed/10223261

5 Kipps CM, Davies RR, Mitchell J, *et al.* Clinical significance of lobar atrophy in frontotemporal dementia: application of an MRI visual rating scale. *Dement Geriatr Cogn Disord* 2007;23:334–42. doi:10.1159/000100973

6 Rosso SM, Heutink P, Tibben A, *et al.* [New insights in frontotemporal dementia]. *Ned Tijdschr Geneeskd* 2000;144:1575–80.http://www.ncbi.nlm.nih.gov/pubmed/10965365

7 Neary D, Snowden JS, Gustafson L, *et al.* Frontotemporal lobar degeneration: A consensus on clinical diagnostic criteria. *Neurology* 1998;51:1546–54. doi:10.1212/WNL.51.6.1546

8 Karageorgiou E, Miller BL. Frontotemporal lobar degeneration: a clinical approach. *Semin Neurol* 2014;34:189–201. doi:10.1055/s-0034-1381735

9 Bocti C, Rockel C, Roy P, *et al.* Topographical patterns of lobar atrophy in frontotemporal dementia and Alzheimer's disease. *Dement Geriatr Cogn Disord* 2006;21:364–72. doi:10.1159/000091838

10 Dols A, van Liempt S, Gossink F, *et al.* Identifying Specific Clinical Symptoms of Behavioral Variant Frontotemporal Dementia Versus Differential Psychiatric Disorders in Patients Presenting With a Late-Onset Frontal Lobe Syndrome. *J Clin Psychiatry* Published Online First: 5 July 2016. doi:10.4088/JCP.15m09844

11 Hornberger M, Shelley BP, Kipps CM, *et al.* Can progressive and non-progressive behavioural variant frontotemporal dementia be distinguished at presentation? *J Neurol Neurosurg Psychiatry* 2009;80:591–3. doi:10.1136/jnnp.2008.163873

12 Bertoux M, Souza LC De, Corlier F, *et al.* Two Distinct Amnesic Pro fi les in Behavioral Variant. *Biol Psychiatry* 2014;75:582–8. doi:10.1016/j.biopsych.2013.08.017

13 Hornberger M, Piguet O, Kipps C, *et al.* Executive function in progressive and nonprogressive behavioral variant frontotemporal dementia. *Neurology* 2008;71:1481–8. doi:10.1212/01.wnl.0000334299.72023.c8

14 Irish M, Graham A, Graham KS, *et al.* Differential impairment of source memory in progressive versus non-progressive behavioral variant frontotemporal dementia. *Arch Clin Neuropsychol* 2012;27:338–47. doi:10.1093/arclin/acs033

15 Mioshi E, Hodges JR. Rate of change of functional abilities in frontotemporal dementia. *Dement Geriatr Cogn Disord* 2009;28:419–26. doi:10.1159/000255652

16 Davies RR, Kipps CM, Mitchell J, *et al.* Progression in frontotemporal dementia: identifying a benign behavioral variant by magnetic resonance imaging. *Arch Neurol* 2006;63:1627–31. doi:10.1001/archneur.63.11.1627

17 Garcin B, Lillo P, Hornberger M, *et al.* Determinants of survival in behavioral variant frontotemporal dementia. *Neurology* 2009;73:1656–61. doi:10.1212/WNL.0b013e3181c1dee7

18 Bookheimer SY, Strojwas MH, Cohen MS, *et al.* Patterns of brain activation in people at risk for Alzheimer's disease. *N Engl J Med* 2000;343:450–6. doi:10.1056/NEJM200008173430701

19 Gorno-Tempini ML, Hillis a E, Weintraub S, *et al.* Classification of primary progressive aphasia and its variants. *Neurology* 2011;76:1006–14. doi:10.1212/WNL.0b013e31821103e6

20 Dick AS, Bernal B, Tremblay P. The language connectome: new pathways, new concepts. *Neuroscientist* 2014;20:453–67. doi:10.1177/1073858413513502

21 Saur D, Kreher BW, Schnell S, *et al.* Ventral and dorsal pathways for language. *Proc Natl Acad Sci U S A* 2008;105:18035–40. doi:10.1073/pnas.0805234105

22 Von Der Heide RJ, Skipper LM, Klobusicky E, *et al.* Dissecting the uncinate fasciculus: disorders, controversies and a hypothesis. *Brain* 2013;136:1692–707. doi:10.1093/brain/awt094

23 Hornberger M, Geng J, Hodges JR. Convergent grey and white matter evidence of orbitofrontal cortex changes related to disinhibition in behavioural variant frontotemporal dementia. *Brain* 2011;134:2502–12. doi:10.1093/brain/awr173

24 Powers JP, Massimo L, McMillan CT, *et al.* White Matter Disease Contributes to Apathy and Disinhibition in Behavioral Variant Frontotemporal Dementia. *Cogn Behav Neurol* 2014;27:206–14. doi:10.1097/WNN.0000000000000044

25 Pérez-Iglesias R, Tordesillas-Gutiérrez D, McGuire PK, *et al.* White Matter Integrity and Cognitive Impairment in First-Episode Psychosis. *Am J Psychiatry* 2010;167:451–8. doi:10.1176/appi.ajp.2009.09050716

26 Crespi C, Cerami C, Dodich A, *et al.* Microstructural white matter correlates of emotion recognition impairment in Amyotrophic Lateral Sclerosis. *Cortex* 2014;53:1–8. doi:10.1016/j.cortex.2014.01.002

27 Ikram MA, van der Lugt A, Niessen WJ, *et al.* The Rotterdam Scan Study: design update 2016 and main findings. *Eur J Epidemiol* 2015;30:1299–315. doi:10.1007/s10654-015-0105-7

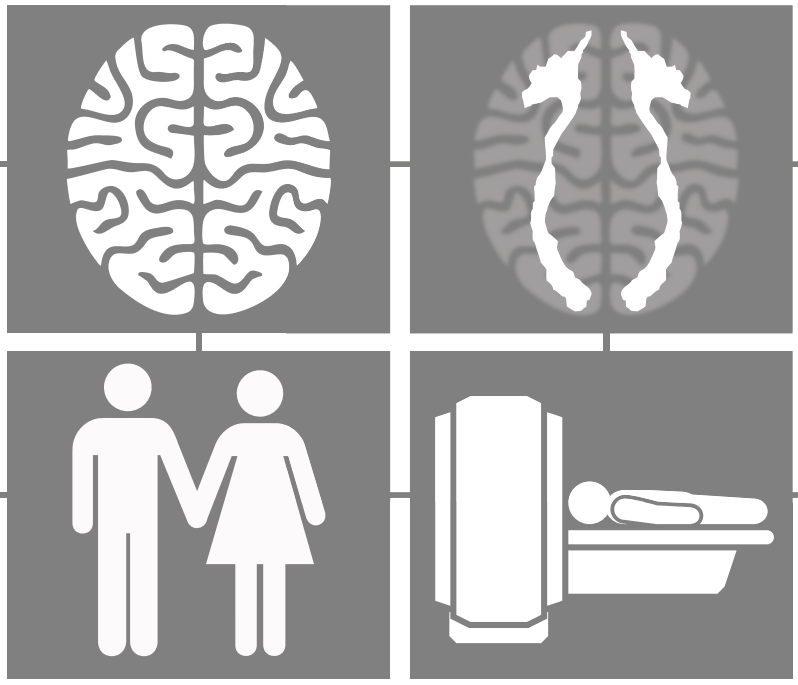

Chapter 6

Summary

Samenvatting

Summary

Presenile dementia (occurring before 65 years of age) [1] is a neurodegenerative disorder affecting white matter (WM) and grey matter (GM) in different regions of the brain. The two most common underlying diseases of presenile dementia are Alzheimer's disease (AD) and frontotemporal dementia (FTD) [2]. FTD is the umbrella term for several types of dementia, such as behavioural variant FTD (bvFTD) and semantic dementia (SD). Additionally, phenocopy frontotemporal dementia (phFTD), a rare syndrome clinically similar to bvFTD, may also belong to this FTD spectrum. In early-stages of these diseases, symptoms may still be mild or unspecific. Consequently, early-stage (differential) diagnosis can be difficult. Magnetic resonance imaging (MRI) of the brain supports diagnosis, but may still appear normal or show unspecific brain abnormalities in early stages of dementia [3–5]. More advanced MRI techniques, such as diffusion tensor imaging (DTI), resting state functional MRI (rs-fMRI) and arterial spin labelling (ASL) may aid differential diagnosis by detecting subtle abnormalities that remain unrevealed using conventional (structural) MRI [6]. Also, we can quantify advanced MRI, which allows for comparing patients to reference values of the healthy population, and allows for combining WM and GM measures to investigate relations between subtle WM and GM changes in dementia.

The first and second technique, DTI and rs-fMRI, can be used to assess brain connectivity, in terms of respectively WM microstructure (e.g. fractional anisotropy, mean diffusivity) and functional connectivity of resting state networks (e.g. default mode network (DMN)). The third technique, ASL, can be used to assess GM perfusion of the whole-brain or in regions of interest. Additionally, by applying advanced post-processing tools to conventional (structural) MRI we may be able identify smaller GM volume changes and combine these with the advanced MRI measures as mentioned above.

In this thesis I investigate the use of these techniques in identifying subtle brain abnormalities, associating brain abnormalities with disease symptomatology, and improving early (differential) diagnosis in several diseases underlying presenile dementia.

Section 2 describes subtle brain abnormalities in early-stage AD and bvFTD using advanced MRI. In **chapter 2.1**, we investigated quantitative measures of tract-specific WM microstructure and functional DMN connectivity to explore clinical applicability for early-stage and long-term differential diagnosis of AD and bvFTD. We observed that functional connectivity of the DMN was not different between groups neither at baseline nor at follow-up. Diffusion abnormalities were ob-

served widely in bvFTD, and regionally in the hippocampal cingulum in AD. The extent of the differences between bvFTD and AD were diminished at follow-up yet abnormalities were still more pronounced in bvFTD, specifically in the cingulate cingulum and inferior fronto-occipital fasciculus. The rate of change was very similar in bvFTD and AD. We concluded that quantitative tract-specific microstructural WM abnormalities, but not quantitative functional connectivity of the DMN, may aid early-stage and long-term differential diagnosis of bvFTD and AD. Specifically, pronounced microstructural WM changes in anterior WM tracts characterise bvFTD, whereas microstructural WM abnormalities of the hippocampal cingulum characterise AD.

In **chapter 2.2** we extended these findings by exploring a combination of quantitative tract-specific WM measures and regional GM volumes and perfusion values. We investigated regional coherence between these measures in AD and bvFTD using a correlational approach. WM-GM coherence, compared with controls, was stronger between cingulum WM and frontotemporal GM in AD, and temporoparietal GM in bvFTD. In addition, in AD compared with controls, coherence was stronger between inferior fronto-occipital fasciculus WM microstructure and occipital GM perfusion. We concluded that WM and GM changes show strong coherence between regions implicated in later stages of AD and bvFTD pathology, which indicates concurrent WM and GM degeneration in disease-specific networks. Additionally, our methodology allowed for the detection of incipient abnormalities that go undetected in conventional between-group analyses.

Section 3 explores subtle brain changes in dementia in relation to early-stage dementia symptomatology. In **chapter 3.1** we investigated associations between cognition and WM microstructure in early-stage AD and bvFTD, to assess whether different WM tracts play a role in early-stage symptomatology of AD and bvFTD. WM microstructure has previously been associated with abnormal as well as normal cognitive functioning. As bvFTD and AD both show abnormalities of WM microstructure, it can be postulated that specific symptomatology in bvFTD and AD is related to specific abnormalities of WM microstructure. This is especially of interest in early-stage bvFTD and AD, when symptoms may still be mild or unspecific, and microstructural WM abnormalities are already present. We observed that attention and executive deficits were associated with WM microstructure of several WM tracts in bvFTD, and to a lesser extent in AD. Language deficits were associated with WM microstructure abnormality in AD, and to a lesser extent, normal language functioning was associated with WM microstructure in bvFTD. Additionally, normal memory functioning in bvFTD, as well as normal visuocon-

structive functioning in AD was associated with WM microstructure abnormality. Interestingly, evident memory deficits were not associated with any WM tract abnormalities in AD. We concluded that there is an association between cognitive functioning and WM microstructure of specific WM tracts in early-stage AD and bvFTD patients. This suggests that specific WM tracts play an important role in cognitive functioning, and are not universally involved in all cognitive domains in early-stage AD and bvFTD.

In **chapter 3.2** we explored whether changes in brain connectivity are reflective of differential symptomatology in SD and bvFTD. Language deficits in SD are associated with left anterior temporal lobe atrophy [7–9], and behavioural deficits in bvFTD are associated with right or bilateral frontal lobe atrophy [7,8,10]. We investigated whether WM microstructure and functional connectivity were also differentially lateralized in SD and bvFTD. Microstructural WM abnormalities were more pronounced in and lateralized towards the left hemisphere in SD in WM tracts associated with semantic processing. In bvFTD microstructural WM abnormalities were more pronounced in the right hemisphere, but were less lateralized than in SD. They were most pronounced in WM tracts associated with behavioural symptoms. Functional connectivity of disease-specific regions (ATL and orbitofrontal cortex (OFC)) was mainly decreased with both hemispheres in SD, and with the right hemisphere in bvFTD. Here symptomatology associations were less straightforward, but generally functional connectivity was observed in GM regions associated with language and behaviour in SD and bvFTD respectively. We concluded that SD and bvFTD show a hemispheric dissociation of brain connectivity in the frontotemporal regions, which underlies their differential symptomatology.

Section 4 continues the discussion on the FTD spectrum of diseases by describing brain abnormalities in phFTD and discussing its relation with bvFTD. PhFTD is a syndrome of much debate, as it shares core characteristics with bvFTD yet without associated cognitive deficits or brain abnormalities on conventional MRI, and without progression. We hypothesised that phFTD belongs to the same disease spectrum as bvFTD and investigated brain abnormalities in phFTD compared to bvFTD using sensitive MR imaging techniques.

In **chapter 4.1** we assessed WM microstructure and functional connectivity of the DMN. We observed that phFTD showed subtle microstructural changes in frontal WM tracts, and subtle increased DMN connectivity. BvFTD showed abnormalities in similar regions as phFTD, but had more extensive microstructural WM changes, and less increased DMN connectivity. In **chapter 4.2** we assessed

regional GM volumes and perfusion. We observed cortical atrophy in the right temporal lobe in phFTD. Additionally, frontotemporal GM volumes were not different from either controls or bvFTD patients, and showed a continuum ranging from the normal to abnormal in bvFTD, with phFTD in between. Perfusion changes were observed in the sense of hyperperfusion in the left frontal lobe. Taken together, findings of **chapters 4.1 and 4.2** are in support of the hypothesis that phFTD and bvFTD may belong to the same disease spectrum and may also indicate that advanced MRI techniques are potentially suited to detect subtle brain changes in phFTD that may improve diagnosis.

We extended these findings by qualitatively describing a subset of phFTD patients at 3-year follow-up in **chapter 4.3.** These patients were qualitatively compared with their baseline measures, and with bvFTD patients and controls. Qualitative comparison was performed for measures of cognition, GM volume, perfusion and WM microstructure. We observed a relatively stable clinical profile. Qualitative comparison showed some progression of language and memory deficits and a stable pattern of structural brain abnormalities, with cognitive scores and structural values generally in between normal and those in bvFTD, and functional changes in the sense of increased perfusion.

We concluded that these findings are still in support of the notion that phFTD and bvFTD may belong to the same disease spectrum. These findings may be used as motivation and a basis for further longitudinal studies in phFTD, specifically exploring the structural versus functional brain changes.

In section 5, I provide an overview of the main findings of this thesis and discuss the methodological considerations, clinical implications and future perspectives. In conclusion, advanced MRI techniques identify subtle brain abnormalities in dementia subtypes not otherwise detected using conventional (structural) MR imaging. These subtle brain abnormalities aid to the understanding of brain processes in dementia, and especially DTI and ASL may aid clinical diagnosis and differentiation of the dementia subtypes. Future research should especially focus on quantitative MRI by establishing reference values for MRI measures.

REFERENCES

1 World Health Organization. Dementia: A public health priority. 2012.

2 Greicius MD, Geschwind MD, Miller BL. Presenile dementia syndromes: an update on taxonomy and diagnosis. *J Neurol Neurosurg Psychiatry* 2002;72:691–700.http://www.ncbi.nlm.nih.gov/pubmed/12023408

3 Gregory CA, Serra-Mestres J, Hodges JR. Early diagnosis of the frontal variant of frontotemporal dementia: how sensitive are standard neuroimaging and neuropsychologic tests? *Neuropsychiatry Neuropsychol Behav Neurol* 1999;12:128–35.http://www.ncbi.nlm.nih.gov/pubmed/10223261

4 Kipps CM, Davies RR, Mitchell J, *et al.* Clinical significance of lobar atrophy in frontotemporal dementia: application of an MRI visual rating scale. *Dement Geriatr Cogn Disord* 2007;23:334–42. doi:10.1159/000100973

5 Rosso SM, Heutink P, Tibben A, *et al.* [New insights in frontotemporal dementia]. *Ned Tijdschr Geneeskd* 2000;144:1575–80.http://www.ncbi.nlm.nih.gov/pubmed/10965365

6 Sperling RA, Aisen PS, Beckett LA, *et al.* Toward defining the preclinical stages of Alzheimer's disease: Recommendations from the National Institute on Aging-Alzheimer's Association workgroups on diagnostic guidelines for Alzheimer's disease. *Alzheimer's Dement* 2011;7:280–92. doi:10.1016/j.jalz.2011.03.003

7 Karageorgiou E, Miller BL. Frontotemporal lobar degeneration: a clinical approach. *Semin Neurol* 2014;34:189–201. doi:10.1055/s-0034-1381735

8 Bocti C, Rockel C, Roy P, *et al.* Topographical patterns of lobar atrophy in frontotemporal dementia and Alzheimer's disease. *Dement Geriatr Cogn Disord* 2006;21:364–72. doi:10.1159/000091838

9 Gorno-Tempini ML, Hillis a E, Weintraub S, *et al.* Classification of primary progressive aphasia and its variants. *Neurology* 2011;76:1006–14. doi:10.1212/WNL.0b013e31821103e6

10 Rascovsky K, Hodges JR, Knopman D, *et al.* Sensitivity of revised diagnostic criteria for the behavioural variant of frontotemporal dementia. *Brain* 2011;134:2456–77. doi:10.1093/brain/awr179

Samenvatting

Preseniele dementie (d.w.z. dementie optredend voor het 65 jarige levensjaar) [1] is een neurodegeneratieve ziekte die de witte en grijze stof aantast in verschillende hersengebieden. De twee meest voorkomende onderliggende aandoeningen van preseniele dementie zijn de ziekte van Alzheimer (AD) en frontotemporale dementie (FTD) [2]. FTD is de overkoepelende term voor verschillende vormen van dementie, zoals de gedragsvariant van FTD (bvFTD) en semantische dementie (SD). Daarnaast is er een zeldzaam syndroom dat klinisch vergelijkbaar is met bvFTD, de zogenaamde phenocopy frontotemporale dementie (phFTD), dat mogelijk ook tot dit FTD spectrum behoort. In het vroege stadium van deze aandoeningen kunnen symptomen nog mild of aspecifiek zijn. Als gevolg hiervan kan het moeilijk zijn om de juiste diagnose te stellen. Beeldvorming met magnetic resonance imaging (MRI) draagt bij aan het stellen van de diagnose. In het vroege stadium van dementie kan de MRI scan echter nog normaal zijn of enkel aspecifieke hersenafwijkingen laten zien, waardoor ook deze niet altijd helpt bij het stellen van de diagnose [3-5].Meer geavanceerde MRI technieken, zoals diffusion tensor imaging (DTI), resting state functionele MRI (rs-fMRI) en arterial spin labelling (ASL) kunnen mogelijk bijdragen aan het stellen van een differentiaal diagnose door het detecteren van subtiele veranderingen in de hersenen die niet zichtbaar zijn op conventionele (structurele) MRI [6]. Daarnaast kunnen we geavanceerde MRI technieken kwantificeren waardoor we patiënten kunnen vergelijken met referentie waarden uit de gezonde populatie. Ook kunnen we maten voor witte en grijze stof combineren, zodat het mogelijk wordt om relaties tussen subtiele veranderingen in de witte en grijze stof bij dementie te bestuderen.

De eerste en tweede techniek, DTI en rs-fMRI, kunnen worden gebruikt om de connectiviteit van de hersenen te onderzoeken. Met DTI maten kunnen we de microstructuur van de witte stof in kaart brengen en met rs-fMRI kunnen we de functionele connectiviteit van resting state netwerken onderzoeken (bv. default mode network (DMN)). De derde techniek, ASL, kan worden gebruikt om doorbloeding van de grijze stof te meten, zowel in het hele brein als in specifieke gebieden. Daarnaast is het mogelijk om veranderingen in het volume van de grijze stof te identificeren, door geavanceerde post-processing software toe te passen op conventionele (structurele) MRI beelden. Deze software kan dan gecombineerd worden met de geavanceerde MRI maten die hierboven genoemd werden.

In dit proefschrift onderzoek ik de toepassing van deze technieken voor het detecteren van subtiele veranderingen in de hersenen, het associëren van hersen-

veranderingen met ziekte symptomatologie, en het verbeteren van vroeg (differentiaal) diagnostiek van de verschillende aandoeningen die onderliggend zijn aan preseniele dementie.

Deel 2 beschrijft het detecteren van subtiele hersenveranderingen in het vroege stadium van AD en bvFTD door gebruik te maken van geavanceerde MRI. In **hoofdstuk 2.1** hebben we gekeken naar de microstructuur van specifieke witte stof banen en functionele connectiviteit van het DMN. Dit hebben we gedaan om klinische toepasbaarheid te onderzoeken voor de differentiële diagnose tussen AD en bvFTD in zowel een vroeg stadium als op de langere termijn. We vonden dat functionele connectiviteit van het DMN niet verschillend was tussen groepen bij de eerste meting en ook niet bij de vervolg meting. Veranderingen in de microstructuur, gemeten met DTI, werden wijdverspreid geobserveerd bij bvFTD, en enkel regionaal in de hippocampale cingulum in AD. De verschillen tussen bvFTD en AD waren kleiner bij de vervolgmeting, alhoewel de afwijkingen nog steeds nadrukkelijker aanwezig waren in bvFTD, met name in de cingulate cingulum en de inferieure fronto-occipitale fasciculus. De mate van verandering over tijd was vergelijkbaar in bvFTD en AD. We concludeerden dat kwantitatieve microstructurele veranderingen in specifieke witte stof banen, maar niet de kwantitatieve functionele connectiviteit van het DMN, kunnen helpen bij de differentiële diagnostiek tussen bvFTD en AD in een vroeg stadium en op de langere termijn. In het bijzonder zijn uitgesproken microstructurele veranderingen in de anterieure witte stof banen karakteristiek voor bvFTD, terwijl microstructurele veranderingen van het hippocampale cingulum karakteristiek zijn voor AD.

In **hoofdstuk 2.2** hebben we deze bevindingen verder uitgebreid door kwantitatieve microstructurele maten voor specifieke witte stof banen te combineren met regionale metingen van volume en doorbloeding in de grijze stof. We onderzochten de samenhang tussen deze maten in zowel AD als bvFTD door middel van een correlationele methode. De samenhang tussen de witte en grijze stof, in vergelijking met controles, was sterker tussen de witte stof microstructuur van het cingulum en de frontotemporale grijze stof in AD, en de temporopariëtale grijze stof in bvFTD. Daarnaast was bij AD, in vergelijking met controles, de samenhang sterker tussen de microstructuur van de inferieure fronto-occipitale fasciculus en de doorbloeding in de grijze stof in de occipitaalkwab. We concludeerden dat veranderingen in de witte en grijze stof een sterke samenhang laten zien tussen regio's die betrokken zijn in de ontwikkeling van pathologie zoals we die kennen in de latere stadia van AD en bvFTD. Dit wijst op een gelijktijdige degeneratie van de witte en grijze stof in ziekte-specifieke netwerken. Bovendien kunnen we met

onze correlationele methodologie beginnende afwijkingen detecteren die met conventionele groepsvergelijkingen onopgemerkt blijven.

Deel 3 onderzoekt subtiele hersenveranderingen in relatie tot de symptomatologie in het vroege stadium van dementie. In **hoofdstuk 3.1** hebben we onderzocht of er associaties zijn tussen cognitie en de microstructuur van de witte stof in het vroege stadium van AD en bvFTD. Hierdoor konden we bekijken of meerdere witte stof banen een rol spelen in de symptomatologie in het vroege stadium van AD en bvFTD. Eerder onderzoek heeft aangetoond dat de microstructuur van de witte stof geassocieerd is met abnormaal en normaal cognitief functioneren. Aangezien zowel bvFTD als AD afwijkingen laten zien in de microstructuur van de witte stof, kan worden aangenomen dat specifieke symptomatologie van bvFTD en AD gerelateerd is aan specifieke afwijkingen van de microstructuur van de witte stof. Dit is met name interessant in het vroege stadium van bvFTD en AD, wanneer symptomen nog mild en aspecifiek kunnen zijn, en afwijkingen in de microstuur van de witte stof wel al aanwezig zijn. We vonden dat stoornissen in de aandacht en executieve functies geassocieerd waren met de microstructuur van de witte stof in verschillende witte stof banen bij bvFTD, en in mindere mate bij AD. Taal afwijkingen waren geassocieerd met afwijkingen in microstructuur van de witte stof bij AD, en in mindere mate was normaal taal functioneren geassocieerd met microstructuur van de witte stof bij bvFTD. Daarnaast was normaal functioneren van het geheugen bij bvFTD, en normaal functioneren van de visuoconstructieve functies bij AD, geassocieerd met afwijkingen in de microstructuur van de witte stof. Interessant is dat evidente geheugen stoornissen niet geassocieerd waren met afwijkingen van de microstructuur van de witte stof bij AD. We concludeerden dat er een associatie is tussen cognitief functioneren en microstructuur van specifieke witte stof banen in het vroege stadium van AD en bvFTD. Dit suggereert dat specifieke witte stof banen een belangrijke rol spelen in het cognitief functioneren, en dat niet alle witte stof banen universeel betrokken zijn bij de cognitieve domeinen die in het vroege stadium van AD en bvFTD zijn aangedaan.

In **hoofdstuk 3.2** hebben we onderzocht of veranderingen in de hersenconnectiviteit de bestaande verschillen in symptomatologie tussen SD en bvFTD reflecteren. Taal afwijkingen bij SD zijn geassocieerd met grijze stof atrofie van de linker anterieure temporaalkwab [7-9], en gedragsafwijkingen bij bvFTD zijn geassocieerd met atrofie van de rechter of bilaterale frontaalkwab [7,8,10]. We onderzochten of microstructuur van de witte stof en functionele connectiviteit van specifieke regio's ook verschillend gelateraliseerd zijn bij SD en bvFTD. Mi-

crostructurele witte stof afwijkingen waren meer uitgesproken in, en gelateraliseerd naar, de linker hemisfeer bij SD. Dit was het geval voor witte stof banen die geassocieerd zijn met de semantische verwerking van taal. Bij bvFTD waren de microstructurele afwijkingen in de witte stof meer uitgesproken in de rechter hemisfeer, maar minder gelateraliseerd dan bij SD. Ze waren het meest uitgesproken in de witte stof banen die geassocieerd zijn met gedragssymptomen. Functionele connectiviteit van ziekte-specifeke regio's (anterieure temporaal kwab en orbitofrontale cortex) was met name verminderd met beide hemisferen bij SD, en met de rechter hemisfeer bij bvFTD. Hier waren de symptomatologische associaties minder vanzelfsprekend, maar over het algemeen werd functionele connectiviteit geobserveerd in grijze stof gebieden die zijn geassocieerd met taal respectievelijk gedrag bij SD en bvFTD. We concludeerden dat er sprake is van een hemisferische dissociatie van hersenconnectiviteit in de frontotemporale regio's tussen SD en bvFTD, wat onderliggend is aan hun verschillende symptomatologie.

Deel 4 zet de discussie over het FTD spectrum van aandoeningen voort door het beschrijven van hersenafwijkingen in phFTD en het exploreren van de relatie tussen phFTD en bvFTD. Het syndroom phFTD is onderwerp van veel debat aangezien phFTD kern eigenschappen van bvFTD laat zien zonder de bijkomende cognitieve afwijkingen of hersenafwijkingen zoals zichtbaar op conventionele MRI, en zonder dat er achteruitgang optreedt. We hypothetiseerden dat phFTD tot hetzelfde ziekte spectrum als bvFTD behoort en we onderzochten hersenafwijkingen bij phFTD in vergelijking met bvFTD, door middel van geavanceerde MR beeldvorming.

In **hoofdstuk 4.1** hebben we gekeken naar de microstructuur van de witte stof en de functionele connectiviteit van het DMN. We observeerden dat phFTD subtiele microstructurele veranderingen in de frontale witte stof banen en subtiele verhoogde DMN connectiviteit liet zien. BvFTD liet afwijkingen in vergelijkbare regio's zien als phFTD, maar had uitgebreidere microstructurele veranderingen van de witte stof, en een minder sterke verhoging van DMN connectiviteit. In **hoofdstuk 4.2** hebben we regionale grijze stof volumes en regionale grijze stof doorbloeding onderzocht. We observeerden corticale atrofie in de rechter temporaal kwab in phFTD. Daarnaast vonden we dat frontotemporale grijze stof volumes niet verschillend waren van zowel controles als bvFTD, en dat er sprake was van een continuüm variërend van normaal tot afwijkend in bvFTD, met phFTD ertussen in. Veranderingen in de doorbloeding werden geobserveerd in de vorm van verhoogde doorbloeding in de linker frontaalkwab. Samengenomen waren de bevindingen van **hoofdstuk 4.1** en **hoofdstuk 4.2** ondersteunend voor de hy-

pothese dat phFTD en bvFTD mogelijk tot hetzelfde ziekte spectrum behoren. Daarnaast wijzen ze er op dat geavanceerde MRI technieken potentieel geschikt zijn voor het detecteren van subtiele hersenafwijkingen in phFTD en die daarmee het stellen van een diagnose mogelijk kunnen verbeteren.

We breiden deze bevindingen in **hoofdstuk 4.3** uit door middel van het kwalitatief beschrijven van een subgroep van phFTD patiënten die drie jaar na de eerste meting nogmaals onderzocht zijn. Deze patiënten hebben we kwalitatief vergeleken met hun eerste meting, en met zowel bvFTD patiënten als controles. Deze kwalitatieve vergelijking werd uitgevoerd voor cognitieve maten, grijze stof volumes en doorbloeding waarden, en de microstructuur van de witte stof. We observeerden een relatief stabiel klinisch profiel, zoals past bij phFTD. De kwalitatieve vergelijking liet enige achteruitgang van taal en geheugen zien en daarnaast een stabiel patroon van structurele hersenafwijkingen. Over het algemeen waren de cognitieve scores en de structurele waarden voor phFTD tussen normaal en bvFTD in, en waren er functionele veranderingen bij phFTD in de vorm van verhoogde doorbloeding. We concludeerden dat deze bevindingen nog steeds ondersteunend zijn voor het idee dat phFTD en bvFTD mogelijk tot hetzelfde ziektespectrum behoren. Deze bevindingen kunnen mogelijk gebruikt worden als motivatie en basis voor verdere longitudinale studies van phFTD, in het bijzonder voor het exploreren van structurele versus functionele hersenveranderingen.

In **deel 5** geef ik een overzicht van de belangrijkste bevindingen van dit proefschrift en bediscussieer ik de methodologische overwegingen, klinische implicaties en toekomst perspectieven. Concluderend identificeren geavanceerde MRI technieken subtiele hersenafwijkingen bij verschillende aandoeningen onderliggend aan dementie die niet zichtbaar zijn met conventionele (structurele) MR beeldvorming. Deze subtiele hersenafwijkingen dragen bij aan het begrip van de hersenprocessen bij dementie, en daarnaast kunnen met name DTI en ASL mogelijk bijdragen aan de klinische diagnose en differentiatie van de verschillende aandoeningen die aan dementie ten grondslag liggen. Toekomstig onderzoek zal zich vooral moeten richten op kwantitatieve MRI door het vaststellen van referentie waarden voor MRI maten.

REFERENTIES

1 World Health Organization. Dementia: A public health priority. 2012.

2 Greicius MD, Geschwind MD, Miller BL. Presenile dementia syndromes: an update on taxonomy and diagnosis. J Neurol Neurosurg Psychiatry 2002;72:691–700.http://www.ncbi.nlm.nih.gov/pubmed/12023408

3 Gregory CA, Serra-Mestres J, Hodges JR. Early diagnosis of the frontal variant of frontotemporal dementia: how sensitive are standard neuroimaging and neuropsychologic tests? Neuropsychiatry Neuropsychol Behav Neurol 1999;12:128–35.http://www.ncbi.nlm.nih.gov/pubmed/10223261

4 Kipps CM, Davies RR, Mitchell J, et al. Clinical significance of lobar atrophy in frontotemporal dementia: application of an MRI visual rating scale. Dement Geriatr Cogn Disord 2007;23:334–42. doi:10.1159/000100973

5 Rosso SM, Heutink P, Tibben A, et al. [New insights in frontotemporal dementia]. Ned Tijdschr Geneeskd 2000;144:1575–80.http://www.ncbi.nlm.nih.gov/pubmed/10965365

6 Sperling RA, Aisen PS, Beckett LA, et al. Toward defining the preclinical stages of Alzheimer's disease: Recommendations from the National Institute on Aging-Alzheimer's Association workgroups on diagnostic guidelines for Alzheimer's disease. Alzheimer's Dement 2011;7:280–92. doi:10.1016/j.jalz.2011.03.003

7 Karageorgiou E, Miller BL. Frontotemporal lobar degeneration: a clinical approach. Semin Neurol 2014;34:189–201. doi:10.1055/s-0034-1381735

8 Bocti C, Rockel C, Roy P, et al. Topographical patterns of lobar atrophy in frontotemporal dementia and Alzheimer's disease. Dement Geriatr Cogn Disord 2006;21:364–72. doi:10.1159/000091838

9 Gorno-Tempini ML, Hillis a E, Weintraub S, et al. Classification of primary progressive aphasia and its variants. Neurology 2011;76:1006–14. doi:10.1212/WNL.0b013e31821103e6

10 Rascovsky K, Hodges JR, Knopman D, et al. Sensitivity of revised diagnostic criteria for the behavioural variant of frontotemporal dementia. Brain 2011;134:2456–77. doi:10.1093/brain/awr179

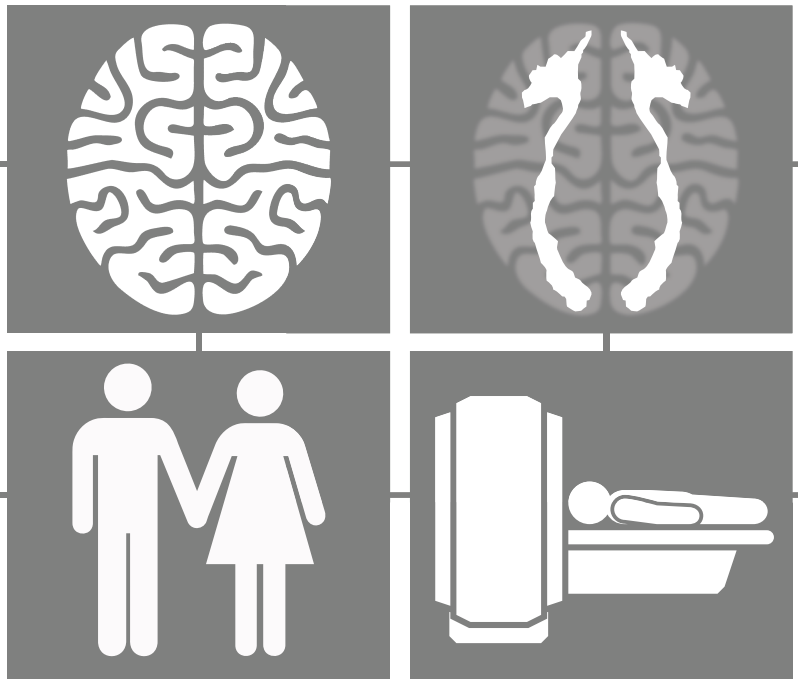

Chapter 7

Dankwoord

List of publications

Funding

PhD portfolio

About the author

Dankwoord

Na vier jaar hard werken, maar zeker niet zonder veel plezier, mag ik met gepaste trots mijn proefschrift klaar noemen. In de afgelopen vier jaar zijn er veel mensen geweest die mij op wat voor manier dan ook hebben bijgestaan, hebben geïnspireerd, me hebben laten lachen, me moed hebben ingepraat en van wie ik veel heb geleerd. Graag wil ik hen allen danken.

Ik wil alle patiënten bedanken voor hun deelname aan de Iris en Iris+ studies. Zij ondergingen meerdere MRI scans, neuropsychologische testen en in geval van de Iris+ studie ook nog psychiatrische onderzoeken. Dit is erg belastend voor patiënten. Vaak gaven ze mij als reden om mee te doen dat zij hoopten dat toekomstige patiënten gebaat zouden zijn bij de onderzoeksresultaten. Ik vind het ontzettend mooi en knap dat mensen die zo ziek zijn, zo onzelfzuchtig kunnen zijn. Ik wil ook alle gezonde deelnemers bedanken die met veel plezier meededen aan de Iris en Iris+ studies, en waar ook zij niets voor terug kregen behalve een mooi plaatje van hun hersenen. Zonder jullie zou ons onderzoek niet gelukt zijn! In het bijzonder wil ik noemen Mart, Kok, Jacques en Jan. Mijn dank!

Graag bedank ik mijn promotoren prof. dr. Aad van der Lugt en prof. dr. John van Swieten. Beste Aad, ik vond het heel fijn dat je altijd betrokken bent geweest bij de grote beslissingen in mijn promotietraject. Ik wil je extra bedanken voor je ondersteuning en inzicht bij het correlatie paper dat tot veel complexe discussies heeft geleid, maar waar we allen uiteindelijk heel blij mee zijn. Daarnaast heb je me in mijn afrondingsfase bijna dagelijks bijgestaan en me geholpen knopen door te hakken. Ik wil je ontzettend bedanken dat je me de kans hebt gegeven om in hele korte tijd een case series op papier te zetten. Beste John, zonder de hulp van jou en het Alzheimercentrum hadden we nooit patiënten kunnen includeren voor onze studies. Ik wil je bedanken voor het meedenken tijdens de MCO's over welke patiënten we wel of niet konden includeren, het benaderen van patiënten wanneer we daarom vroegen, en je neurologische en kritische blik op mijn papers.

Beste copromotor dr. Marion Smits, lieve Marion, ik ben ontzettend blij dat je me na mijn onderzoeksstage de kans hebt gegeven om te blijven en mijn promotietraject te starten. Ik heb zo ontzettend veel van je geleerd de afgelopen jaren, niet alleen inhoudelijk op gebied van neuroimaging maar ook als wetenschappelijk onderzoeker in het algemeen. Je hebt altijd laten zien dat je vertrouwen in mij en mijn werk had. Alles was altijd bespreekbaar en mogelijk. Ik kon voor elk onderwerp bij je terecht, of dit nou persoonlijk of werk-gerelateerd was, je hebt me altijd gesteund. En nog steeds zet je je voor me in door me te helpen bij mijn

tijdelijke baan in het Erasmus MC en mijn mogelijke toekomstige post-doc buiten ons ziekenhuis. Ik prijs mezelf gelukkig dat ik in jouw onderzoeksgroep opgeleid ben tot onderzoeker. Ik had me geen betere mentor kunnen wensen.

Graag bedank ik de leden van mijn promotiecommissie voor het willen plaatsnemen in mijn commissie. Prof. dr. C. van Duijn en prof. dr. F. Barkhof, bedankt dat jullie mijn proefschrift kritisch hebben doorgenomen en besloten hebben dat het waardig is voor verdediging. Beste dr. Vernooij, beste Meike, graag bedank ik jou voor hetzelfde, en ook voor ons werkcontact. Dear professor Waldman, dear Adam, it is an honour that you are willing to travel to The Netherlands to be part of my committee. Thank you very much! Beste prof. Niessen, beste Wiro, ik vind het ontzettend fijn dat jij de samenwerking tussen onze onderzoeksgroepen representeert in mijn commissie. Hartelijk dank! Beste dr. Papma, beste Janne, we hebben over de jaren heen niet alleen samengewerkt maar elkaar ook op persoonlijk vlak beter leren kennen. Ik vind het een eer dat ik met jou de inhoud van mijn proefschrift mag bespreken.

My dear paranimfen, I am incredibly happy you are standing beside me. It would not be the same without the Radiology girls rebels Beatles monsters ;). Rebecca, lieve Stekkie, vorig jaar naast jou, dit jaar naast mij. Precies zoals wij veel werk hebben verzet: zij aan zij voor Iris en Iris+. Ik vind het zo fijn dat we zowel super collega's als hele goede vriendinnen zijn. Soms is een blik, houding of woord al voldoende ;). Dingen die me nog regelmatig laten glimlachen: Disco Inferno, Grumpy Cat meets Immortal in Vienna, jouw bijzondere geluiden repertoire, de gesloten toren, Venetië in 1 uur, FMI! en sinds kort ook Dr. Sterrenthee ;). Ik hoop op nog veel meer glimlach herinneringen :). Carolina, my dear Mendezzie, it means the world to me that you are willing to fly all the way from Chile to Holland for my defence. You are my favourite cookie monster. I loved being your office mate for all these years, even when you ate my food, or hid my chewing gum and left me to find an empty box with a note saying 'I love you Blondie'. I loved being friends while you were still living in Holland, and I love that I still have you as my friend even though you live miles away.

Dear prof. Wardlaw, dear Joanna, thank you for providing me with the opportunity to work in and learn from your research group at the Brain Research Imaging Centre in Edinburgh. Dr. Muñoz Maniega, dear Susana, I very much enjoyed working with you during my visit. I am happy we are continuing our collaboration and extending our work. I also want to thank dr. Mark Bastin, dr. Dominic Job, and

Moira Henderson, for their help and making me feel welcome. Caroline, het was fijn om Belgische/Nederlandse onderonsjes te hebben :).

Zonder mijn kamergenoten met wie ik kan lachen, sparren, kletsen, werken, en alles mee kan delen, zou mijn PhD een stuk minder bijzonder zijn geweest. Anouk, over de jaren heen ben je een hele goede vriendin van mij geworden. Bedankt voor al je hulp, je support, lieve woorden, gezellige etentjes, momenten met Bram, en je vriendschap die mij erg dierbaar is. Ik vind het heel bijzonder dat ik naast jou mag staan bij jouw verdediging. Taihra, ik ben zeer onder de indruk van jouw sterke kanten, en waardeer jouw vertrouwen in mij ontzettend. Renske, bedankt dat we altijd van alles kunnen delen over onze interesses, met name muziek :). Ik vond het super om met jou naar Scumbag te gaan! En ook de zelfverdedigingscursus was ontzettend leuk! Rinske, ons paper was alles behalve mindful ;), maar je hebt er iets prachtigs van gemaakt! Ik vond het leuk om nauw met je samen te werken en ben altijd erg blij met jouw humor en gezelschap. Anouk, Taihra, Renske, Rinske, Rebecca en Carolina, room 13, simply the best!

Mijn collega's van de radiologie en nucleaire geneeskunde. Sjel, dank voor alle leuke avonden uit, je gezelschap tijdens het He/Hs tijdperk, en je spelleider expertise ;). Daniel, ex-kantoorgenoot en mede muziekliefhebber, bedankt voor je gevoel voor humor en alle gezellige avonden in Paddy's. Ghassan, thank you for all the fun(ny) moments and open conversations! Ton, ontzettend bedankt voor de opmaak van mijn proefschrift. Mart, heel erg bedankt voor al je computer gerelateerde ondersteuning. En alle andere fijne collega's van de radiologie en nucleaire geneeskunde: Jolanda, Annelise, Joost, Laurens, Maartje, Jasper, Rianne, Hanneke, Piotr, Hazel, Anika, Soeraida, Nora, en Marjolein; en van De Nieuwe Kans: Reshmi en Josjan; allen ontzettend bedankt voor jullie gezelligheid en fijne samenwerking over de jaren heen.

Dear colleagues of the BIGR, I am glad Radiology moved to the 25th floor so we all had the chance to meet :)! Pierre, you funny Frenchman :), you make every pub session fun! I don't think I'll ever forget that FFF pubsession and subsequent bikeride home, resulting in the invention of Balisto Tortue ;). Marius, bedankt voor alle gesprekken en afspraken over DTI :). Carolyn, Pierre, Gennady, Esther, Ruben, Valerio, Jean-Marie, Hua, Esben, thank you all for your company at PhD dinners and the research drinks, random chats in the hallway, fun whatsapp group-conversations, pub sessions, and movie nights at work. Ook dank aan de borrelcommissie, het was heel leuk om de afdelingsborrel met jullie te organiseren: Hakim, Marcel, Ewoud, Matthias en Renske, bedankt!

Mijn Neuro collega's :)! Janne, Sophie, Lieke, Lize, Elise, Jessica, Tsz, Jeroen, Leonie, Esther, Sanne, Djoeke en Sanne, bedankt voor de jaren samenwerking en jullie gezelligheid. Ik ben zeer onder de indruk van jullie inzet voor het dementie onderzoek! Frank Jan, jij in het bijzonder bedankt voor je hulp met inclusie van patiënten voor de Iris en Iris+ studie. Ans, bedankt voor je hulp bij het inplannen en zoeken van NPO's.

Tonya, bedankt dat ik met je mocht sparren over mijn toekomst en dat ik tijdens HBM 2014 en 2016 zo welkom was in jouw onderzoeksgroep. Dear Ryan, I very much appreciated that I could bother you with resting state questions every now and then. Ryan en Philip, HBM Geneva was great thanks to you!

Rick, Sanne en Leontine, ik vond het ontzettend leuk om jullie te begeleiden. Bedankt voor jullie harde werk en gemotiveerde ondersteuning van ons fMRI team. En Leontine, jij in het bijzonder bedankt voor je enthousiasme en interesse zelfs na je stage!

Het fMRI studententeam, en in het bijzonder Frenchey en Madelon, op jullie kon ik bouwen tijdens het scannen, wat toch vaak gepaard ging met veel stress! Sylvia, van jou heb ik alles over de veiligheid van de MRI geleerd, en in return kon ik jou weer helpen als de fMRI setting niet mee werkte ;).

Goede vrienden zijn hard nodig tijdens een promotie traject :). Enrico, we zien elkaar niet vaak, maar desondanks ben je één van mijn beste vrienden. Ik weet dat ik bij jou altijd en eeuwig terecht kan. Voor flauwe humor, het top2000 spel, serieuze gesprekken, uitwisselen van muziek en films, en niet onbelangrijk: concerten. Ik hoop dat we Bruce Springsteen nog heel vaak samen gaan zien! Noah, bedankt voor je rationele gedachtegang, je statistiek hulp, etentjes, sporturen, koffie momenten, en de nuchtere inbreng in emotionele situaties. We maken weleens het grapje, na negen jaar nog steeds vrienden ondanks al die "leuke" grapjes van jou :-p, maar ik hoor ze graag nog jaren aan :)! Alex, ik ben heel erg blij dat je je bij ons hebt aangesloten, en ons nog niet zat bent :p. Bedankt voor Lou onder je hoede nemen. Bedankt voor alle gesprekken, etentjes, sportschooluurtjes en koffiemomenten. Jij ziet vaak al aan me wat er in me omgaat zonder dat ik iets hoef te zeggen. Dank voor vriendschap door dik en dun (hier gaat Noah een opmerking over maken…). Charlotte, bedankt voor de tijd dat we tegelijkertijd promoveerden en elkaar konden ondersteunen bij alle leuke en minder leuke dingen. Alle andere lieve vrienden uit het Weeshuis: Loes, Josjan, Max, Gerwin, Ari,

Ivanka, Harmen, Casper, Arjan, Daan, Els, Elvira, Yorick, Josepha, Jasmin, Tommie. Ik vind het bijzonder om zo'n grote groep vrienden te hebben waarin iedereen prettig gestoord is, zichzelf is en waarin iedereen welkom is. Alle tijd met jullie is altijd geweldig en daarvoor dank ik jullie! Lieve Julie, Wouter, Anouk, David en Erik, ook jullie wil ik erg bedanken voor jullie vriendschap en leuke tijden :)!

Claudia, bedankt. De vlag staat nog altijd op mijn bureau :-).

Ik wil mijn leuke en lieve familie bedanken: Oma Bep, Marco, Katelijne, Ronald, Jeroen, Tessa, Linda, Nick, Jaap, Lotte, Bas en Julika. Ook dank aan alle guppies die me altijd blij maken als ik ze zie: Pepijn, Ella, Wessel, Jasmijn, Roan, Aron, Noel en Annika. In het bijzonder wil ik graag Tiny en Kok bedanken voor deelname als gezonde controles, en Ada en Lau voor het enthousiast mee rennen in de Head First Race. Angela, jou wil ik bedanken voor je interesse in mijn onderzoek en de leuke en lieve whatsappjes :). Ben, mijn gekke oom, bedankt voor al je rare grapjes die me altijd veel lol brengen en het delen van mijn liefde voor de wetenschap. Lieve Suus, Suzy-Q, door samen met jou op te groeien ben je voor mij meer als een zus dan als mijn nicht. Daar zal ik je altijd dankbaar voor zijn. Ik vind het erg bijzonder dat je zo geïnteresseerd bent in mijn onderzoek, en dat je zoals het jou betaamt ;) altijd alle details wil weten. Lieve Dennis, ik vind jouw kennis van ik geloof zo'n beetje alles altijd heel geruststellend. "Oh dat weet Dennis wel joh!" hoor ik mezelf of Suus dan ook best vaak zeggen ;). Dank voor de gezellige uitjes met Suus en dank voor de vele interessante gesprekken. Dear Mary, thank you for being such a lovely small human! I am very happy to have you in my life and I am very much looking forward to seeing you grow up :).

Oma en Opa, Nel en Dik, mijn rotsen in de Rotterdamse branding. Lieve Opa, ik weet hoe belangrijk je doorleren vond. Ik vind het jammer dat je nooit zal weten dat ik dat gedaan heb, maar ik weet zeker dat je trots was geweest. Ik mis je. Lief lief O'tje, de zaterdagavond bij jou is één van de beste momenten van de week. Jij staat voor thuis.

Mijn lieve A-team, Anna en Arend, jullie staan altijd achter mij. Verhuizen naar Edinburgh voor mijn studie, weer terug naar Rotterdam, hup naar Maastricht, promoveren in Rotterdam, en zelfs nu, nu ik weer een nieuw avontuur begin in Edinburgh zijn jullie overal bij betrokken. Bedankt voor al jullie support, goede zorgen, etentjes, de zaterdagavonden bij Oma, onze vakantie in New York, hardop meezingen in de auto, goede gesprekken, lekker gek doen, muziek uitwisselen,

uit onze plaat gaan bij Danny V, alles is okay en niets is te gek. Ik ben zo ontzettend blij dat jullie mijn ouders zijn.

Lieve Mat, I was often asked how I was able to have a long distance relationship while finishing my thesis. The answer is very simple: you. Thank you for being so incredibly supportive! Thank you for discussing my research with me, sending me flowers to remind me that finishing my thesis is a happy ;) time, helping me improve the fifth “troublemaker” proposition with your native language skills, and really making an effort celebrating all the small steps that led me to completing my thesis. There is no one like you lieffie. Not so long now until we can live in the same country :).

List of publications

1 **Meijboom R**, Steketee RM, de Koning I, Osse RJ, Jiskoot LC, de Jong FJ, van der Lugt A, van Swieten JC, Smits M. *Functional connectivity and microstructural white matter changes in phenocopy frontotemporal dementia*. European Radiology. 2016 July 19. [Epub ahead of print]

2 Steketee RM*, **Meijboom R***, de Groot M, Bron EE, Niessen WJ, van der Lugt A, van Swieten JC, Smits M. *Concurrent white and gray matter degeneration of disease-specific networks in early-stage Alzheimer's disease and behavioral variant frontotemporal dementia*. Neurobiology Aging. 2016; 43:119-28.

*These authors contributed equally to this work.

3 **Meijboom R**, Steketee RM, Ham LS, van der Lugt A, van Swieten JC, Smits M. *Hemispheric dissociation of microstructural white matter and functional connectivity abnormalities in semantic and behavioural variant frontotemporal dementia*. Accepted in Journal of Alzheimer's Disease after revision (2016).

4 Steketee RM, **Meijboom R**, Bron EE, Osse RJ, de Koning I, Jiskoot LC, Klein S, de Jong FJ, van der Lugt A, van Swieten JC, Smits M. *Structural and functional brain abnormalities place phenocopy frontotemporal dementia (FTD) in the FTD spectrum*. Neuroimage Clinical. 2016 Apr; 11:595-605.

5 Steketee RM, Bron EE, **Meijboom R**, Houston GC, Klein S, Mutsaerts HJ, Mendez Orellana CP, de Jong FJ, van Swieten JC, van der Lugt A, Smits M. *Early-stage differentiation between presenile Alzheimer's disease and frontotemporal dementia using arterial spin labeling MRI*. European Radiology. 2016; 26(1):244-53.

6 Gotink RA, **Meijboom R**, Vernooij MW, Smits M, Hunink MG. *8-week Mindfulness Based Stress Reduction induces brain changes similar to traditional long-term meditation practice - A systematic review. Brain and Cognition.* 2016; 108:32-41

7 Bron EE, Smits M, van der Flier WM, Vrenken H, Barkhof F, Scheltens P, Papma JM, Steketee RM, Méndez Orellana C, **Meijboom R**, Pinto M, Meireles JR, Garrett C, Bastos-Leite AJ, Abdulkadir A, Ronneberger O, Amoroso N, Bellotti R, Cárdenas-Peña D, Álvarez-Meza AM, Dolph CV, Iftekharuddin KM, Eskildsen SF, Coupé P, Fonov VS, Franke K, Gaser C, Ledig C, Guerrero R, Tong T, Gray KR, Moradi E, Tohka J, Routier A, Durrleman S, Sarica A, Di Fatta G, Sensi F, Chincarini A, Smith GM, Stoyanov ZV, Sørensen L, Nielsen M, Tangaro S, Inglese P, Wachinger C, Reuter M, van Swieten JC, Niessen WJ, Klein S; Alzheimer's Disease Neuroimaging Initiative. *Standardized evaluation of algorithms for computer-aided diagnosis of dementia based on structural MRI: the CADDementia challenge*. Neuroimage. 2015; 111:562-79.

8 Bron EE, Smits M, Papma JM, Steketee RM, **Meijboom R**, de Groot M, van Swieten JC, Niessen WJ, Klein S. *Multiparametric computer-aided differential diagnosis of Alzheimer's disease and frontotemporal dementia using structural and advanced MRI*. [Submitted]

9 **Meijboom R**, Steketee RM, Jiskoot LC, van der Lugt A, van Swieten JC, Smits M. *Microstructural white matter is associated with specific cognitive domains in early-stage behavioural variant frontotemporal dementia and Alzheimer's disease*. [Submitted]

10 **Meijboom R**, Steketee RM, Ham LS, Mantini D, Bron EE, van der Lugt A, van Swieten JC, Smits M. *Quantitative early-stage and long-term differentiation of Alzheimer's disease and behavioural variant frontotemporal dementia using tract-specific microstructural WM and functional connectivity measures*. [Submitted]

11 *Longitudinal changes in phenocopy frontotemporal dementia: a case series*. [In preparation]

Funding

All studies in this thesis were supported by a personal fellowship granted to dr. M. Smits by the Erasmus University Rotterdam (2009-2013).

The functional connectivity methods employed in chapter 2.1 were supported by a Wellcome Trust grant (no 101253/Z/13/Z) granted to dr. D. Mantini.

Publication of this thesis was financially supported by the Graduate School Neurosciences Amsterdam Rotterdam (ONWAR).

Publication of this thesis was financially supported by Alzheimer Nederland.

PhD portfolio

Name PhD candidate:	Rozanna Meijboom
Erasmus MC department:	Radiology and Nuclear Medicine
Research school:	Graduate school Neurosciences Amsterdam Rotterdam (ONWAR)

PhD training	***Year***	***ECTS***
General courses		
Introduction course ONWAR (Amsterdam, Rotterdam/NL)	2012	1.4
Introduction course Centre for Patient Oriented research (CPO, Erasmus MC/NL)	2013	0.3
Basiscursus Regelgeving Klinisch Onderzoek (BROK, Erasmus MC, Rotterdam/NL)	2013	0.9
Regression analysis Netherlands Institute for Health Sciences (NIHES, Erasmus MC/NL)	2013	1.4
Biomedical English Writing and Communication (Erasmus MC/NL)	2014	3.0
Grant writing (ONWAR, Amsterdam/NL)	2015	1.8
Scientific Integrity (Erasmus MC/NL)	2015	0.3
Specific courses		
Resting State functional MRI: Analysis and interpretation (European society for Magnetic Resonance in Medicine and Biology (ESMRMB),Magdeburg/DE)	2012	0.7
Perfusion MRI (International Society for Magnetic Resonance in Medicine (ISMRM), Amsterdam/NL)	2012	1.3
Functional Neuroanatomy (ONWAR, Amsterdam/NL)	2013	1.4
Clinical fMRI and DTI (ESMRMB, Rotterdam/NL)	2013	0.7
ASL in dementia (COST AID, Verona/IT)	2013	0.8
Degenerative diseases of the nervous system (ONWAR, Amsterdam/NL)	2014	1.4
FSL course (Oxford/UK)	2014	1.5
International and national conferences and presentations		
European conference of Radiology (ECR, Vienna/AT)	2012	1.4
Electronic Poster		
European society for Magnetic Resonance in Medicine and Biology (ESMRMB, Toulouse/FR)	2013	0.8
Oral Presentations		

Human Brain Mapping (HBM, Hamburg/DE) *Poster Presentation*	2014	1.3
European society for Magnetic Resonance in Medicine and Biology (ESMRMB, Edinburgh/UK) *Electronic Poster Presentation* *Moderator teaching session*	2015	0.8
Human Brain Mapping (HBM, Geneva/CH) *Poster Presentation*	2016	1.2

Meetings

ONWAR Annual meetings, (Zeist-Driebergen/NL)	2012-2015	3.5
COST ASL Initiative in Dementia meetings (Amsterdam/NL, Brussels/BE)	2012-2013	0.5
Alzheimer Nederland Mix & Match research meeting (Utrecht/NL)	2014, 2016	0.5
ISMRM Benelux chapter (Ghent/BE)	2015	0.3
Reproducibility, credibility and validity Centre for Education and Learning (Rotterdam/NL)	2016	0.3

Other

Short term research project in the research group of Prof. dr. J. Wardlaw at Brain Research Imaging Centre (BRIC), University of Edinburgh (Edinburgh/UK) *Normal appearing white matter (WM) tracts intersecting with WM hyperintensities*	2016	5.8

Teaching	***Year***	***ECTS***
Supervision Master theses of three fourth-year medical students (Erasmus MC/NL)	2013-2015	8.4
Coordinator monthly work meetings fMRI research group (Erasmus MC/NL)	2012-2014	2.0
Coordinator monthly research meetings fMRI research group (Erasmus MC/NL)	2012-2014	1.3
Coordinator monthly joint meetings fMRI, BIGR and KNICR groups (Erasmus MC/NL)	2014	0.7
Total		***45.7***

About the author

Rozanna Meijboom was born in Rotterdam, The Netherlands, on 23rd December 1988. She completed bilingual (Dutch/English) university preparatory education at Wolfert van Borselen Scholengemeenschap in Rotterdam and obtained the International Baccalaureate (IB: A1 higher) degree in 2007. She then briefly studied Psychology and Linguistics at University of Edinburgh (Edinburgh/UK). She obtained her Bachelor degree in Psychology at Erasmus University Rotterdam in 2011, with a specialization in Brain and Cognition and a minor in Computer Science. She continued her studies at Maastricht University (Maastricht/NL), where she obtained her Master degree in Neuropsychology (2012). As part of her Master degree, she conducted an extensive research project on the use of task-based functional MRI as an early diagnostic tool in presenile dementia. This project was performed at the department of Radiology at Erasmus MC - University Medical Centre Rotterdam (Rotterdam/NL) and supervised by dr. R.M.E. Steketee and dr. M. Smits.

In 2012 she started her PhD project, focussing on neuroimaging in dementia as part of the Iris and Iris+ studies performed at Erasmus MC - University Medical Centre Rotterdam (Rotterdam/NL). She was supervised by prof.dr. A. van der Lugt (promotor) and dr. M. Smits (co-promotor) at the department of Radiology and Nuclear Medicine, and by prof.dr. J.C. van Swieten (promotor) at the department of Neurology. Her PhD project was conducted in close collaboration with the Alzheimer Centre Southwest Netherlands.

During her PhD she also performed a short-term research project (2016) focussing on white matter tracts intersecting with white matter hyperintensities at the Brain Research Imaging Centre (BRIC) at the University of Edinburgh (Edinburgh/UK), supervised by prof.dr. J. Wardlaw and dr. S. Muñoz Maniega.

Rozanna is currently living in Rotterdam and continues her research into advanced imaging in dementia at the Department of Radiology and Nuclear Medicine. Additionally, she has an honorary research contract with the Brain Research Imaging Centre at the University of Edinburgh to continue her work on white matter intersections.